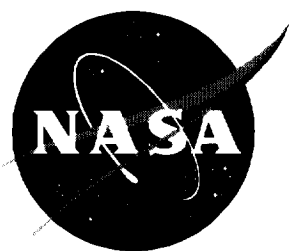NASA Technical Paper 3409

Time Series Comparisons of Satellite and Rocketsonde Temperatures in 1978–79

Ellis E. Remsberg, Praful P. Bhatt, and Francis J. Schmidlin
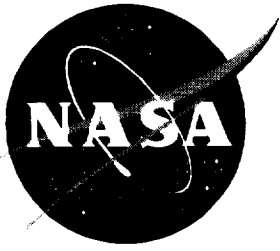
April 1994

Time Series Comparisons of Satellite and Rocketsonde Temperatures in 1978–79

Ellis E. Remsberg
Langley Research Center • Hampton, Virginia

Praful P. Bhatt
SAIC • Hampton, Virginia

Francis J. Schmidlin
Wallops Flight Facility • Wallops Island, Virginia

April 1994

Symbols

$\bar{d}$	mean temperature difference, K, (see eq. (1))
m	sample size
p	pressure, hPa (or 100 Pa)
s	sample standard deviation, K, (see eq. (2))
T	temperature, K
t	Student's t-test statistic (see eq. (3))
x	station temperature value from single sounding, K
Z	geopotential height, km
z	geometric altitude, km

Subscripts:

j	pair number (see eq. (1))
m	sample size (see eq. (3))
1	satellite (see eq. (1))
2	in situ (see eq. (1))

Abbreviations:

FSU	former Soviet Union
IFS	inflatable falling sphere
LAIPAT	LIMS inverted profile archive tape
LAMAT	LIMS map archive tape
LIMS	Limb Infrared Monitor of the Stratosphere
MD	mean difference
NMC	National Meteorological Center
NOAA	National Oceanic and Atmospheric Administration
RAOB	radiosonde observation
ROCOB	rocketsonde observation
SAO	semiannual oscillation
SD	standard deviation
SSU	stratospheric sounding unit
TIROS	Television and Infrared Operational Satellite
TOVS	TIROS Operational Vertical Sounder
UTC	universal time coordinate
VTPR	Vertical Temperature Profile Radiometer
WMO	World Meteorological Organization

Summary

The Limb Infrared Monitor of the Stratosphere (LIMS) experiment made observations from the Nimbus 7 satellite in 1978 and 1979. Temperature-versus-pressure, $T(p)$, profiles were derived from its limb radiance measurements, and those profiles were used to register the radiances from other channels and to retrieve species concentration profiles from those radiances. Therefore, biases in the $T(p)$ results must be known in order to estimate the accuracy of those species profiles. LIMS temperatures have been validated in the past with colocated radiosonde and rocketsonde measurements. The present report describes time series comparisons between satellite and rocketsonde $T(p)$ values at station locations. This approach to validation retains nearly all the rocketsonde profiles, increasing sample size significantly (to 665). As a result, one can know better whether there is a bias that varies as a function of pressure altitude, latitude, or season.

The results indicate no clearly significant bias for LIMS versus Datasonde from 10 hPa to 1 hPa at low and mid latitudes. There is a positive LIMS bias of 2 to 3 K in the upper stratosphere at high latitudes for the Northern Hemisphere in both winter and spring. LIMS is progressively colder than Datasonde from 0.4 hPa (about -3 K) to 0.1 hPa (about -9 K) at all latitudes. A similar comparison between LIMS and the more accurate falling sphere measurements reveals an equivalent mid-latitude LIMS bias at 0.4 hPa but a much smaller bias at 0.1 hPa (-4.6 K). Because the biases do not vary noticeably with season, it is concluded that they are not a function of atmospheric state. This result confirms the robustness of the LIMS temperature retrieval technique.

LIMS comparisons with the Soviet M-100 rocketsonde show significant biases in both the stratosphere and the mesosphere; the Datasonde is considered more useful as a validation standard. National Meteorological Center (NMC)/Datasonde mean differences are very similar to those for LIMS/Datasonde at 10 and 5 hPa. However, the quality of the NMC comparisons is reduced at 2, 1, and 0.4 hPa, primarily due to a lack of nadir radiance data from those levels during the 1978–79 period. Standard deviations for the differences are generally larger at all levels for NMC data than for LIMS data, indicating that the LIMS analyses follow the true temperature variations better than the NMC analyses.

1. Introduction

Temperature-versus-pressure, $T(p)$, profiles are a fundamental product of satellite midinfrared limb emission sounders of the middle atmosphere. Specifically, Gille and House (1971) and Bailey and Gille (1978) showed that one can retrieve $T(p)$ by using observed radiances versus relative altitudes from two radiometer channels that view the atmospheric limb in the ν_2 (or 15 μm) region of the CO_2 spectrum. The "narrow" bandpass CO_2 channel, located near the center of that band, has an emissivity-versus-pressure profile that approaches a value of 1 near a "reference" altitude of 30 km. At that level the effective radiating temperature is very close to the atmospheric temperature, according to the blackbody function. That temperature is then used to calculate an effective emissivity in the more transparent (or "wide") CO_2 channel. The "reference" pressure for the 30-km point is then determined from a curve of the "wide" channel emissivity versus pressure. The hydrostatic equation is then used to calculate the whole $T(p)$ profile from the observed "wide" channel profile of radiance versus relative altitude. This process is iterated to achieve a final $T(p)$ profile in the stratosphere. Absolute altitudes for each pressure level are determined later by a hydrostatic integration of $T(p)$ with the aid of an independent analysis of the height of the 50-hPa surface.

The pressures associated with the $T(p)$ results from the Nimbus 7 Limb Infrared Monitor of the Stratosphere (LIMS) experiment were used to register the measured radiance profiles from each of its channels (Gille and Russell 1984). Then, the $T(p)$ values were applied to those radiances for the retrieval of the concentration profiles of LIMS constituents O_3, H_2O, HNO_3, and NO_2. This means that the LIMS constituent concentrations can be affected by a bias in those temperatures. In particular, whenever the tangent-layer signal becomes low, the retrieved concentrations are more sensitive to temperature bias. Error studies carried out on the LIMS species show that temperature bias error is the largest source of error in the species retrievals at most pressure levels. Because LIMS temperatures and species concentrations vary with pressure (or altitude), latitude, and season, the effect of a temperature bias can change accordingly.

Temperature observations from meteorological rocketsondes (ROCOB's) and radiosondes (RAOB's) are considered as correlative data for validating satellite measurements. In a comparison of colocated LIMS profiles with ROCOB's and RAOB's, Gille et al. (1984a) showed that the mean differences were generally within ± 2 K below the 1-hPa level (altitude of about 48 km). The comparisons with ROCOB's become less reliable at higher altitudes as sources of errors for ROCOB's become more pronounced.

Several rocketsonde techniques have been employed in the past by different countries. To be able to derive maximum information from limited rocketsonde soundings, the compatibility of various systems was studied. Intercomparison campaigns were carried out at Kourou, French Guiana (Finger et al. 1975), and at Wallops Island, Virginia (Schmidlin et al. 1980). Gille et al. (1984b) also used LIMS temperatures as a transfer standard between ROCOB's obtained with instruments from the US and the former Soviet Union (FSU)—identified as "USSR rocketsondes" in their paper and in the remainder of this report.

Remsberg et al. (1984) also carried out temperature comparisons with correlative measurements as part of LIMS O_3 validation activities and found good agreement. Remsberg (1986) compared LIMS zonal-mean temperatures with a 4-year temperature climatology derived from Rayleigh backscatter lidar measurements at 44° N during March, April, and May, when effects of zonal waves are weak. The agreement between those two data sets was better than 3.5 K between 37 and 64 km.

Time series comparisons at single stations show differences in both the phase and the amplitude of temperature waves. For example, Miles et al. (1987) and Grose et al. (1988) carried out comparisons of LIMS temperatures with RAOB data at Invercargill, New Zealand, and Berlin, Germany, respectively, by employing the Fourier coefficient values on the LIMS map archive tape (LAMAT) product (Remsberg et al. 1990). In each case the phase of the LAMAT temperature time series agreed with the changes observed by the RAOB's, but with some reduction in temperature wave amplitude. Although the LIMS LAMAT product contains some spatial smoothing, one can determine a temperature value for the exact location of a correlative measurement station. Miles et al. (1987) reported LIMS LAMAT minus RAOB mean differences (MD) at 100 hPa that were less than 1.2 K with rms differences of less than 2.5 K. The agreement between RAOB and LIMS inverted profile archive tape (LAIPAT) data at Invercargill was even better, with MD less than 0.3 K, and rms differences of 1.6 K. The LAIPAT comparisons were limited to fewer samples, however.

Recently, Remsberg et al. (1992) compared LIMS and National Meteorological Center (NMC) temperatures with RAOB temperatures in the Arctic lower stratosphere. They used a set of 22 stations with nearly uniform longitudinal and latitudinal coverages from 60° N and 84° N. The LIMS and NMC temperature analyses were compared with RAOB data at pressure levels between 100 and 10 hPa. The LIMS temperatures showed very good agreement (MD less

than ±0.3 K) with RAOB's for pressure levels between 70 to 30 hPa as averaged over a 7-month period. The corresponding NMC minus RAOB MD values were within ±0.3 K from 100 to 30 hPa. The satellite/RAOB comparisons at 10 hPa were limited somewhat because of fewer radiosondes ascending to this level, especially during winter. Generally, the number of sondes that reach 10 hPa in winter is 10 percent of the total (McInturff 1978).

The time series comparison approach employed by Remsberg et al. (1992) is very useful and is complementary to the colocated vertical profile comparisons reported in Gille et al. (1984a). Any seasonal or shorter period component in one or the other data set can be identified, in principle. Because of a decrease of RAOB data from altitudes at the 10-hPa level and above, ROCOB's are important for a validation of LIMS temperatures in the upper stratosphere and mesosphere. Therefore, in this report we extend the comparison process upwards in altitude, and present time series of both LIMS LAMAT and NMC temperatures versus US and USSR ROCOB's between pressure altitudes of 10 and 0.1 hPa, as outlined in section 2. Parallel with the previous comparison exercises, we then compare time series of station temperatures derived from the LIMS and NMC analyses. We consider factors that influence the accuracy of those data sets as well as the influence of their vertical resolutions. Furthermore, we report any latitudinal or seasonal trend between the data sets.

ROCOB's must be used with some caution. For example, McInturff (1978) reports that, on average, about one-third of ROCOB's were unusable for NMC's weekly synoptic analyses in the 1970's. While the acceptance rate for most stations was better than 80 percent, only about 40 percent were "usable" from Primrose Lake, Canada, from Thule, Greenland, and from Thumba, India. This relatively low acceptance rate was not biased toward any particular sonde type.

Recently, Schmidlin et al. (1991) showed that the Super Loki inflatable falling sphere (IFS) technique provides temperatures inferred from density determinations that are more accurate than the measured Super Loki Datasonde temperatures in the mesosphere. The aerodynamic heating and radiative heating/cooling effects, which can introduce large errors for Datasonde temperatures in the mesosphere that must be corrected, do not affect the inferred IFS temperatures. In the stratosphere, random-like, but small-scale, vertical structure is induced in the derived IFS temperature profile because of the effect of vertical winds on the lightweight sphere; the vertically smoothed temperature profile is more accurate. An absence of significant biases for the IFS technique

provides a means of standardization of Datasonde ROCOB's. By combining the results from the comparison of the IFS and the US Datasonde temperatures with our intercomparison studies, the accuracy of the LIMS and NMC satellite temperatures is reassessed.

Section 3 contains a brief description of the data sets. The comparison method and results are presented for individual stations in section 4, and the findings for LIMS/ROCOB's are reported by latitude zone in section 5. Conclusions about $T(p)$ accuracy are discussed in section 6. Two appendices present the data comparisons in detail, both graphically and in tabular form.

2. Approach

The LIMS/ROCOB comparison statistics in Gille et al. (1984a) were obtained from individual LIMS profiles that met strict space and time colocation criteria with a rocket sounding. As a result, many rocket profiles were not included in their statistical sets. They did not report a monthly or even a seasonal statistical breakdown from their sample. Because the present time series comparison is based on the LIMS-mapped Fourier coefficient product, we are able to calculate a $T(p)$ value at the exact station location from the coefficients. Although a mapping of the LIMS profiles leads to a smoothed temperature, we can include all the rocket profiles in our comparisons and thereby increase sample size significantly. ROCOB comparisons with these smoothed satellite data lead to larger standard deviations (SD) for a set of paired observations, but the mean differences (MD) are not affected much (Miles et al. 1987). A determination of changes of MD with pressure, latitude, or season is the primary goal of this study.

The comparison results are presented in two ways. First, the LIMS/NMC/ROCOB time series plots are presented for each station at the standard NMC analysis pressure levels of 10 hPa (approximate altitude 31 km), 5 hPa (36 km), 2 hPa (43 km), 1 hPa (48 km), and 0.4 hPa (55 km). LIMS/ROCOB comparisons are also reported at 0.1 hPa (65 km). Using the plots, one can visually evaluate whether the satellite data follow the observed temperature variations seen in a rocket time series. In effect, the time series plot represents an estimate of the information content of the satellite data at any given pressure altitude. The time series plots also reveal any significant biases between the data sets. Secondly, we present the monthly differences for each station in both tabular form and graphical form, but we do not address their statistical significance because of the small sample sizes. Near-seasonal statistics are

generated at each station and compared with estimates of accuracy for each of the data sets. We also compare the 7-month statistics with the results in figure 11 of Gille et al. (1984a).

The findings are discussed according to groups of pressure levels: (a) 10 hPa; (b) 5, 2, and 1 hPa; and (c) 0.4 and 0.1 hPa. We determine the statistical differences for the US versus USSR ROCOB's and compare our findings with those of Gille et al. (1984b), who proposed using LIMS as a transfer standard between the US and USSR ROCOB's for 1978 79. To do this, plots of the monthly differences as a function of station latitude are evaluated for the above pressure level groupings. Separate 7-month average statistics are presented for just the IFS comparisons.

3. Data Sets

3.1. LIMS Data

The Nimbus 7 LIMS instrument was operational from October 25, 1978, to May 28, 1979. LIMS $T(p)$ results on the LAIPAT product were retrieved from CO_2 radiances measured between 64° S and 84° N at approximately 4° latitude intervals, at a vertical resolution of about 2.5 km, but with a vertical point spacing of 1.5 km. The $T(p)$ results were then interpolated to 18 pressure levels from 100 to 0.05 hPa and synoptically mapped to 1200 UTC using a Kalman filter technique. This Fourier coefficient product (termed LAMAT) was created at each standard latitude and pressure level (Remsberg et al. 1990). The standard NMC levels used here are a subset of the LAMAT levels.

The LAMAT data also contain geopotential height information $Z(p)$ at each pressure level, from which $T(Z)$ or $T(z)$ can be generated at a station, where z is geometric altitude. The LIMS distributions of $Z(p)$ were obtained by use of the 50-hPa geopotential field as a reference and then integrating upward using the LIMS $T(p)$ information. Because $T(z)$ is a fundamental product of the Datasonde, one can also make LIMS/ROCOB comparisons of either $T(z)$ or $T(Z)$.

Temperatures from the ascending and descending orbital segments (obtained at ≈1 PM and ≈11 PM at most latitudes) are different by less than 1 K in the lower stratosphere. In order to have the full six zonal wave number or 30° longitudinal resolution in our LIMS analysis, we rely on the results obtained by combining data from all the orbital segments. Therefore, no provision has been made for any diurnal temperature change. We note that diurnal variations are significant in the upper stratosphere/lower

mesosphere at low latitudes, as estimated from separate zonal mean LIMS coefficients obtained at those two local times (Hitchman and Leovy 1985). Resolution in the tangent-layer, limb-view direction is 200 to 300 km or somewhat better than the 4° sampling resolution of the LAMAT data in the meridional direction. Remsberg et al. (1990) report that the LAIPAT temperatures have been mapped to an accuracy of about ± 1 K. Thus, if there is no diurnal variation or other bias in the original retrieved LIMS profiles, that value represents the average uncertainty of the mapped LIMS temperatures at a station location.

3.2. In Situ Data

In situ meteorological rocketsonde observations (ROCOB's) provide high-resolution profiles of density, temperature, and winds with altitude. Because of the relatively high cost involved, however, ROCOB's have been obtained routinely at only a few sites (e.g., about a maximum of 30 sites in 1965). Further, the frequency of observations at each station was about one sounding per week. We consider 14 stations that were making soundings with Datasondes during the LIMS period. The M-100 instrument was used at four USSR land-based sites. The set of 18 rocket stations used for the present study is listed in table 1.

The Datasonde and M-100 temperatures are subject to large errors at upper levels (Krumins and Lyons 1972; Nestler 1983). For example, major corrections were operationally applied to account for aerodynamic heating due to the rapid fall of each instrument. Corrections for heat lag, radiation, and sensor emissivity were also included. For the US Datasonde these combined corrections are about 2 K at 40 km and 8 K at 60 km, while for the USSR M-100 they are much larger, particularly in the mesosphere, as reported from a 1973 rocketsonde intercomparison campaign (Finger et al. 1975). Because a large correction is less accurate, improvements were made to the M-100 payload (the M-100B system) for which the corrections are smaller, and a second intercomparison was conducted with the Datasonde in 1977 (Schmidlin et al. 1980). An IFS sensor system was also part of that 1977 intercomparison. According to Schmidlin et al. (1980) and Koshelkov (1983), there was a gradual changeover by the USSR to the modified payload after 1978. But the printed copies of the profiles for our study still carry the M-100 sensor designation in the heading with no further comment on the nature of the corrections. Because we are not certain whether the 1978–79 USSR ROCOB temperatures were obtained with the original M-100

or the improved M-100B payload design and their associated corrections, we consider comparisons with the USSR ROCOB's to be qualitative at best.

Magnetic tape versions of the ROCOB's used in this study are available at the Wallops Flight Facility. Additional quality control criteria were not applied to each ROCOB, but, in general, the time series plots to be presented herein indicate that the use of strict acceptance criteria would have been counterproductive. In fact, it is an inspection of the plots themselves that defines the quality of each of the data sets. A brief description of the $T(p)$ profiles for each ROCOB type is given below. We have interpolated these $T(p)$ profiles using cubic spline techniques in logarithm of pressure to give temperatures at the standard pressure levels for the present satellite validation study. The ROCOB profiles were interpolated rather than the satellite data because the vertical point spacing is no better than about 3.5 km for the mapped satellite data. In general, interpolation affects the random error for a set of profile differences, but not its mean difference.

3.2.1. US Datasonde. The US Datasonde instrument, technique, and error sources are given in Schmidlin et al. (1980), Nestler (1983), and references therein. The precision or repeatability of the Datasonde $T(z)$ is 1 K up to 53 km (Schmidlin 1981). However, above this level the Datasonde repeatability deteriorates exponentially to about 3.8 K at 65 km and 7.5 K at 70 km. The pressure profile in the ROCOB was calculated by a tie-on of the rocket temperature-altitude $T(z)$ profile to the geometric height derived from the 50-hPa level (normally) of a colocated RAOB sounding, and then integrated upward hydrostatically using the $T(z)$ from the ROCOB. Occasionally, the rocket and RAOB profiles did not overlap in altitude, and in those cases there was an extrapolation of the RAOB data upward to achieve a tie-on point for pressure. In general, ROCOB's from the US sites were made around local noon.

Occasionally, a ROCOB $T(p)$ is misregistered. One particular example is given in figure 1, which shows a LIMS/ROCOB comparison for May 7, 1979, at Thule. Note that the Datasonde $T(p)$ in the left panel has its stratopause near 0.3 hPa. The right panel shows the Datasonde measurement in its more fundamental $T(z)$ form. The colocated LIMS $T(Z)$ profile is derived from the geopotential height field Z on the LAMAT product; thus there is a slight LIMS/ROCOB discrepancy because we have not distinguished between geopotential versus geometric altitude. Nevertheless, the temperature versus "altitude" comparison is also poor. A colocated

4

RAOB sounding extends to 10 hPa and is nearly iso-thermal from there to 100 hPa, as is the LIMS profile. Deep isothermal layers are typical of the high-latitude lower stratosphere in spring. If the ROCOB/RAOB tie-on criterion is based on good temperature agreement at the lowest altitude of this ROCOB sounding (about 30 km), then that require-ment was met. In this case, because the RAOB sounding does not extend well above the 10-hPa level where the temperature is increasing, the observer cannot know that the ROCOB is incorrect, and not just anomalous. In fact, as one can see in appendix A, it is really the temperature time series comparisons in the upper stratosphere from Heiss Island and Thule that strongly suggest an altitude registration prob-lem for the ROCOB in figure 1. The problem is most likely due to uncertainties in angular pointing for the GMD-4 tracking system used at Thule at that time. (The more precise FPS-16 system was used at most US stations.) Misregistration becomes much less of a problem at low and mid latitudes, where the tem-perature profile varies with height even in the low to mid stratosphere. In those cases, misregistration would give a clear mismatch with a colocated RAOB, causing the ROCOB to be unusable or rejected.

3.2.2. USSR M-100.
A brief description of the M-100 system and instrument is given by Schmidlin et al. (1980) and Finger et al. (1975). The M-100 often had a measurement of static pressure from a Pirani heat manometer. The procedure for obtain-ing the final $T(p)$ in those soundings involved iter-ating between both this measured pressure and a hydrostatic calculation of the pressure profile until a match was achieved. Schmidlin et al. (1980) dis-cusses two data-processing methods considered by the USSR. The "standard" processing method was used for the M-100 ROCOB's and is based on samples obtained every 30 sec during descent, which means that the corrections applied to them operationally are not very accurate in the mesosphere. The "prospec-tive" processing method was used with data obtained from the M-100B sensor design of the 1980's, and it is based on samples taken every 5 sec.

We decided to include the temperatures from the four USSR stations in this report because the indi-vidual time series plots are informative and because we can use them to assess any statistical differences between the overall set of US and USSR ROCOB's. Generally, because of the high northern latitude loca-tions of two of the USSR sites, observation times fall during local nighttime there from November to the first week of February but change to local daytime from March to May.

3.2.3. US Super Loki Sphere or IFS.
As part of the ongoing intercomparison studies during 1978–79, soundings with the IFS sensor were ob-tained at Ascension, Barking Sands, Wallops Island, Cape Canaveral, White Sands, and Point Mugu. These occasions are identified by an "×" on the points in the time series plots. Those soundings can be used to test the adequacy of the corrections being applied to the Datasonde temperatures in the meso-sphere. The IFS $p(z)$ profile is obtained from the den-sity profile by integrating the hydrostatic equation downward from an assumed state at the top (near 90 km), and then temperature is obtained using the gas law. Therefore, IFS $T(p)$ is not dependent on a colocated RAOB sounding (Schmidlin 1984).

After deployment for a given launch, the sphere is inflated to a superpressure of nominally 10 hPa. If complete inflation is not achieved, then the sphere becomes compressed prematurely at its lowest alti-tudes, causing the density profile (and inferred tem-perature) to be less accurate.

3.3. National Meteorological Center (NMC) Data

The NMC temperature data used here refer to analyses at 1200 UTC at stratospheric levels (Finger et al. 1965; NMC Office Note 84, "Packing and Iden-tification of NMC Grid Point Data," June 1989). At 10 hPa the 1978–79 NMC Northern Hemisphere anal-yses used RAOB data as input, but only after the data had been corrected for solar heating and radia-tive cooling effects (see below). Both the original and the corrected RAOB data are stored at the Na-tional Climatic Data Center (NCDC). Many of the original RAOB's contain corrections applied at the stations or "pretransmission" corrections (McInturff et al. 1979; McInturff and Finger 1968). In general, these corrections were applied to soundings from the 1978–79 VAISALA, Kew, A-22, and RKZ sondes, but there is no information in the World Meteorological Organization (WMO) transmission code to let NMC (or any other user) know for sure that the correc-tion was applied. Still, an examination by NMC of the 0000 UTC and 1200 UTC transmissions for even those corrected soundings reveals differences that at times are of the order of 1 to 2 K. Therefore, NMC ap-plied a solar heating correction to make the daytime data compatible with the nighttime data. A correc-tion for long-wave cooling was also made at 10 hPa, but the effect was assumed the same for all the sonde types.

Because fewer RAOB's ascend to 10 hPa, espe-cially in polar winter, the 10-hPa analyses also relied on 50-percent persistence plus a 50-percent upward

regression derived using climatological temperature data (Finger et al. 1965). The temperature persistence was based on the previous and following 0000 UTC RAOB reports. Where RAOB data existed, much weight was put on them for the analysis. The Southern Hemisphere analyses at 10 hPa were based on a combination of operational satellite and RAOB data. The information content for the 1978–79 NMC analyses equatorward of 20° N or S is based on an extrapolation from about 20° latitude (Randel 1987).

For both hemispheres the NMC analyses from 5 to 0.4 hPa are based on satellite soundings. From September 24, 1978, to February 23, 1979, the NMC temperature analyses for 5 to 0.4 hPa were derived using regression equations (Gelman and Nagatani 1977) based on radiances from the Vertical Temperature Profile Radiometer (VTPR) flown on the NOAA 5 satellite, and from February 25, 1979, to January 20, 1980, on radiances from the Stratospheric Sounding Unit (SSU) on NOAA 6 (channels 25 and 26). Both the VTPR and the SSU are nadir-viewing instruments and have a vertical resolution of the order of 10 to 17 km. The weighting functions for SSU channels 25 and 26 have a vertical width of about 15 km and are centered at about 15 and 6 hPa, respectively. Thus, the analyses are based on radiances from deep atmospheric layers. The regression relationships also depend on a climatological set of colocated rocketsonde/satellite soundings (Gelman et al. 1982; Anon. 1978; Gelman and Nagatani 1977). Because the USSR rocketsonde data in that climatology were made warmer in the mesosphere to make them compatible with the Datasonde measurements, the 1978–79 NMC temperature analyses at 0.4 hPa are also dependent on Datasonde accuracy (Anon. 1978). Finally, as at 10 hPa, the NMC temperatures were extrapolated equatorward from 20° N or S at these higher analysis levels.

In our study the NMC fields have been modified for easier use in the analysis of stratospheric temperature fields. The original gridded NMC data are represented by the coefficients of a harmonic series at 45 latitudes with a separation of 4° in latitude (88° S to 88° N). The stratospheric data sets were fit with 25 zonal coefficients (a zonal mean term plus 12 sine and 12 cosine terms or 12 wave numbers), which gives a longitudinal resolution of 15°. Temperatures were then obtained at the exact longitude of each station for our comparisons, which, in effect, is an interpolation from the original 25 coefficients. Thus, the zonal resolution for the NMC temperatures is potentially better than that from the six zonal wave number LAMAT data, particularly at low and mid

latitudes. Of course, our 1978–79 10 hPa comparisons still depend on operational NMC analyses that are based solely on the number of RAOB reports available when the analysis was made.

Gelman et al. (1982 and 1986) and Finger et al. (1993) compared NMC temperatures with ROCOB's for periods when there was an operational changeover between two satellites with similar instruments. Based on those comparisons, they report temperature adjustments for each of the pressure levels as a function of latitude. Thus, after adjustment it is easier to evaluate small trends in temperature over a period when a succession of two or more satellites was operating. For the present study we made the NMC temperature fields compatible by applying the recommended adjustments from 5 hPa to 0.4 hPa.

4. Satellite/ROCOB Station Results

The figures in appendix A are plots of LIMS, ROCOB, and NMC time series temperature comparisons at the 10-, 5-, 2-, 1-, 0.4-, and 0.1-hPa pressure levels for all stations listed in table 1. Summary figures in appendix A are also shown of the monthly mean $T(p)$ differences for LIMS minus ROCOB at each station. The monthly and 7-month summaries at each station are useful in assessing whether there might be a LIMS temperature bias that varies with pressure-altitude or station location.

Statistics of temperature differences for LIMS minus ROCOB, LIMS minus NMC, and NMC minus ROCOB were calculated for each station for the VTPR/LIMS (Nov.–Feb.) period, the SSU/LIMS (Feb.–May) period, and the entire 7-month period. The monthly mean differences are also calculated for individual stations. November–February and February–May represent approximate winter and spring seasons, respectively, for the Northern Hemisphere. The winter period is characterized by stratospheric warming activity, while the springtime atmosphere is less perturbed and relaxing toward a radiative equilibrium state. Those "seasonal" and 7-month average results are tabulated in appendix B for each of the six (five for NMC) pressure levels.

Previous satellite validation studies found some rather large differences with ROCOB measurements, especially at upper levels (for example, Gille et al. 1984a and 1984b; Petzoldt 1979). We wanted to investigate those differences in more detail. Results in appendix A also indicate some persistent, large biases even at 10 hPa, particularly for the high-latitude USSR stations. Therefore, we applied a rejection criterion of temperature difference greater than ±20 K in order to edit out profile pairs that contain a potentially spurious result. At 0.4 and 0.1 hPa it could be

argued that even greater differences are likely, given the uncertainties for the several rocket measurement systems.

In the "samples" column for the summary figures in appendix A and the tables in appendix B, the quantity on the left side of the slash (/) is the number of observations that entered into the calculations, while the quantity on the right is the number of observations that exceeded our 20 K criterion. For the NMC/ROCOB comparison, the right-hand number also reflects any missing days in the NMC analysis. The 20 K criterion was not applied in LIMS/NMC comparisons.

The mean differences for the paired observations and their standard deviations have been compiled in appendix B at each station and for each of the three time periods (7 months, Nov. Feb., and Feb. May). It is assumed that both observations (satellite and ROCOB) are representative of the same volume of the atmosphere, and it is our expectation that both observation techniques will register the true atmospheric temperature. Therefore, we have calculated quantities that can be used to test the hypothesis that the sample mean difference is zero (Guenther 1973). The sample mean difference (or $\bar{d}$) at a station is given by

$$\bar{d} = \frac{\sum_j d_j}{m} \qquad (1)$$

where $d_j = x_{j1} - x_{j2}$; x_{j1} and x_{j2} are the satellite and ROCOB values, respectively, for pair j; and m is the number of pairs for that time period and pressure level. The corresponding standard deviations of the differences is defined from

$$s^2 = \frac{\sum_j (d_j - \bar{d})^2}{(m - 1)} \qquad (2)$$

The Student's t-test statistic is defined as

$$t_{m-1} = \frac{\bar{d}}{s/\sqrt{m}} \qquad (3)$$

and can be determined from the quantities in appendix B. The quantity in the denominator of equation (3) is the standard deviation of the mean difference. For a given confidence interval, one can estimate whether the calculated $\bar{d}$ is significantly different than zero, and thus whether there is a significant seasonal bias in $T(p)$ for at least one of the measurement techniques.

The LIMS and NMC temperatures are for 1200 UTC. For the US sonde stations, the observations are taken near local noon. However, the

time difference with ROCOB's can be as much as 12 hr, depending on the longitude of a station (e.g., Kwajalein −8.7° N, 168° E). The observations for USSR sondes at Volgograd and Heiss Island are in darkness from November to the first week of March. The Thumba observations are within 4 hr of 1200 UTC.

4.1. 10 hPa

In general, the rocketsonde measurement errors at 10 hPa are small and the differences from the LIMS and NMC analyses are small (see tables in appendix B). In the tropics the temporal small-scale variability is more pronounced in the ROCOB's than in the LIMS or NMC results. Some of the ROCOB variability may be due to the tie-on uncertainties for Datasonde $T(p)$ profiles. Also the ROCOB's contain effects of small-scale oscillations due to tides and gravity waves. The damped amplitudes in the LIMS and NMC temperature time series in the figures for 10 hPa in appendix A are attributed primarily to their lower zonal resolutions and to constraints in the map analysis products. At Molodezhnaya and Heiss Island and to a smaller extent at Fort Sherman, Kwajalein, Thule, Thumba, and Volgograd, LIMS is almost always warmer than ROCOB's. At Wallops Island LIMS is colder than ROCOB's for most months. Four of those eight stations obtained ROCOB's with the M-100 system for which significant corrections were applied routinely at the sites, particularly at the upper levels. Part of the comparison biases may also be due to the finite (2.5 km) vertical resolution for LIMS, but, if so, it should be noticeable for all low- and mid-latitude stations, regardless of season. We have obtained LIMS retrievals with a higher resolution algorithm, and they do give temperatures that are colder by about 0.5 K to 1.0 K at 10 hPa for a sample day, January 13, 1979 (Solomon et al. 1986).

A slight bias in ROCOB temperatures (or, more likely, its pressure registration) would show up most clearly in tropical $T(p)$ data because of their strong vertical gradients in the stratosphere. Diurnal temperature variations can also be a factor at low latitudes. Hitchman and Leovy (1985) found day temperatures colder than night by up to 1.4 K in the zonally and 216-day-averaged LIMS results near 10° N and 10 hPa; this difference is related to the semiannual oscillation and is most pronounced in Northern Hemisphere spring. LIMS temperatures used in the present study are merely an average of the local day and night values. Consider the apparent biases at Kwajalein (fig. A4) and Fort Sherman (fig. A5), where ROCOB's were taken near midday,

local time. The 1200 UTC LIMS results in those figures ought to be too warm due to not accounting for this diurnal temperature tide. The comparisons at Thumba (fig. A3) may be affected also.

The NMC time series comparisons with ROCOB's are similar to those for LIMS at the individual stations in appendix A, except that the NMC temperatures show less seasonal variability equatorward of about 10° latitude. The NMC analyses for Fort Sherman in figure A5 are a bit colder than the ROCOB's—in opposition to the corresponding LIMS result. Of course, we are mindful that the NMC $T(p)$ analyses are based on RAOB data that include bias "corrections" for solar radiative heating effects at low sun angle (sunrise), leading to a 1200 UTC NMC temperature at Fort Sherman that may be too cold. The 10-hPa NMC results for Thumba contain almost no "short" period variations, most likely because very few RAOB reports from that region of the world were incorporated into the operational NMC analyses (Randel 1987).

For mid- and high-latitude stations both LIMS and NMC contain the large-scale temperature variations also seen in the ROCOB's. LIMS and NMC faithfully reproduce the warming events of December and January at Fort Churchill, Poker Flat, Primrose Lake, and Volgograd. These findings for LIMS agree with those from the LIMS/RAOB time series comparisons for Berlin (52° N) at 10 hPa in Grose et al. (1988). Some biases remain for the polar stations. For example, Gille et al. (1984b) reported LIMS warmer than ROCOB's at Heiss Island by about 6 K on average and warmer than ROCOB's at Thule by about 2 K. The comparisons in appendices A and B are in accord with their findings. Even so, the quality of the high-latitude LIMS results is judged better than for NMC, because the standard deviations for the LIMS/ROCOB differences are almost always smaller than those for NMC/ROCOB.

The monthly mean differences for LIMS minus ROCOB's are plotted as a function of station latitude in figure 2 for 10 hPa. The three Northern Hemisphere USSR stations are marked by open circles ("$\odot$"). Sample size per month is small for all stations and is given to the left of the "slash" at the right margins of each plot. Those samples were included in the final statistics; samples to the right of the "slash" were rejected. The last panel in the sequence in figure 2 is the 7-month statistics, where the horizontal bars represent the standard deviations with respect to the MD for the 7-month period. There is no clear latitudinal trend in the LIMS/ROCOB comparisons.

We focus on those instances where persistent monthly biases can be noted from the summary figures in appendix A; the 10-hPa LIMS/ROCOB statistics at individual stations are given in appendix B for two seasonal periods. For example, table B11 for Wallops Island has a value of $\bar{d}$ of -4.2 K for the November–February period with $s = 3.1$ K and $m = 13$ (see eqs. (1) and (2)). Table B12 for Volgograd has a value of $\bar{d}$ of 2.5 K for the February–May period with $s = 2.0$ K and $m = 40$. Table B5 for Fort Sherman has a value of $\bar{d}$ of 2.4 K with $s = 2.5$ K and for $m = 32$ for the 7-month period. Finally, table B18 for Heiss Island has a 7-month value of $\bar{d}$ of 5.4 K with $s = 3.4$ K and $m = 65$. In each case, the differences, according to equation (3), are significant at the 99-percent confidence level.

Figure 3 shows the NMC/ROCOB results, and the MD's are similar in magnitude but opposite in sign at low latitudes to those for LIMS/ROCOB in figure 2. The 7-month average standard deviations are about equal. There are significant biases at Molodezhnaya (table B1, Feb.–May), Thumba (table B3), Wallops Island (table B11, Nov.–Feb.), and Heiss Island (table B18, Feb.–May). NMC/ROCOB standard deviations are larger than LIMS/ROCOB values at Fort Churchill, Thule, and Heiss Island.

Figure 4 shows LIMS/NMC differences at 10 hPa. Sample size is much greater here, comprising essentially all days of each month. There are pronounced and persistent differences at low latitudes. Comparisons with ROCOB's are closer for LIMS at Ascension, Kwajalein, and Thumba, but closer for NMC at Fort Sherman. Randel (1987) notes that the 1978–79 NMC analyses equatorward of about 20° N or S are based on an extrapolation from 20° latitude, a process that may be less accurate over Asia where almost no RAOB reports were available for the operational analyses.

At Ascension (8° S) the LIMS/ROCOB and the NMC/ROCOB differences are not significant. This finding is at odds with that for Ascension and for Natal, Brazil (6° S, 325° E) in Barnes et al. (1991), where they found NMC warmer than ROCOB by about 6 K and 7 K, respectively, at 10 hPa in spring 1985. We note that NMC no longer made use of RAOB data in their 10 hPa Southern Hemisphere analyses after October 16, 1980, but relied solely on TOVS analyses (Gelman et al. 1986). More importantly, March 1985 was a transition period between NOAA 7 and NOAA 9 for the NMC analyses. Although the so-called NMC adjustment factors at 5 hPa were different by 3.8 K for those two satellites, no factors were developed for 10 hPa even though

temperatures at that level are based on TOVS SSU data, too.

The LIMS/NMC differences at Thule (77° N) and Heiss Island (81° N) in January and February (fig. 4) are relatively large, but there is good agreement between them in spring. Even so, both the LIMS and NMC comparisons with the M-100 at Heiss Island show differences that are clearly positive in spring (figs. 2 and 3). LIMS and NMC comparisons with Datasondes at Thule are not as consistent, particularly for November–February. When NMC is compared with Thule ROCOB's (table B17), there is no significant seasonal bias, although the SD is quite large. As noted in the discussion of figure 1, the altitude registration is also not accurate for some springtime Datasonde soundings at Thule.

4.2. 5, 2, and 1 hPa

The LIMS minus Datasonde time series comparisons in appendix A at 5, 2, and 1 hPa are similar in value and character to the comparisons at 10 hPa (see summaries in figs. 5, 6, and 7). There is no clear bias with latitude. Station standard deviations in appendix B are larger near the stratopause because of increasing $T(p)$ measurement and colocation uncertainties as well as effects from tides and gravity waves. There are significant biases in winter at 5 hPa for Barking Sands (3.3 K) and Wallops Island (-4.4 K) and at 2 hPa for Primrose Lake (4.6 K). In spring there is a bias at 5 hPa for Primrose Lake (2.9 K) and at 2 hPa for Fort Churchill (5.5 K). But there is no springtime bias at Shemya or Poker Flat at 2 hPa. An inspection of individual profile comparisons at Fort Churchill reveals a sharp decrease in the Datasonde $T(p)$ values from 1 hPa to 2 hPa that is not followed so well by LIMS because of its finite vertical resolution.

The LIMS minus M-100 results have larger biases, and they stand out in the 7-month summary plots in figures 5, 6, and 7. Measurements at Thumba (table B3) show a 7-month difference that increases from 0.3 K at 5 hPa to 4.4 K at 1 hPa. Part of this difference profile can be explained by diurnal temperature variations (Gille et al. 1984b). Measurements at Thumba station were taken near twilight or at night (local time of 7 PM to 12 PM). Differences for the two high-latitude stations are significant and consistently positive for both seasons. This is a clear indication of bias, most likely due to an overcorrection for the large aerodynamic heating term in the reduction of the M-100 sensor data. The November–February bias of about 10 K at 1 hPa for Volgograd (table B12) and Heiss Island (table B18) agrees closely with the

recommended 8 K adjustment for the corresponding winter period (May–Aug.) for M-100 data at Molodezhnaya at 68° S (see table 3 in Koshelkov 1983).

NMC minus ROCOB comparisons are summarized in figures 8, 9, and 10 and in appendix B. NMC temperatures at these levels are based on satellite data (VTPR or SSU). In contrast to LIMS minus ROCOB comparisons, monthly differences at stations are variable and have a tendency to change sign with altitude (and perhaps atmospheric state). Station standard deviations are largest during the winter months. Nadir satellite temperature sounders have vertical resolutions of the order of 17 km in the upper stratosphere (Peckham 1974; Nash and Forrester 1986; Jackson et al. 1990). Under disturbed atmospheric conditions, NMC's use of regression of the observed VTPR (or SSU) radiances against a climatology of rocket profiles may misrepresent atmospheric temperature at a given pressure-altitude, even though the deep-layer averaged temperatures are accurate (Gelman and Nagatani 1977).

An interesting example of this insensitivity to real atmospheric variations occurs at White Sands during the second half of December 1978. The 5-hPa time series plot (fig. A9) shows a cooling trend from December 12 to 17, reaching a minimum before starting to warm up again, according to both LIMS and ROCOB's. A nearly opposite trend is seen at 2 and 1 hPa in both LIMS and ROCOB's during the same time period. However, the finer structure present in the higher resolution LIMS and rocket data is absent in the NMC analysis. NMC temperatures at all three levels are nearly constant during December at White Sands; NMC is about 25 K colder than ROCOB's in mid December at 1 hPa! In fact, the NMC statistics that we report at 1 hPa are actually better than they should be because 3 of the 17 measurements in December exceeded our 20 K cutoff criterion and were not included in the seasonal difference. Similar problems for the December 1978 NMC analysis occur at four other mid-latitude stations (Barking Sands, Cape Canaveral, Point Mugu, and Wallops Island).

NMC temperatures for this December period were derived from VTPR channels 1 and 2. Channel 1 measurements are centered at 30 hPa, and 80 percent of its energy comes from the 100- to 2-hPa region. Channel 2 peaks at 10 hPa, and 80 percent of its energy comes from the 100- to 5-hPa region (Gelman and Nagatani 1977). This smearing of energy over such a wide altitude range can lead to inaccurate analyses at 1 hPa. In another example, there is also a substantial NMC/ROCOB bias at

9

Poker Flat at 1 hPa for late January. However, the NMC VTPR analyses tend to follow the ROCOB temperature time series at high latitudes better, most likely because variations in satellite nadir radiance measurements are of larger amplitude and occur over deep layers for winter at high latitudes.

Over the SSU period (or spring 1979 for these comparisons), NMC temperatures were obtained from channels 25 and 26. It must be stressed that channel 27—centered near 1.5 hPa—was not operational for this particular SSU instrument, causing some degradation in NMC temperature accuracy at 2 and 1 hPa. For example, this may be the reason for the large and statistically significant NMC/ROCOB bias for Poker Flat at 2 and 1 hPa during March, April, and May, when wave activity was weak. NMC displays excellent agreement at 2 hPa with the springtime ROCOB's at Fort Churchill, but not at 1 hPa. Most likely, the climatological profiles, used for regression by NMC, have a shape that is also different from the real atmosphere at that station (as defined by the ROCOB's for 1979). The transition from VTPR to SSU in the NMC analyses occurs on February 23, but any remaining uncorrected discontinuities in the NMC time series are hard to distinguish from the temperature fluctuations that also occurred then.

Another interesting result can be seen at 1 hPa for the higher latitudes in the panels for March and April. Figure 7 shows that LIMS matches the Datasonde very well near 50° N and 80° N, but not M-100. Conversely, figure 10 shows that NMC tends to be colder than Datasonde but warmer than M-100. Because the NMC results are constrained more by a ROCOB climatology at this time, it is reasonable that the NMC analyses reflect that climatology. But since the high-latitude M-100 results at 1 hPa are significantly colder than LIMS (by about 10 K) and since NMC applied an adjustment of only 2 K to the M-100 data at 50 km when they compiled their rocket climatology (Anon. 1978), it is likely that their high-latitude climatology defines an atmospheric state based on both the Datasonde soundings and the undercorrected M-100 soundings. Hence, the retrieved NMC $T(p)$ values at 1 hPa ought to split the differences between the two rocket sensors, as it seems to do in figure 10.

The results of NMC minus Datasonde comparisons corresponding to the two different satellite periods are reported in Gelman et al. (1982). Generally, the station MD's in appendix B are smaller at 5 and 2 hPa for both periods than in that reference. This is to be expected because, as stated earlier in section 3, our NMC results do incorporate their

recommended adjustment factors to make the different NOAA satellite measurements compatible. However, our SD values are still comparable with those from Gelman et al. (1982) for both the corresponding VTPR period and the SSU period.

Finally, a summary of the LIMS/NMC comparisons is provided in figures 11, 12, and 13. In general, there is better agreement at low latitudes at 5 and 2 hPa than at 10 hPa (compare fig. 4). However, a bias appears for the mid-latitude stations, leading to a distinct latitudinal dependence in the monthly plots. The character of that bias at 2 hPa is very similar for each of the SSU months of March to May. The station SD values in appendix B are small, in spring compared with winter, when the atmosphere is more variable. Several locations have statistically significant biases. In particular, there is a bias for the four stations from 29° N to 38° N for March at 5 hPa (fig. 11), which should not be related to the loss of the top SSU channel. For comparison, figure 5 shows only weak LIMS/ROCOB biases at Wallops Island and Point Mugu and none at White Sands. Figure 8 shows larger negative NMC/ROCOB biases at all three stations. It is likely that this apparent NMC discrepancy in figure 11 is related to the coarse vertical resolution of the SSU and the regression procedure used to derive $T(p)$ values from its radiances. Those constraints could also account for a high-latitude LIMS/NMC springtime bias at 2 and 1 hPa (figs. 12 and 13).

4.3. 0.4 and 0.1 hPa

LIMS/ROCOB comparisons were made at both 0.4 and 0.1 hPa (appendices A and B), and the summary results are provided in figures 14 and 15. The 7-month LIMS minus Datasonde comparisons show that LIMS is a bit cold at 0.4 hPa, but clearly so at 0.1 hPa. Figures 14 and 15 indicate no clear seasonal or latitudinal dependence in those differences. A top-of-profile effect may cause the LIMS temperatures at 0.1 hPa to be too cold by up to 2 K, but only when mid-mesosphere temperatures are cold enough to cause the radiance signal to approach the LIMS noise level. This retrieval bias occurs because an isothermal guess temperature is used initially at profile top. The effect of this guess disappears after several iterations, except within about 3 km from the profile top. Retrievals generally begin at 0.05 to 0.08 hPa. At any rate, this effect does not explain the large negative bias (−9 K) at 0.1 hPa in figure 15.

LIMS temperatures are warmer than those from the M-100, an effect that is the opposite of that with the Datasonde. Mean differences with the M-100 decrease progressively from about 8 K at 1 hPa to

10

about 4 K at 0.1 hPa. The SD increases, however, from 1 hPa to 0.1 hPa. The 7-month summaries in figures 14 and 15 show that both the sample differences and the standard deviations increase with latitude at 0.4 and 0.1 hPa.

The highest analysis level for NMC is 0.4 hPa. Time series plots for each station (in appendix A) show a nearly constant NMC result at that level. There is also no SAO signature at low latitudes. On the other hand, there is no bias in the 7-month results for NMC minus Datasonde (fig. 16). This may be because the VTPR and SSU channels are insensitive to atmospheric temperatures from that level, such that the NMC regression procedure relies almost entirely on the long-term Datasonde climatology. There is a relatively low correlation coefficient (0.55) for the VTPR/ROCOB regression relation for temperature at 0.4 hPa (Anon. 1978). Presumably, that coefficient would be even smaller for the present SSU period with its top channel missing.

The transition from VTPR to SSU in late February in the NMC analyses is marked by a noticeable increase in temperature at Thule and Heiss Island (appendix A) at 1.0 and 0.4 hPa. This increase is opposite the direction of the temperature trend recorded by both ROCOB's and LIMS. After the nearly 2-week transition period, NMC does follow the ROCOB's more closely.

Figure 17 indicates pronounced LIMS minus NMC differences at 0.4 hPa both by month and by latitude. Based on the rocket comparisons, one might conclude that both LIMS and NMC have significant errors, but of course, that conclusion also depends on the accuracy of the rocket $T(p)$ in the mesosphere. Nevertheless, the individual station rocket/satellite time series analyses in appendix A do show that the rocket temperature trends were followed much better by LIMS than by NMC, indicating that the LIMS temperatures are more precise.

4.4. Comparisons at 68° S

Appendices A and B also include results for the USSR station Molodezhnaya (68° S, 46° E). Because the LIMS data do not extend beyond 64° S, the LIMS/ROCOB comparisons are not as useful for validation purposes, especially in autumn (April and May) when the Southern Hemisphere polar vortex is well formed and there is a larger meridional temperature gradient at high southern latitudes. To see this better, we have included two NMC curves one for 64° S and another for 68° S. While the effect of the gradient is apparent, there is still a significant bias with the rocket data in autumn. The NMC/ROCOB

statistics in appendix B were calculated using NMC data at 68° S, and they show a large bias, too.

During summer, when the gradients in the mid stratosphere are weaker, there is very good agreement between LIMS, NMC, and the rocket data at 5 and 10 hPa. Both LIMS and NMC are warmer than the M-100 at 2, 1, and 0.4 hPa, as was the case for the other three USSR rocket stations. The LIMS $T(p)$ time series at 0.1 hPa is nearly constant from October to April with a gradual warm up in autumn.

5. Comparisons by Latitude Zone

5.1. LIMS/Datasonde

This section focuses on the LIMS/Datasonde comparisons. We have grouped those paired results by latitude zone to search further for any mean differences. There are five stations at low latitudes (8° S to 22° N), four at mid latitudes (29° N to 38° N), and five at high latitudes (53° N to 77° N). Equations (1) and (2) have been applied to these larger samples, and the results are given in table 2 and figures 18, 19, and 20. Horizontal bars represent the sample standard deviations from table 2. Mean differences are judged significant if they are outside the 95-percent confidence intervals for these larger samples. The important issues are how do the mean differences compare with the estimates of systematic error in $T(p)$ for LIMS and Datasondes and do they vary with latitude, season, or pressure.

LIMS is significantly warmer at 10 hPa by about 1 K for low and high latitude, according to equation (3). The high-latitude bias is similar for winter and spring, indicating that the problem is not likely due to a misregistration of any Datasonde profiles. A bias of 1 K is of the order of the expected accuracy of $T(p)$ at 10 hPa for both LIMS and Datasonde. A LIMS bias of this order could be attributed simply to uncertainties in the transmittances for CO_2 (Gille et al. 1984a), although such a bias is expected to be fairly uniform with latitude.

For the pressure range, 5 hPa to 1 hPa, there is a significant LIMS/Datasonde bias at high latitudes, but not at low or mid latitudes. The bias is most pronounced at 2 hPa in winter, when LIMS is warmer by 3.6 K (table 2). The standard deviation of that mean, $s/\sqrt{m}$, is 0.5 K, so the 95-percent confidence interval is about twice that, only ±1.0 K. On average, LIMS is warmer at all three pressure levels at high latitudes in both winter and spring.

At 0.4 and 0.1 hPa LIMS is cooler than Datasonde for all three latitude zones. The mean difference of about −9 K at 0.1 hPa is also much greater

than the theoretical LIMS, root-sum-square (rss), $T(p)$ error estimate of ± 4.6 K in Gille et al. (1984a, their table 2). It is also larger than the remaining uncorrected Datasonde biases reported by Nestler (1983).

Gille et al. (1984a) reported mean and standard deviation differences for three stations—Ascension, White Sands, and Fort Churchill. Our station results from appendix B are similar, although we do show smaller mean differences at White Sands and larger ones at Fort Churchill. From the theoretical LIMS rss errors in Gille et al. (1984a), the $T(p)$ error at 10 to 1 hPa for a single profile is somewhat smaller than the 7-month SD values in our table 2. But then our SD values also include any uncertainties in the Datasonde $T(p)$. Our 7-month MD values at low and mid latitudes are much smaller than the LIMS rss errors, indicating that many of the systematic LIMS $T(p)$ errors are quasi-random when averaged over many profiles.

5.2. LIMS/Sphere

The falling sphere (IFS) technique has been used for $T(p)$ validation, primarily in the mesosphere. Schmidlin et al. (1991) indicate average IFS minus Datasonde differences in $T(z)$ of less than 3 K from 30 to 60 km with a repeatability of order ± 3 K. Their results are shown in figure 21. The LIMS/Datasonde comparisons in figures 18 to 20 have shapes that are very similar to figure 21 and are just as accurate, even taking into account the additional estimates of LIMS $T(p)$ error due to its finite vertical resolution and the fit of its mapped coefficients to the original retrieved profiles.

Schmidlin et al. (1991) and Quiroz and Gelman (1976) did find Datasonde warmer than the IFS $T(p)$ values by about 5 K at 0.1 hPa (about 65 km in fig. 21). It is believed that the IFS is the more accurate in situ technique in the mesosphere. Therefore, we use the Datasonde as the common data set for the two LIMS/in situ comparisons and find that LIMS minus IFS should be only about -4 K at 0.1 hPa. That difference is of the order of the rss error for the LIMS $T(p)$. We infer then that the low- and mid-latitude LIMS $T(p)$ values are accurate from 10 hPa to 0.4 hPa, but too cold at 0.1 hPa.

As a check on our inferred LIMS/IFS differences, we calculated LIMS differences with the approximately 70 IFS soundings that appear at 6 mid-latitude stations in the time series plots in appendix A. These IFS comparisons are more meaningful for us because they are collocated in time (same day and year), as well as space. The individual station

and 6-station average results are given in table 3 and figure 22 along with the 7-month mid-latitude LIMS/Datasonde plot from figure 19. Standard deviations for LIMS/IFS are rather large, presumably because of the small-scale effects of the vertical winds in an individual sphere determination of $T(p)$. Because the standard deviation about the mean is larger for the IFS comparisons, it is concluded that a $T(p)$ profile from a single Datasonde may be more representative of the atmosphere than the $T(p)$ from a single sphere. IFS sample size is smaller at 5 and 10 hPa, because the sphere often deflates somewhat before descending to those levels. Still, the LIMS/IFS differences are within ± 3 K over most of the pressure range. At 0.1 hPa LIMS minus IFS is equal to -4.6 K ± 4.8 K, a result that is remarkably similar to our inferred LIMS/IFS bias based on the findings in Schmidlin et al. (1991) and based on the LIMS/lidar comparisons in Remsberg (1986).

6. Discussion and Conclusions

The present time series approach to satellite temperature validation has enabled us to make use of all the rocketsonde data, thus increasing both sample size (to 665) and statistical confidence. Furthermore, one can more easily judge the quality of the measured temperatures at a station by observing the general agreement in their variations for both quiet and disturbed atmospheric conditions. The high precision of Limb Infrared Monitor of the Stratosphere (LIMS) temperature-versus-pressure profile $(T(p))$ values is particularly evident in our station time series plots.

There are no clear trends with season for LIMS minus Datasonde $T(p)$ for any latitude zone, indicating that the LIMS $T(p)$ retrieval accuracy is not a function of atmospheric state. This is an important point, because it confirms the robustness of the LIMS temperature retrieval technique. There is no stratospheric LIMS bias at low and mid latitudes. However, we do find a positive LIMS bias for both seasons at high latitudes of the upper stratosphere, and it is hard to imagine how the Datasonde could be accurate at low and mid latitudes, but not at high latitudes. It is also unlikely that a latitudinally varying LIMS bias could be explained by transmittance errors or a smoothing of the true $T(p)$ due to the vertical resolution of LIMS. We have found a minor error (about 0.25 percent) in our first guess for the altitude above the center of the Earth of the tangent layer for our reference pressure level. Because this value is used in the hydrostatic calculation of the LIMS $T(p)$, it leads to a systematic $T(p)$ error that is increasingly positive at high latitudes of the upper stratosphere. The effect of this error for a

mesospheric $T(p)$ is less clear and more difficult to sort out, at least by comparison with the Datasondes at high latitudes. (We have no sphere profiles for high latitudes during the LIMS period.) More work is needed with an improved LIMS algorithm plus updated spectral databases for the LIMS CO_2 channels to evaluate these effects in detail.

Gille et al. (1984b) proposed using LIMS $T(p)$ data as a transfer standard between the Datasonde and the M-100. We found differences in this study that are very similar to those of Gille et al. (1984b, their figs. 2, 3, and 4). Those differences also agree qualitatively with the recommended adjustments to the M-100 temperature climatologies for high-latitude stations, at least at 50 km (Koshelkov 1983). However, the positive LIMS bias, noted above, would affect its use as a transfer standard at high latitudes.

The 7-month National Meteorological Center (NMC)/Datasonde comparisons at 10 hPa show good agreement, except at low latitudes, where the 1978–79 NMC analyses are based on extrapolations of RAOB data equatorward of about 20° N. NMC/Datasonde mean differences are very similar to those for LIMS/Datasonde at 5 hPa, a level where nadir-radiance data were available to NMC during 1978–79. SD values at 5 hPa, however, are larger for NMC as compared with LIMS, indicating that the LIMS analyses follow the true temperature variations better than the NMC analyses. At 2, 1, and 0.4 hPa the 1978–79 NMC retrievals are weighted toward their historical ROCOB climatology, and, as a result, the NMC/Datasonde time series comparisons show larger differences at those levels. The largest differences occur during winter and are attributed to the low vertical resolution of the nadir-viewing sounders and a nonrepresentative climatology, as shown in the White Sands time series. Several stations (e.g., Poker Flat) also have relatively large NMC/ROCOB mean differences during springtime at 2 and 1 hPa, perhaps because of the relative insensitivity of SSU channels 25 and 26 to stratopause temperatures.

The findings herein suggest that there is no statistically significant $T(p)$ bias affecting the LIMS species in the upper stratosphere at low and mid latitudes. The $T(p)$ bias at high latitudes affects LIMS species there in two ways. First, there is a bias in the registration of the measured species radiance profiles with pressure. Second, a $T(p)$ bias affects the calculation of blackbody radiances, which must be accounted for in a limb emission retrieval. Both effects, while small, must be evaluated further. Finally, because LIMS temperatures seem to be too

cold at pressure levels above 0.4 hPa at all latitudes, the LIMS ozone values may be too large at those levels.

NASA Langley Research Center
Hampton, VA 23681-0001
January 5, 1994

References

Anon. 1978: *Synoptic Analyses, 5-, 2-, 1-, and 0.4-Millibar Surfaces for July 1976 Through June 1977*. NASA RP-1032.

Bailey, P. L.; and Gille, J. C. 1978: An Approximate Method For Non-Linear Inversion of Limb Radiance Observations. *Remote Sensing of the Atmosphere Inversion Methods and Applications*, Alain L. Fymat and Vladimir E. Zuev, eds., Elsevier Scientific Publ. Co., pp. 115 122.

Barnes, Robert A.; McMaster, Leonard R.; Chu, William P.; McCormick, M. Patrick; and Gelman, Melvyn E. 1991: Stratospheric Aerosol and Gas Experiment II and ROCOZ-A Ozone Profiles at Natal, Brazil A Basis For Comparison With Other Satellite Instruments. *J. Geophys. Res.*, vol. 96, pp. 7515 7530.

Finger, F. G.; Woolf, H. M.; and Anderson, C. E. 1965: A Method for Objective Analysis of Stratospheric Constant-Pressure Charts. *Mon. Weather Review*, vol. 93, pp. 619 638.

Finger, F. G.; Gelman, M. E.; Schmidlin, F. J.; Leviton, R.; and Kennedy, B. W. 1975: Compatibility of Meteorological Rocketsonde Data as Indicated by International Comparison Tests. *J. Atmos. Sci.*, vol. 32, pp. 1705 1714.

Finger, F. G.; Gelman, M. E.; Wild, J. D.; Chanin, M. L.; Hauchecorne, A.; and Miller, A. J. 1993: Evaluation of NMC Upper-Stratospheric Temperature Analyses Using Rocketsonde and Lidar Data. *Bull. American Meteorol. Soc.*, vol. 74, no. 5, pp. 789 799.

Gelman, M. E.; and Nagatani, R. M. 1977: Objective Analyses of Height and Temperature at the 5-, 2-, and 0.4-mb Levels Using Meteorological Rocketsonde and Satellite Radiation Data. *Space Research XVII*, M. J. Rycroft, ed., Pergamon Press, pp. 117 122.

Gelman, M. E.; Miller, A. J.; Nagatani, R. M.; and Bowman, H. D., II 1982: Mean Zonal Wind and Temperature Structure During the PMP-1 Winter Periods. *Adv. Space Res.*, vol. 2, no. 10, pp. 159 162.

Gelman, M. E., Miller, A. J.; Johnson, K. W.; and Nagatani, R. M. 1986: Detection of Long-Term Trends in Global Stratospheric Temperature From NMC Analyses Derived From NOAA Satellite Data. *Adv. Space Res.*, vol. 6, no. 10, pp. 17 26.

Gille, John C.; and House, Frederick B. 1971: On the Inversion of Limb Radiance Measurements I: Temperature and Thickness. *J. Atmos. Sci.*, vol. 28, no. 8, pp. 1427 1442.

Gille, John C.; and Russell, James M., III 1984: The Limb Infrared Monitor of the Stratosphere: Experiment Description, Performance and Results. *J. Geophys. Res.*, vol. 89, no. D4, pp. 5125–5140.

Gille, John C.; Russell, James M., III; Bailey, Paul L.; Gordley, Larry L.; Remsberg, Ellis E.; Lienesch, James H.; Planet, Walter G.; House, Frederick B.; Lyjak, Lawrence V.; and Beck, Sharon A. 1984a: Validation of Temperature Retrievals Obtained by the Limb Infrared Monitor of the Stratosphere (LIMS) Experiment on Nimbus 7. *J. Geophys. Res.*, vol. 89, no. D4, pp. 5147–5160.

Gille, J. C.; Bailey, P. L.; and Beck, S. A. 1984b: A Comparison of U.S. and USSR Rocketsondes Using LIMS Satellite Temperature Sounding as a Transfer Standard. *J. Geophys. Res.*, vol. 89, pp. 11,711 11,715.

Grose, W. L.; Miles, T.; Labitzke, K.; and Pantzke, E. 1988: Comparison of LIMS Temperatures and Geostrophic Winds With Berlin Radiosonde Temperature and Wind Measurements. *J. Geophys. Res.*, vol. 93, pp. 11,217 11,226.

Guenther, William C., 1973: *Concepts of Statistical Inference*, Second ed. McGraw-Hill, Inc.

Hitchman, Matthew H.; and Leovy, Conway, B. 1985: Diurnal Tide in the Equatorial Middle Atmosphere as Seen in LIMS Temperatures. *J. Atmos. Sci.*, vol. 42, no. 6, pp. 557–561.

Jackson, D. R.; Harwood, R. S.; and Renshaw, E. 1990: Tests of a Scheme For Regression Retrieval and Time-Space Interpolation of Stratospheric Temperature From Satellite Measurements. *Q. J. Royal Meteorol. Soc.*, vol. 116, pp. 1449 1470.

Koshelkov, I. P. 1983: Proposal for a Reference Model of the Middle Atmosphere of the Southern Hemisphere, *Adv. Space Res.*, vol. 3, no. 1, pp. 3 16.

Krumins, M. V.; and Lyons, W. C. 1972: *Corrections For the Upper Atmosphere Temperatures Using a Thin Film Loop Mount.* AD-747973, NOLTR-72-152, U.S. Navy. (Available from DTIC as AD 747 973.)

McInturff, Raymond M.; and Finger, Frederick G. 1968: *The Compatibility of Radiosonde Data at Stratospheric Levels Over the Northern Hemisphere.* ESSA TM-WBTM-DATAC 2, U.S. Dep. of Commerce. (Available from DTIC as AD 686 296.)

McInturff, Raymond M., ed. 1978: *Stratospheric Warmings: Synoptic, Dynamic and General-Circulation Aspects.* NASA RP-1017.

McInturff, R. M.; Finger, F. G.; Johnson, K. W.; and Laver, J. D. 1979: *Day-Night Differences in Radiosonde Observations of the Stratosphere and Troposphere.* NOAA-TM-NWS-XMC-63, National Meteorological Center, 1979. (Available from NTIS as PB80 117 989.)

Miles, T.; Grose, W. L.; Russell, J. M. III; and Remsberg, E. E. 1987: Comparison of Southern Hemisphere

Radiosonde and LIMS Temperatures at 100 mb. *Q. J. Royal Meteorol. Soc.*, vol. 113, pp. 1382–1386.

Nash, J.; and Forrester, G. F. 1986: Long-Term Monitoring of Stratospheric Temperature Trends Using Radiance Measurements Obtained by the TIROS-N Series of NOAA Spacecraft. *Adv. Space Res.*, vol. 6, no. 10, pp. 37 44.

Nestler, M. S. 1983: *A Comparative Study of Measurements From Radiosondes, Rocketsondes, and Satellites.* NASA CR-168343.

Peckham, G. 1974: The Information Content of Remote Measurements of Atmospheric Temperature by Satellite Infrared Radiometry and Optimum Radiometer Configurations. *Q. J. Royal Meteorol. Soc.*, vol. 100, pp. 406 419.

Petzoldt, K. 1979: Investigation of Stratospheric Warmings With Different Inversion Techniques for Infrared Satellite Radiances. *Remote Sounding of the Atmosphere From Space*, H.-J. Bolle, ed., Pergamon Press, Inc., pp. 89 100.

Quiroz, R. S.; and Gelman, M. E. 1976: An Evaluation of Temperature Profiles From Falling Sphere Soundings. *J. Geophys. Res.*, vol. 81, no. 3, pp. 406 412.

Randel, W. J. 1987: *Global Atmospheric Circulation Statistics, 1000 1mb.* PB88-168240, NCAR/TN-295-STR, National Center for Atmospheric Research. (Available from NTIS as PB88 168 240.)

Remsberg, E. E.; Russell, J. M., III; Gille, J. C.; Bailey, P. L.; Gordley, L. L.; Planet, W. G.; and Harries, J. E. 1984: The Validation of Nimbus 7 LIMS Measurements of Ozone. *J. Geophys. Res.*, vol. 89, pp. 5161 5178.

Remsberg, E. E. 1986: The Accuracy of Nimbus 7 LIMS Temperatures in the Mesosphere. *Geophys. Res. Lett.*, vol. 13, pp. 311 314.

Remsberg, Ellis E.; Haggard, Kenneth V.; and Russell, James M., III 1990: Estimation of Synoptic Fields of Middle Atmosphere Parameters From Nimbus-7 LIMS Profile Data. *J. Atmos. & Ocean. Technol.*, vol. 7, pp. 689–705.

Remsberg, Ellis E.; Bhatt, Praful P.; and Miles, Thomas 1992: A Comparison of Nimbus 7 Limb Infrared Monitor of the Stratosphere and Radiosonde Temperatures in the Lower Stratosphere Poleward of 60N. *J. Geophys. Res.*, vol. 97, no. D12, pp. 13,001 13014.

Schmidlin, F. J.; Duke, J. R.; Ivanovsky, A. I.; and Chernyshenko, Y. M. 1980: *Results of the August 1977 Soviet and American Meteorological Rocketsonde Intercomparison Held at Wallops Island, Virginia.* NASA RP-1053.

Schmidlin, F. J. 1981: Repeatability and Measurement Uncertainty of the United States Meteorological Rocketsonde. *J. Geophys. Res.*, vol. 86, pp. 9599 9603.

Schmidlin, F. J. 1984: Intercomparisons of Temperature, Density and Wind Measurements From In Situ and Satellite Techniques. *Adv. Space Res.*, vol. 4, no. 6, pp. 101–110.

Schmidlin, F. J.; Lee, H. S.; and Michel, W. 1991: The Inflatable Sphere A Technique for the Accurate Measurement of Middle Atmosphere Temperatures. *J. Geophys. Res.*, vol. 96, pp. 22,673 22,682.

Solomon, S.; Kiehl, J. T.; Kerridge, B. J.; Remsberg, E. E.; and Russell, J. M., III 1986: Evidence for Nonlocal Thermodynamic Equilibrium in the Nu3 Mode of Mesospheric Ozone. *J. Geophys. Res.*, vol. 91, pp. 9865 9876.

Table 1. Rocketsonde Stations

Serial no.	Station identification	Latitude, deg	Longitude (east), deg	Station name	Instrument type
1	89542	−67.7	46	Molodezhnaya	USSR M-100
2	61902	−8.0	346	Ascension Island	US Datasonde
3	43373	8.5	77	Thumba	USSR M-100
4	91366	8.7	168	Kwajalein	US Datasonde
5	78801	9.3	280	Fort Sherman	US Datasonde
6	78861	17.1	298	Antigua	US Datasonde
7	91162	22.0	200	Barking Sands	US Datasonde
8	74794	28.5	279	Cape Canaveral	US Datasonde
9	72269	32.4	254	White Sands	US Datasonde
10	72391	34.1	241	Point Mugu	US Datasonde
11	72402	37.8	285	Wallops Island	US Datasonde
12	34560	48.7	44	Volgograd	USSR M-100
13	70414	52.7	174	Shemya	US Datasonde
14	71124	54.8	250	Primrose Lake	US Datasonde
15	71913	58.7	266	Fort Churchill	US Datasonde
16	70192	65.0	213	Poker Flat	US Datasonde
17	04202	76.6	291	Thule	US Datasonde
18	20046	80.6	58	Heiss Island	USSR M-100

Table 2. LIMS Minus Datasonde Statistics by Latitude Zone

	Mean difference, K, at—						Total of samples/Number rejected at—						Standard deviation, K, at—					
	10 hPa	5 hPa	2 hPa	1 hPa	0.4 hPa	0.1 hPa	10 hPa	5 hPa	2 hPa	1 hPa	0.4 hPa	0.1 hPa	10 hPa	5 hPa	2 hPa	1 hPa	0.4 hPa	0.1 hPa
Low-latitude sector																		
7 month	1.2	−0.1	0.1	0.3	−2.2	−7.8	217/0	217/0	216/0	214/0	196/0	78/6	2.8	3.9	3.9	3.7	3.6	4.7
Nov.–Feb.	0.7	−0.6	0.1	0.1	−2.5	−8.5	110/0	110/0	109/0	108/0	98/0	34/5	2.8	3.6	3.9	3.9	3.9	4.6
Feb.–May	1.8	0.4	0.1	0.5	−2.0	−7.3	107/0	107/0	107/0	106/0	98/0	44/1	2.6	4.1	3.9	3.5	3.3	4.7
Mid-latitude sector																		
7 month	−1.0	0.3	0.4	−0.8	−4.0	−9.4	219/0	218/0	215/0	214/0	193/1	53/7	3.1	3.8	4.2	3.9	4.4	5.0
Nov.–Feb.	−0.6	−0.4	−0.4	−1.6	−5.2	−10.5	124/0	123/0	120/0	120/0	115/1	27/6	3.4	3.8	4.6	4.3	3.7	4.9
Feb.–May	0.4	1.3	1.4	0.2	−2.2	−8.3	95/0	95/0	95/0	94/0	78/0	26/1	2.7	3.6	3.5	3.0	4.7	5.0
High-latitude sector																		
7 month	1.2	1.7	2.8	1.9	−2.7	−10.0	230/1	230/1	229/2	222/4	178/0	66/8	2.9	3.5	4.7	4.6	4.8	6.1
Nov.–Feb.	1.3	1.9	3.6	2.9	−1.7	−8.5	101/0	101/0	101/0	96/2	80/0	32/5	3.0	3.8	5.2	5.6	5.9	7.1
Feb.–May	1.1	1.6	2.2	1.1	−3.6	−11.4	129/1	129/1	128/2	126/2	98/0	31/3	2.8	3.2	4.2	3.5	3.4	4.7

Table 3. LIMS Minus Sphere 7-Month Statistics at Mid Latitudes

	Mean difference, K, at—						Total of samples/Number rejected at —						Standard deviation, K, at—					
	10 hPa	5 hPa	2 hPa	1 hPa	0.4 hPa	0.1 hPa	10 hPa	5 hPa	2 hPa	1 hPa	0.4 hPa	0.1 hPa	10 hPa	5 hPa	2 hPa	1 hPa	0.4 hPa	0.1 hPa
Ascension Island	0.0	0.0	0.0	0.0	−2.4	−3.9	0/0	0/0	0/0	0/0	1/0	2/0	0.0	0.0	0.0	0.0	0.0	6.0
Barking Sands	4.8	4.7	3.3	−0.4	0.1	−1.5	4/0	4/1	5/0	6/0	5/1	8/0	6.3	3.2	3.2	5.4	1.4	1.7
Cape Canaveral	−2.3	1.1	3.0	−1.1	−3.2	−2.0	4/0	6/0	6/0	6/0	6/0	7/1	10.7	5.6	9.5	9.3	4.9	3.5
White Sands	−2.2	−0.1	1.1	−3.5	−3.9	−6.3	7/3	18/2	22/1	23/0	23/0	24/0	10.3	5.2	8.7	7.9	5.1	5.6
Point Mugu	3.7	2.8	3.5	0.1	−3.5	−3.2	5/0	8/0	10/0	10/0	10/0	11/0	6.0	6.9	4.9	4.5	5.8	3.9
Wallops Island	0.1	5.1	2.7	2.8	−1.0	−5.8	6/0	9/0	13/0	19/0	19/1	19/1	2.6	5.9	6.1	4.6	4.4	4.4
Combined	0.5	2.0	2.3	−0.6	−2.6	−4.6	26/3	45/3	56/1	64/0	64/2	71/2	7.7	5.8	7.1	6.8	4.9	4.8
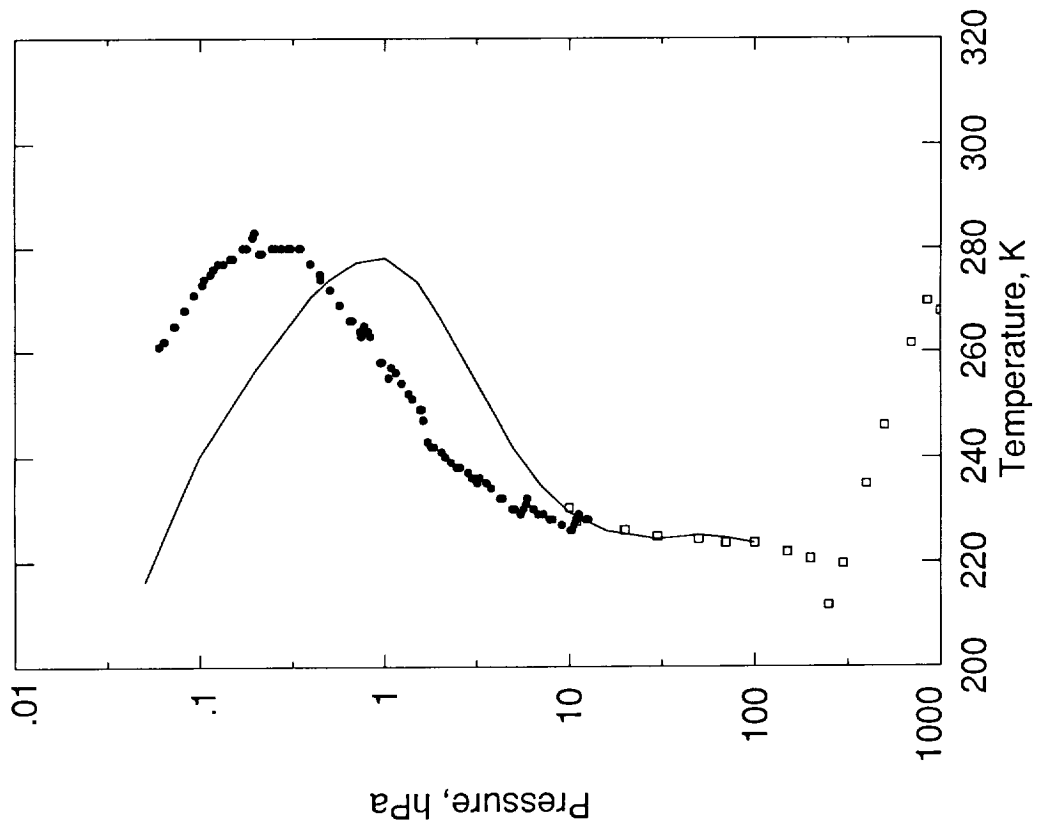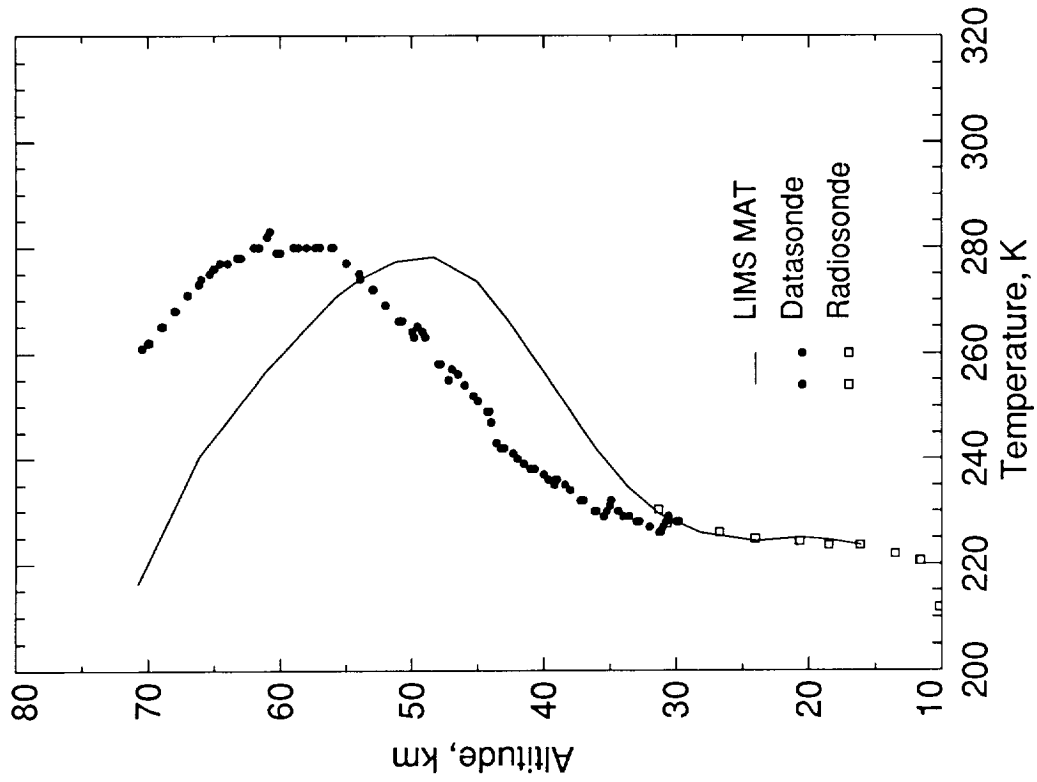
Figure 1. Temperature profile comparisons at Thule (May 7, 1979).
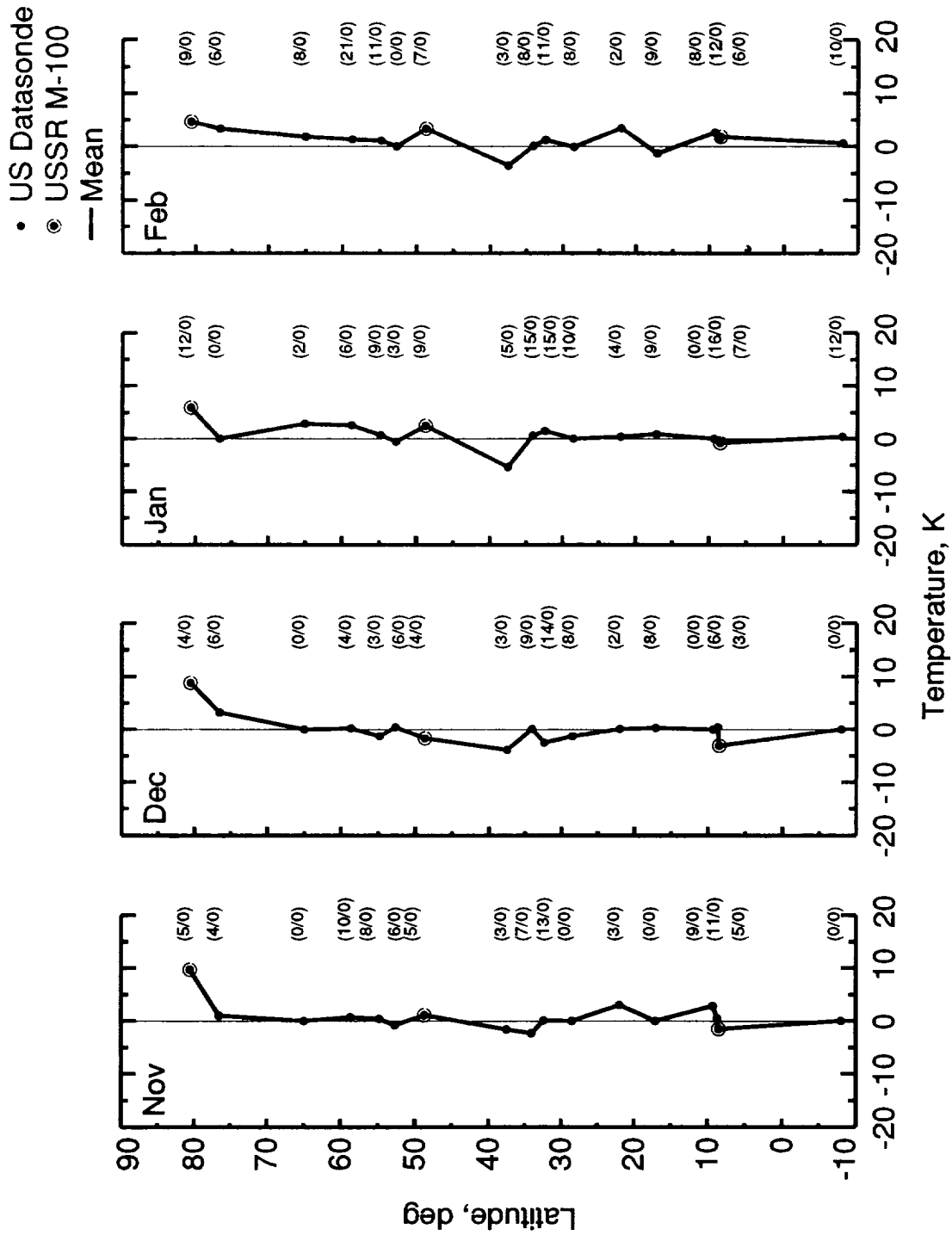
Figure 2. LIMS minus rocketsonde temperature differences by month and station latitude at 10 hPa. Horizontal bars in last panel represent standard deviation about 7-month average difference.
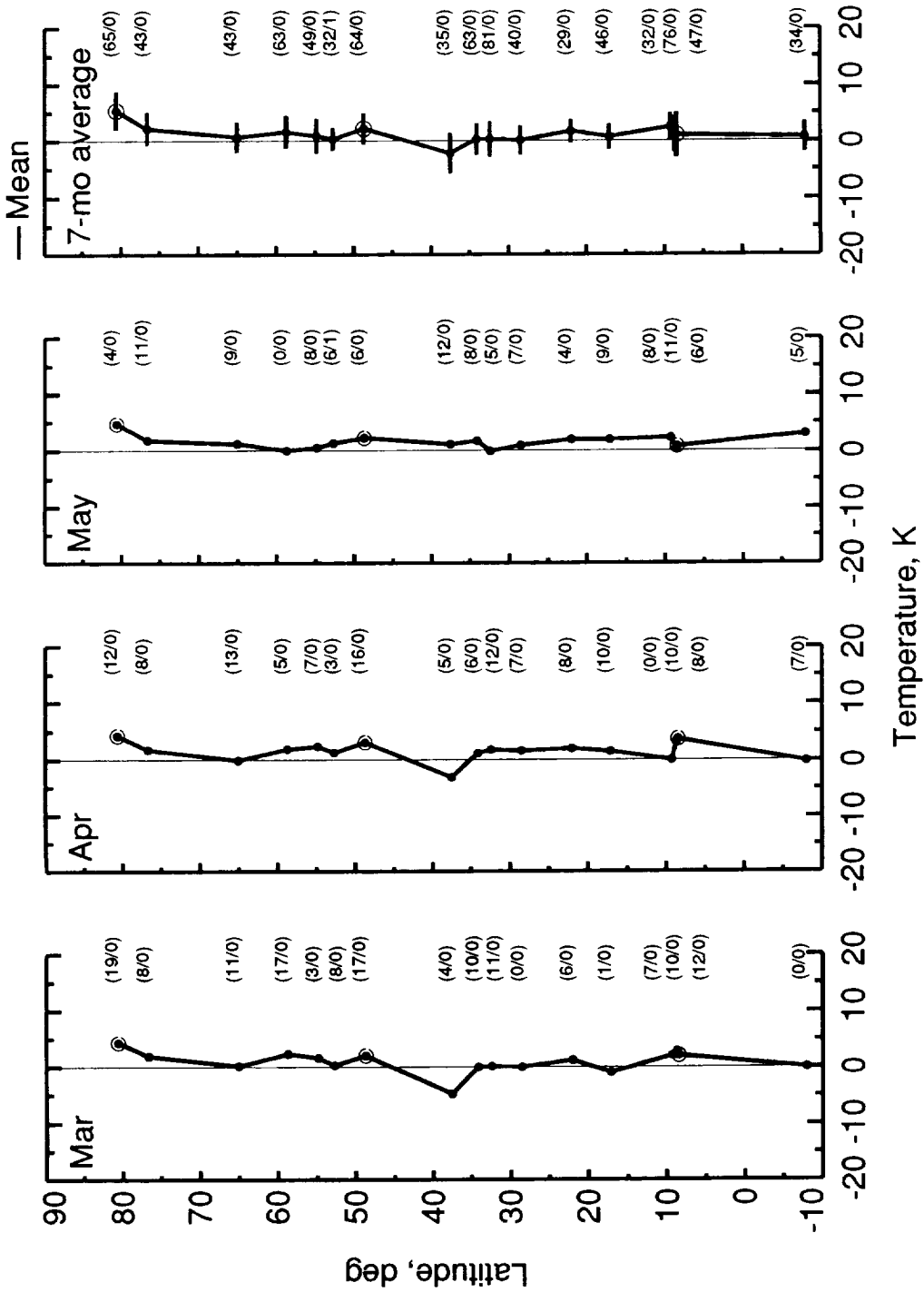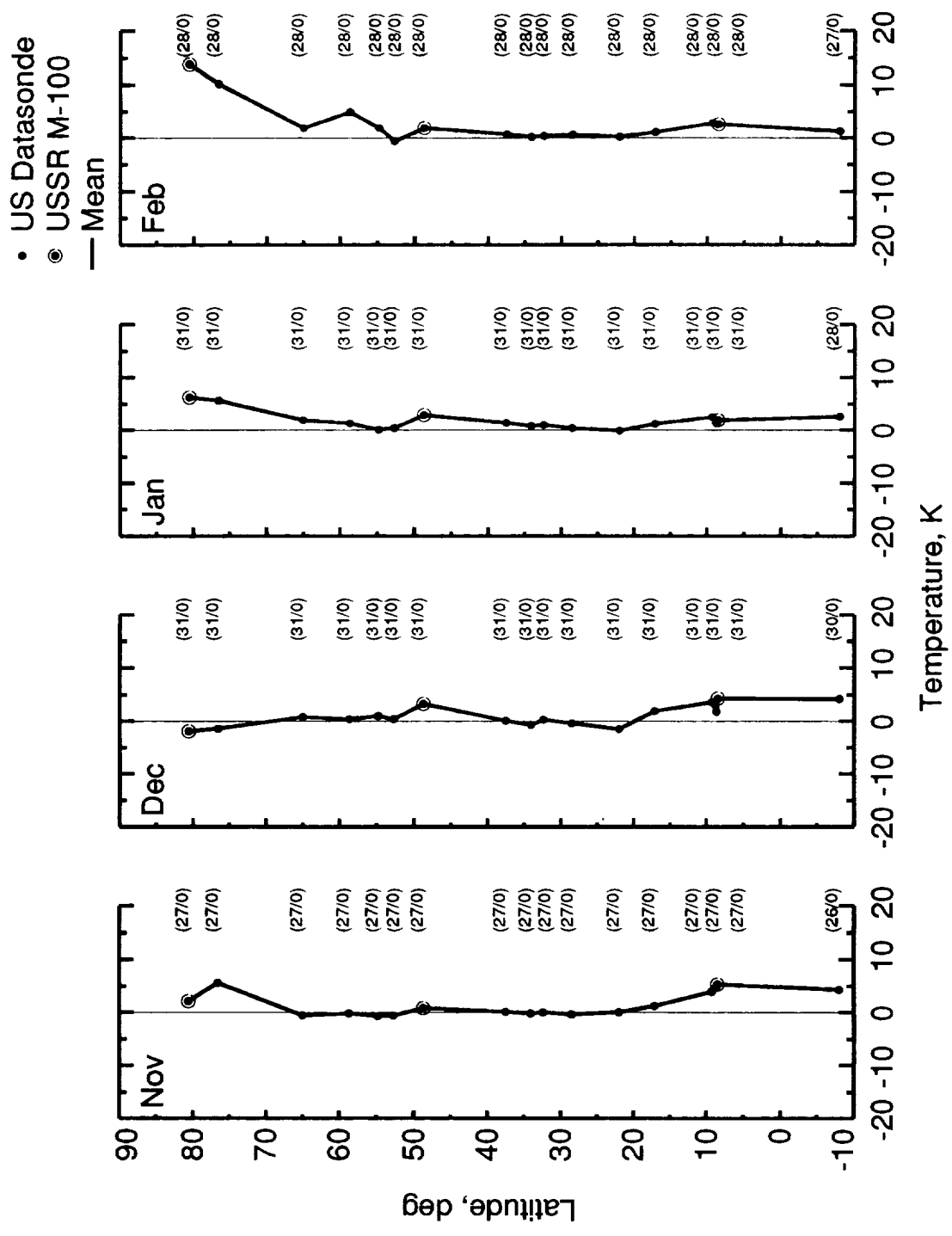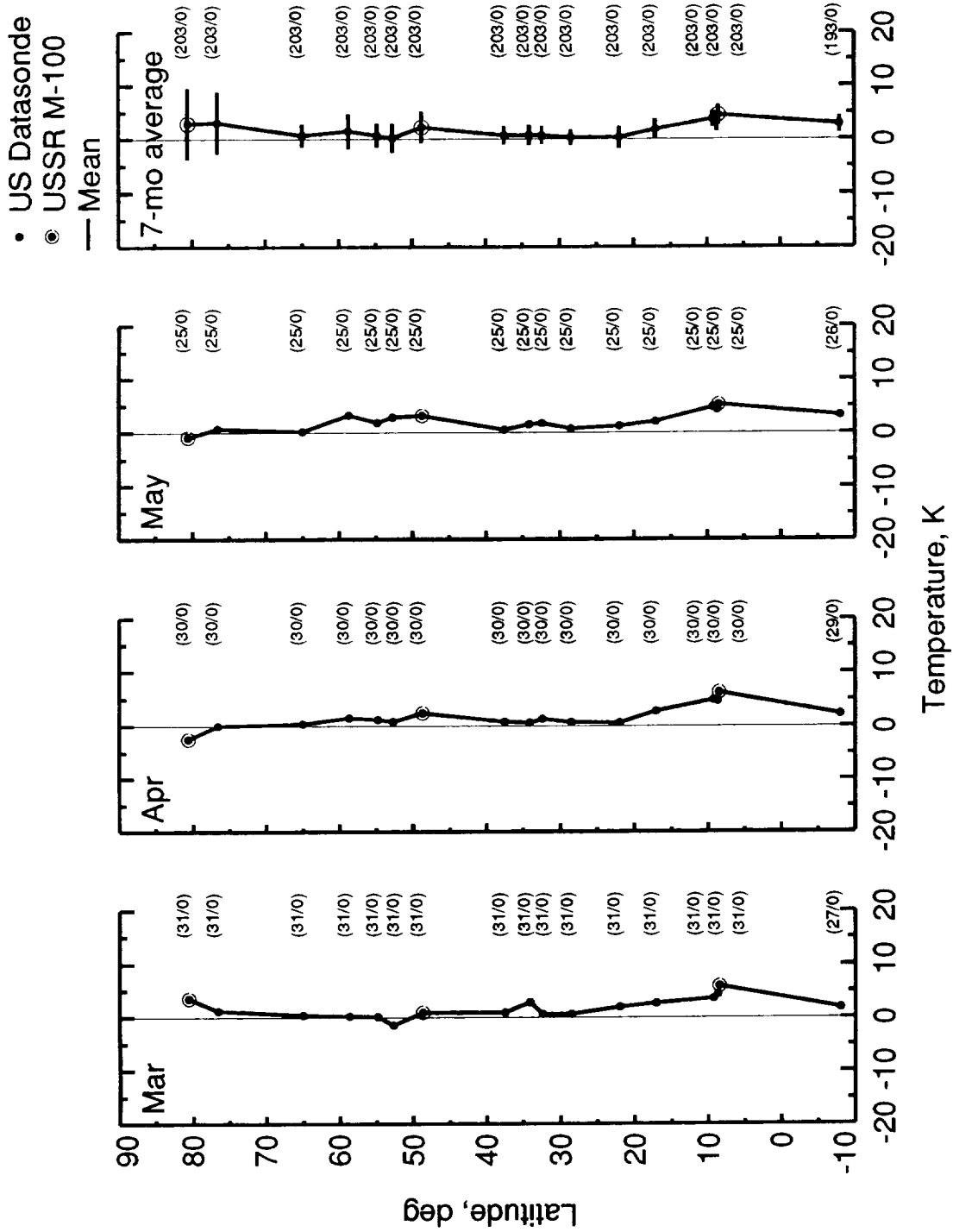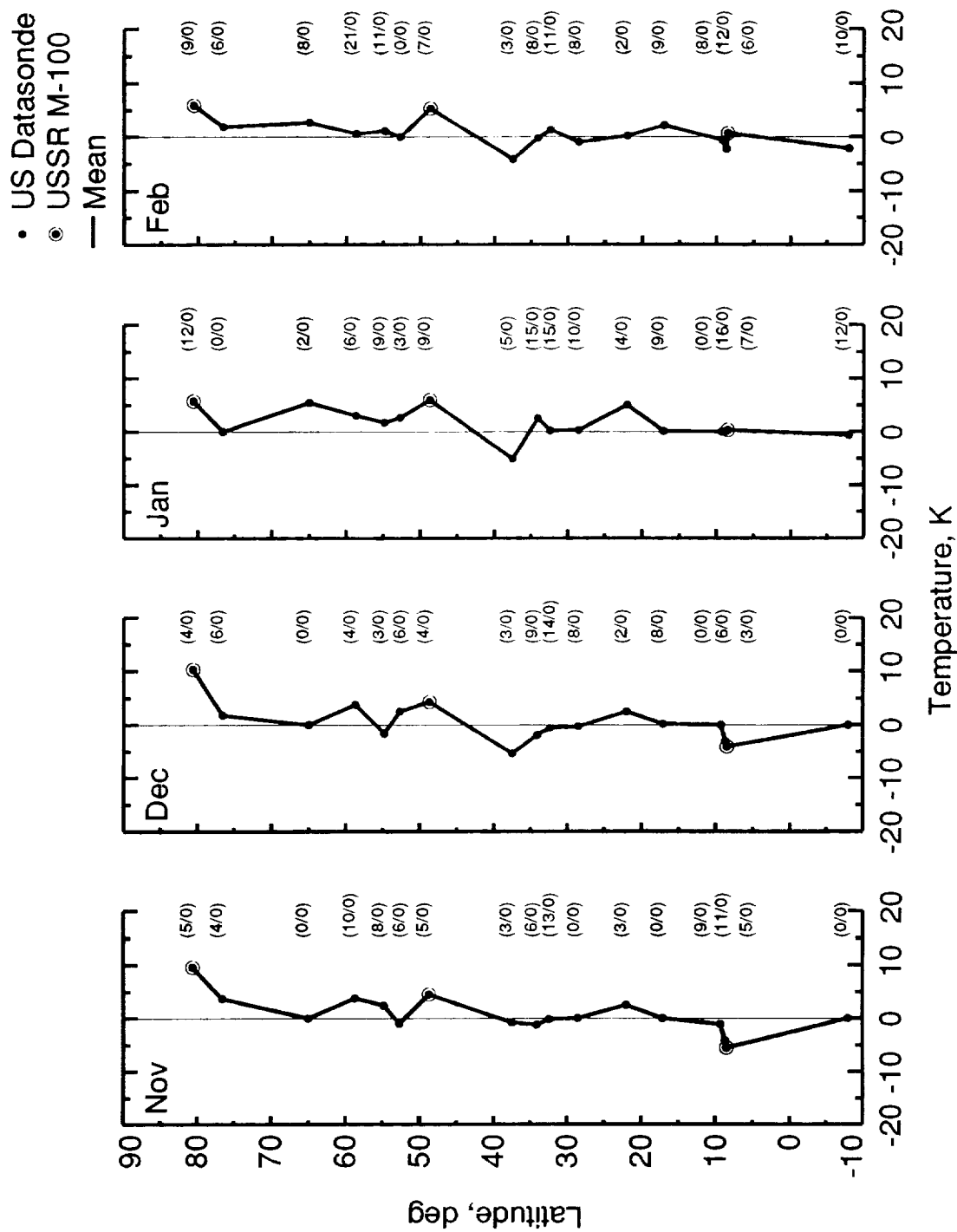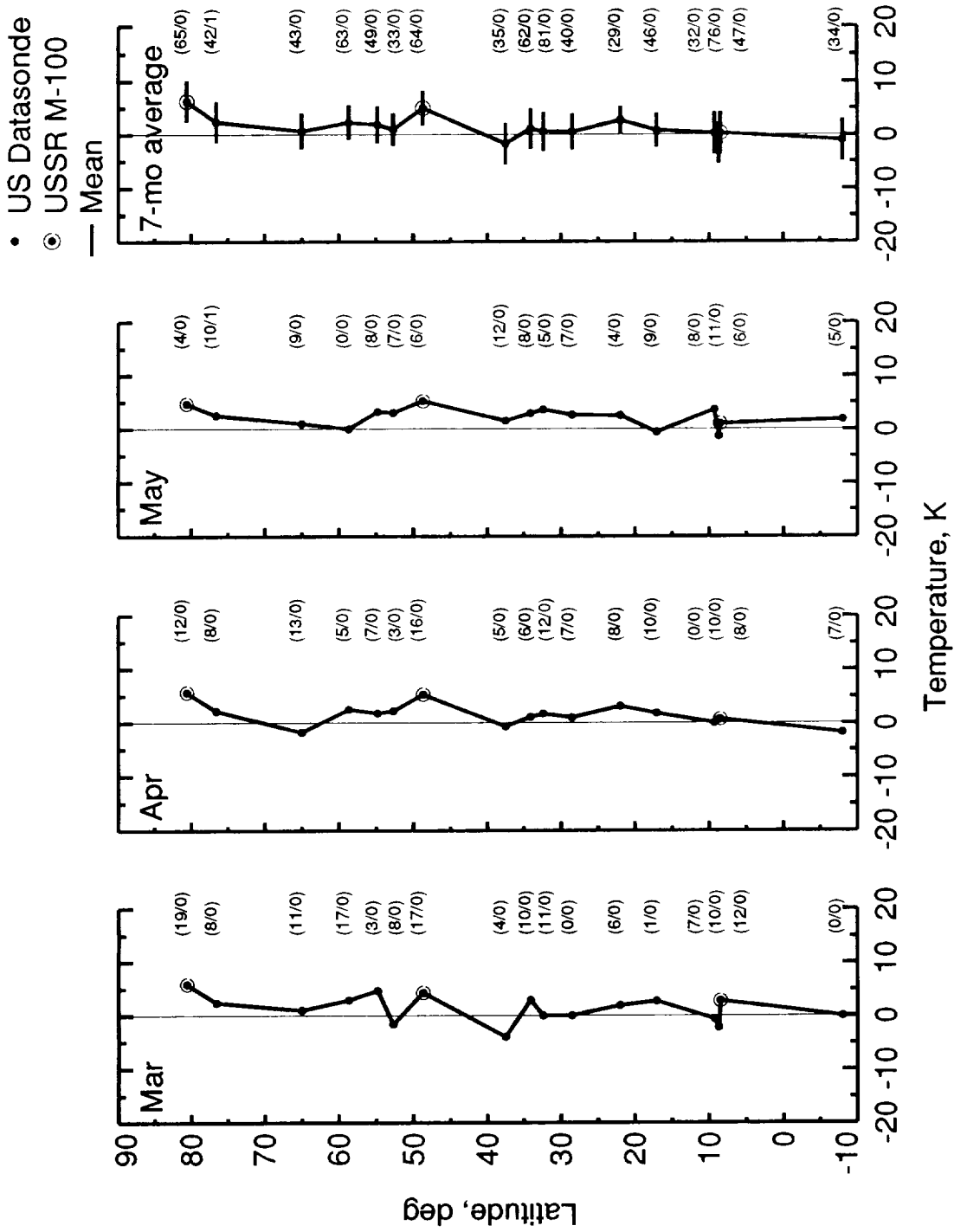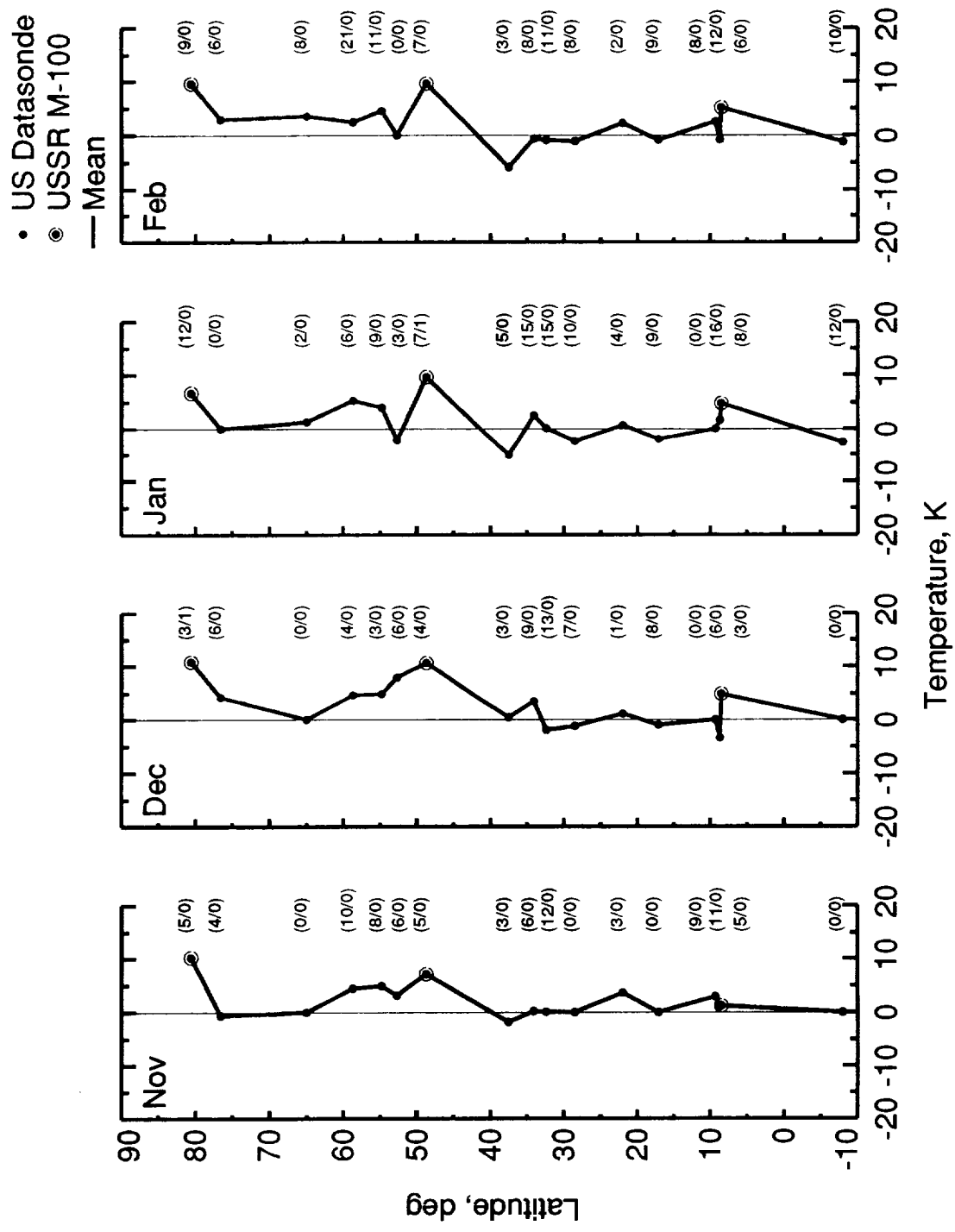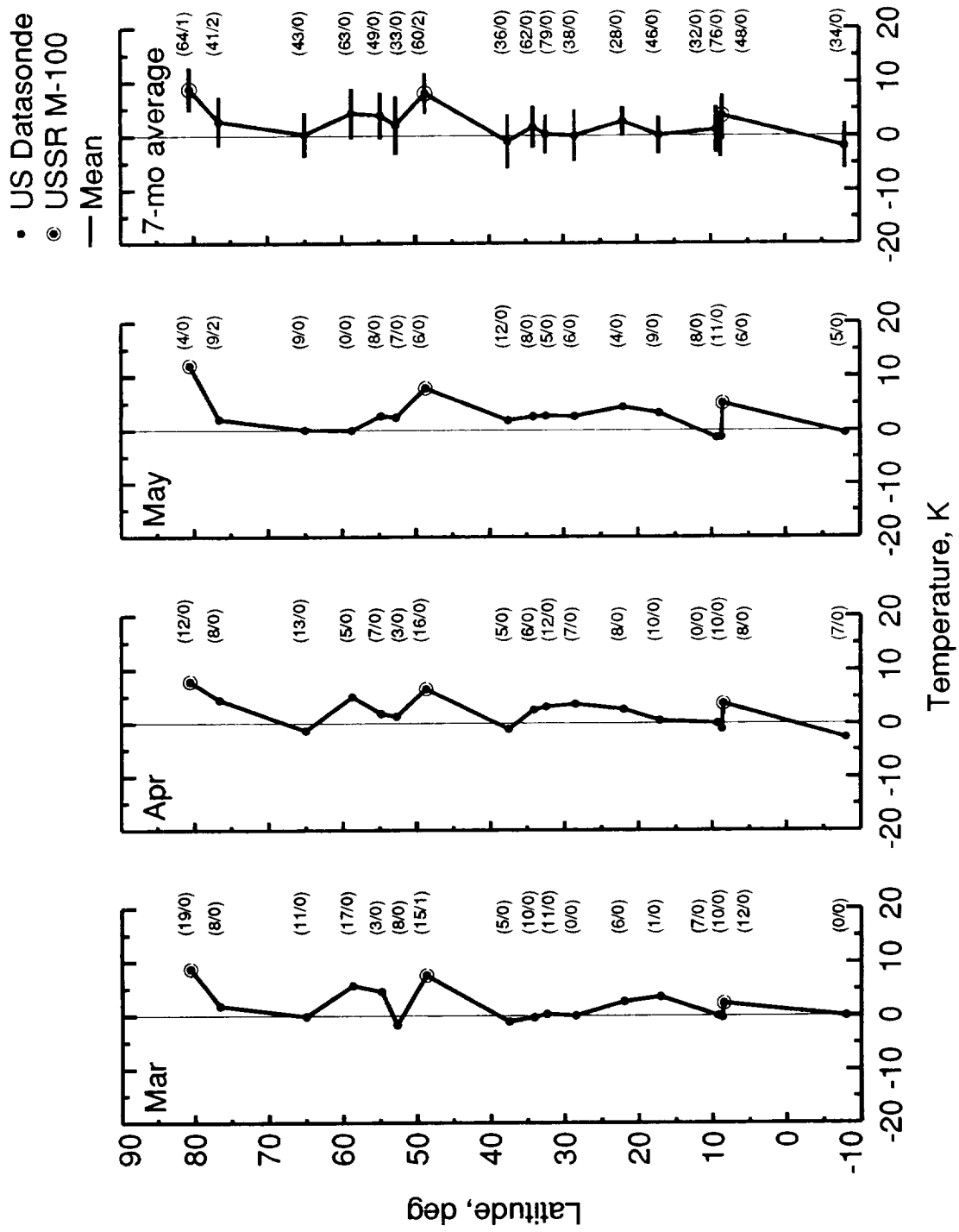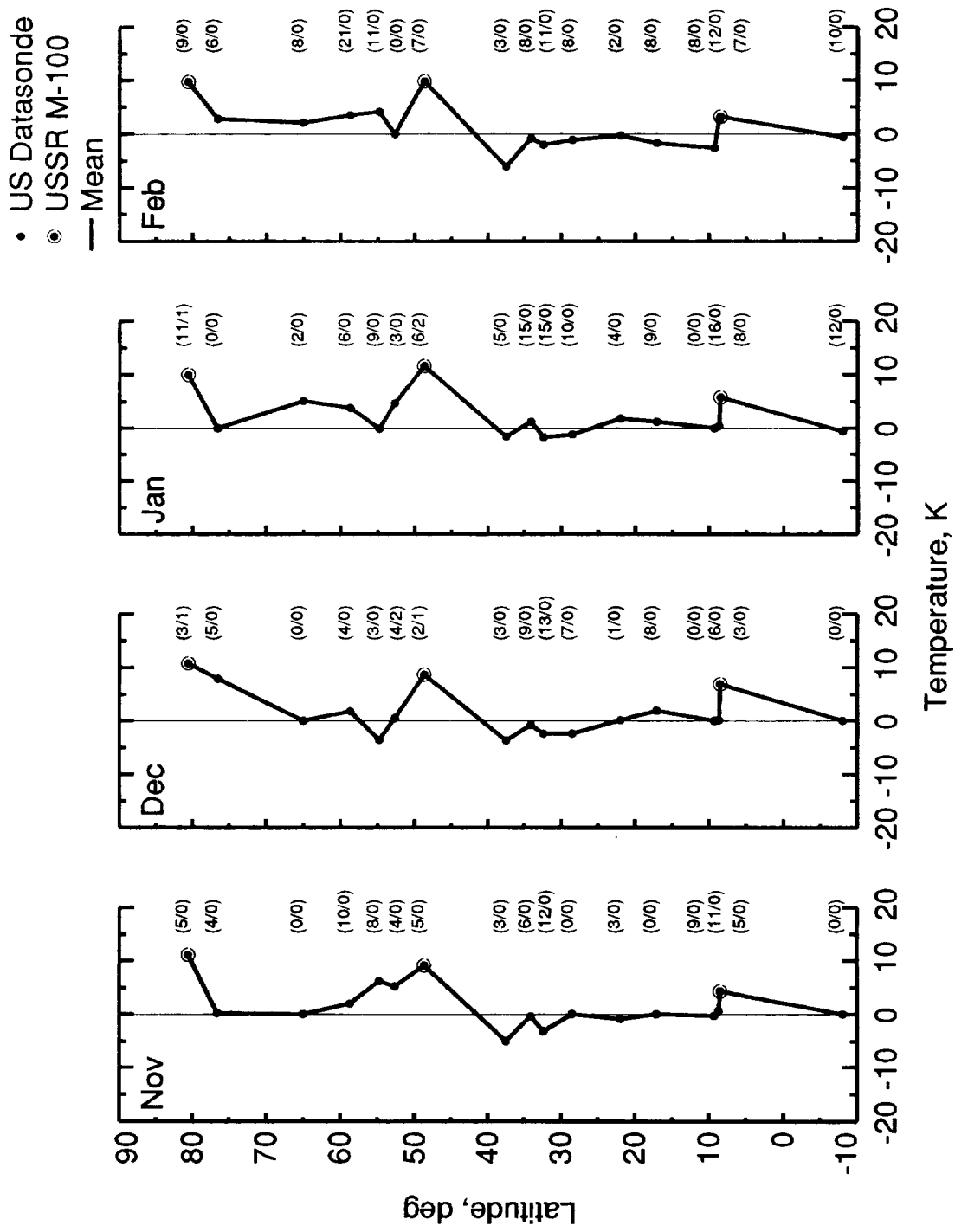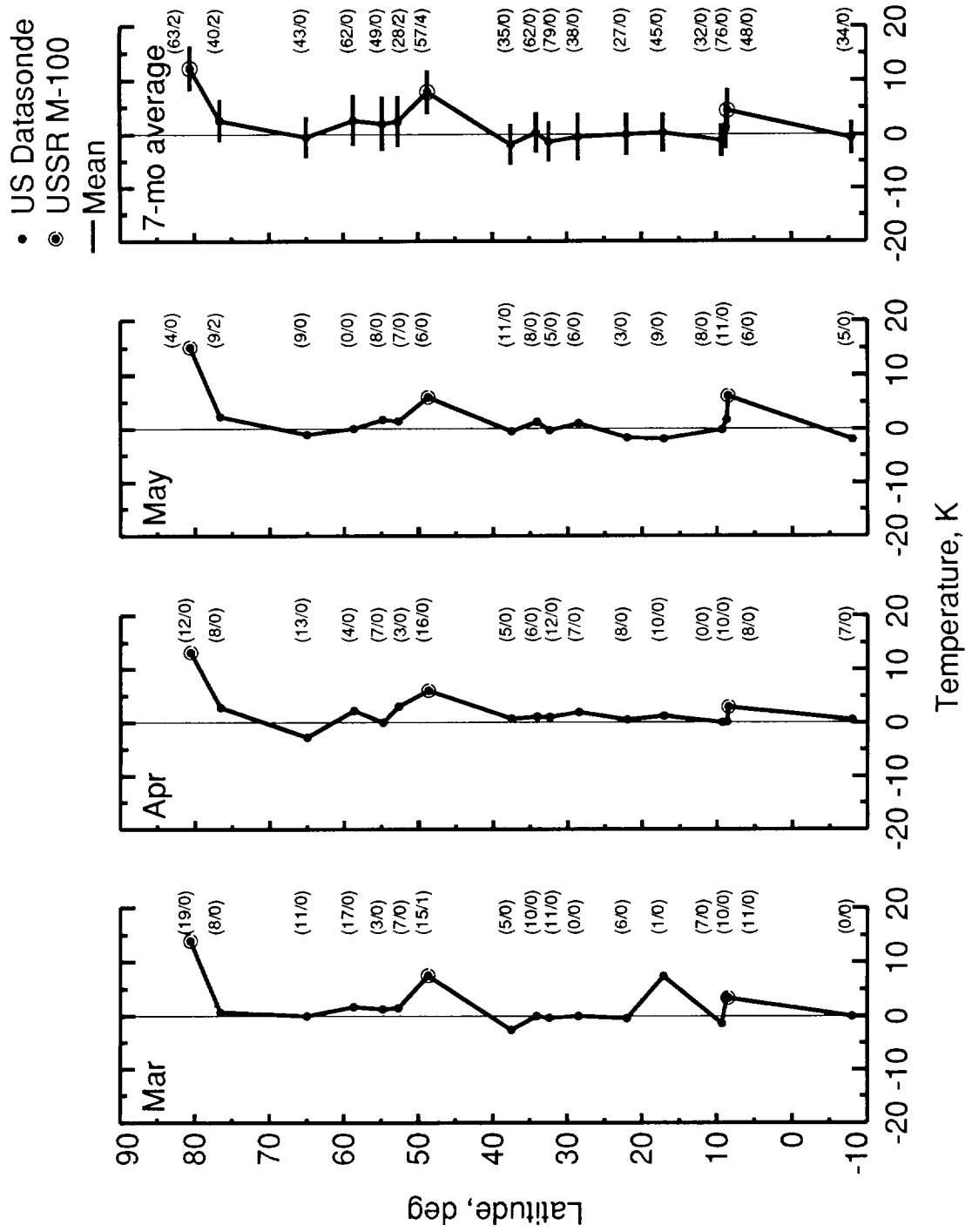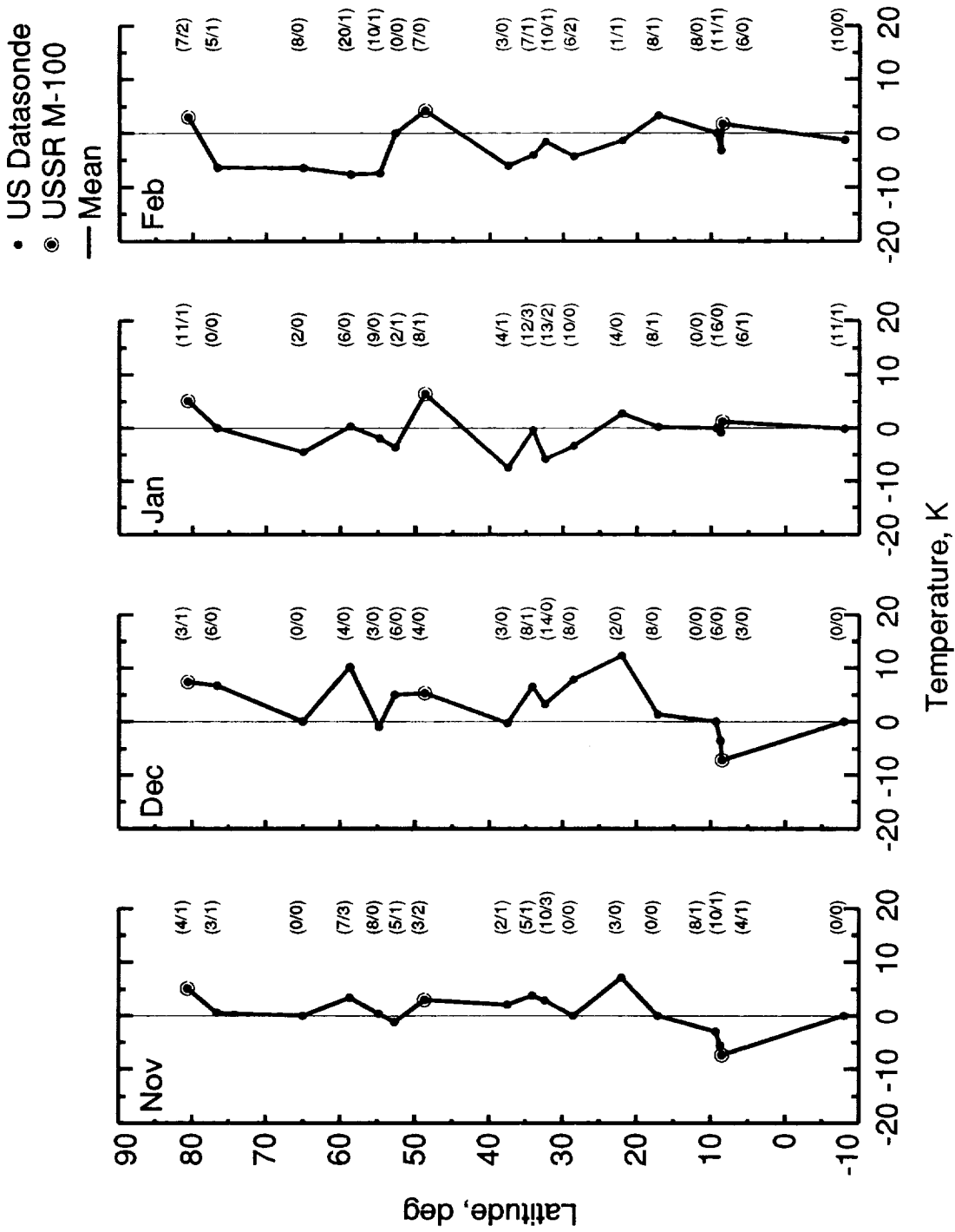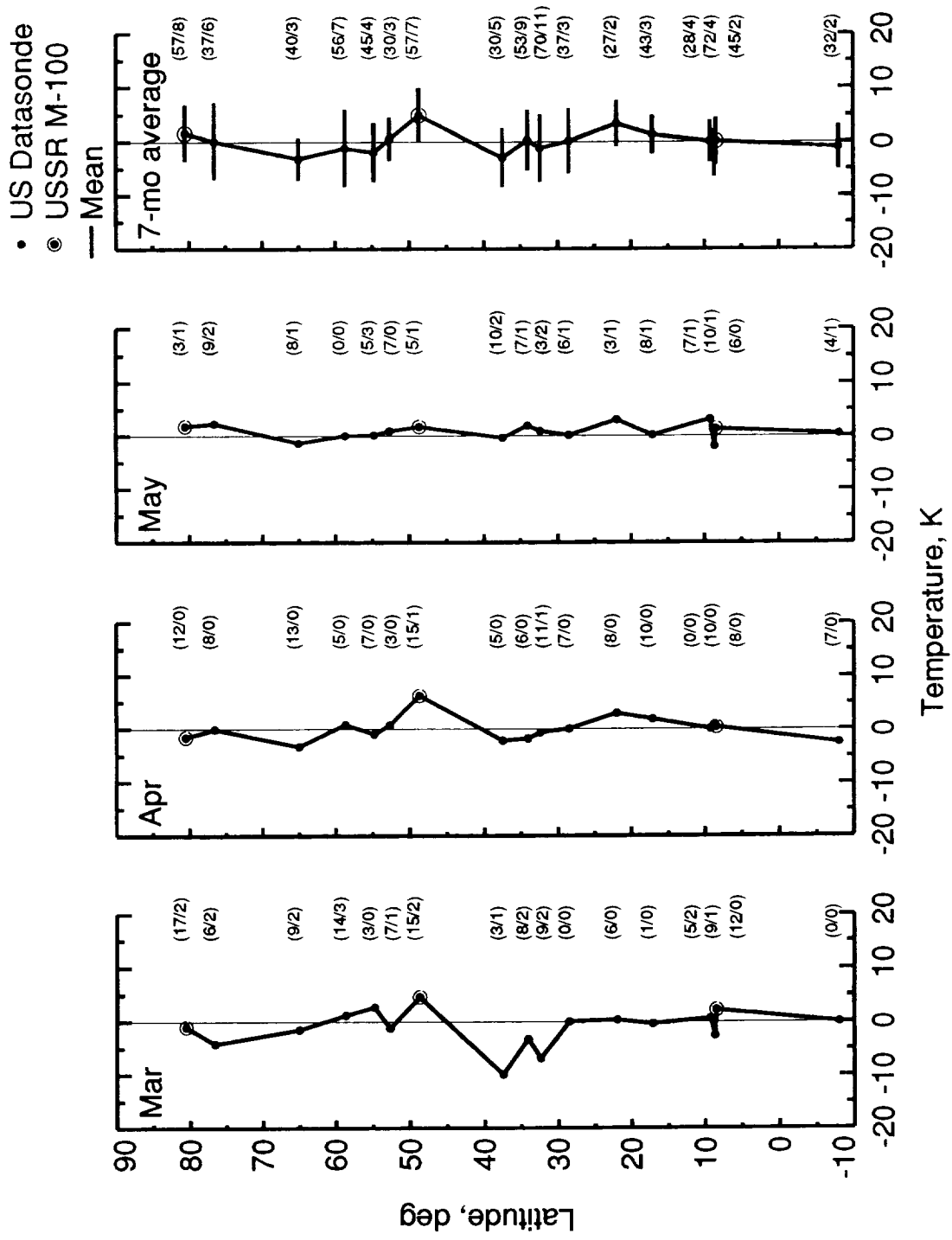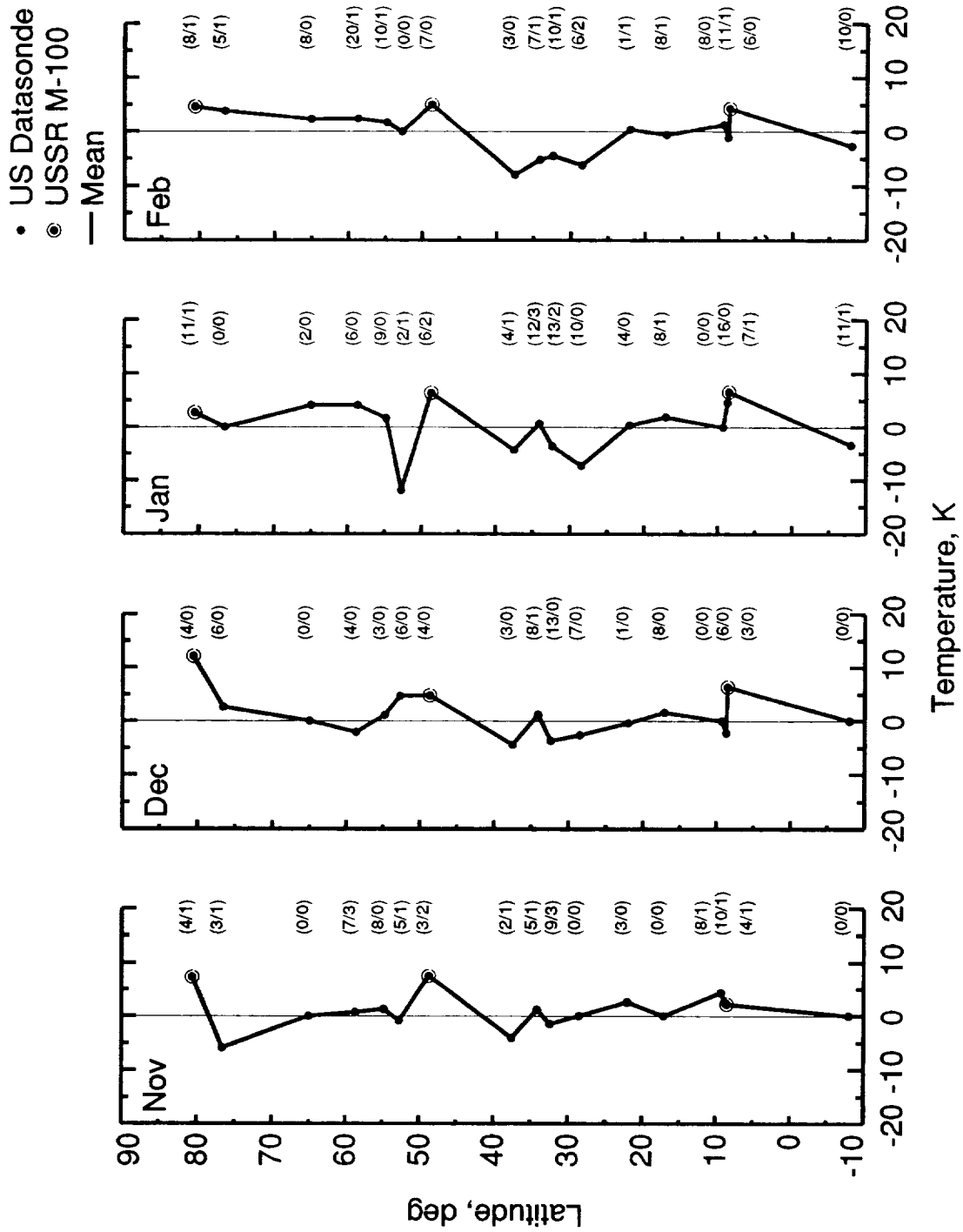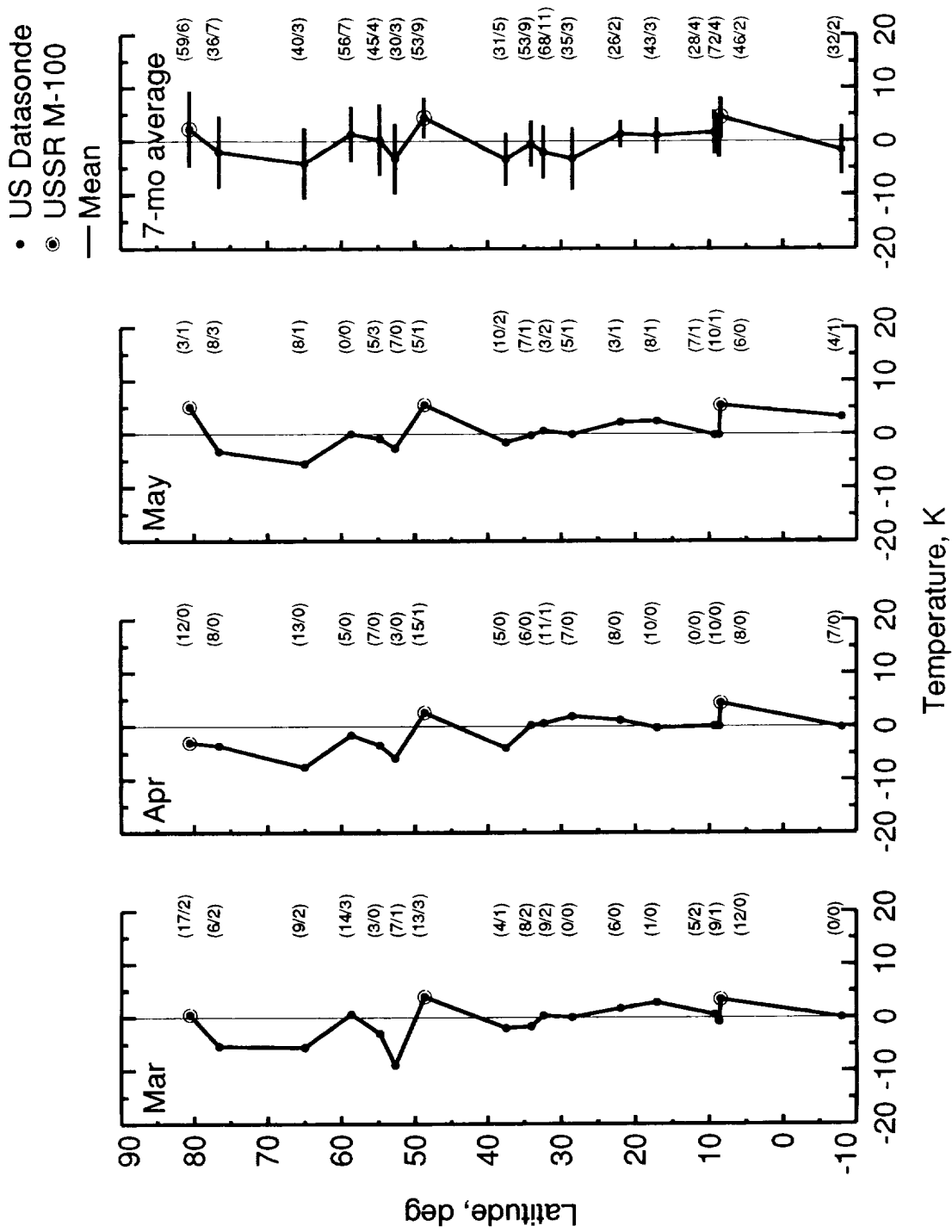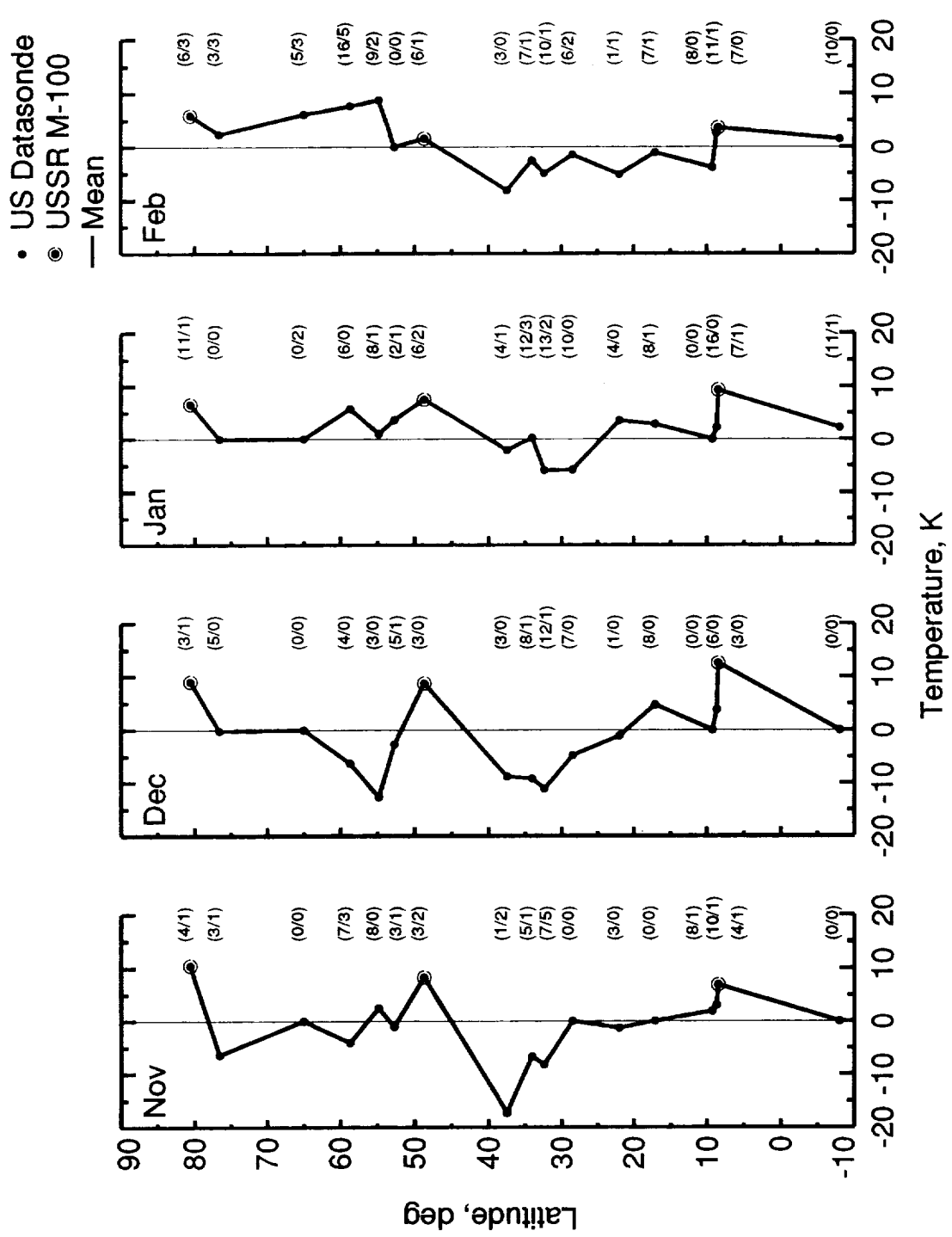
Figure 2. Concluded.

21
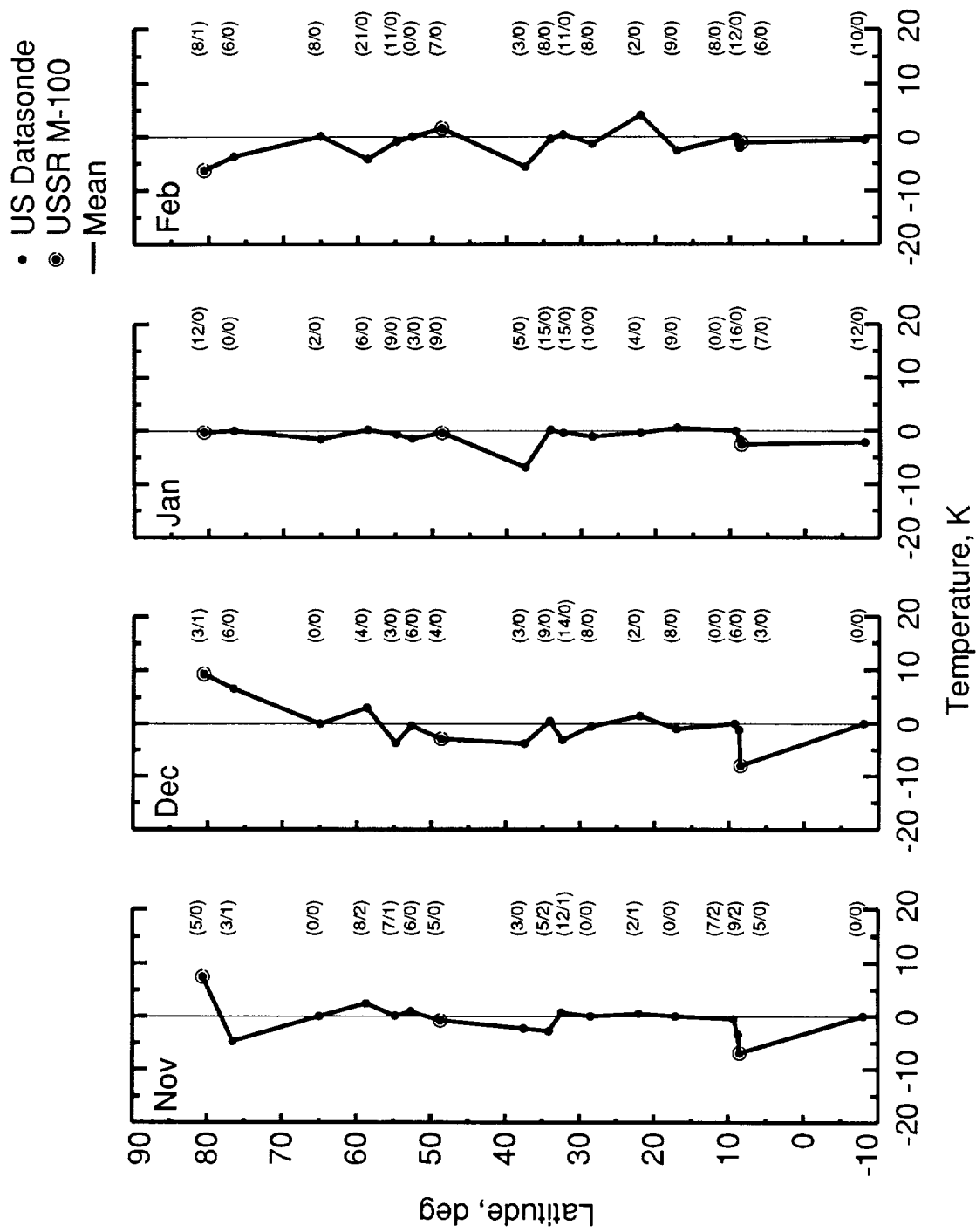
Figure 3. NMC minus rocketsonde temperature differences by month and station latitude at 10 hPa. Horizontal bars in last panel represent standard deviation about 7-month average difference.
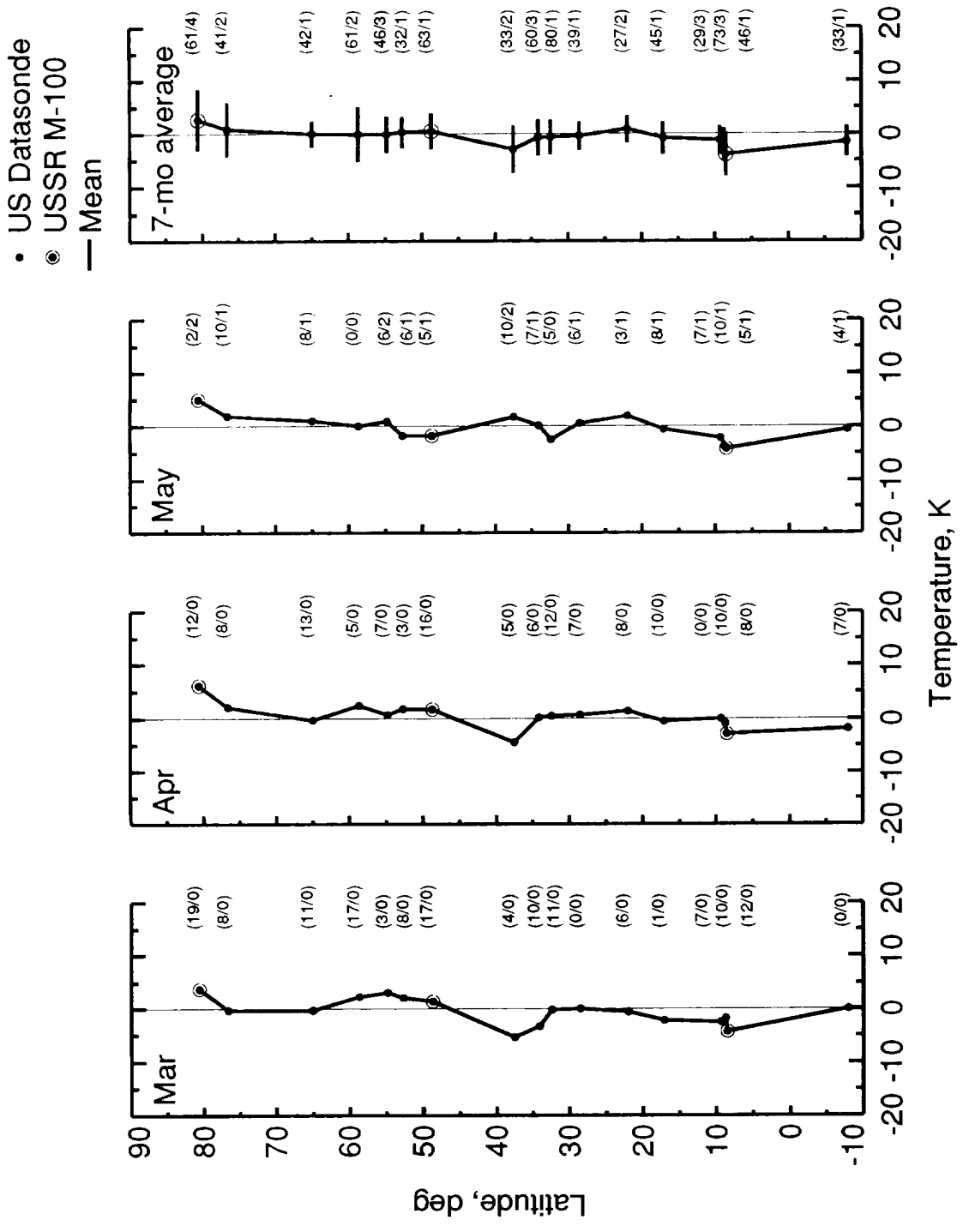
Figure 3. Concluded.

23

Figure 4. LIMS minus NMC satellite temperature differences by month and station latitude at 10 hPa. Horizontal bars in last panel represent standard deviation about 7-month average difference.
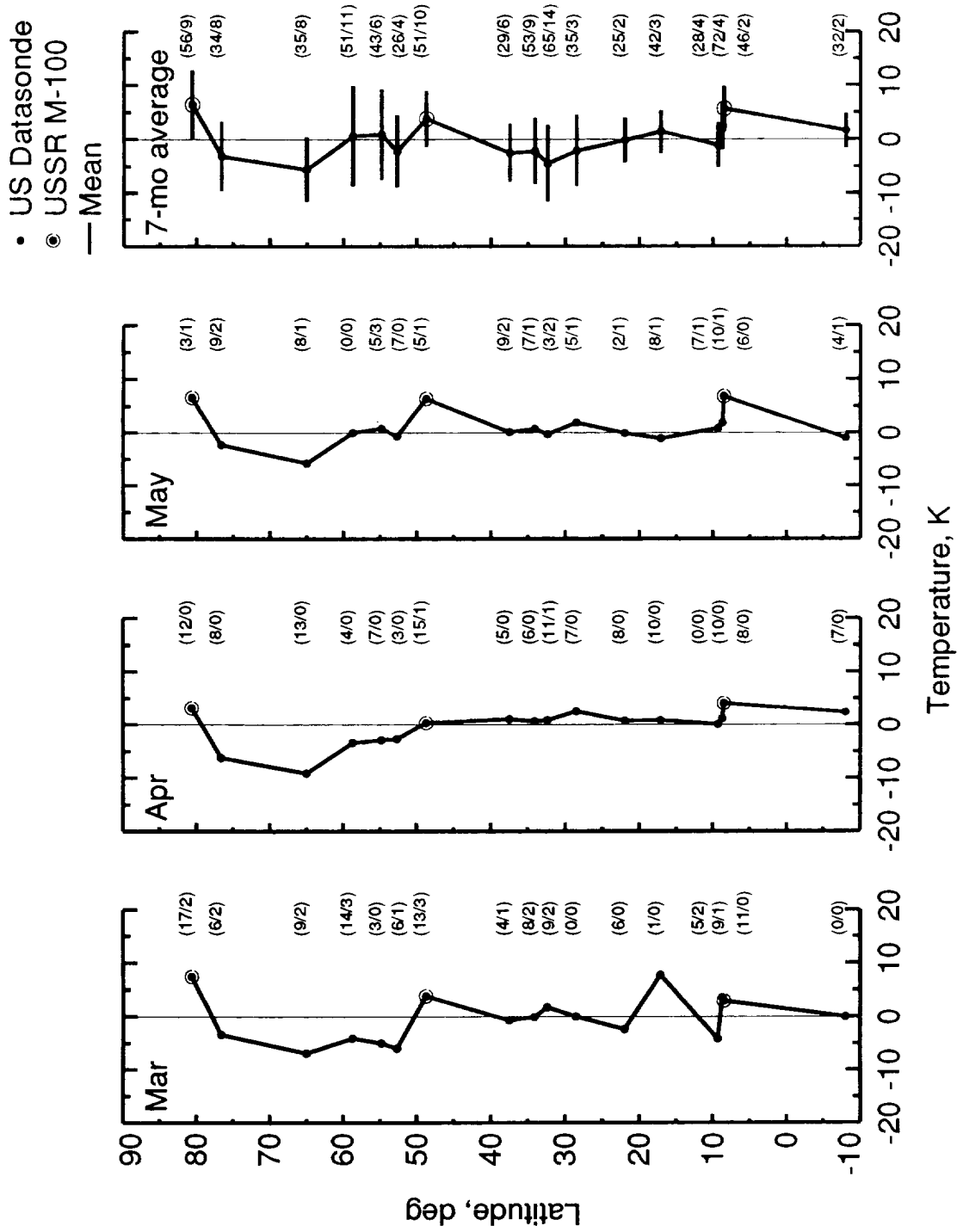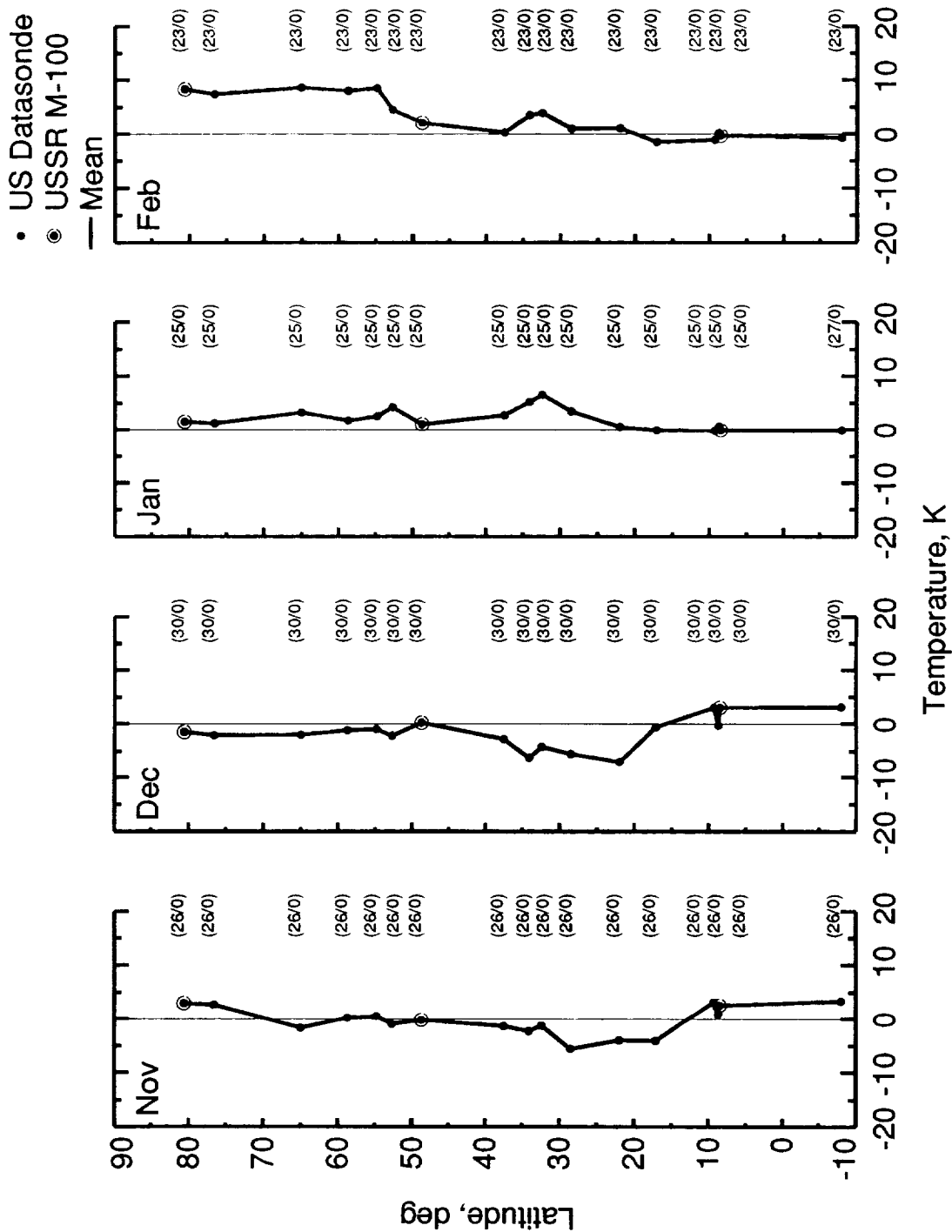
Figure 4. Concluded.

Figure 5. LIMS minus rocketsonde temperature differences by month and station latitude at 5 hPa. Horizontal bars in last panel represent standard deviation about 7-month average difference.

26

Figure 5. Concluded.

27

Figure 6. LIMS minus rocketsonde temperature differences by month and station latitude at 2 hPa. Horizontal bars in last panel represent standard deviation about 7-month average difference.

Figure 6. Concluded.

29

Figure 7. LIMS minus rocketsonde temperature differences by month and station latitude at 1 hPa. Horizontal bars in last panel represent standard deviation about 7-month average difference.
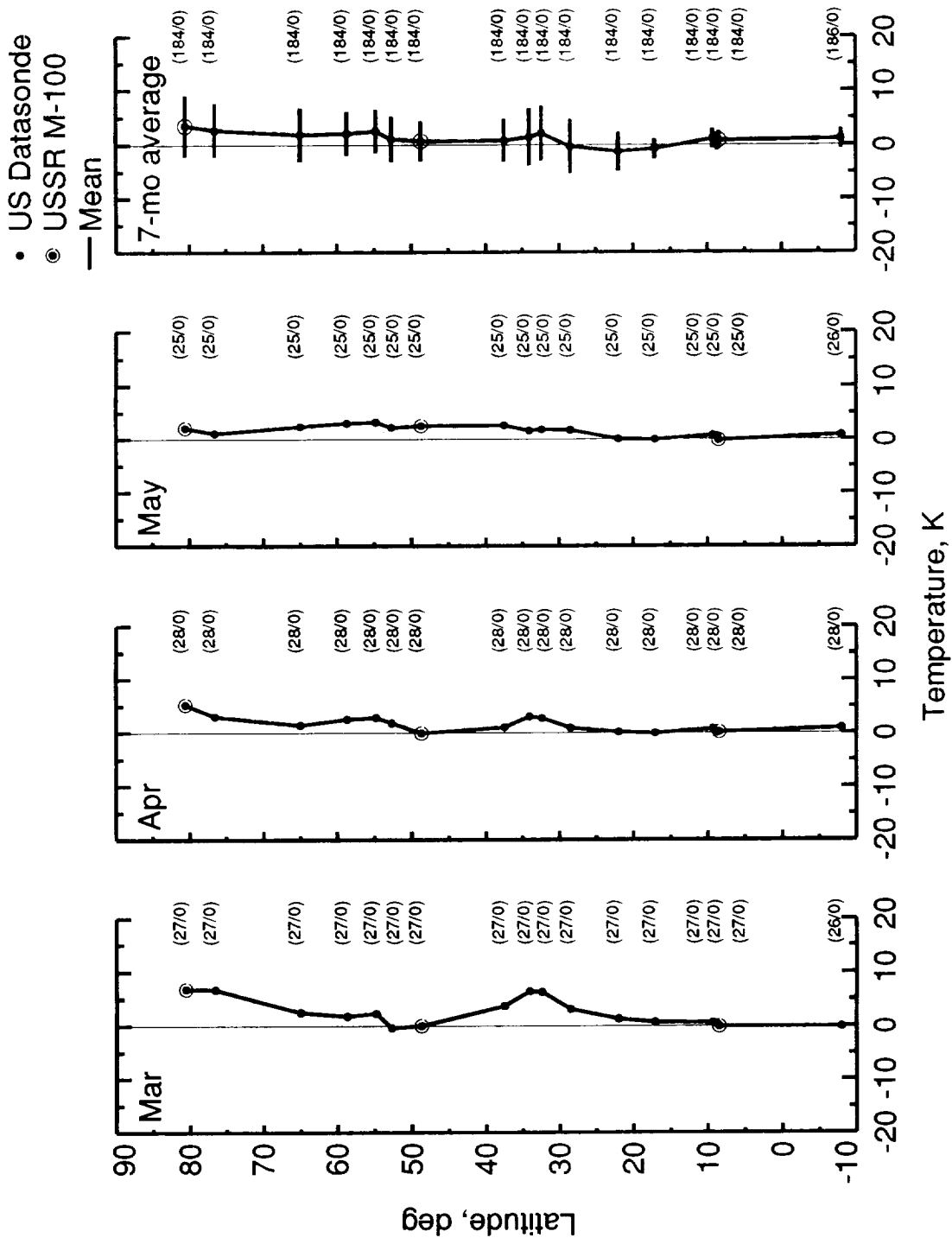
Figure 7. Concluded.

31

Figure 8. NMC minus rocketsonde temperature differences by month and station latitude at 5 hPa. Horizontal bars in last panel represent standard deviation about 7-month average difference.
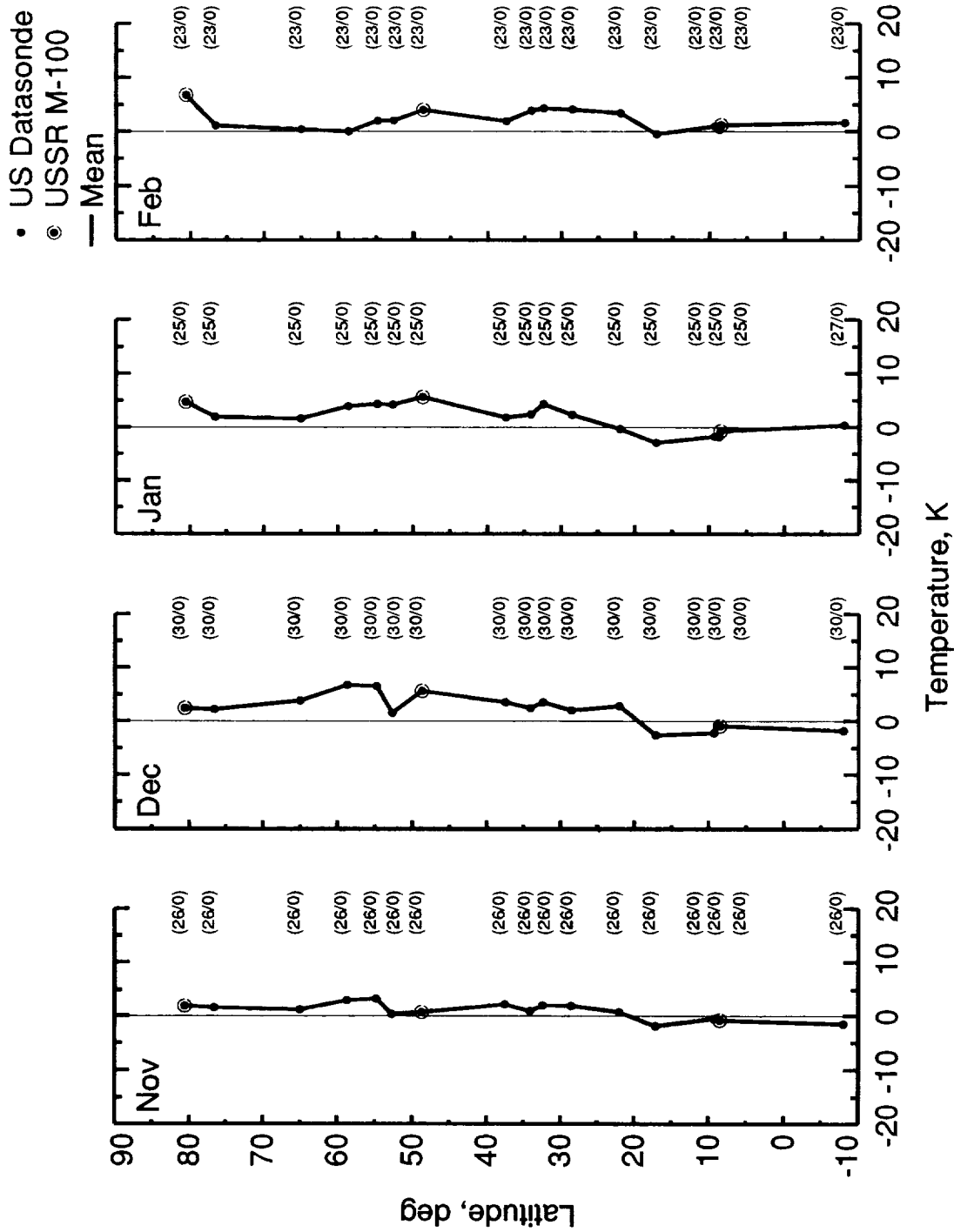
32

Figure 8. Concluded.

33

Figure 9. NMC minus rocketsonde temperature differences by month and station latitude at 2 hPa. Horizontal bars in last panel represent standard deviation about 7-month average difference.
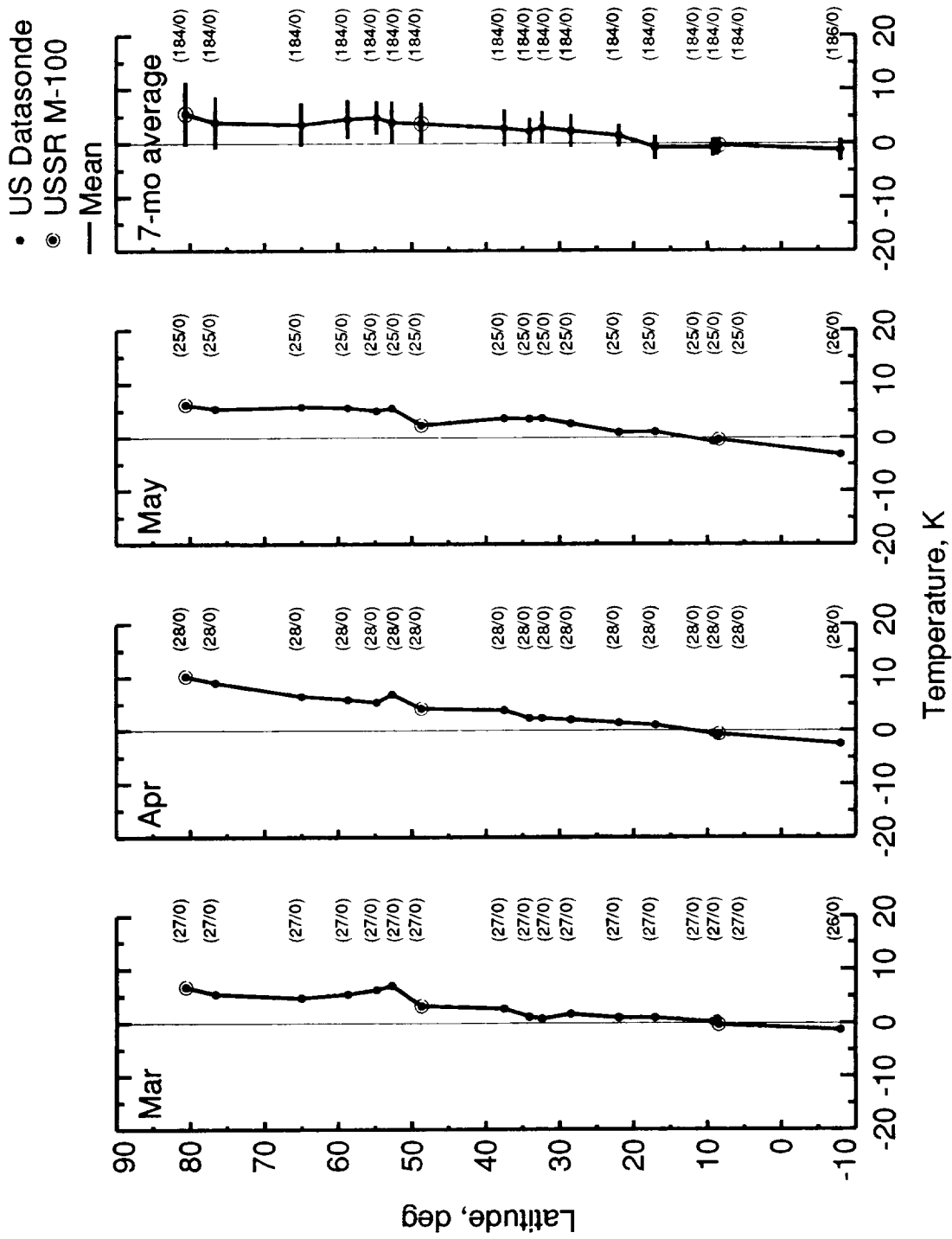
34

Figure 9. Concluded.

35

Figure 10. NMC minus rocketsonde temperature differences by month and station latitude at 1 hPa. Horizontal bars in last panel represent standard deviation about 7-month average difference.

Figure 10. Concluded.

Temperature, K

Latitude, deg

- US Datasonde
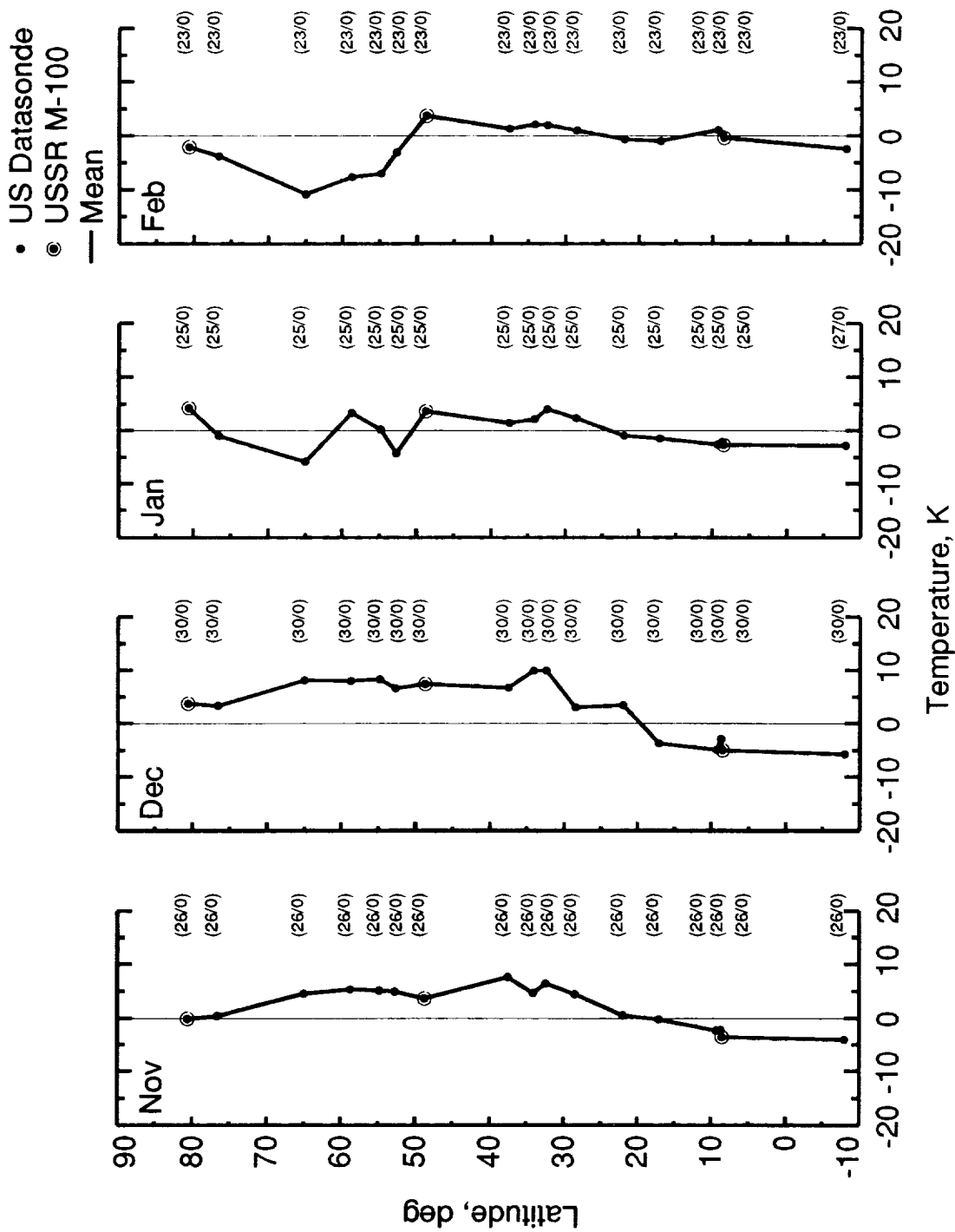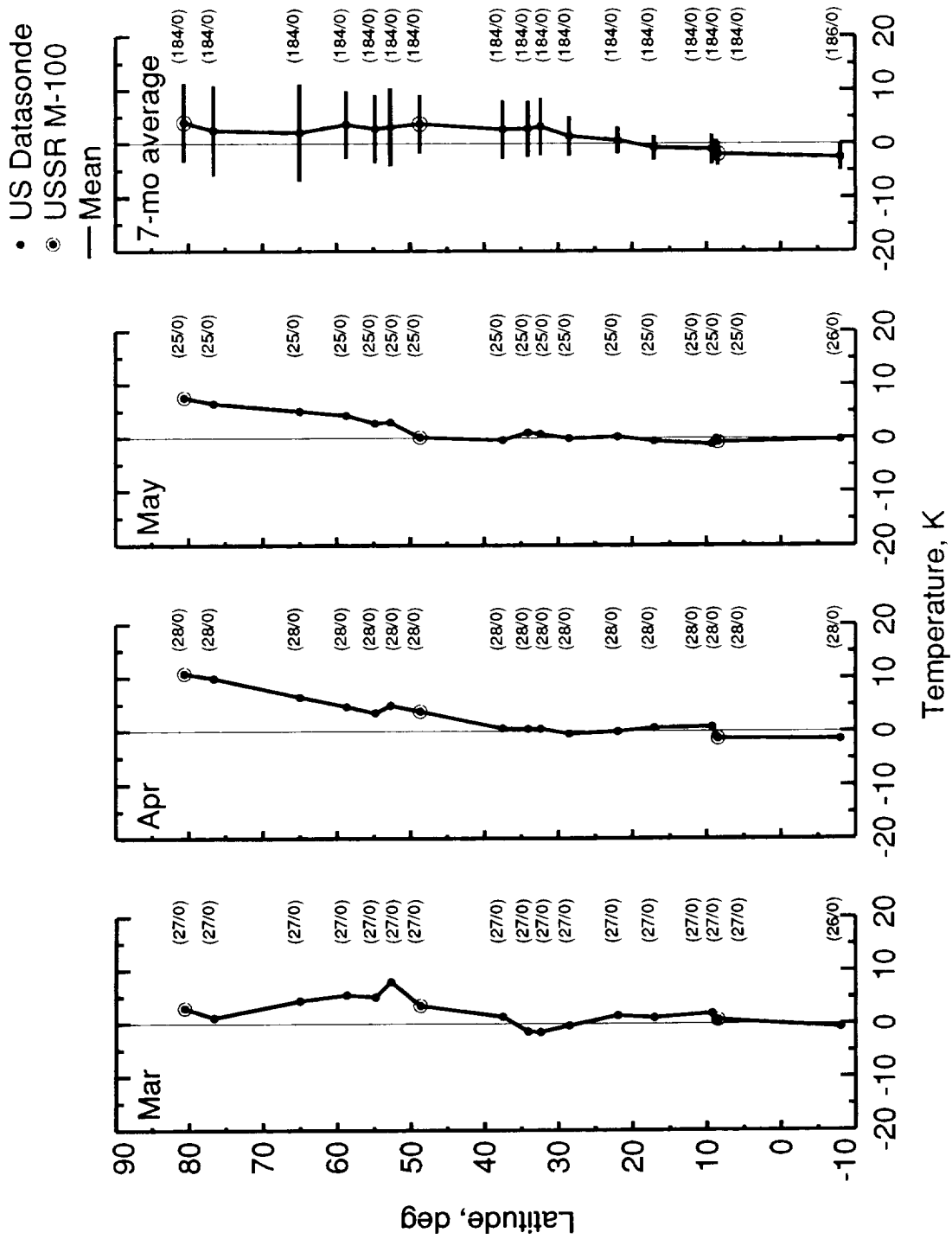⊚ USSR M-100
— Mean

7-mo average

Mar

Apr

May

Figure 11. LIMS minus NMC satellite temperature differences by month and station latitude at 5 hPa. Horizontal bars in last panel represent standard deviation about 7-month average difference.

Figure 11. Concluded.

39

Figure 12. LIMS minus NMC satellite temperature differences by month and station latitude at 2 hPa. Horizontal bars in last panel represent standard deviation about 7-month average difference.

Figure 12. Concluded.

41

Figure 13. LIMS minus NMC satellite temperature differences by month and station latitude at 1 hPa. Horizontal bars in last panel represent standard deviation about 7-month average difference.
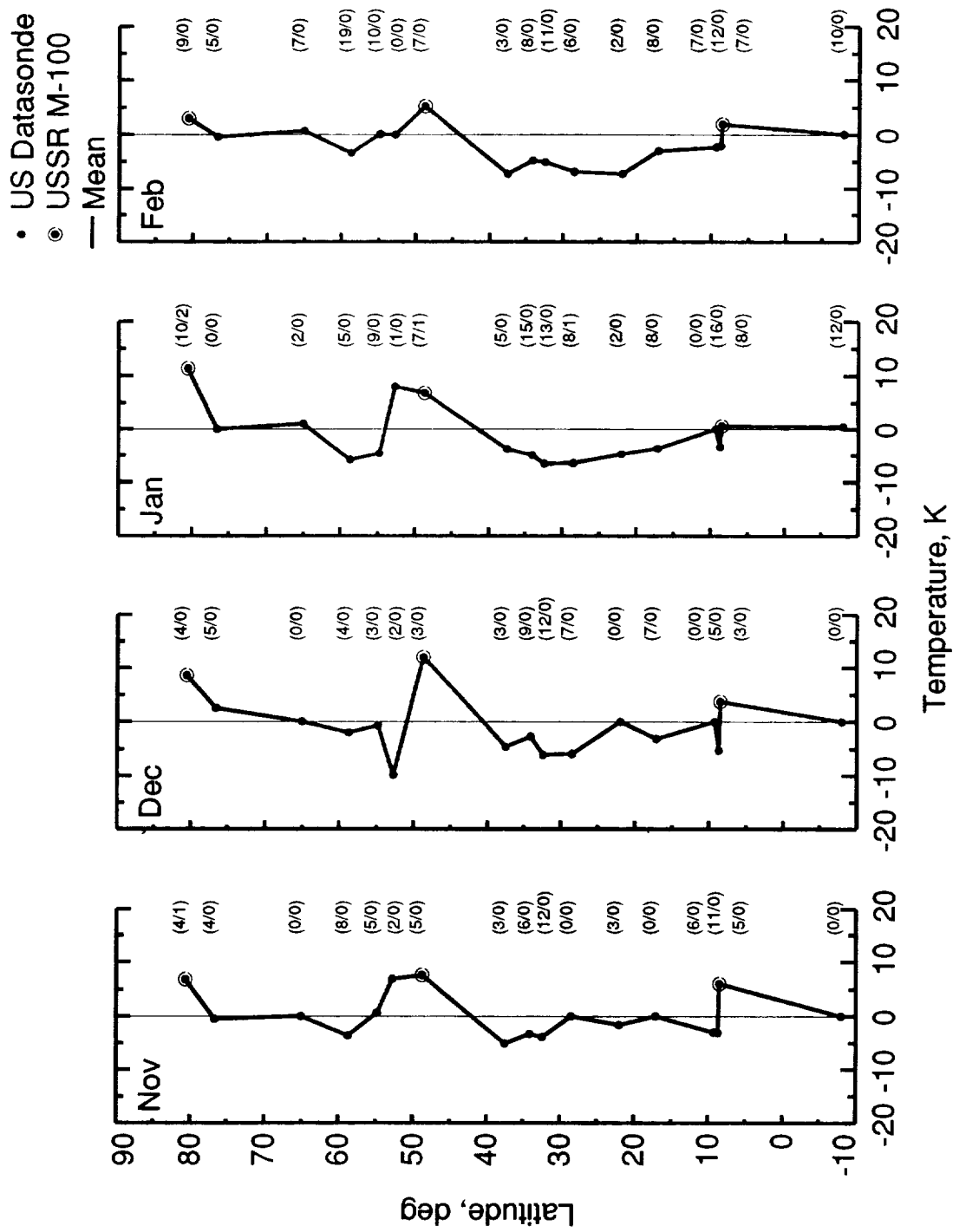
42

Figure 13. Concluded.

43

Figure 14. LIMS minus rocketsonde temperature differences by month and station latitude at 0.4 hPa. Horizontal bars in last panel represent standard deviation about 7-month average difference.
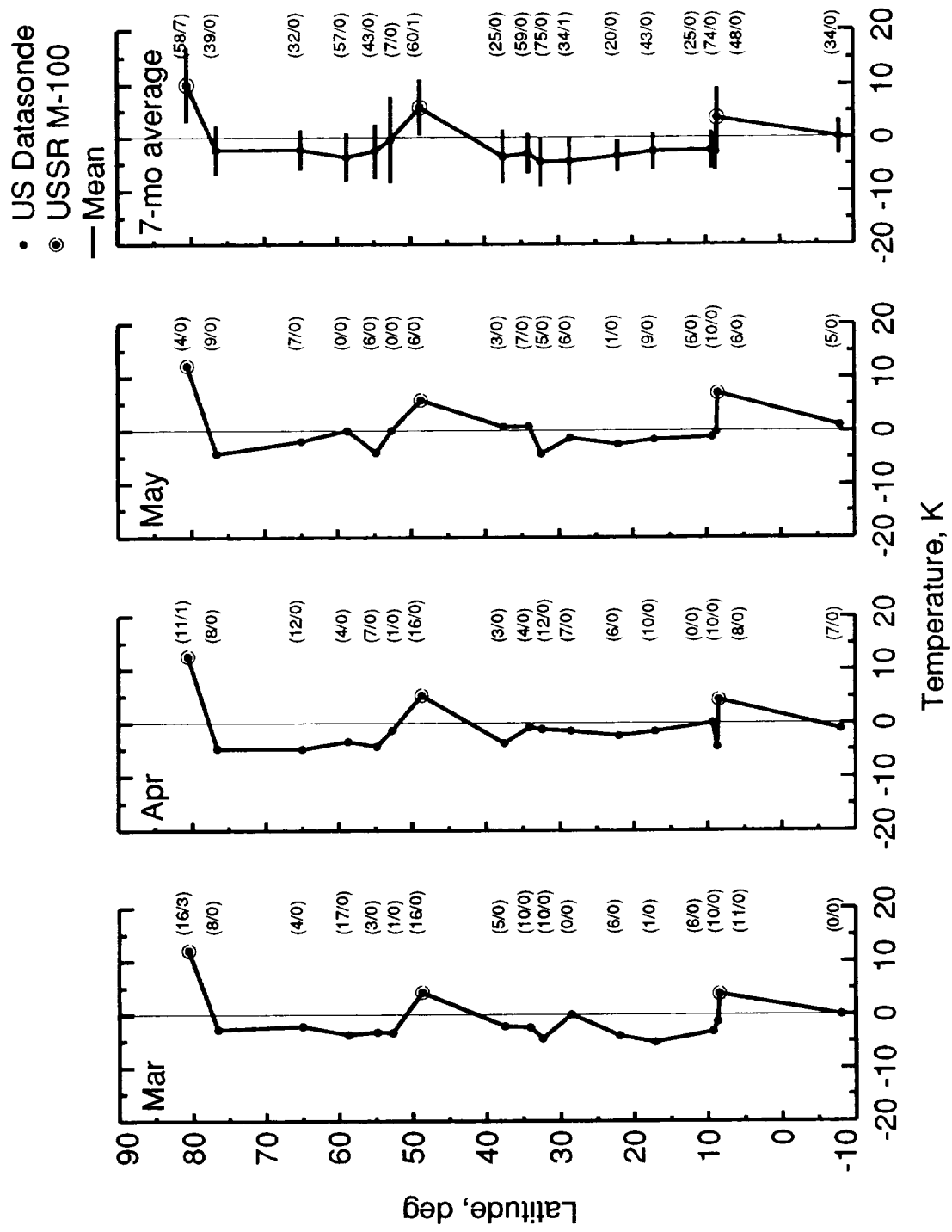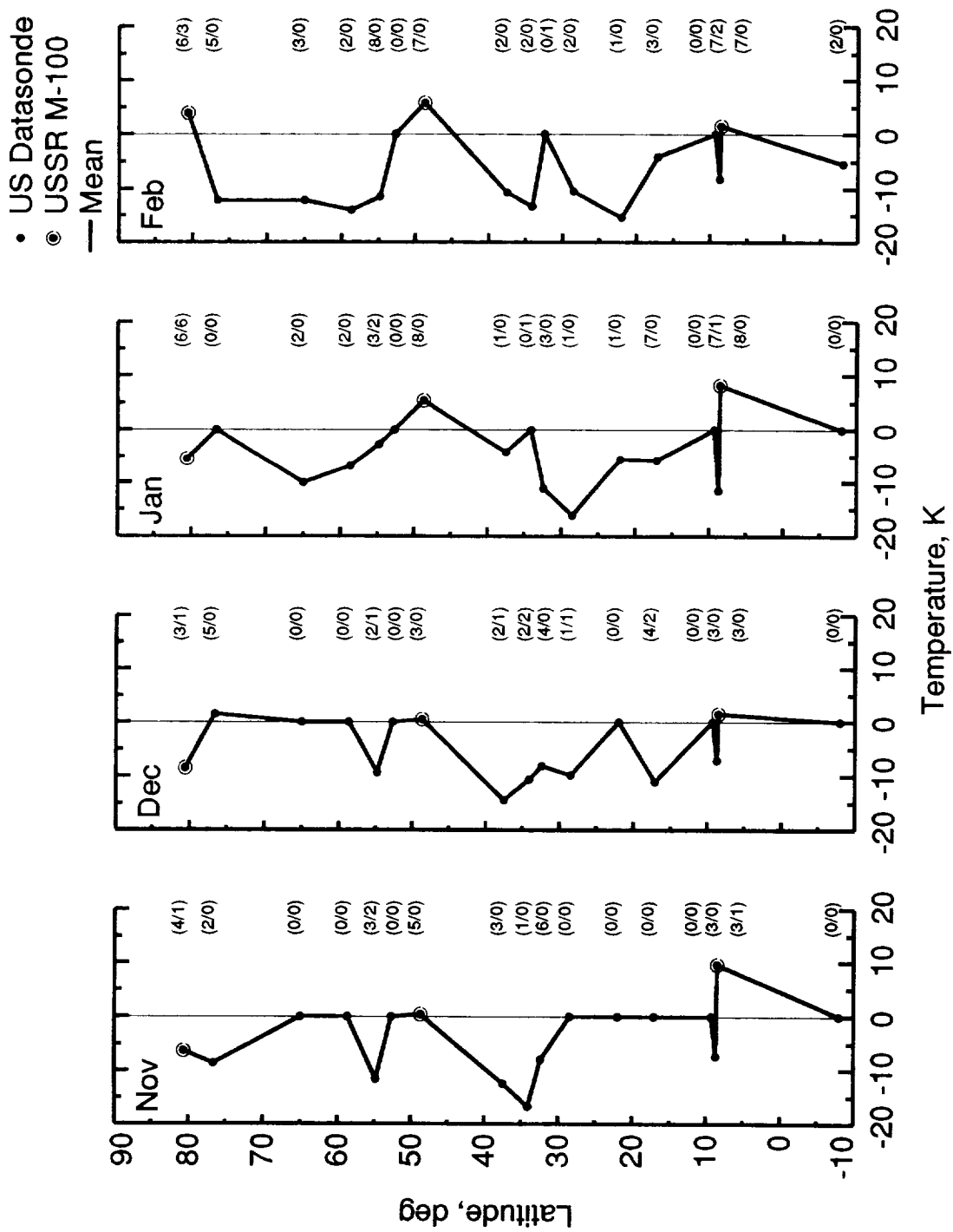
Figure 14. Concluded.

45

Figure 15. LIMS minus rocketsonde temperature differences by month and station latitude at 0.1 hPa. Horizontal bars in last panel represent standard deviation about 7-month average difference.

Figure 15. Concluded.

47

Figure 16. NMC minus rocketsonde temperature differences by month and station latitude at 0.4 hPa. Horizontal bars in last panel represent standard deviation about 7-month average difference.
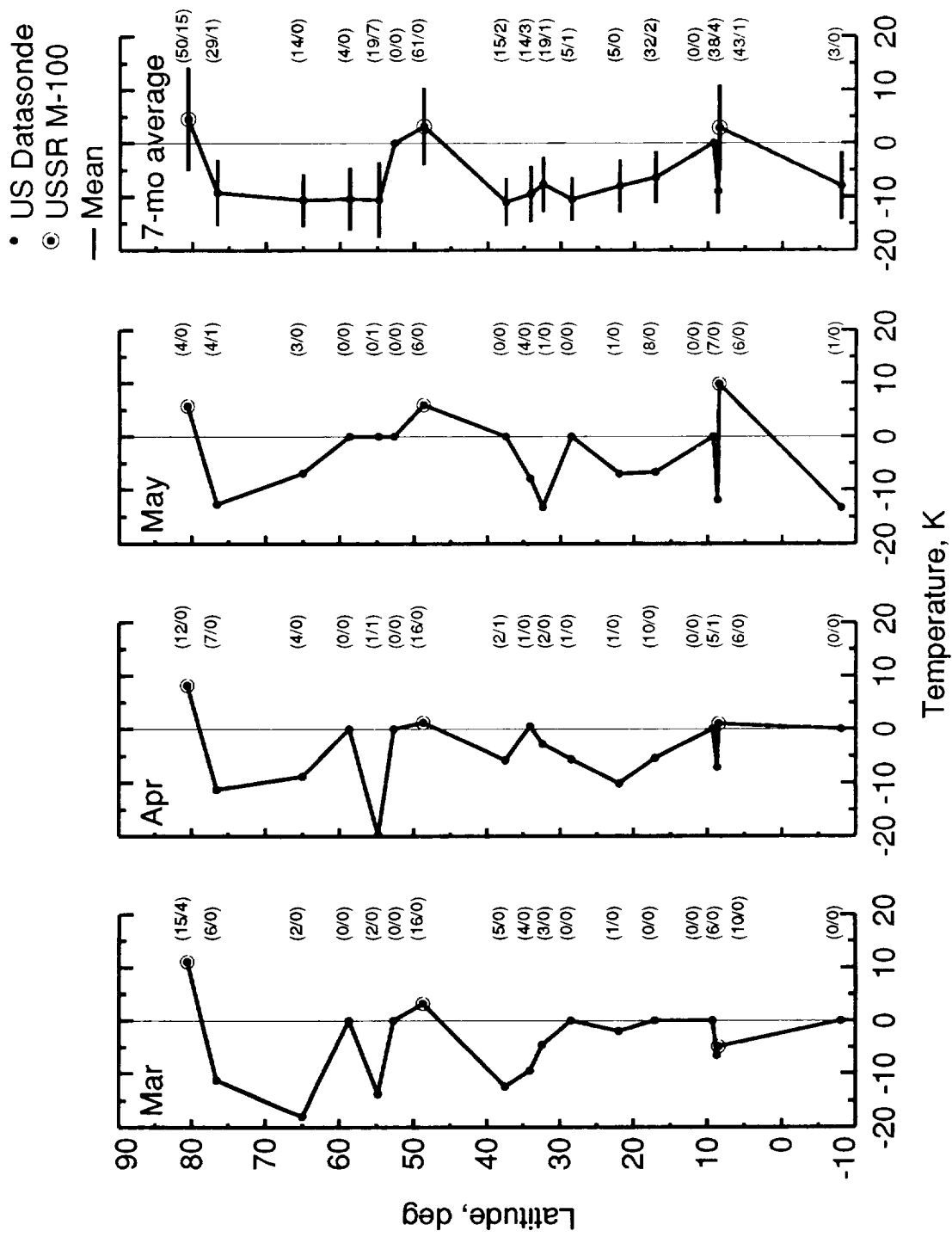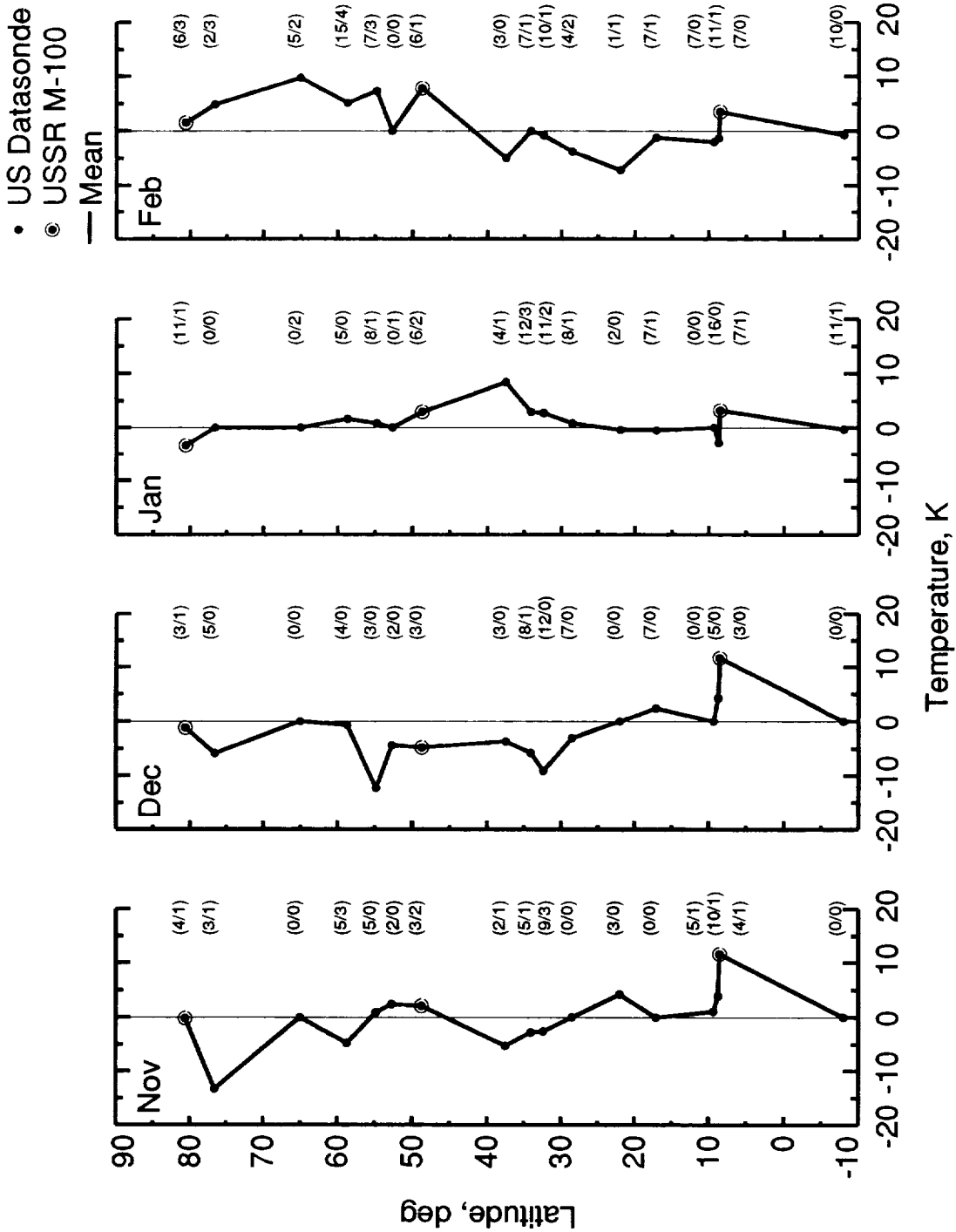
48

Figure 16. Concluded.

49

Figure 17. LIMS minus NMC satellite temperature differences by month and station latitude at 0.4 hPa. Horizontal bars in last panel represent standard deviation about 7-month average difference.
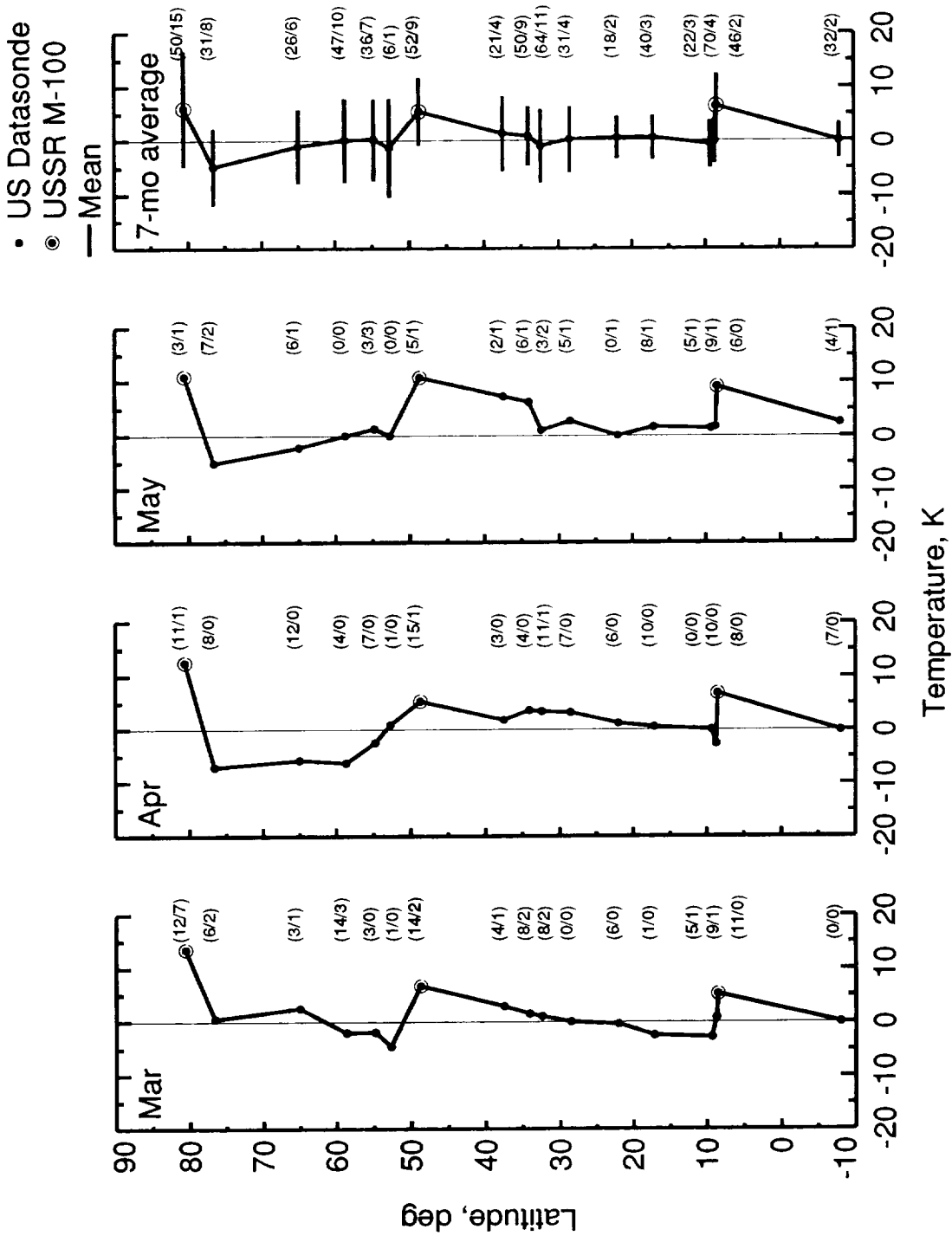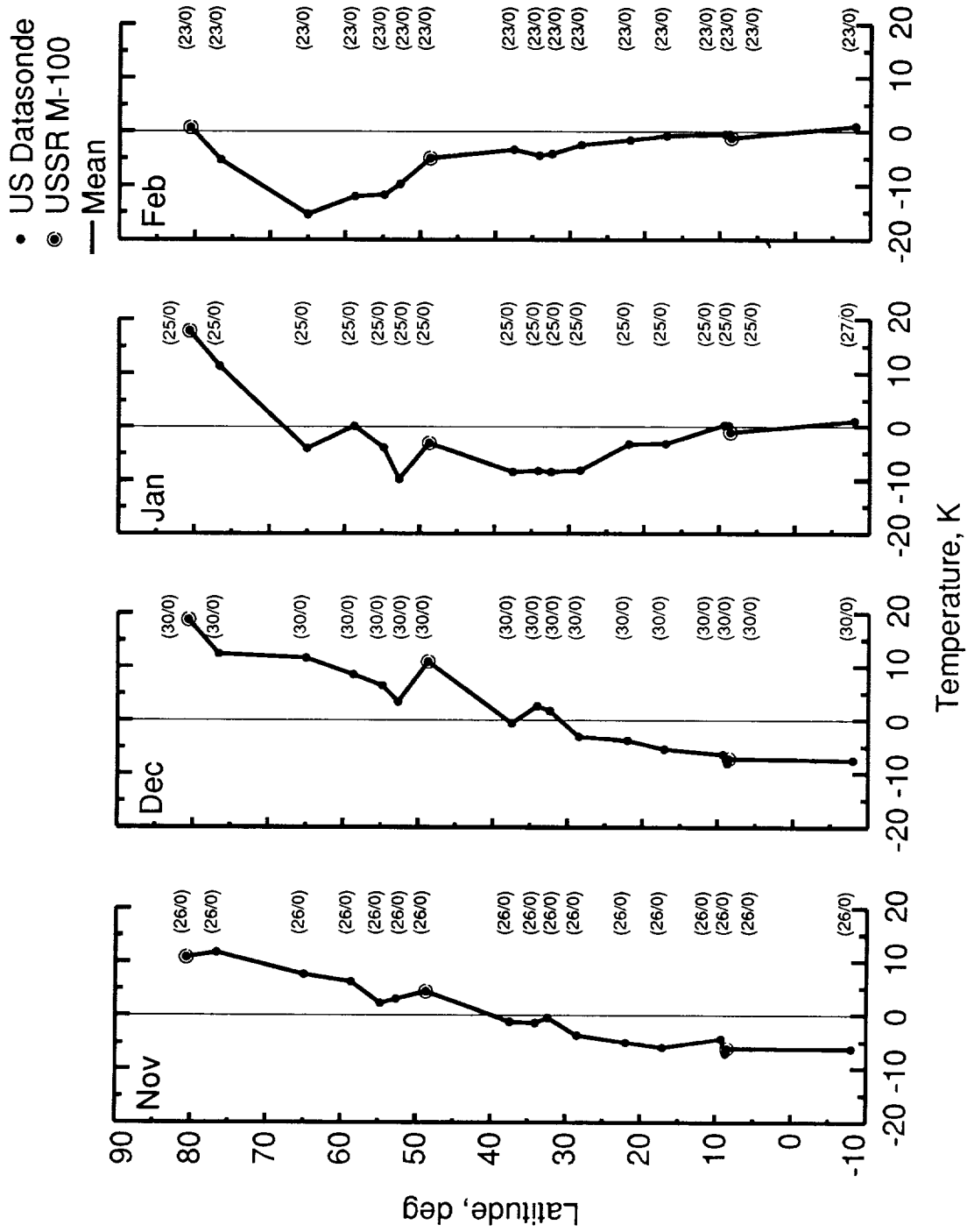
Figure 17. Concluded.

51

Figure 18. Seasonally averaged LIMS minus Datasonde (US) temperature differences for low latitudes. Horizontal bars represent standard deviation about average difference.

Figure 19. Seasonally averaged LIMS minus Datasonde (US) temperature differences for mid latitudes. Horizontal bars represent standard deviation about average difference.
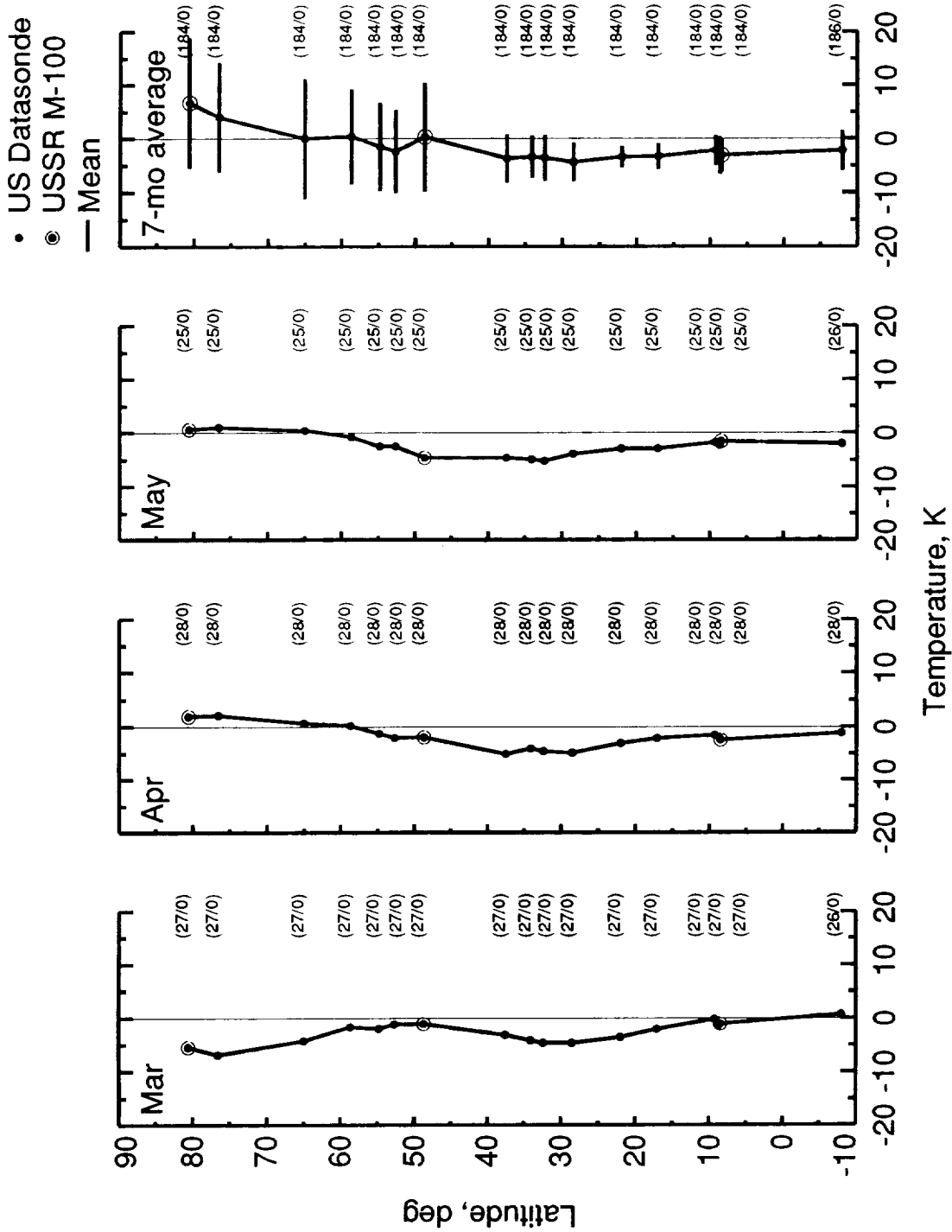

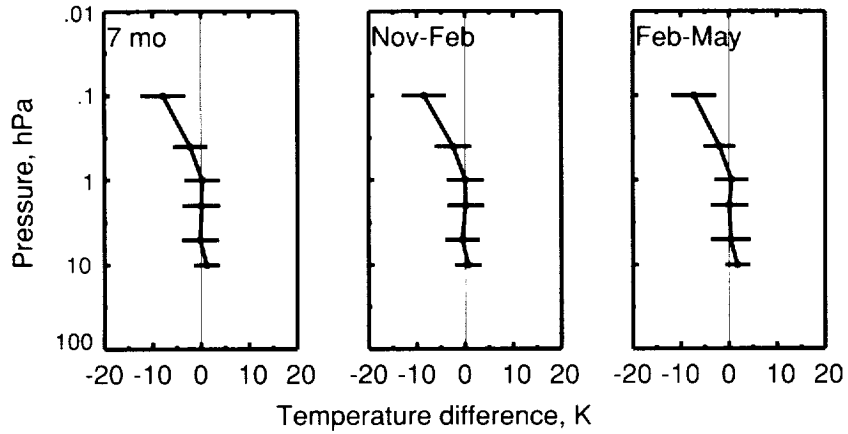Figure 20. Seasonally averaged LIMS minus Datasonde (US) temperature differences for high latitudes. Horizontal bars represent standard deviation about average difference.
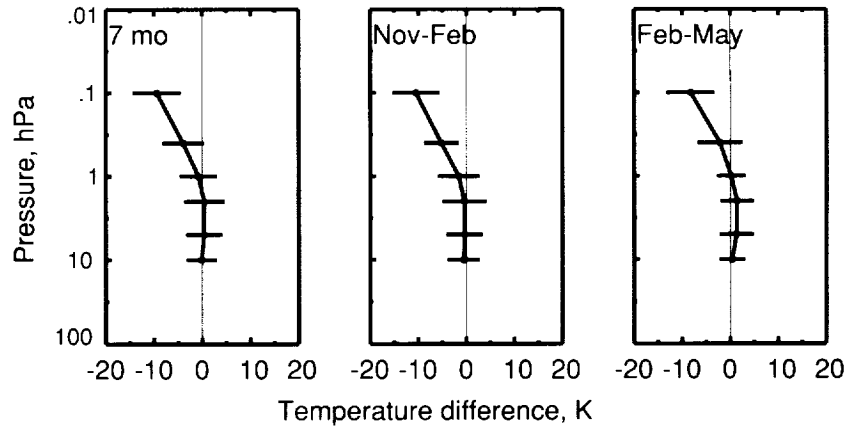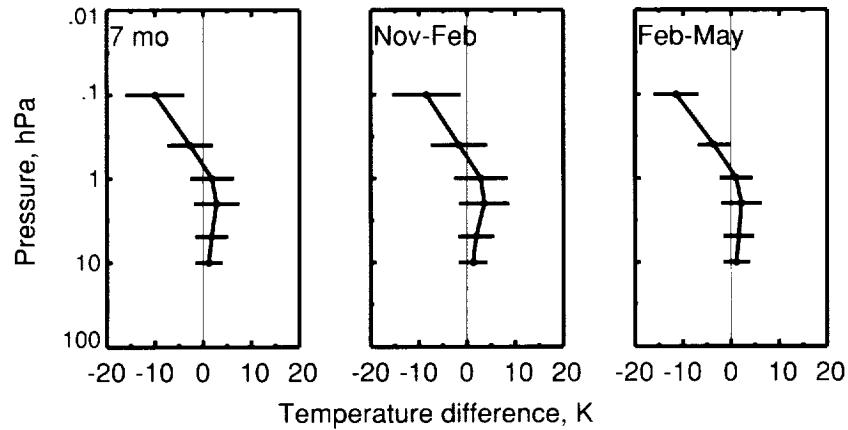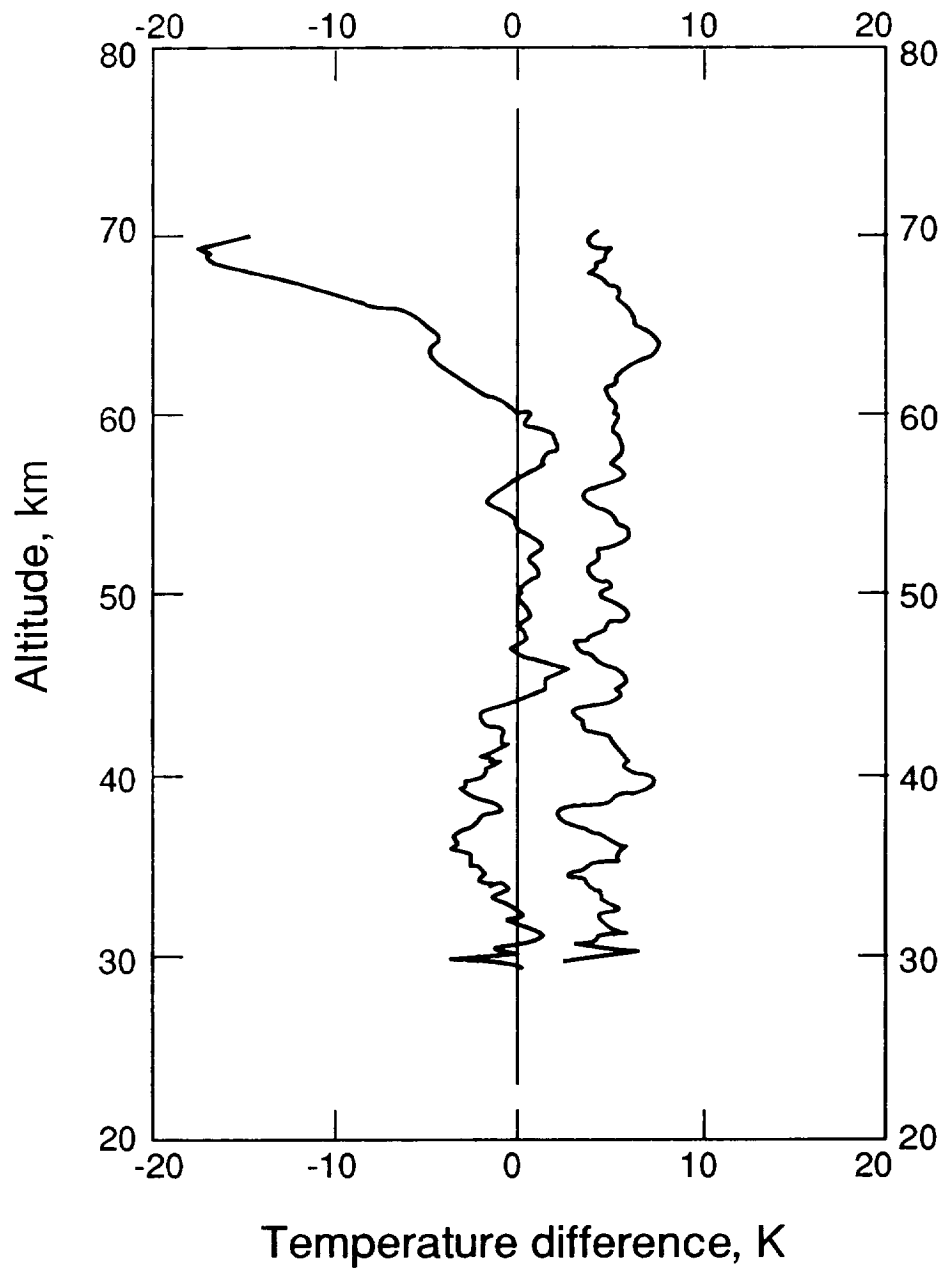
Figure 21. Sphere minus Datasonde differences from Schmidlin et al. (1991). Left curve is mean difference, right curve standard deviation of differences.
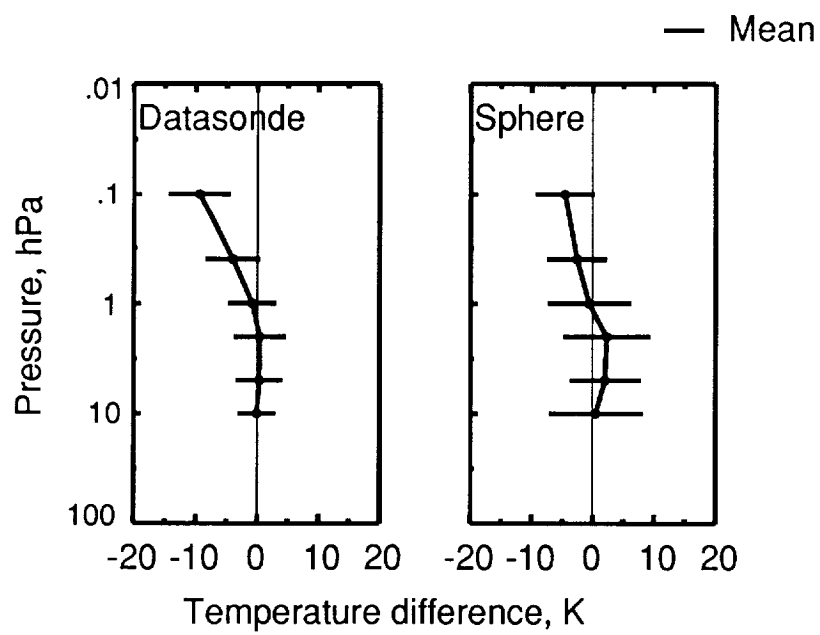
Figure 22. LIMS minus ROCOB temperature differences at mid latitudes.

Appendix A
Temperature Time Series Plots and Statistics Plots at Each Station

This appendix contains temperature (K) time series (day) plots as well as monthly mean differences at each of the rocketsonde stations listed in table 1 of this report. The time series plots are for the 10-, 5-, 2-, 1-, 0.4-, and 0.1-hPa levels. The solid lines are LIMS data, and the dotted lines are NMC data for the latitude and longitude of the rocketsonde station. The filled circles represent rocketsonde data; a filled circle with an "×" on it indicates a falling sphere data point. In figure A1 for Molodezhnaya, the LIMS data are from 64° S (LIMS data do not exist south of 64° S), and the dashed line represents NMC data at 64° S for comparison with LIMS. The dotted line is NMC data at the station latitude (68° S).

The monthly average profile plots that follow the time series plots for each station represent the mean differences for LIMS versus Datasonde or M-100. Rocketsonde observations were not available for all months at some stations. The 7-month average difference is also given, where the horizontal bars are the standard deviations about those differences. The first number in the parentheses on the right-hand border of each figure indicates the total number of samples that went into the calculation of the statistics. The second number indicates the number of observations that were excluded on the basis of a rejection criterion of 20 K (see text). The numerical values for individual stations, used in preparing these plots, are given in appendix B.

The NMC data do not exist above the 0.4-hPa level (i.e., at 0.1 hPa in this study).
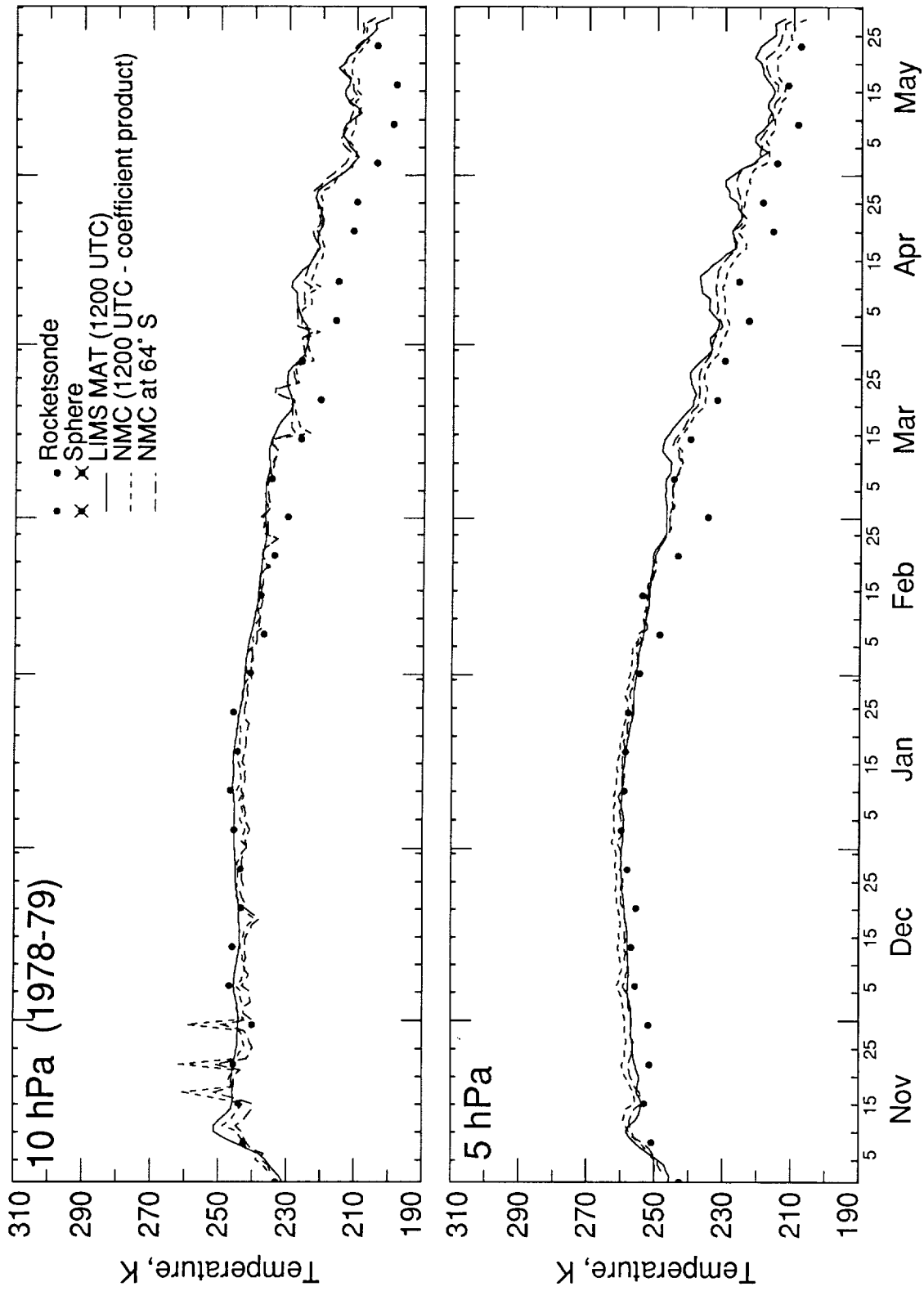
Figure A1. Molodezhnaya, USSR (68° S, 46° E).

The plot legend:
- • Rocketsonde
- × Sphere
- —— LIMS MAT (1200 UTC)
- —·— NMC (1200 UTC - coefficient product)
- —·· — NMC at 64° S

Top panel: 10 hPa (1978-79), Temperature, K
Bottom panel: 5 hPa, Temperature, K

X-axis months: Nov, Dec, Jan, Feb, Mar, Apr, May
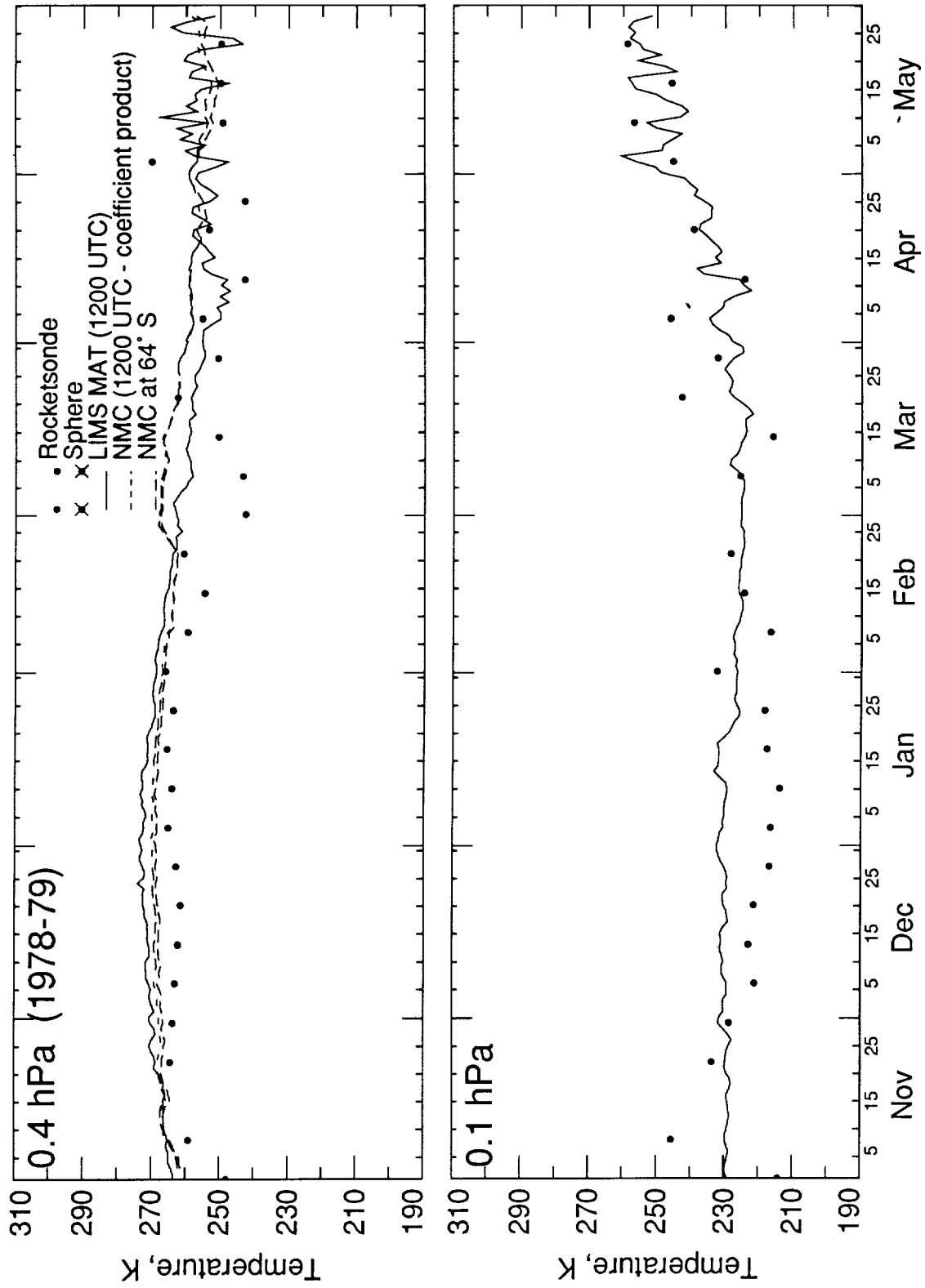
Figure A1. Continued.

Figure A1. Continued.

(LIMS minus rocketsonde temperature)

Mean

Feb

(3/0)
(3/1)
(4/0)
(4/0)
(4/0)
(4/0)

7-mo average

(27/0)
(27/2)
(28/1)
(30/0)
(30/0)
(30/0)

Jan

(5/0)
(5/0)
(5/0)
(5/0)
(5/0)
(5/0)

May

(4/0)
(3/1)
(3/1)
(4/0)
(4/0)
(4/0)

Dec

(4/0)
(4/0)
(4/0)
(4/0)
(4/0)
(4/0)

Apr

(3/0)
(4/0)
(4/0)
(4/0)
(4/0)
(4/0)

Nov

(4/0)
(4/0)
(4/0)
(5/0)
(5/0)
(5/0)

Mar

(4/0)
(4/0)
(4/0)
(4/0)
(4/0)
(4/0)

Pressure, hPa

.01
.1
1
10
100

Pressure, hPa

.01
.1
1
10
100

Temperature difference, K

-20 -10 0 10 20
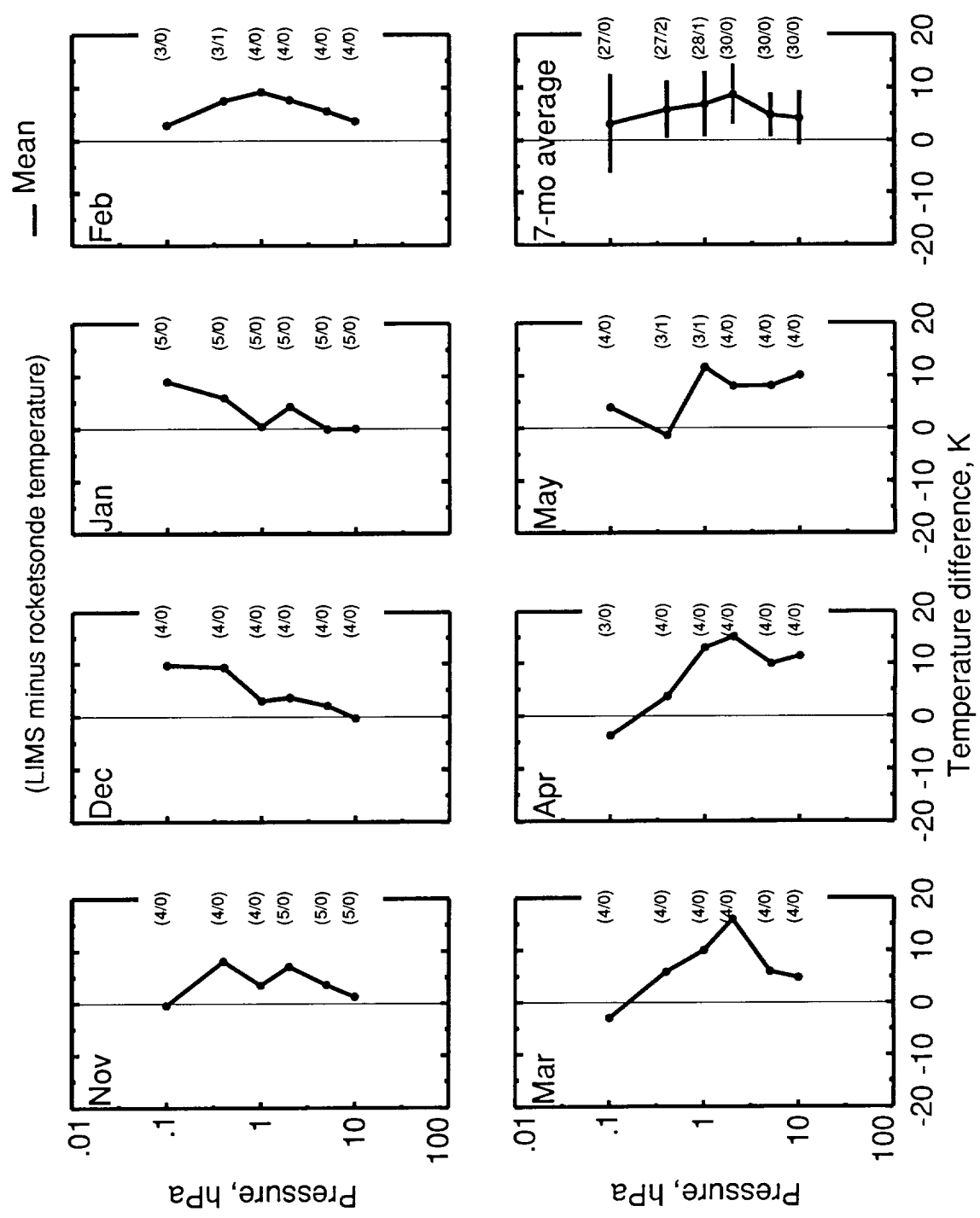
Figure A1. Concluded.

59

Figure A2. Ascension Island (8° S, 346° E).

Figure A2. Continued.
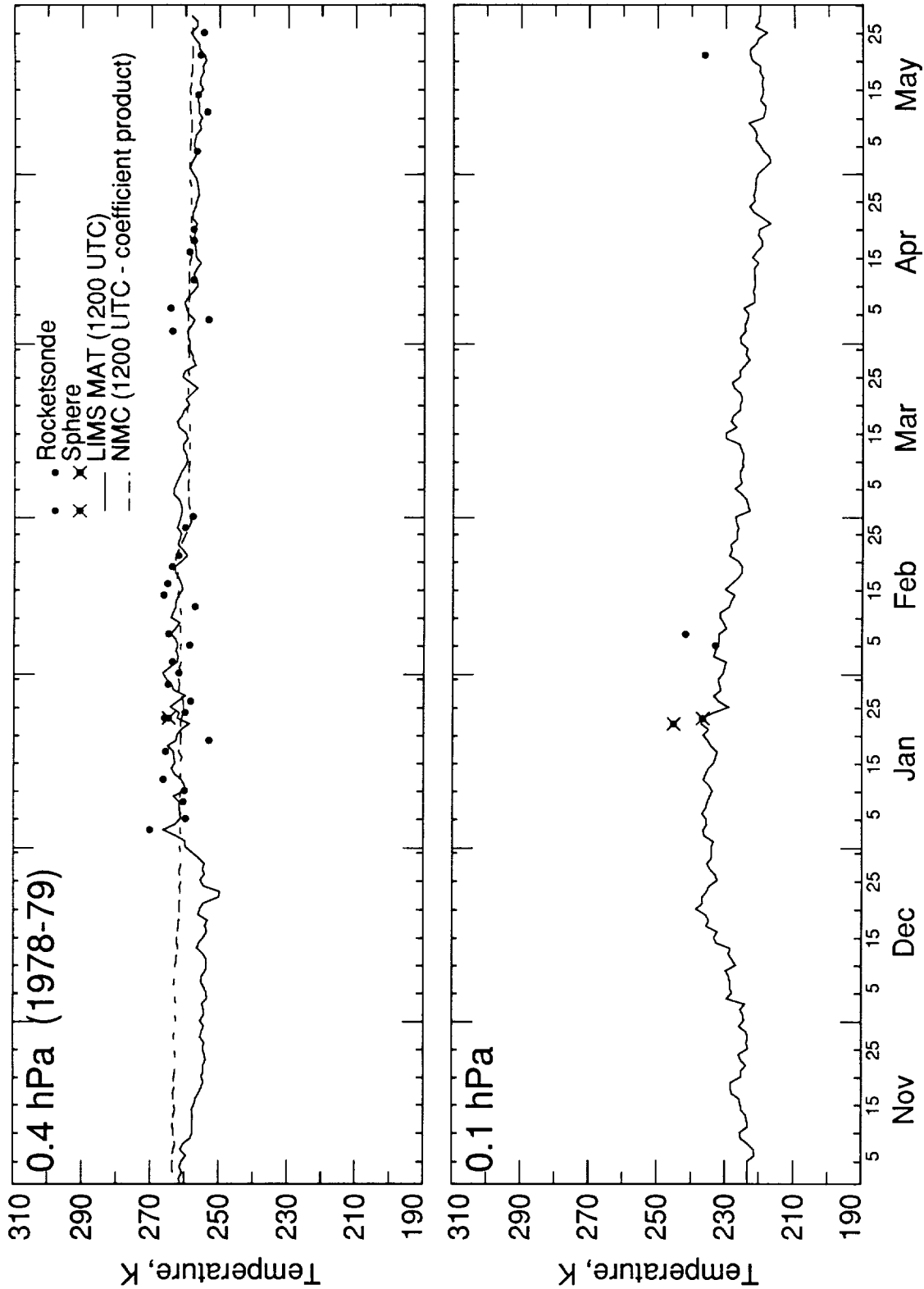
Figure A2. Continued.
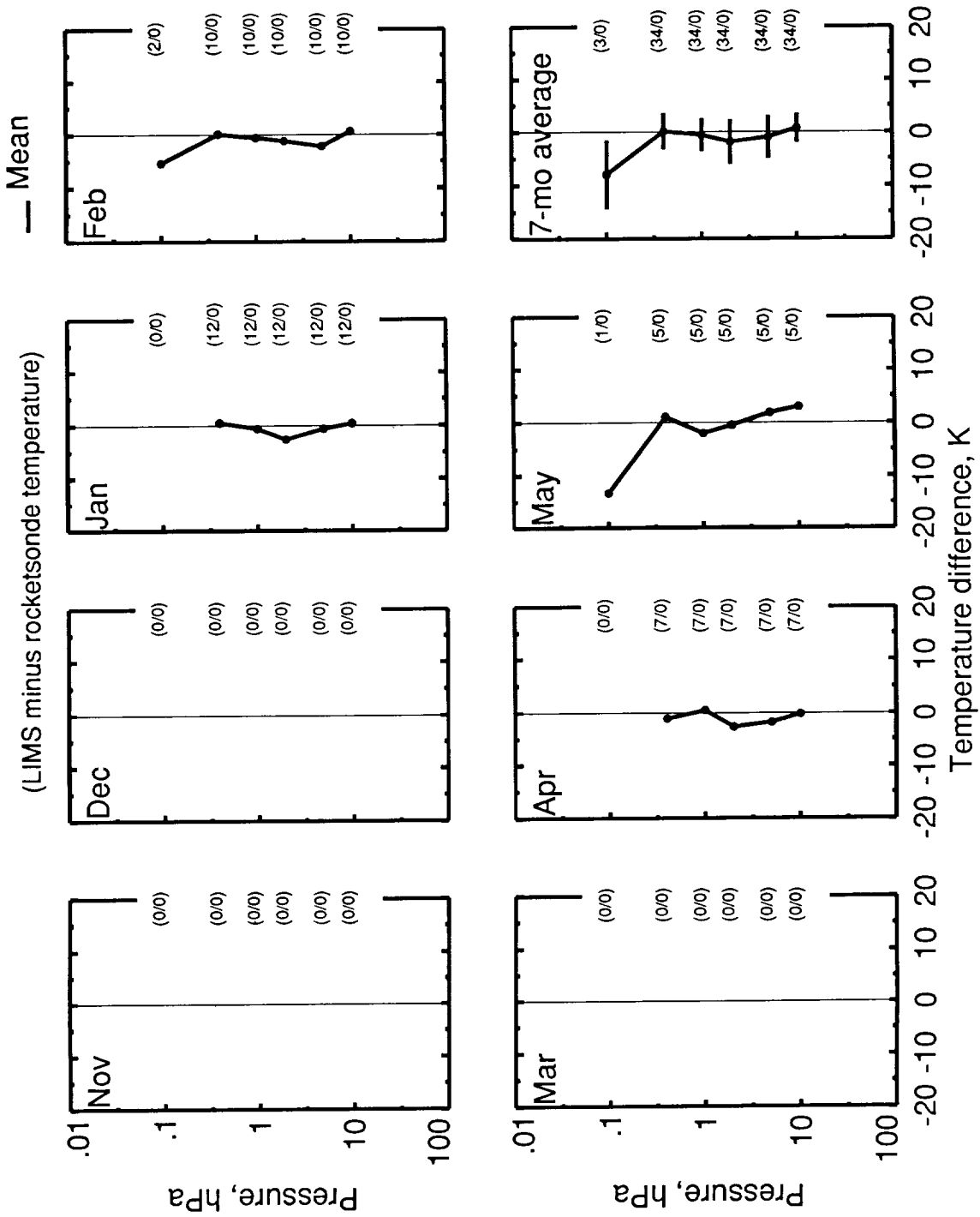
Figure A2. Concluded.

63

Figure A3. Thumba, India (9° N, 77° E).
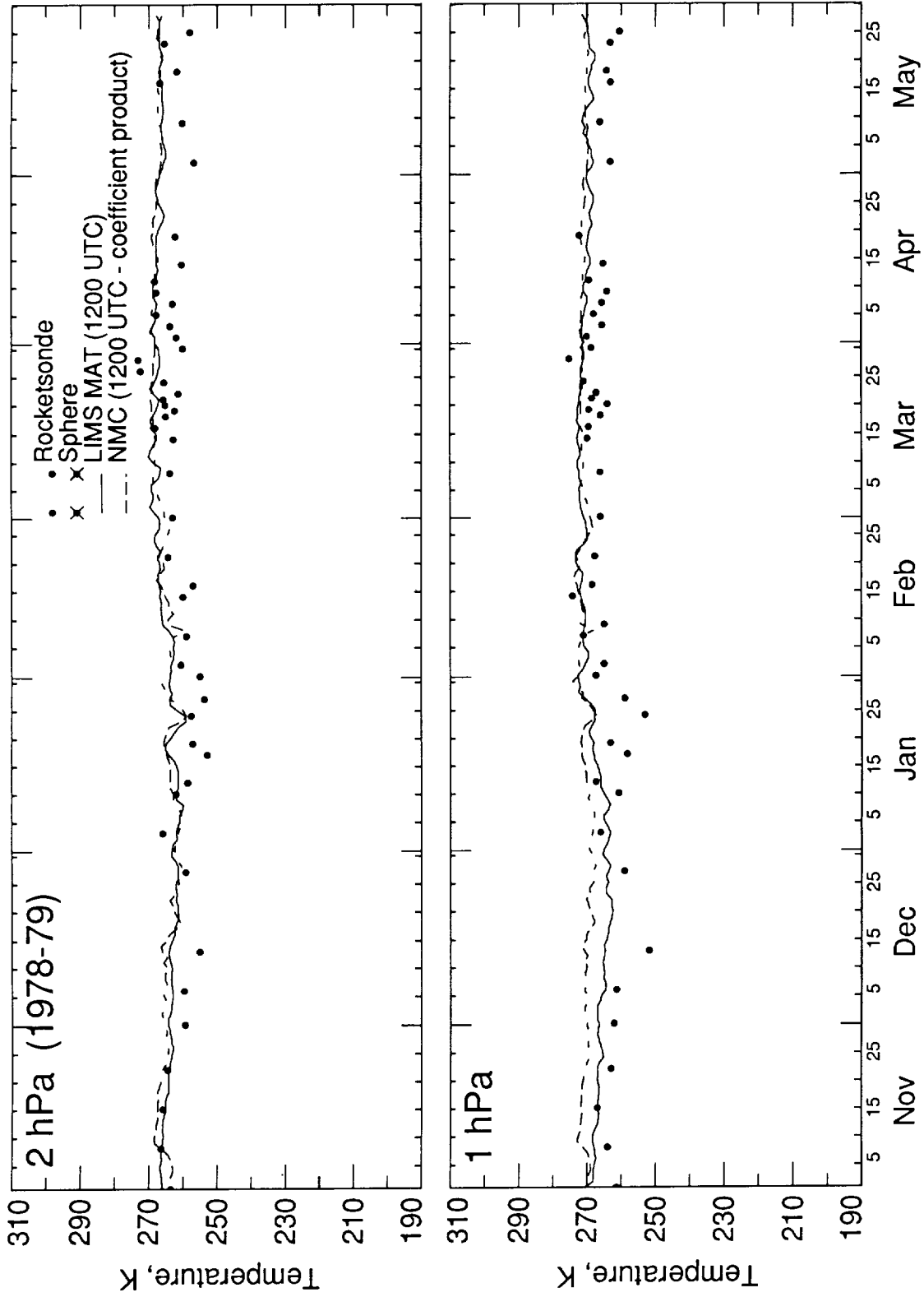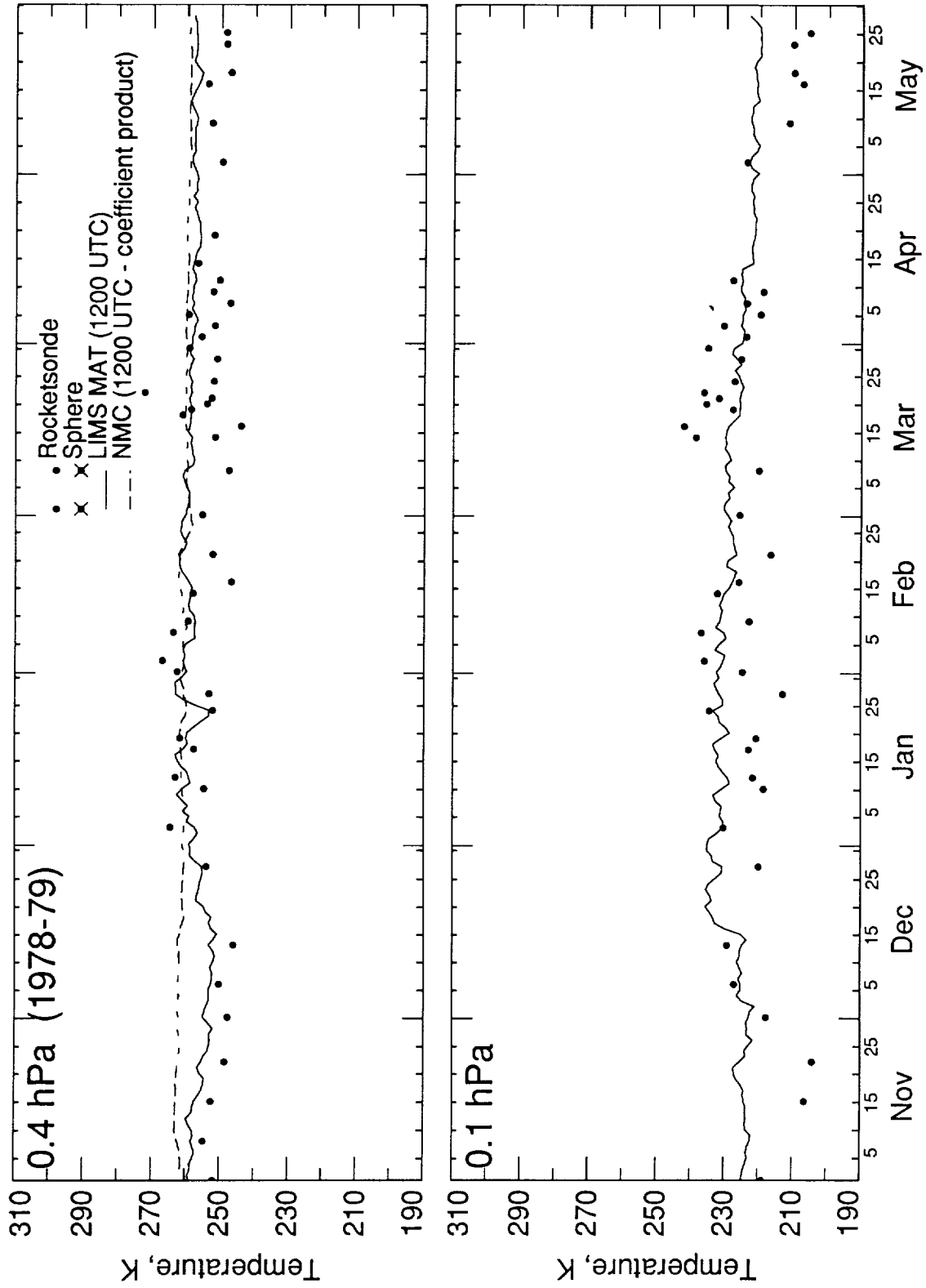
Figure A3. Continued.

Figure A3. Continued.

66
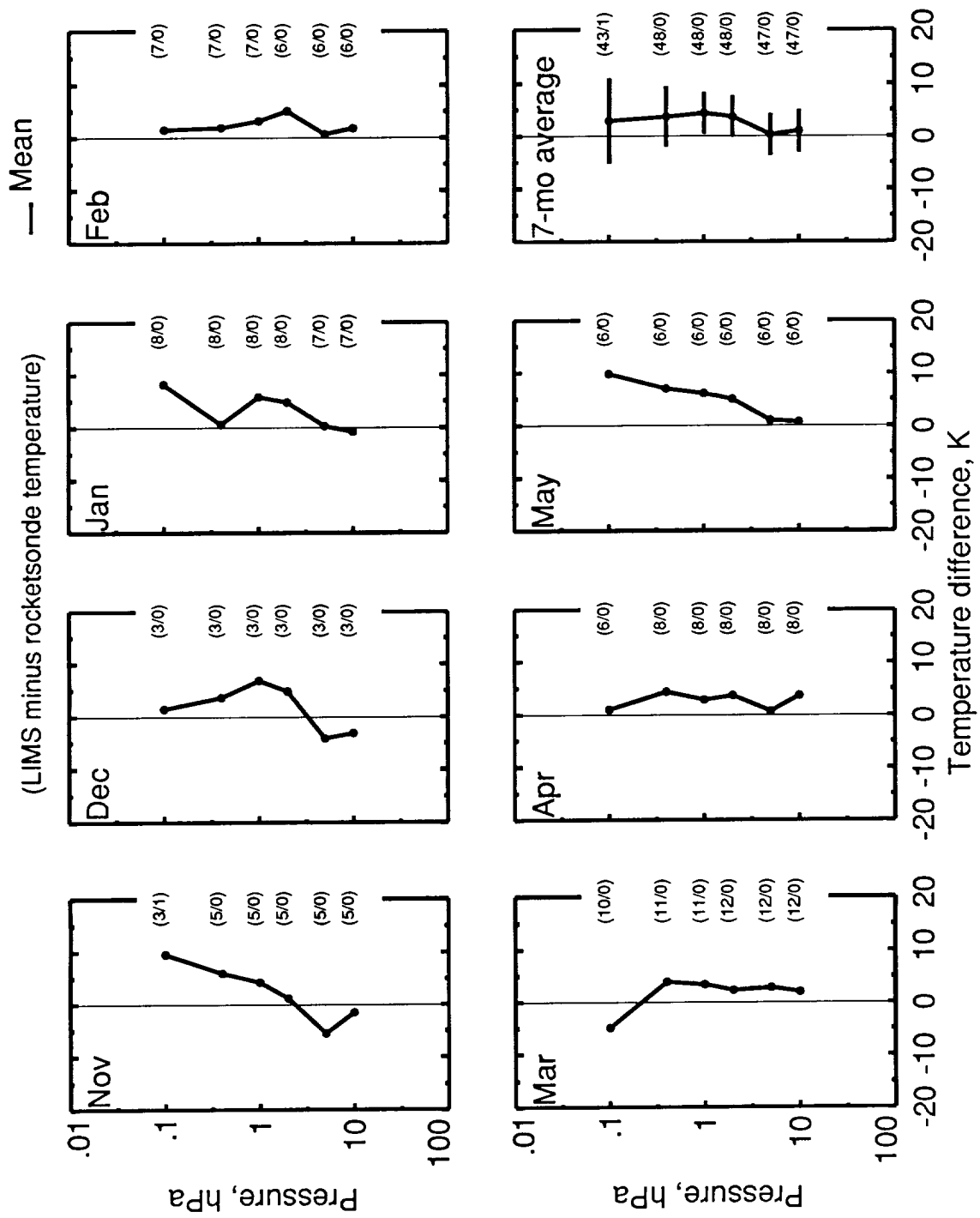
Figure A3. Concluded.

Figure A4. Kwajalein (9° N, 168° E).

68

Figure A4. Continued.

69
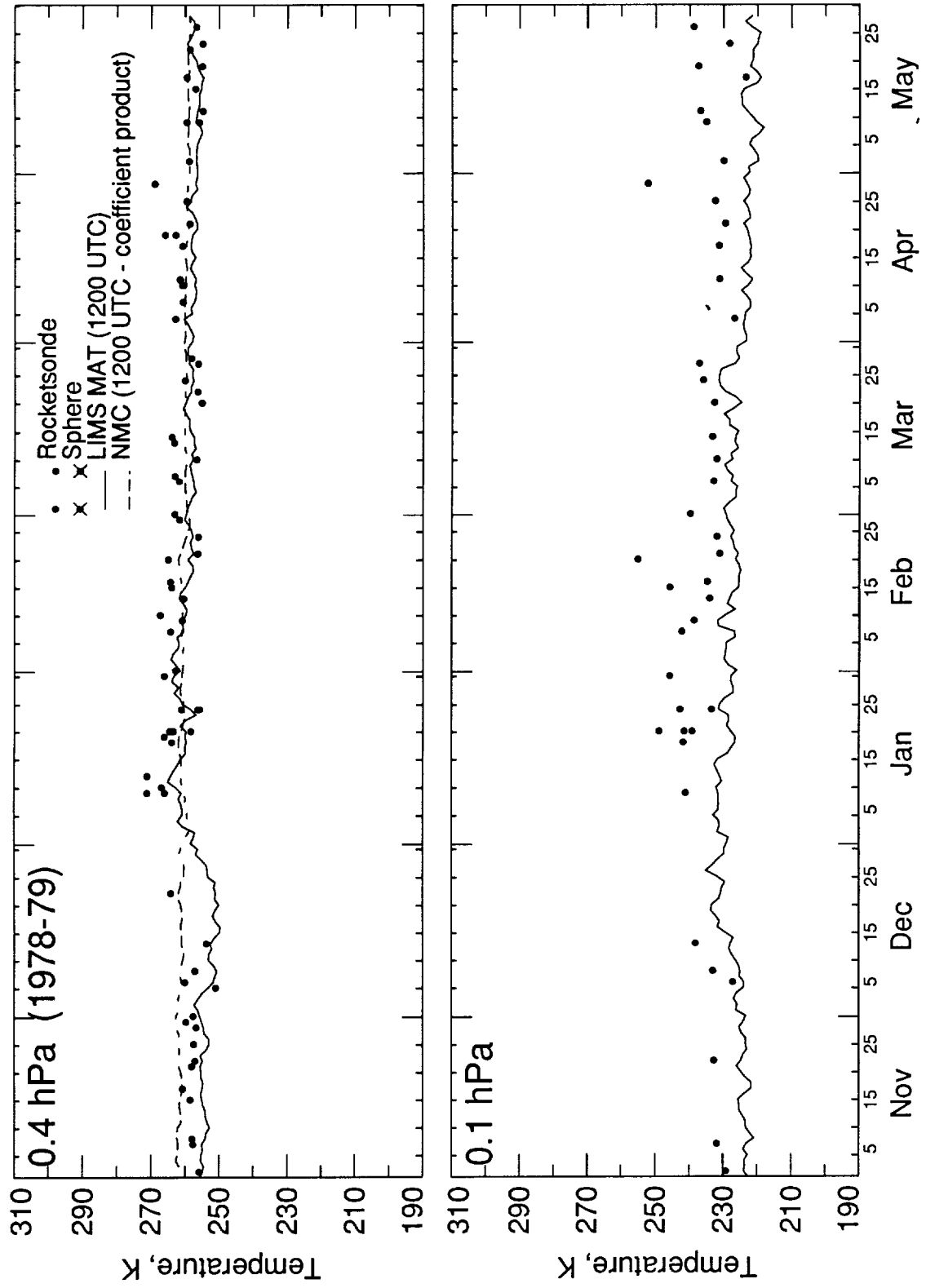
Figure A4. Continued.
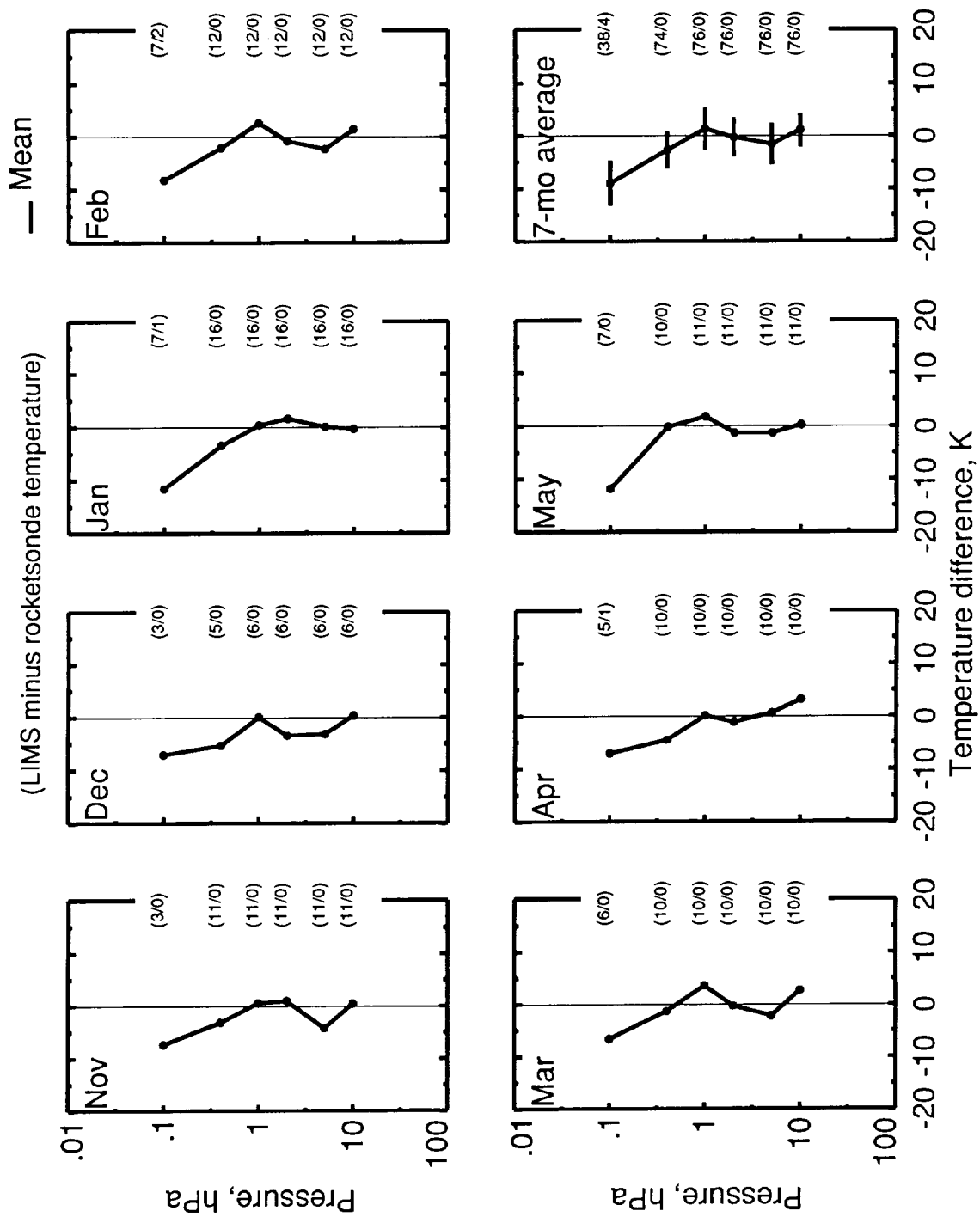
Figure A4. Concluded.

71

Figure A5. Fort Sherman (9° N, 280° E).
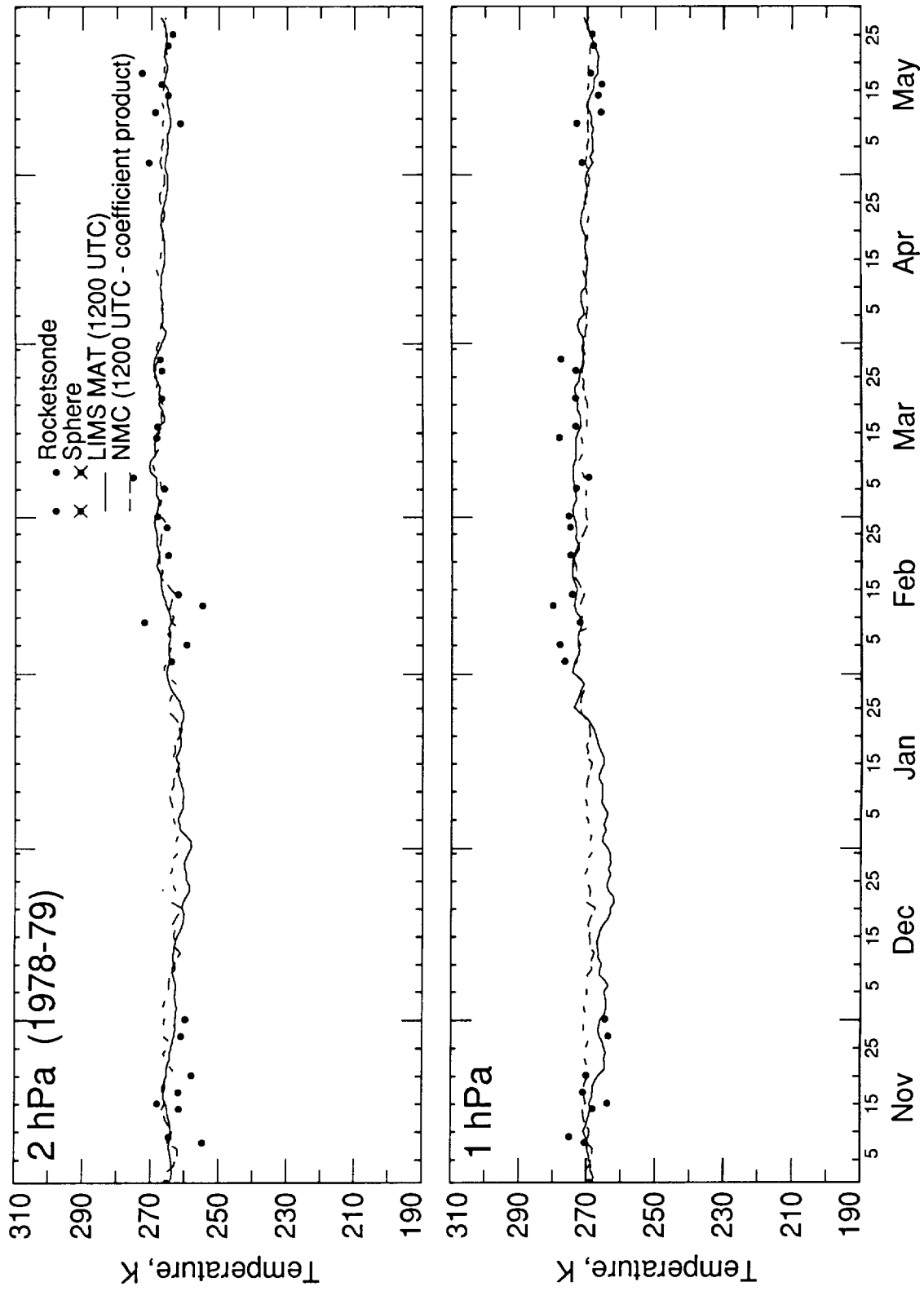
Figure A5. Continued.
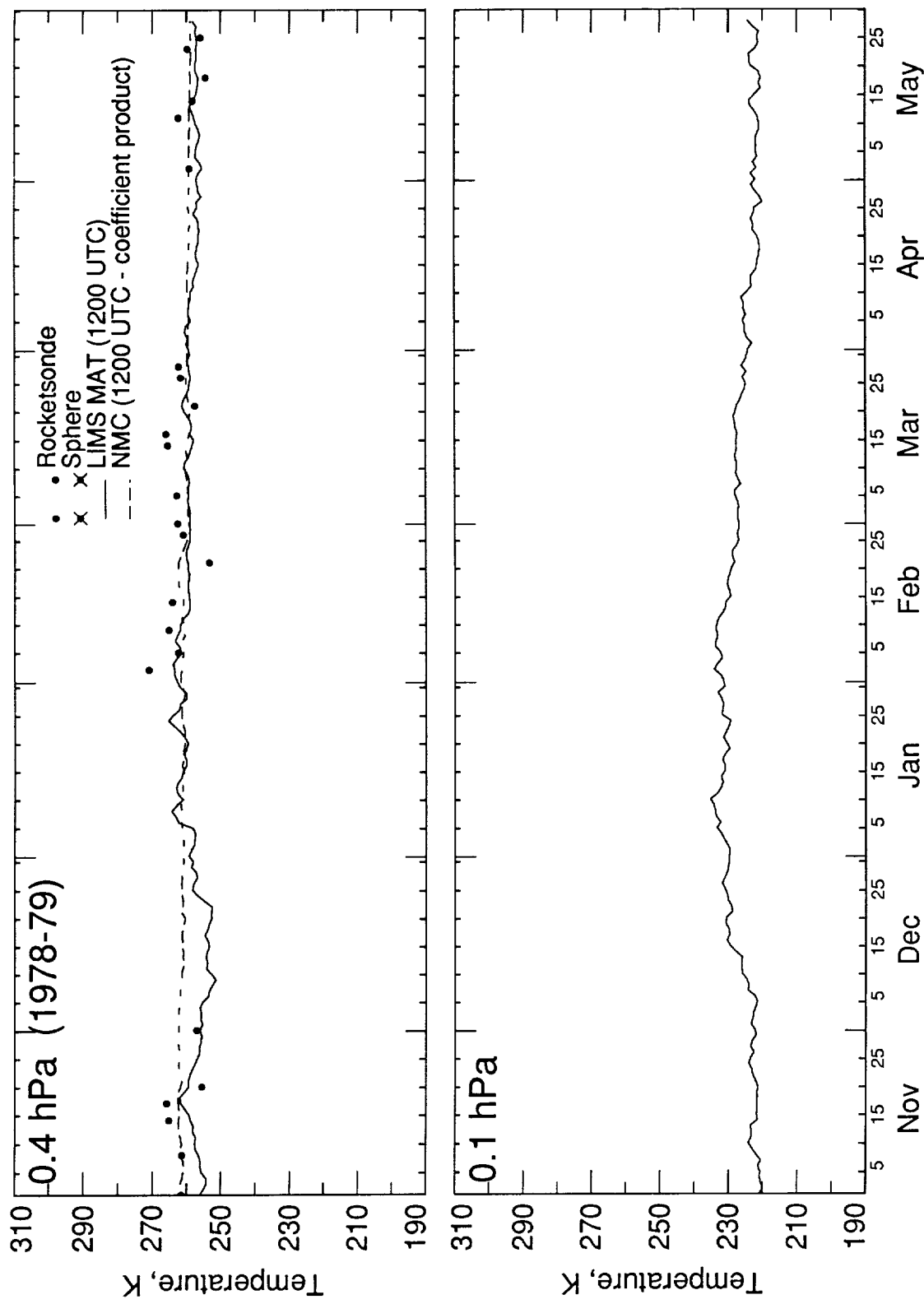
Figure A5. Continued.
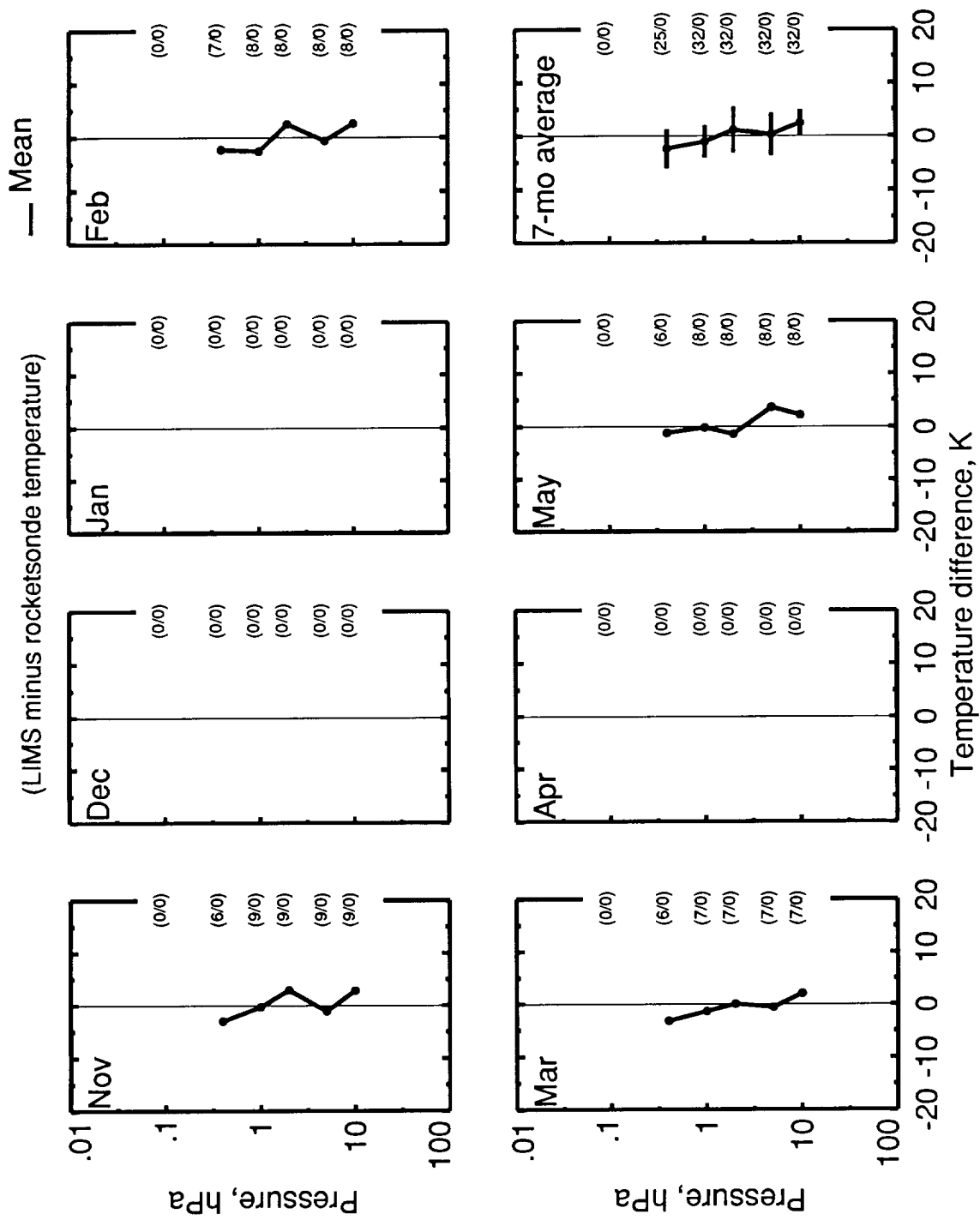
Figure A5. Concluded.

Figure A6. Antigua (17° N, 298° E).

76
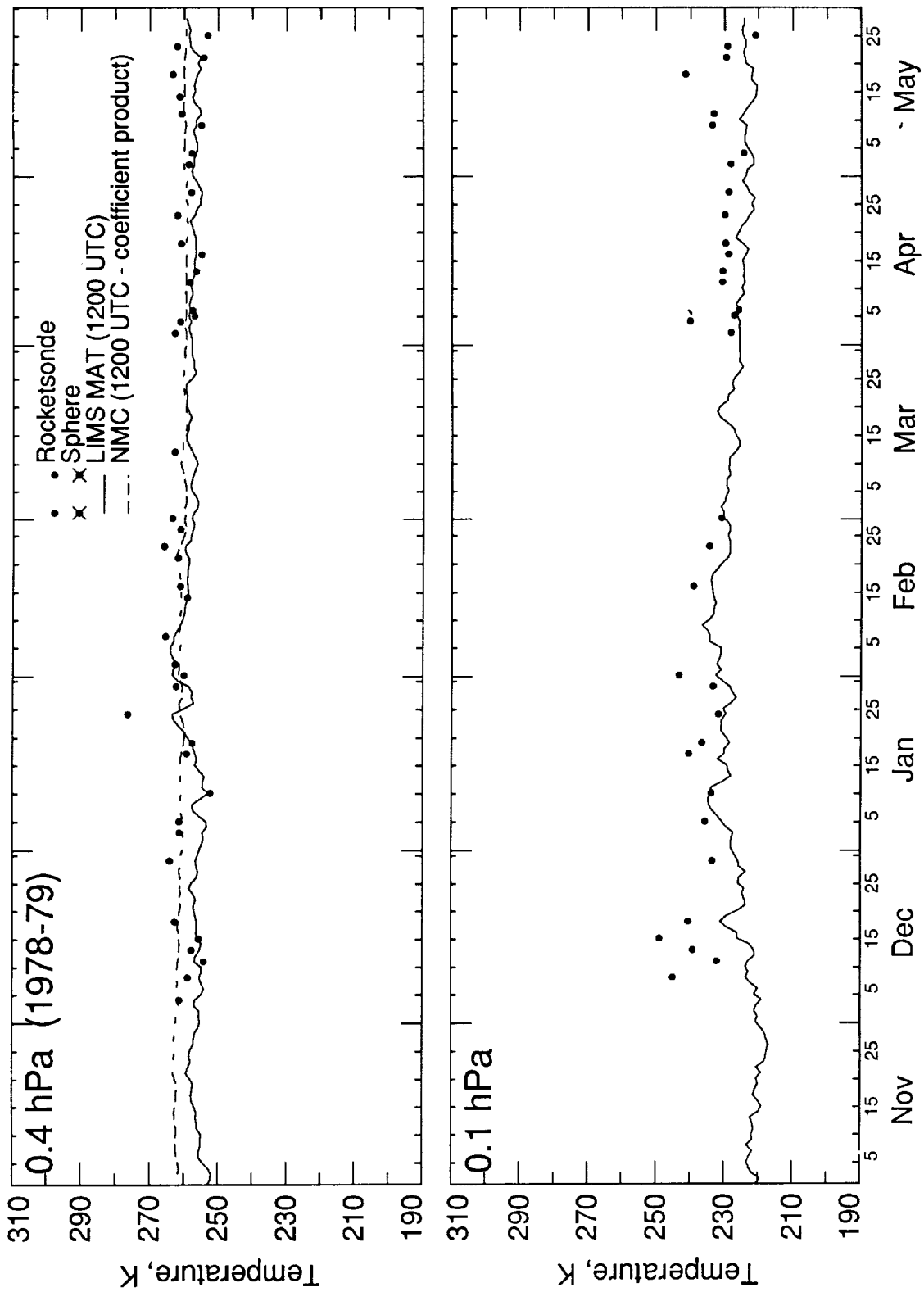
Figure A6. Continued.

Figure A6. Continued.

Mean

Feb

(3/0)
(8/0)
(8/0)
(9/0)
(9/0)
(9/0)

7-mo average

(32/2)
(43/0)
(45/0)
(46/0)
(46/0)
(46/0)

Jan

(7/0)
(8/0)
(9/0)
(9/0)
(9/0)
(9/0)

May

(8/0)
(9/0)
(9/0)
(9/0)
(9/0)
(9/0)

(LIMS minus rocketsonde temperature)

Dec

(4/2)
(7/0)
(8/0)
(8/0)
(8/0)
(8/0)

Apr

(10/0)
(10/0)
(10/0)
(10/0)
(10/0)
(10/0)

Nov

(0/0)
(0/0)
(0/0)
(0/0)
(0/0)
(0/0)

Mar

(0/0)
(1/0)
(1/0)
(1/0)
(1/0)
(1/0)

Pressure, hPa

Pressure, hPa

Temperature difference, K
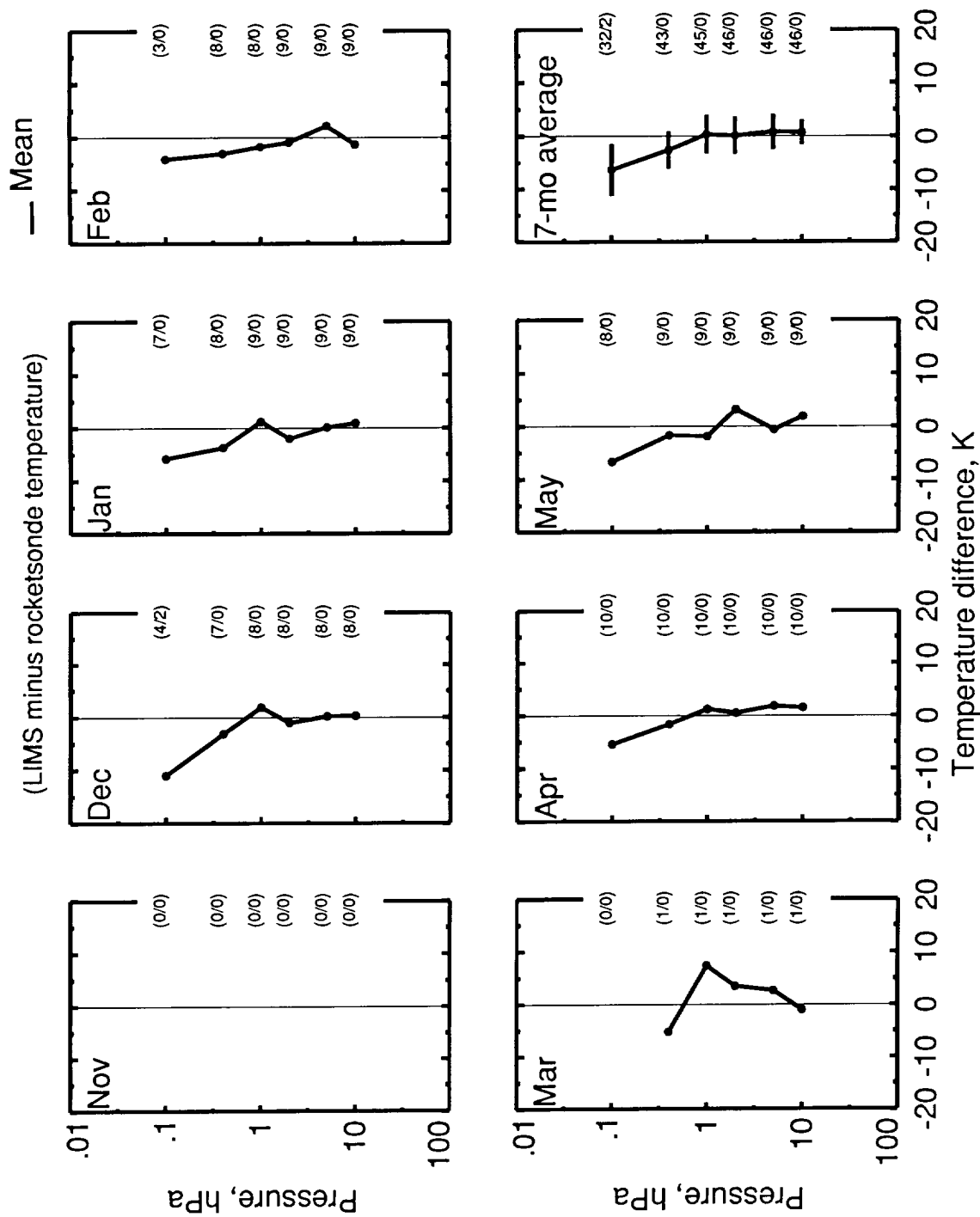
Figure A6. Concluded.
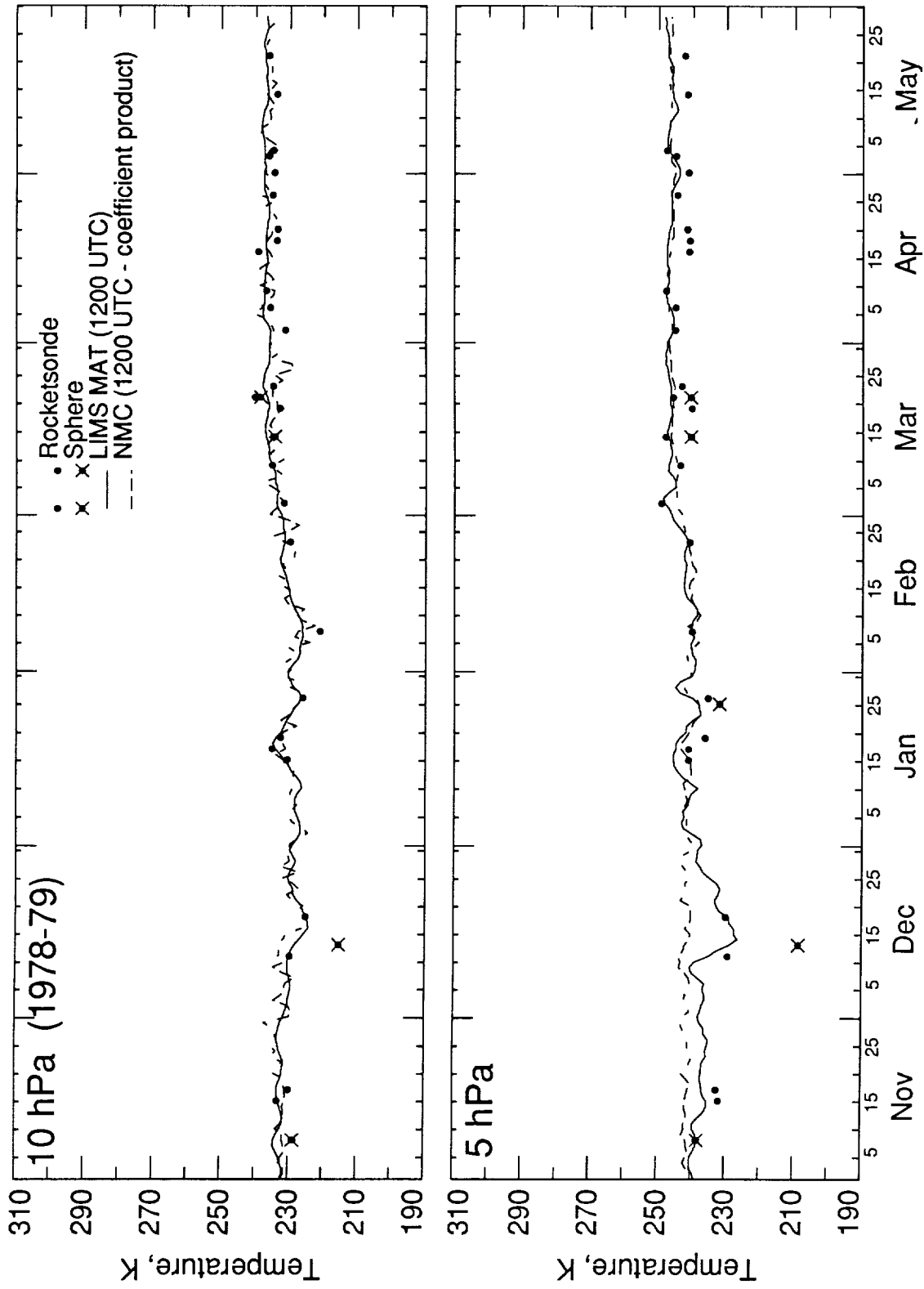
Figure A7. Barking Sands (22° N, 200° E).
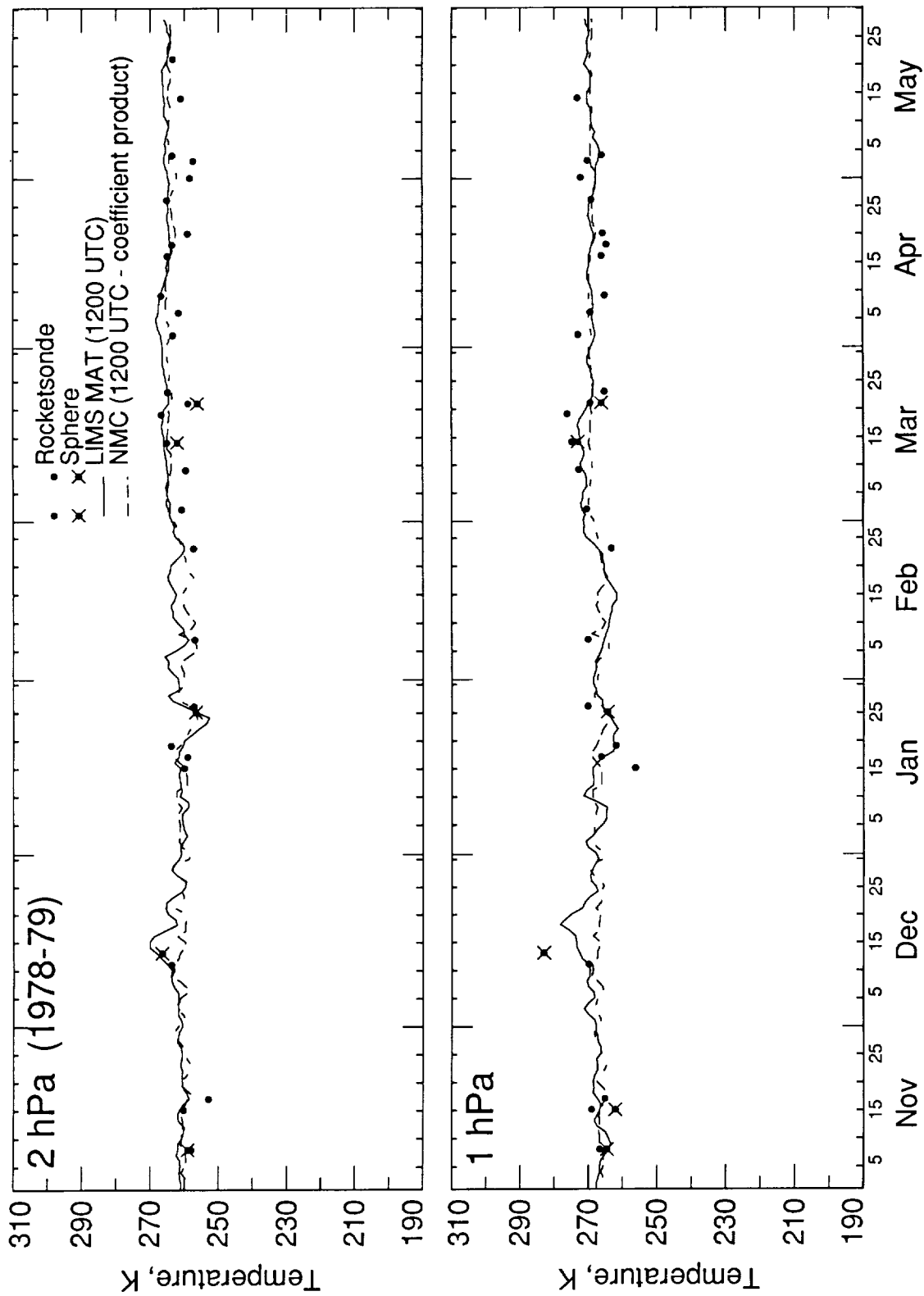
Figure A7. Continued.
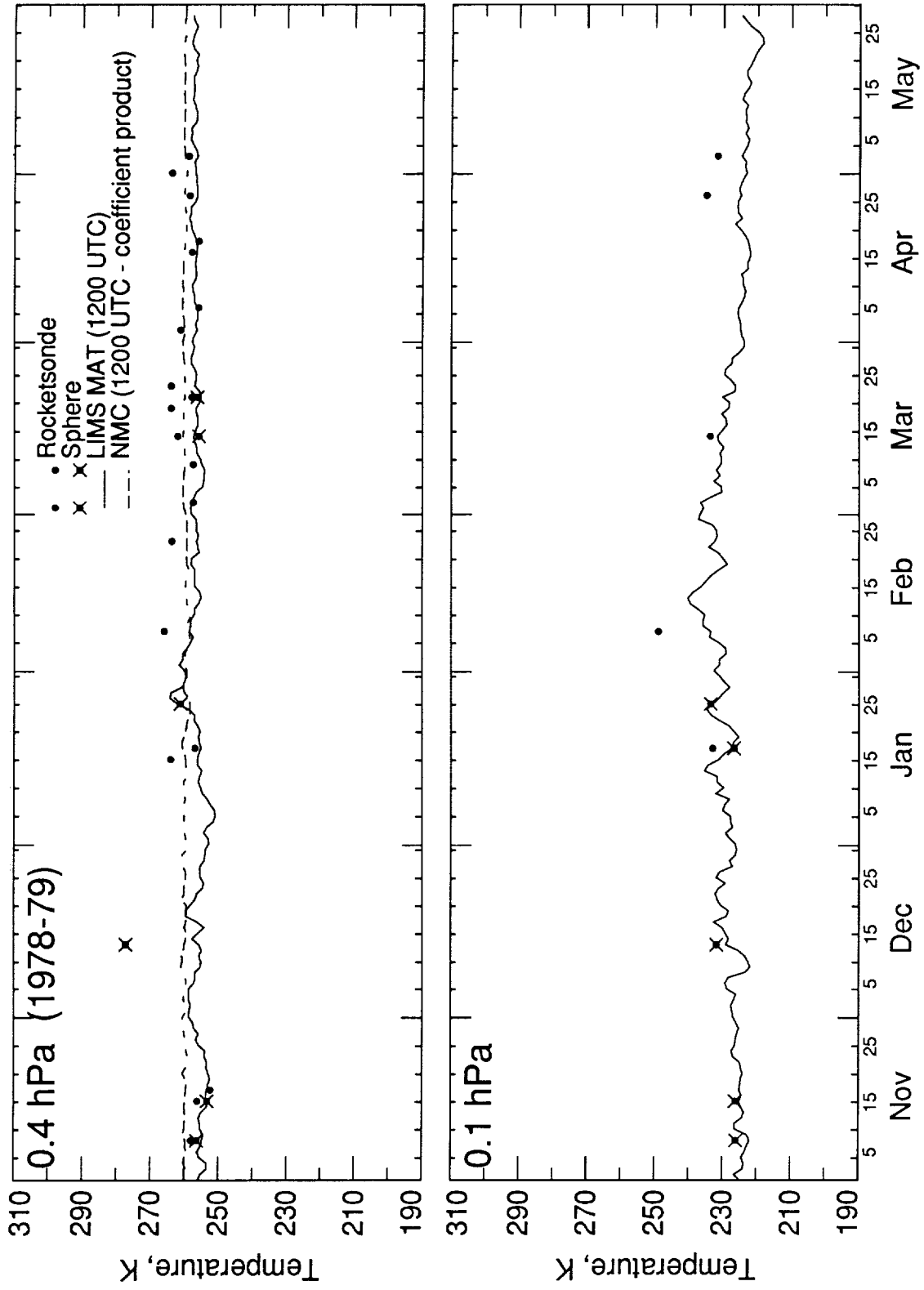
Figure A7. Continued.
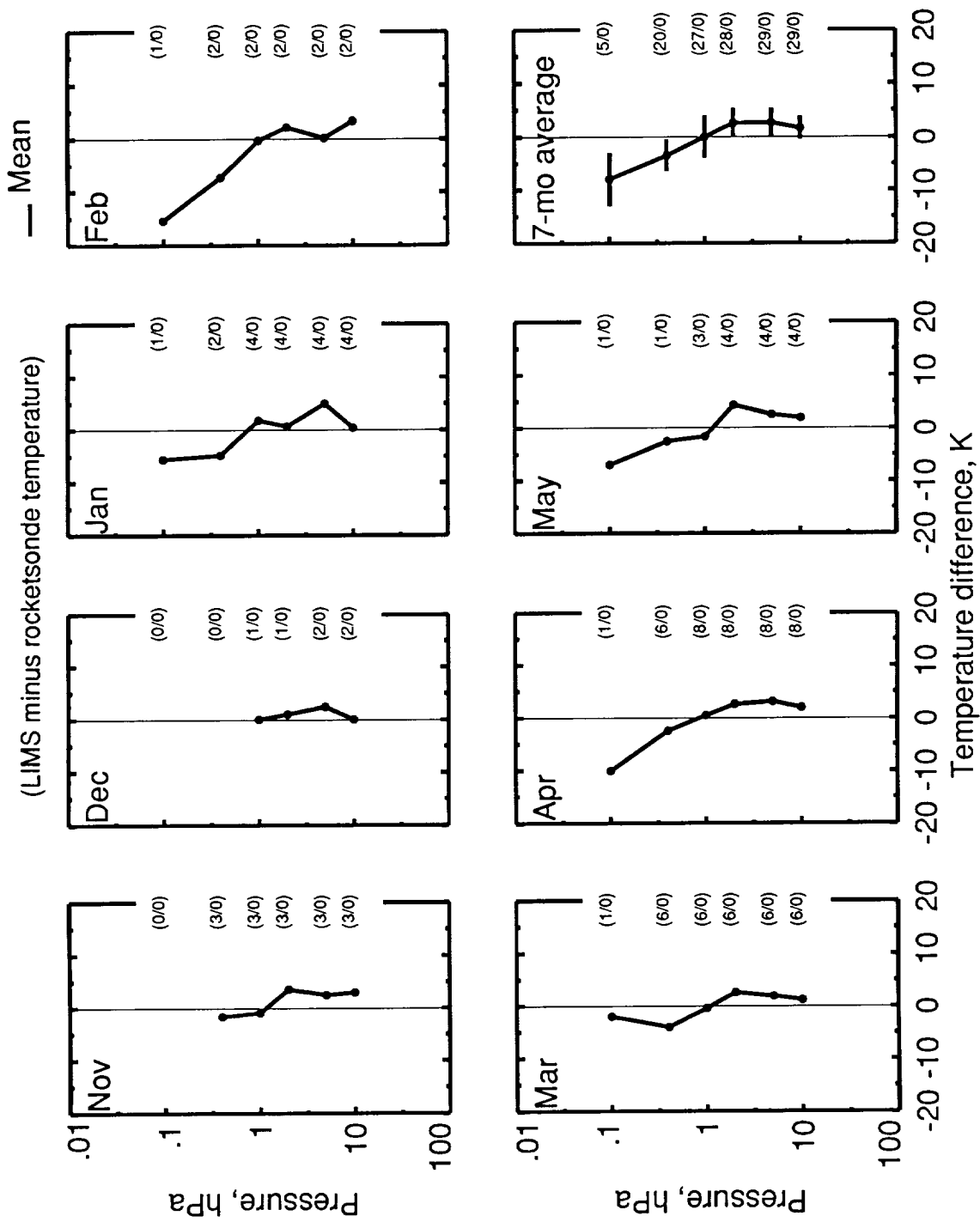
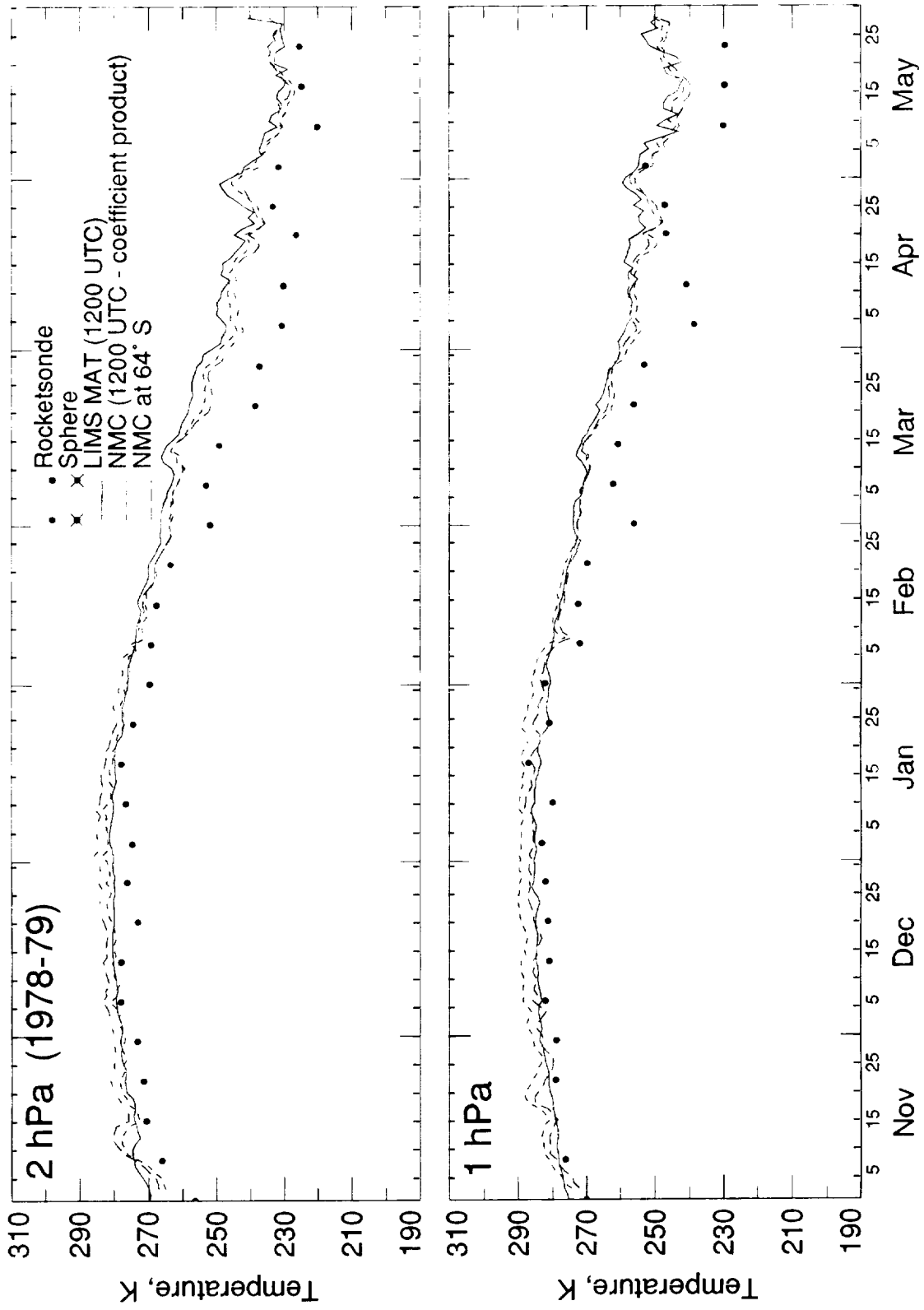Figure A7. Concluded.
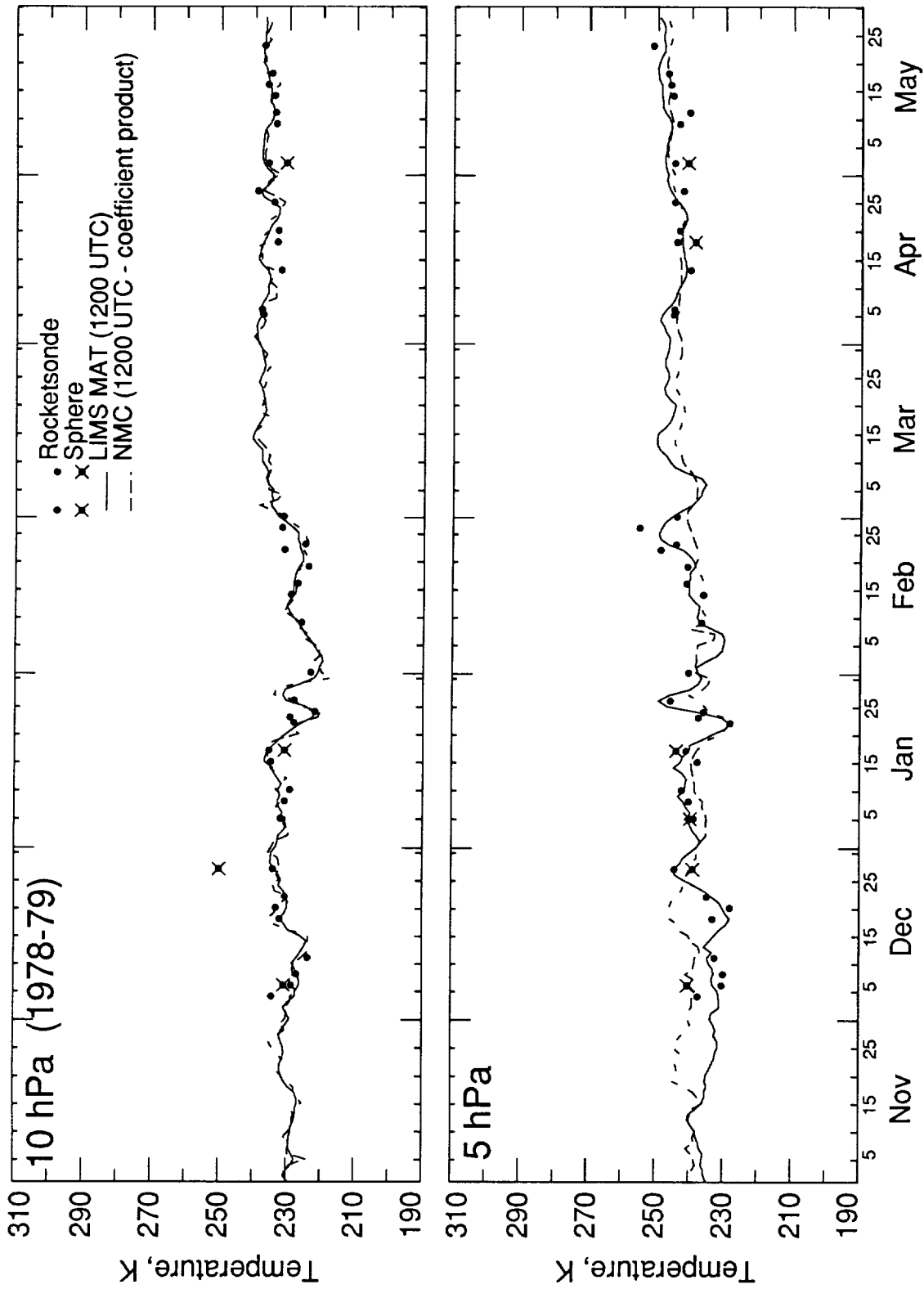
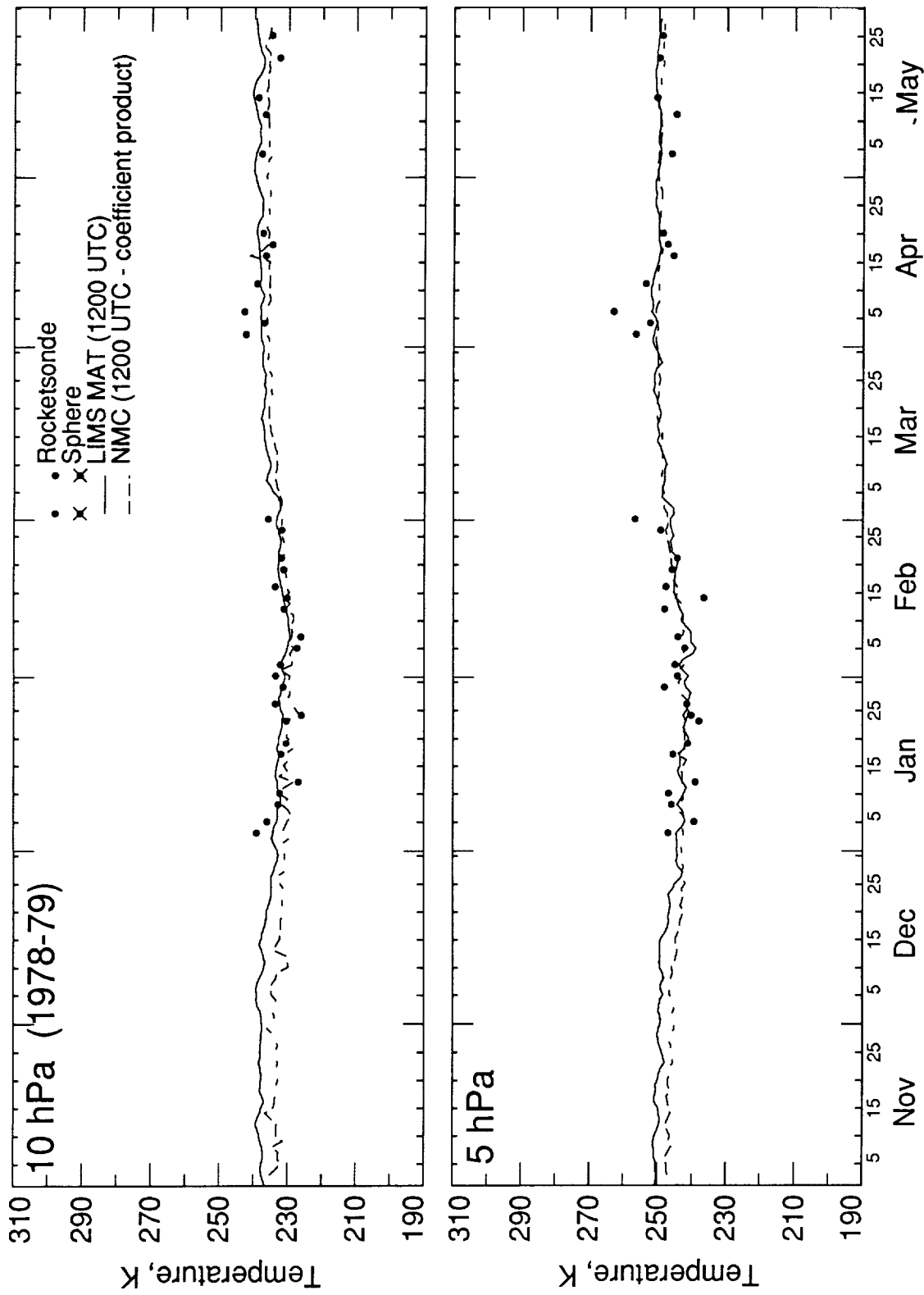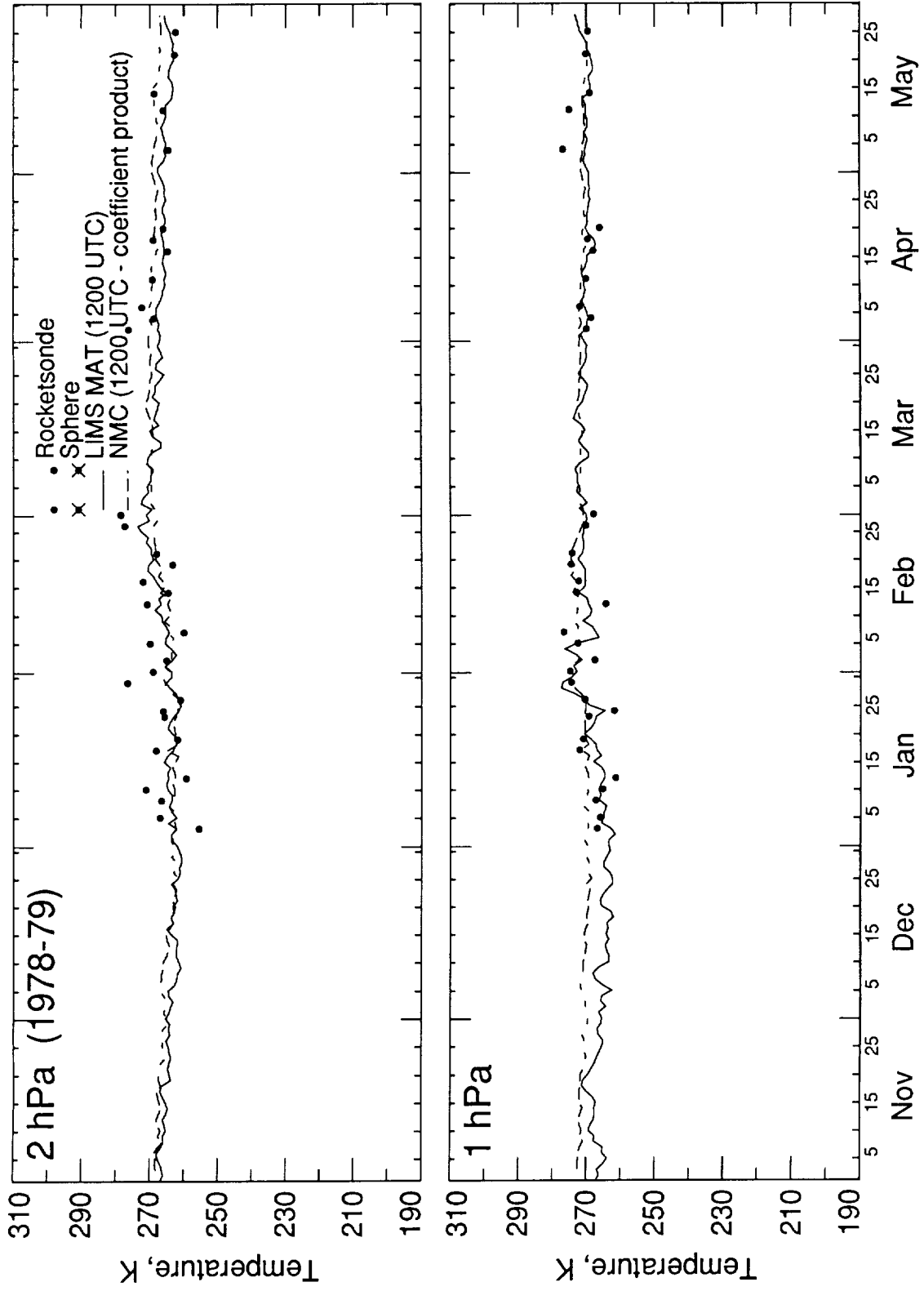Figure A8. Cape Canaveral (29° N, 279° E).
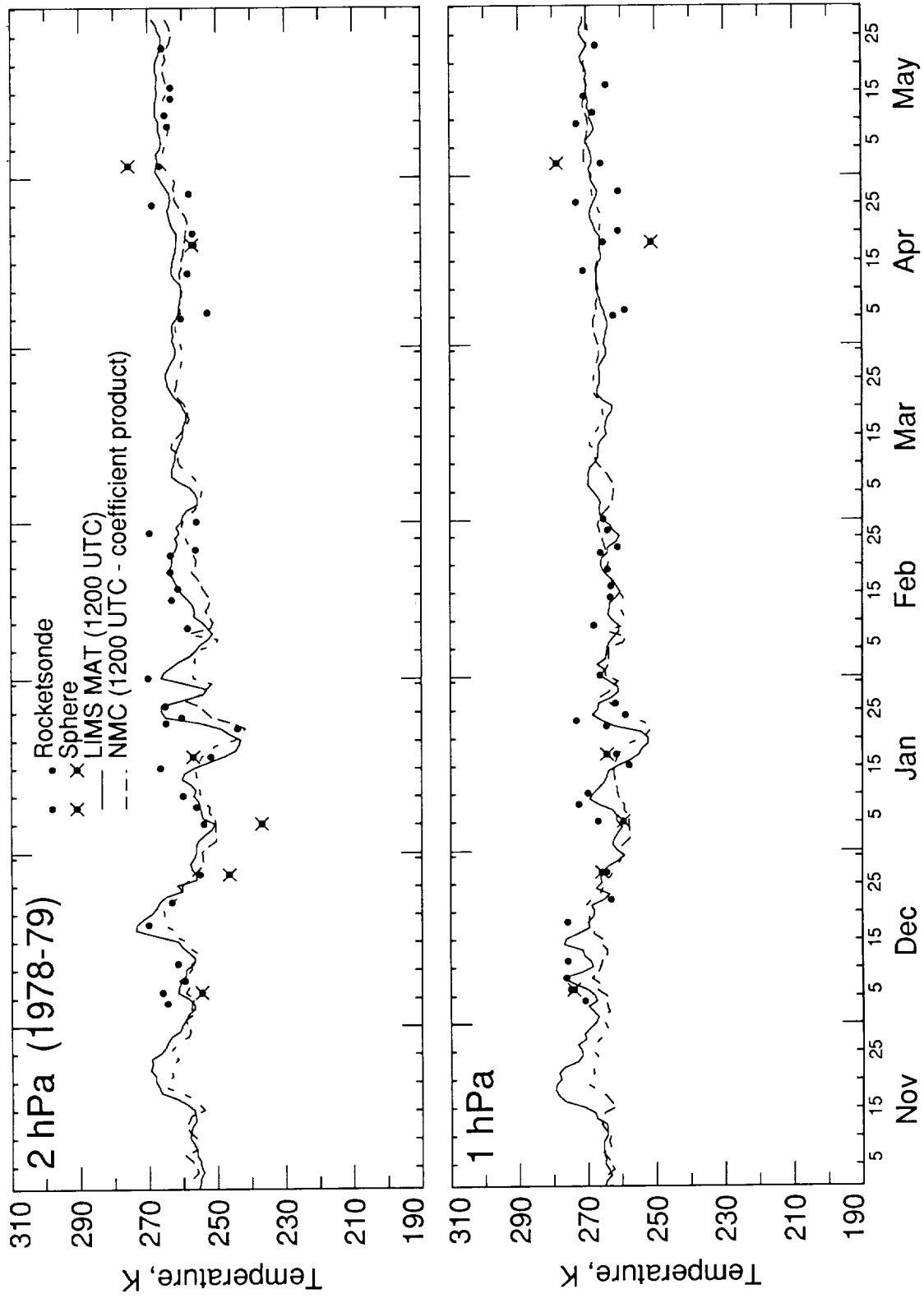
Figure A8. Continued.
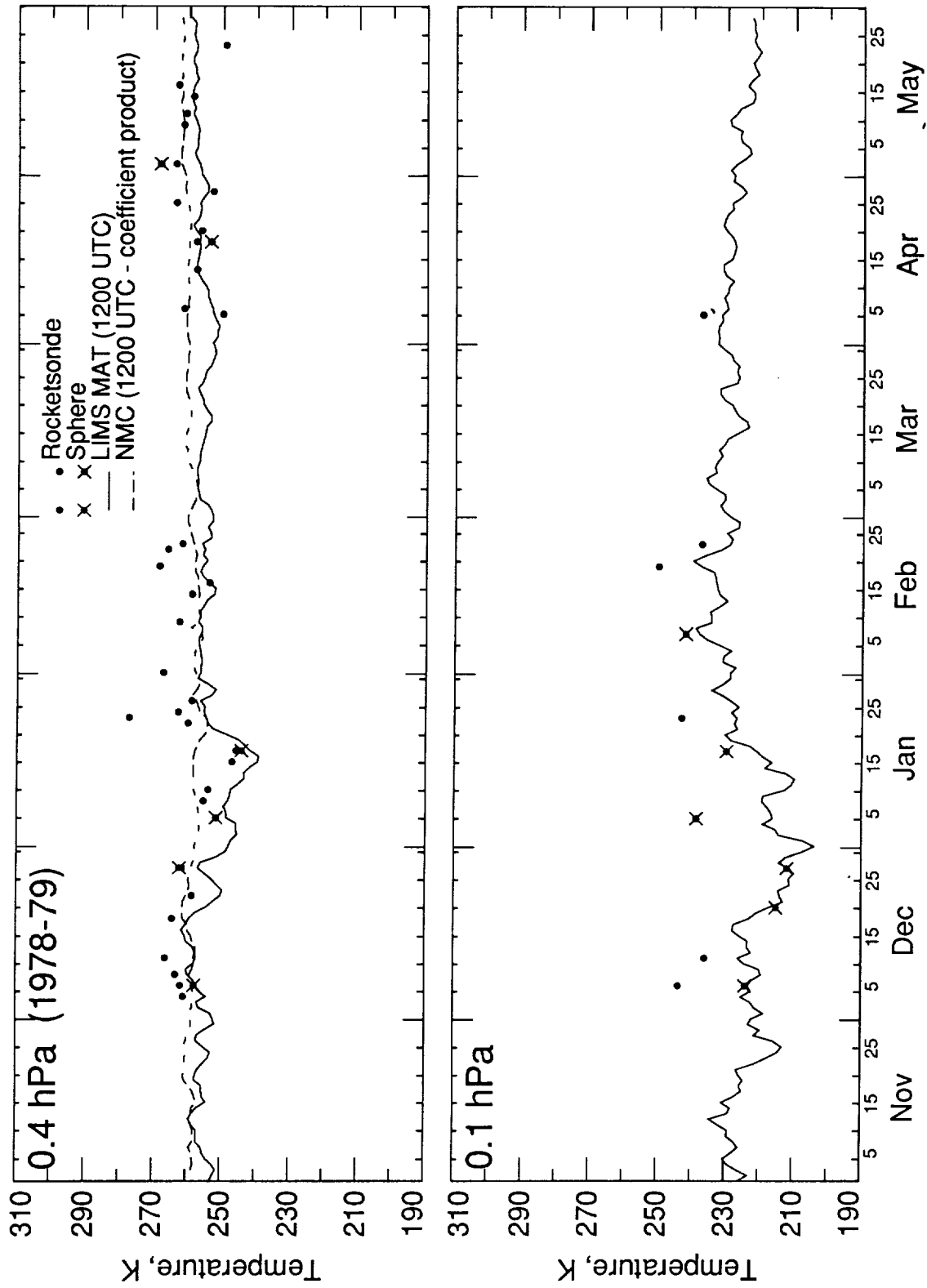
Figure A8. Continued.

Figure A8. Concluded.

(LIMS minus rocketsonde temperature)

— Mean

Feb

(2/0)
(6/0)
(8/0)
(8/0)
(8/0)
(8/0)

7-mo average

(5/1)
(34/1)
(38/0)
(38/0)
(40/0)
(40/0)

Jan

(1/0)
(8/1)
(10/0)
(10/0)
(10/0)
(10/0)

May

(0/0)
(6/0)
(6/0)
(6/0)
(7/0)
(7/0)

Dec

(1/1)
(7/0)
(7/0)
(7/0)
(8/0)
(8/0)

Apr

(1/0)
(7/0)
(7/0)
(7/0)
(7/0)
(7/0)

Nov

(0/0)
(0/0)
(0/0)
(0/0)
(0/0)
(0/0)

Mar

(0/0)
(0/0)
(0/0)
(0/0)
(0/0)
(0/0)

Pressure, hPa

.01
.1
1
10
100

Temperature difference, K

-20 -10 0 10 20

87
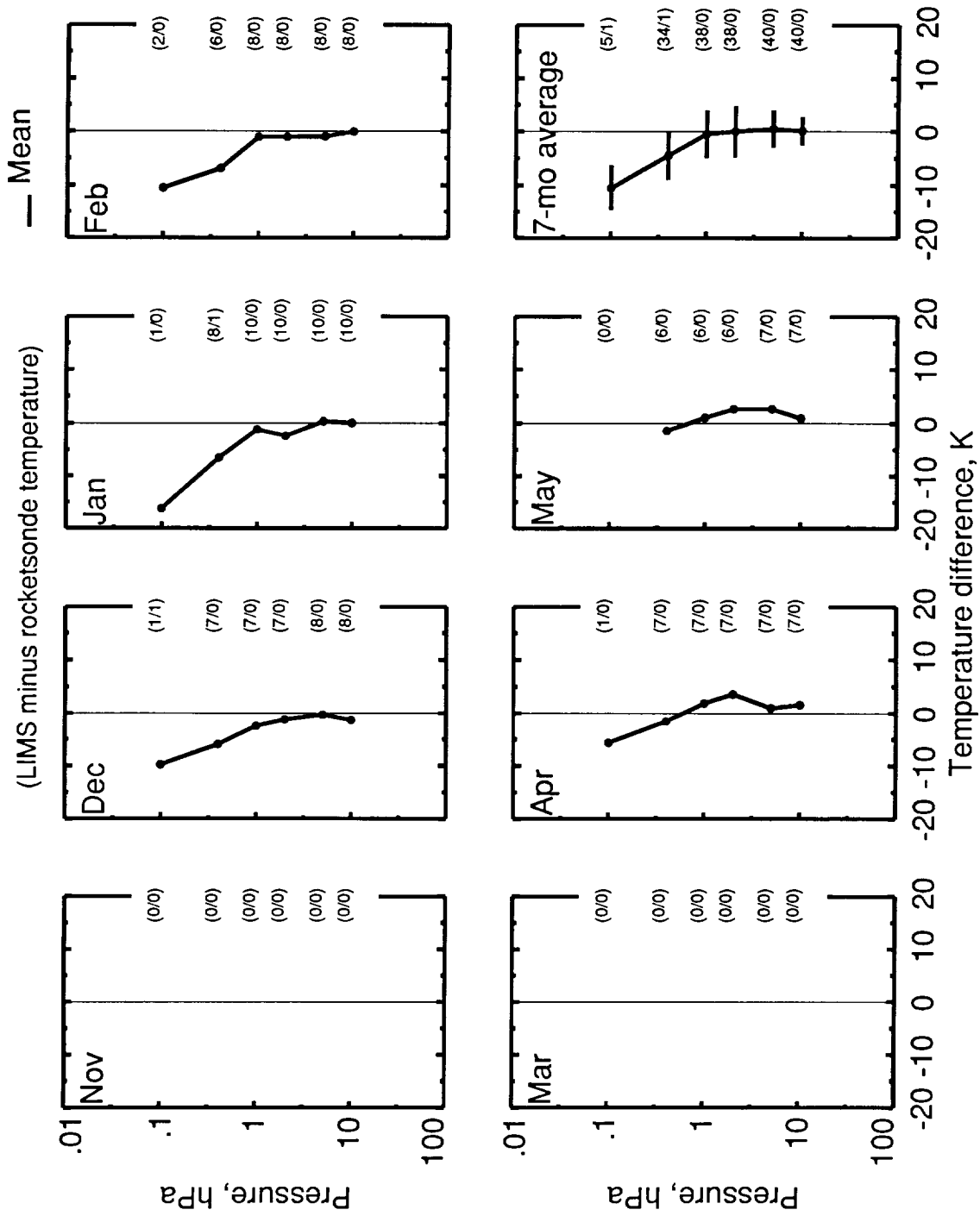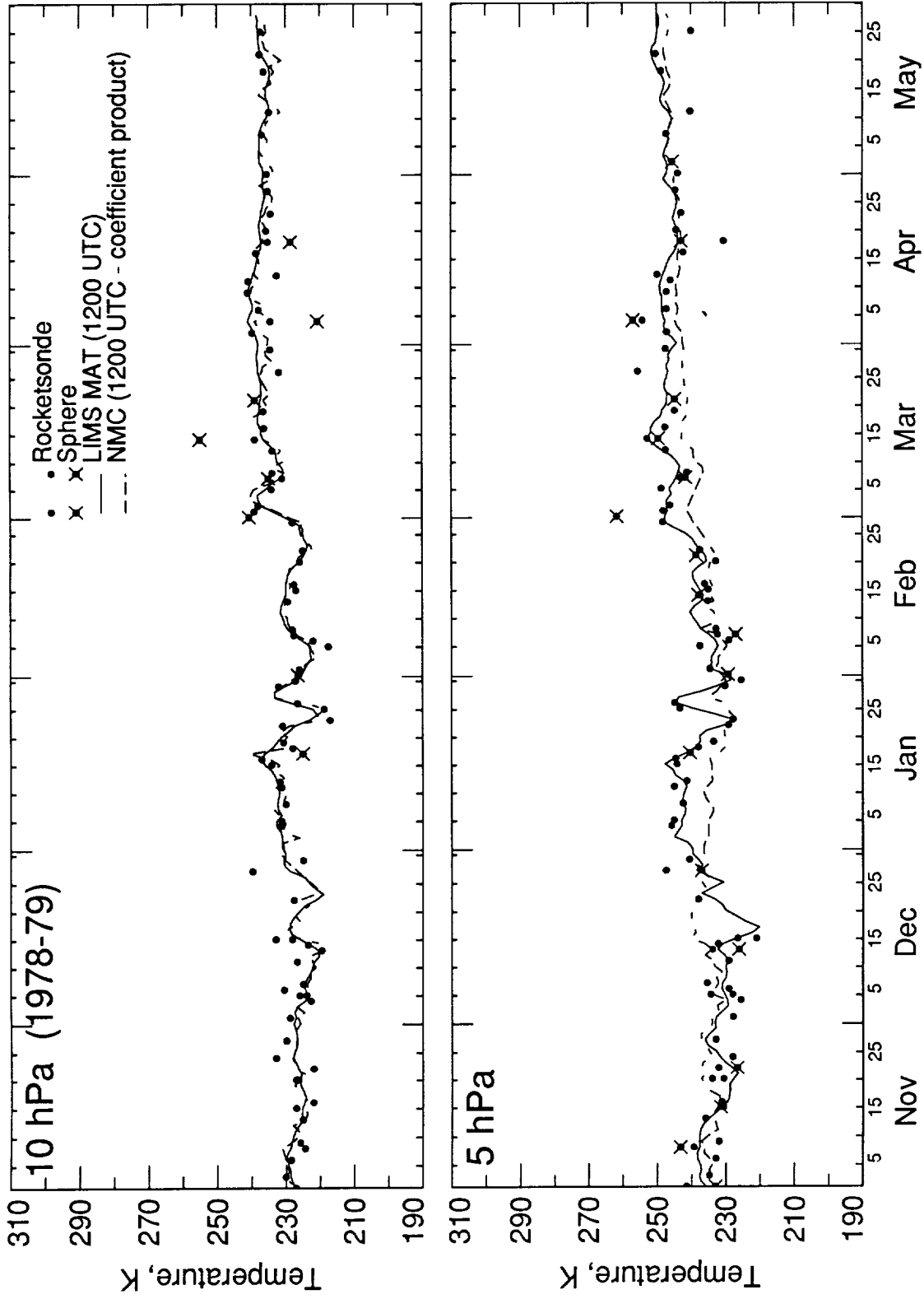
Figure A9. White Sands (32° N, 254° E).

88
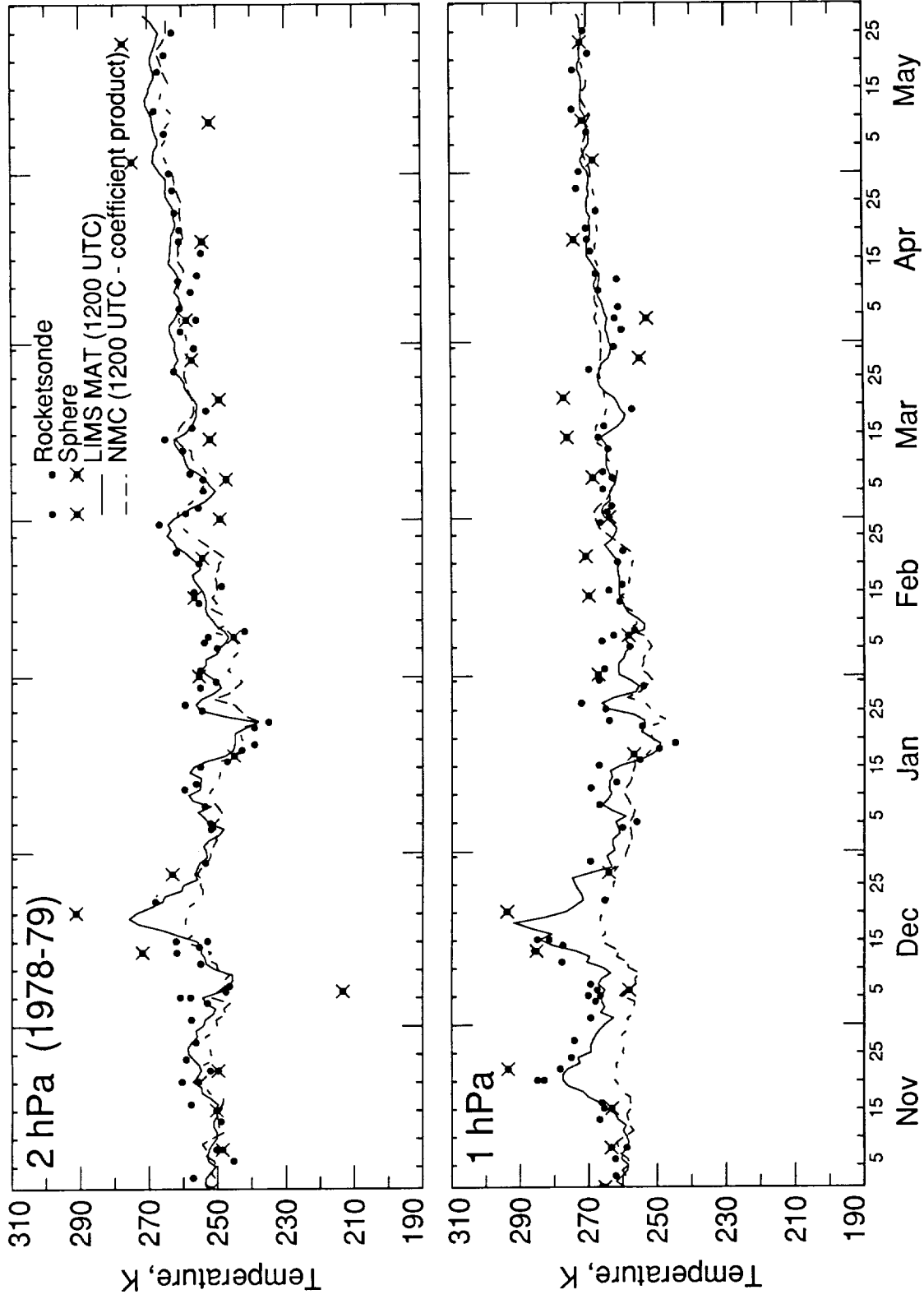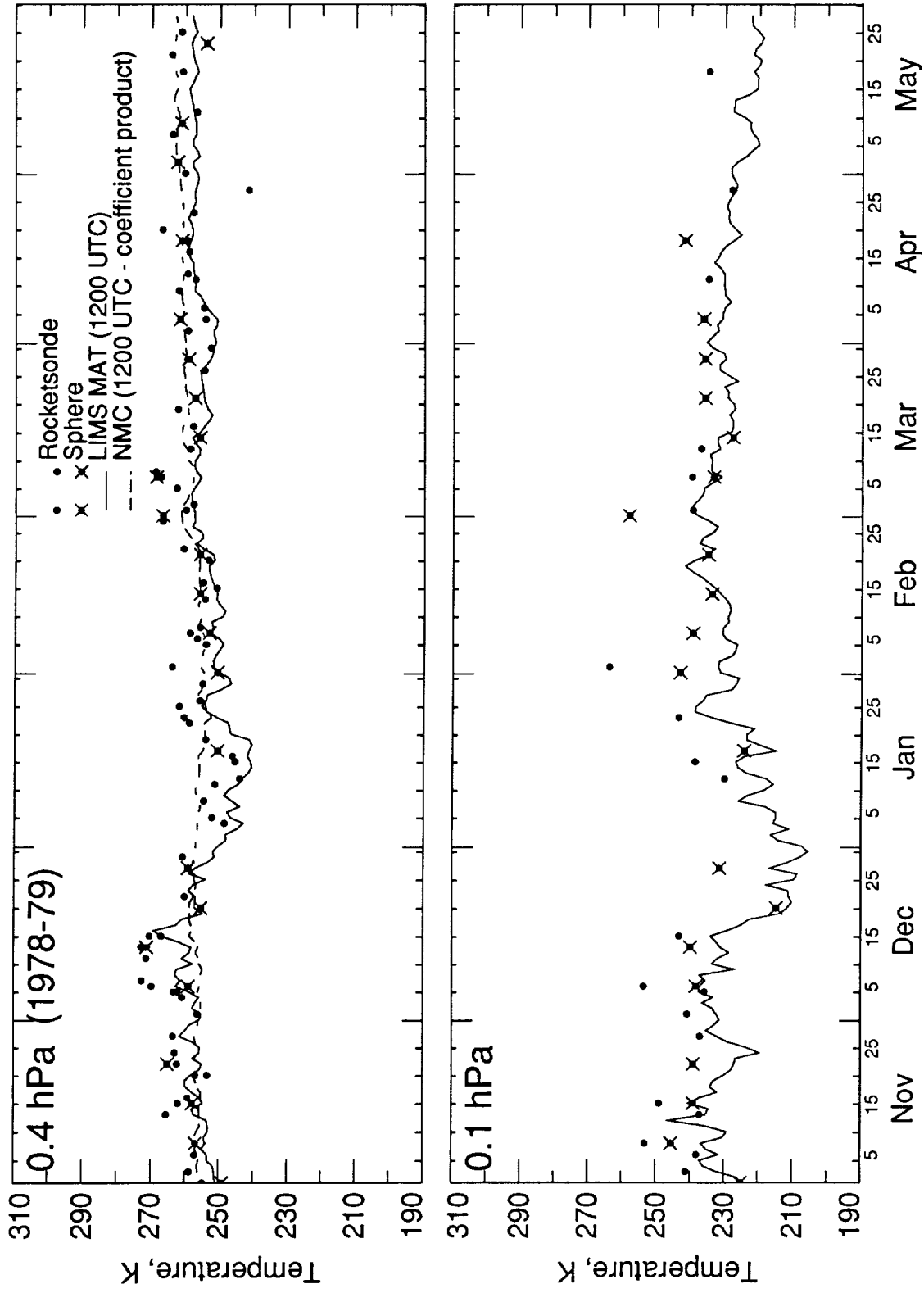
Figure A9. Continued.

Figure A9. Continued.

90

— Mean

(LIMS minus rocketsonde temperature)

Feb

(0/1)
(11/0)
(11/0)
(11/0)
(11/0)
(11/0)

Jan

(3/0)
(13/0)
(15/0)
(15/0)
(15/0)
(15/0)

Dec

(4/0)
(12/0)
(13/0)
(13/0)
(14/0)
(14/0)

Nov

(6/0)
(12/0)
(12/0)
(12/0)
(13/0)
(13/0)

7-mo average

(19/1)
(75/0)
(79/0)
(79/0)
(81/0)
(81/0)

May

(1/0)
(5/0)
(5/0)
(5/0)
(5/0)
(5/0)

Apr

(2/0)
(12/0)
(12/0)
(12/0)
(12/0)
(12/0)

Mar

(3/0)
(10/0)
(11/0)
(11/0)
(11/0)
(11/0)

Pressure, hPa

.01 .1 1 10 100

-20 -10 0 10 20

Temperature difference, K
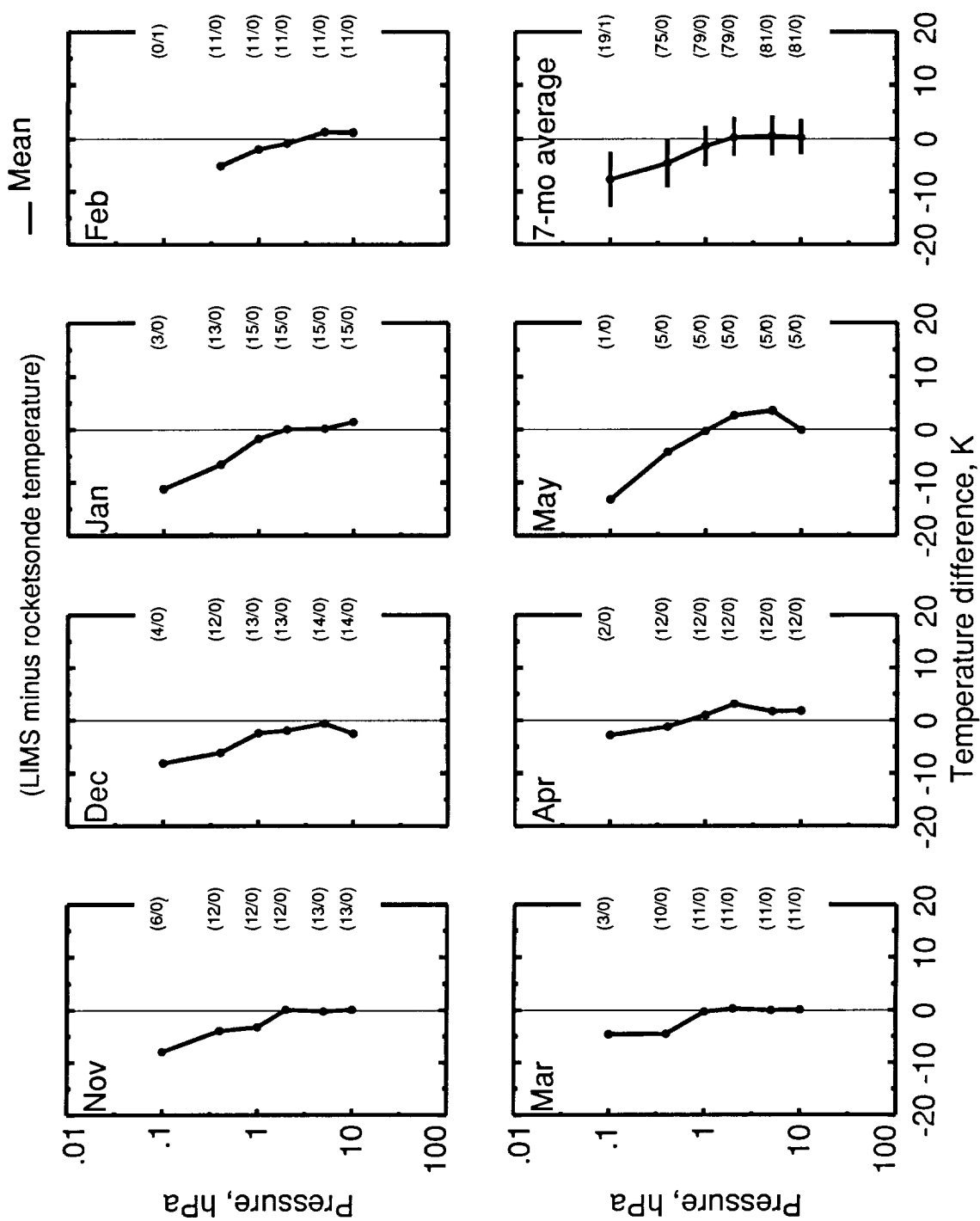
Figure A9. Concluded.

91
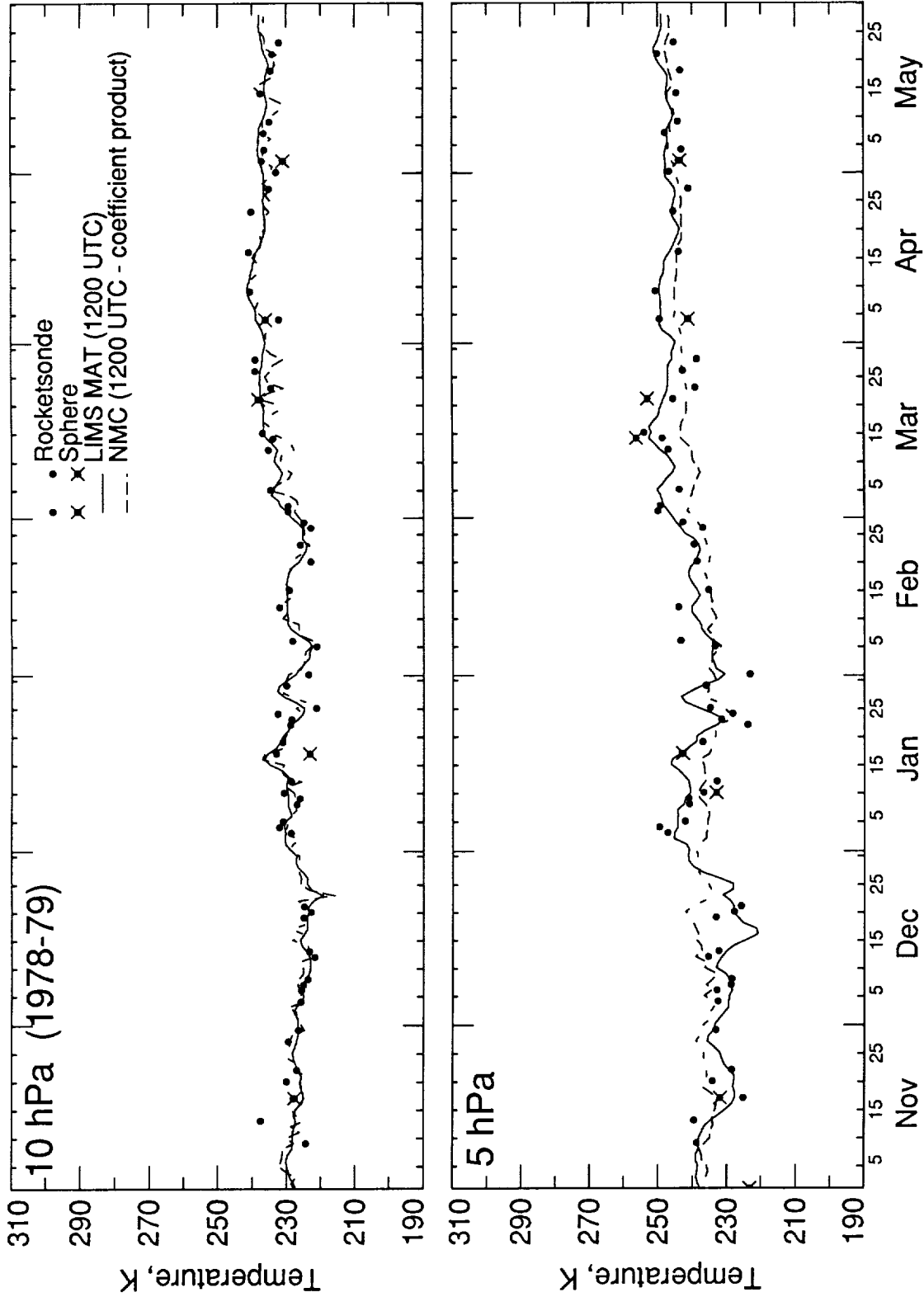
Figure A10. Point Mugu (34° N, 241° E).

Figure A10. Continued.

93
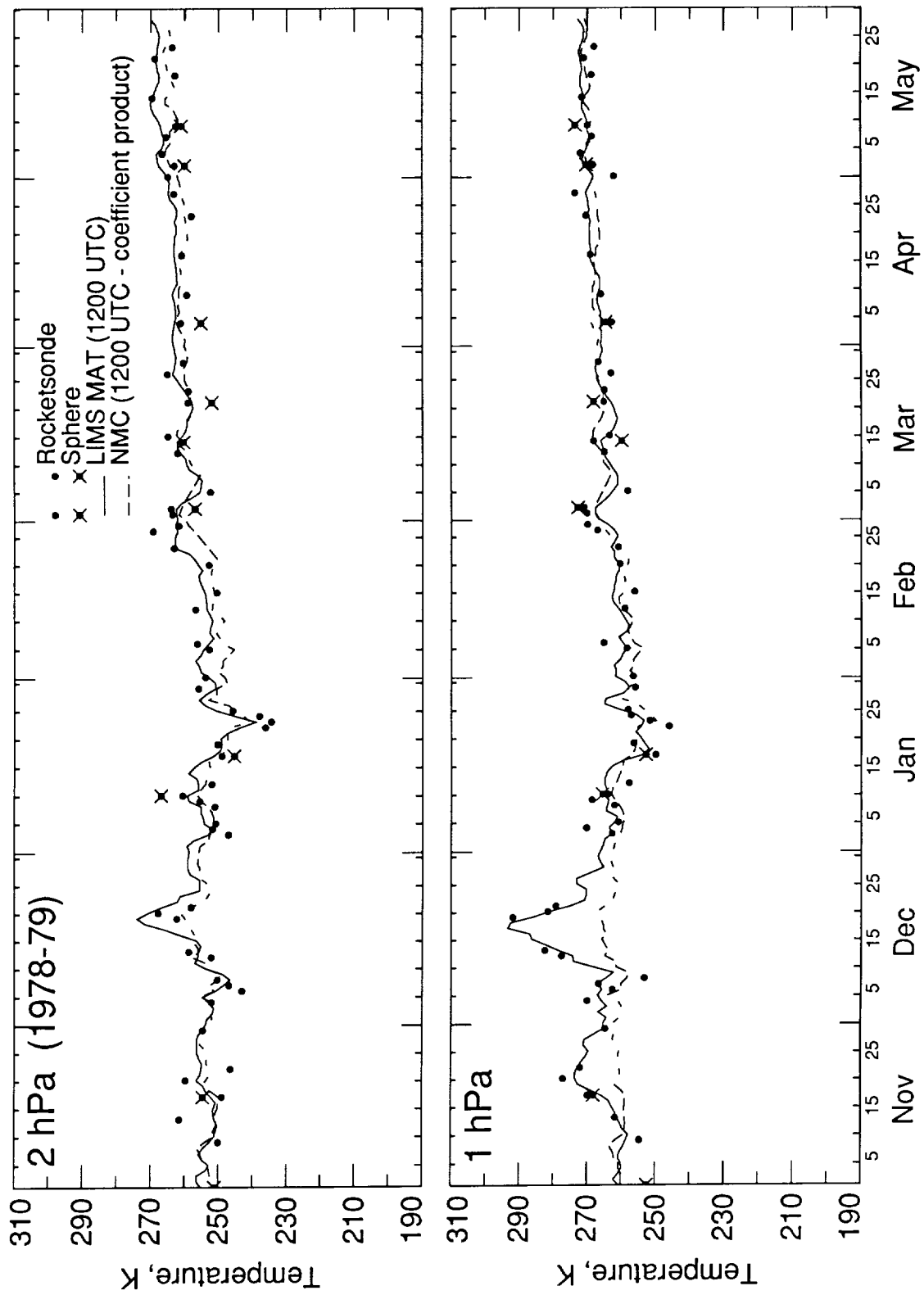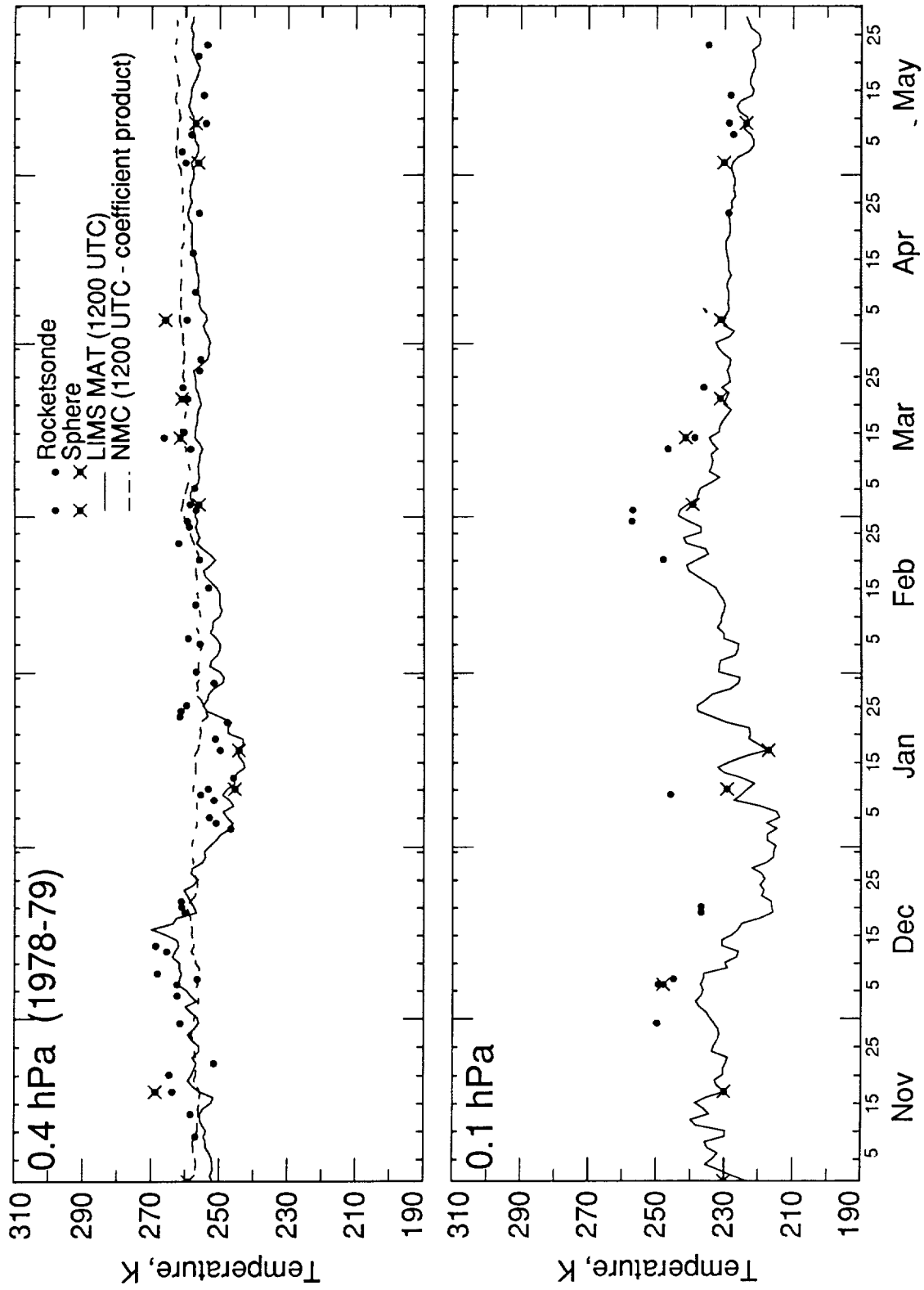
Figure A10. Continued.
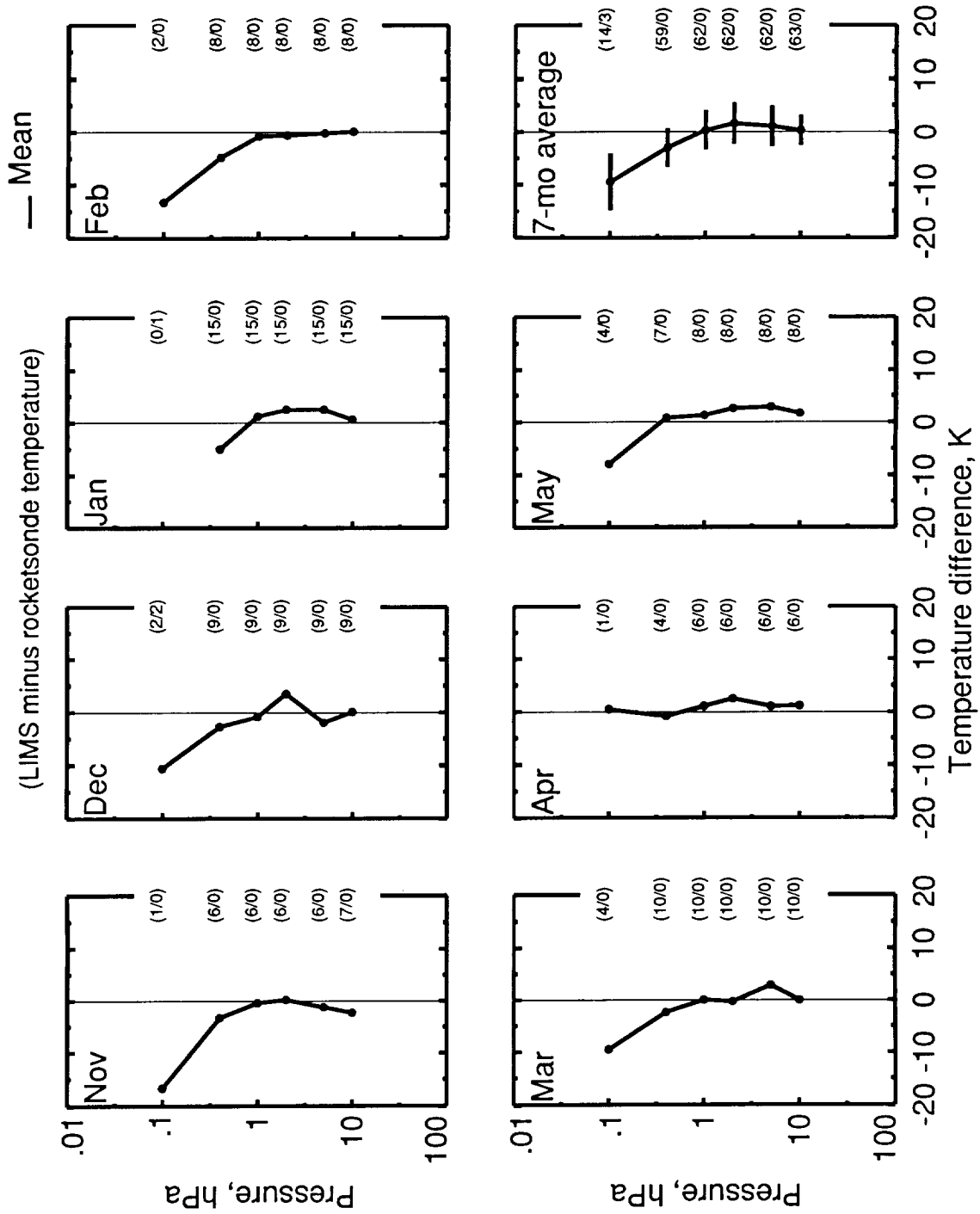
Figure A10. Concluded.

C-2
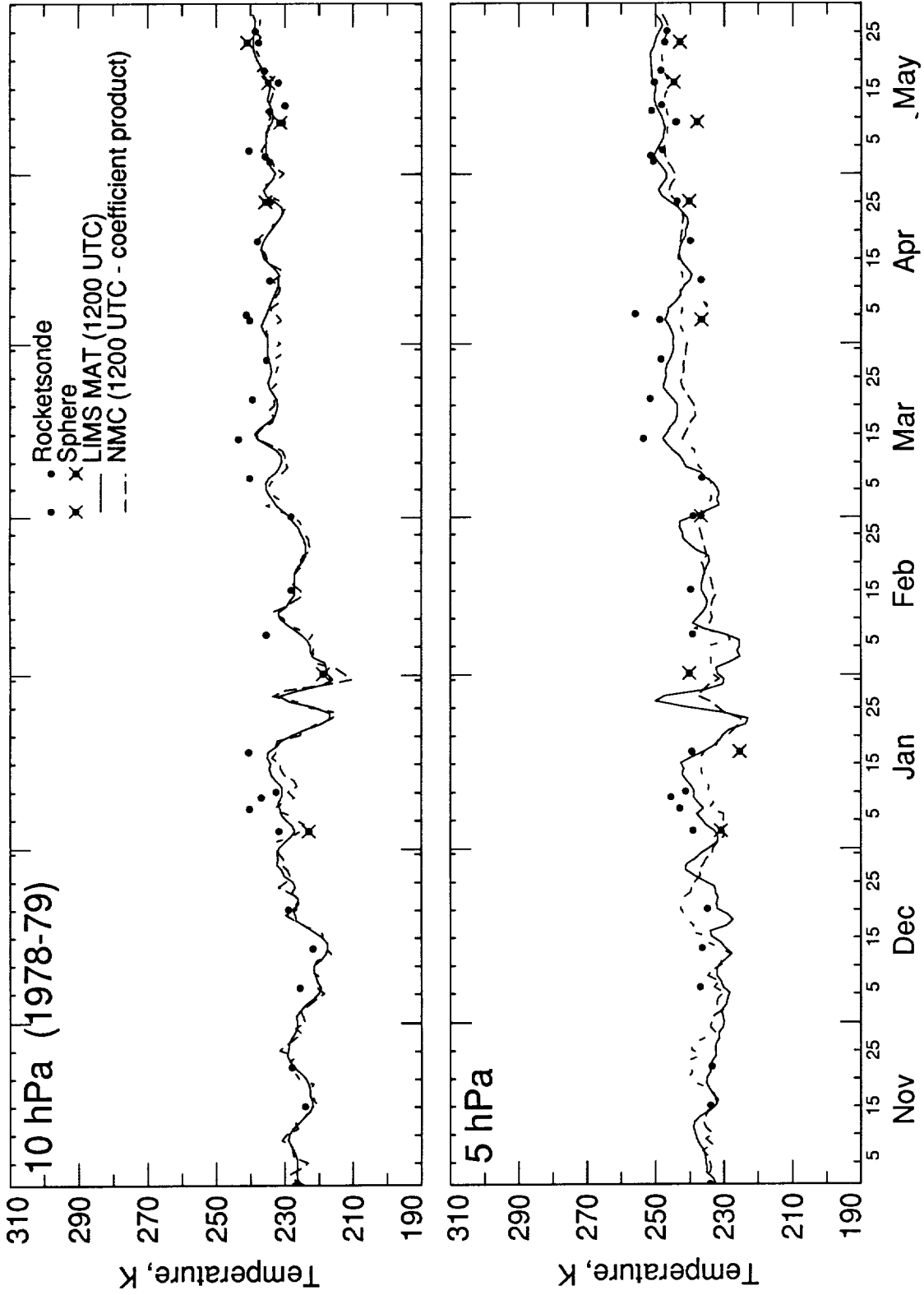
Figure A11. Wallops Island (38° N, 285° E).
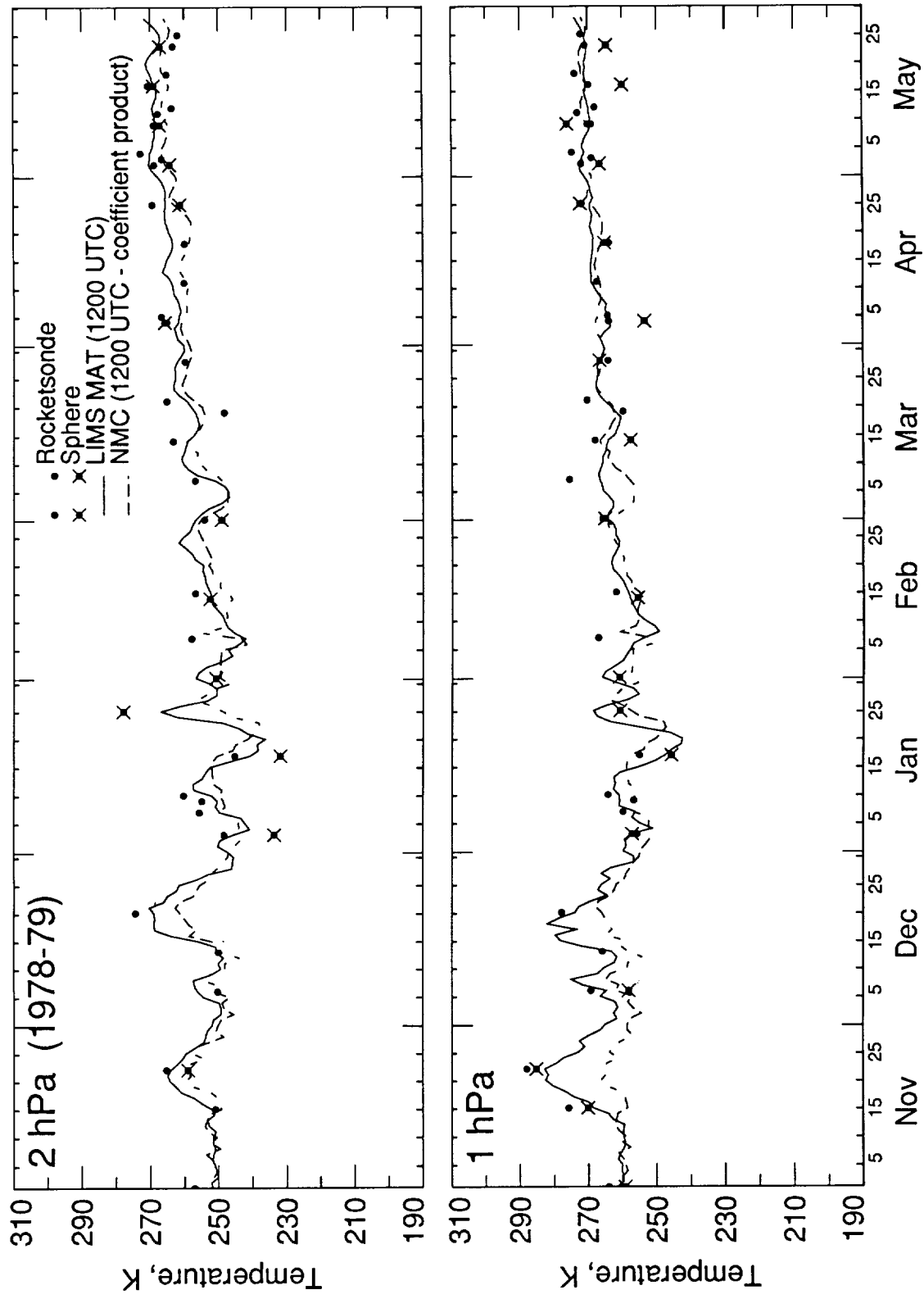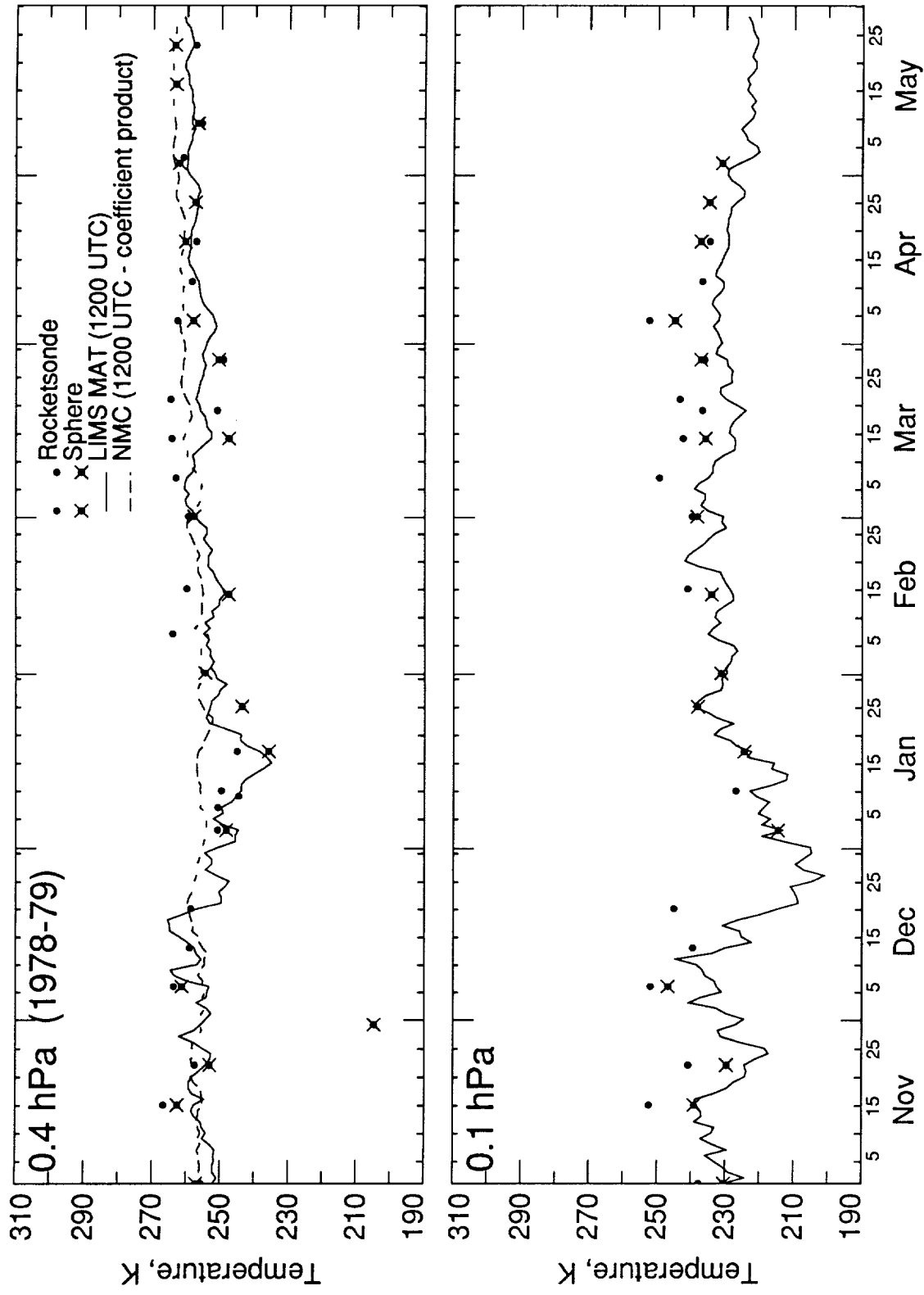
Figure A11. Continued.

Figure A11. Continued.

(LIMS minus rocketsonde temperature)

— Mean
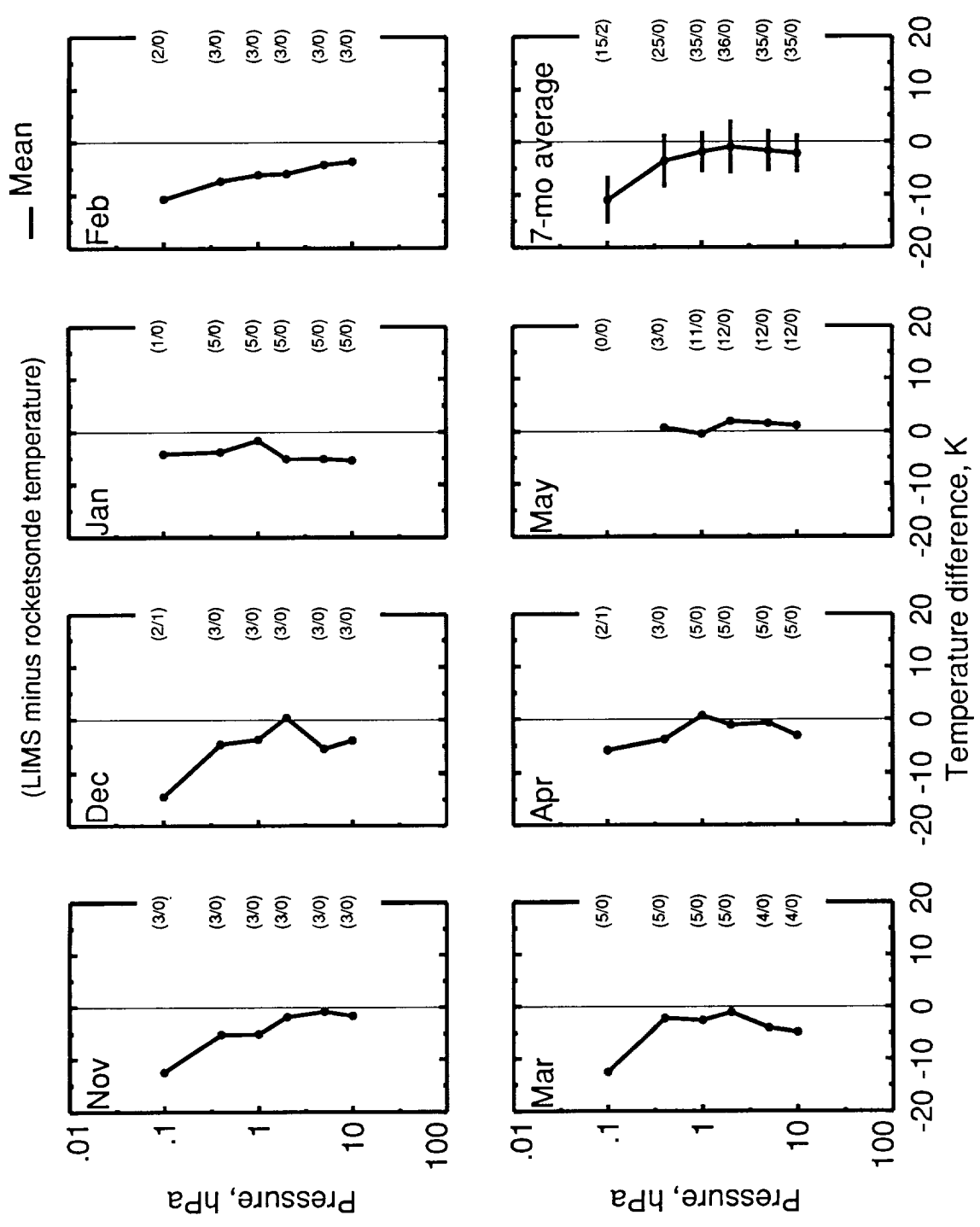
Figure A11. Concluded.

99
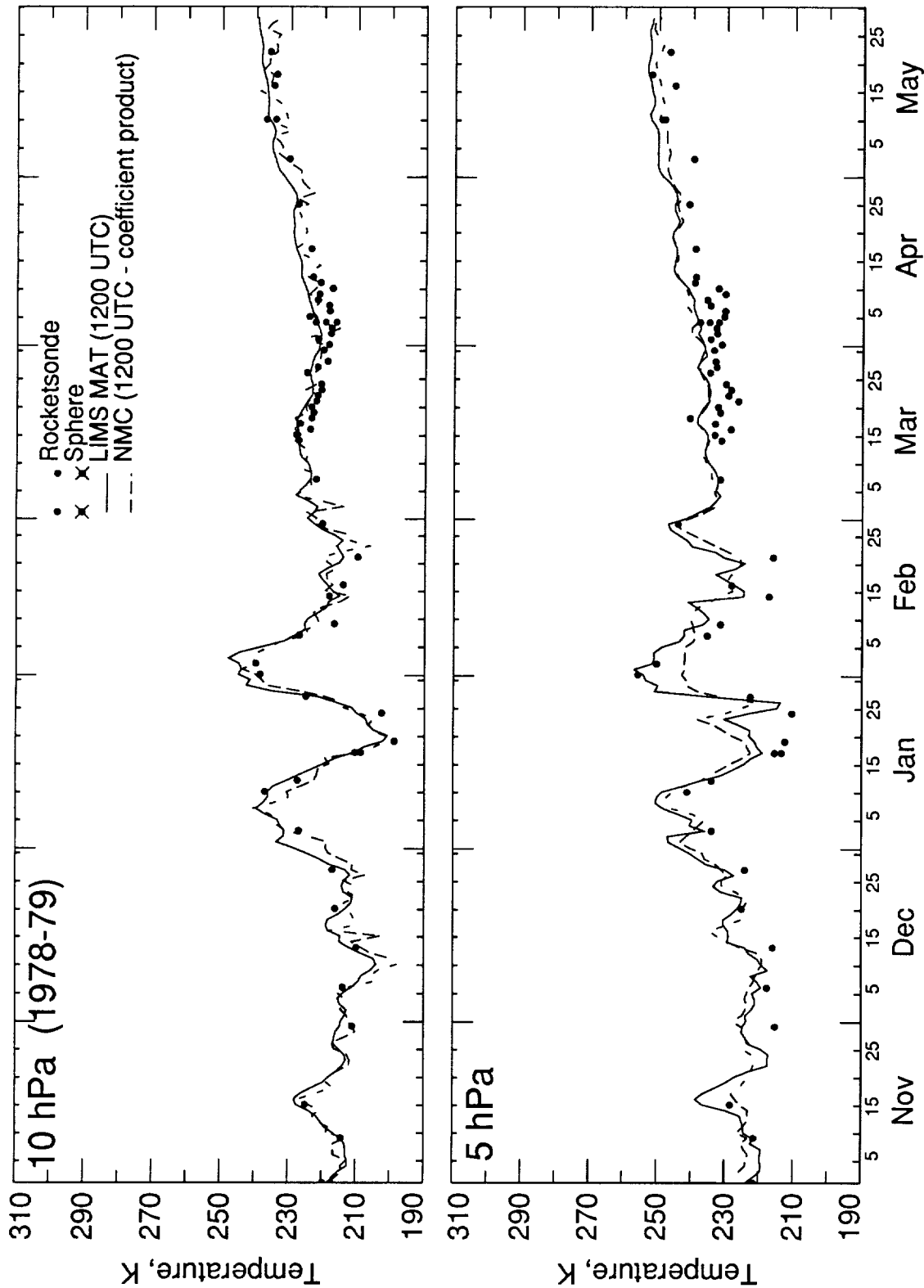
Figure A12. Volgograd, USSR (49° N, 44° E).
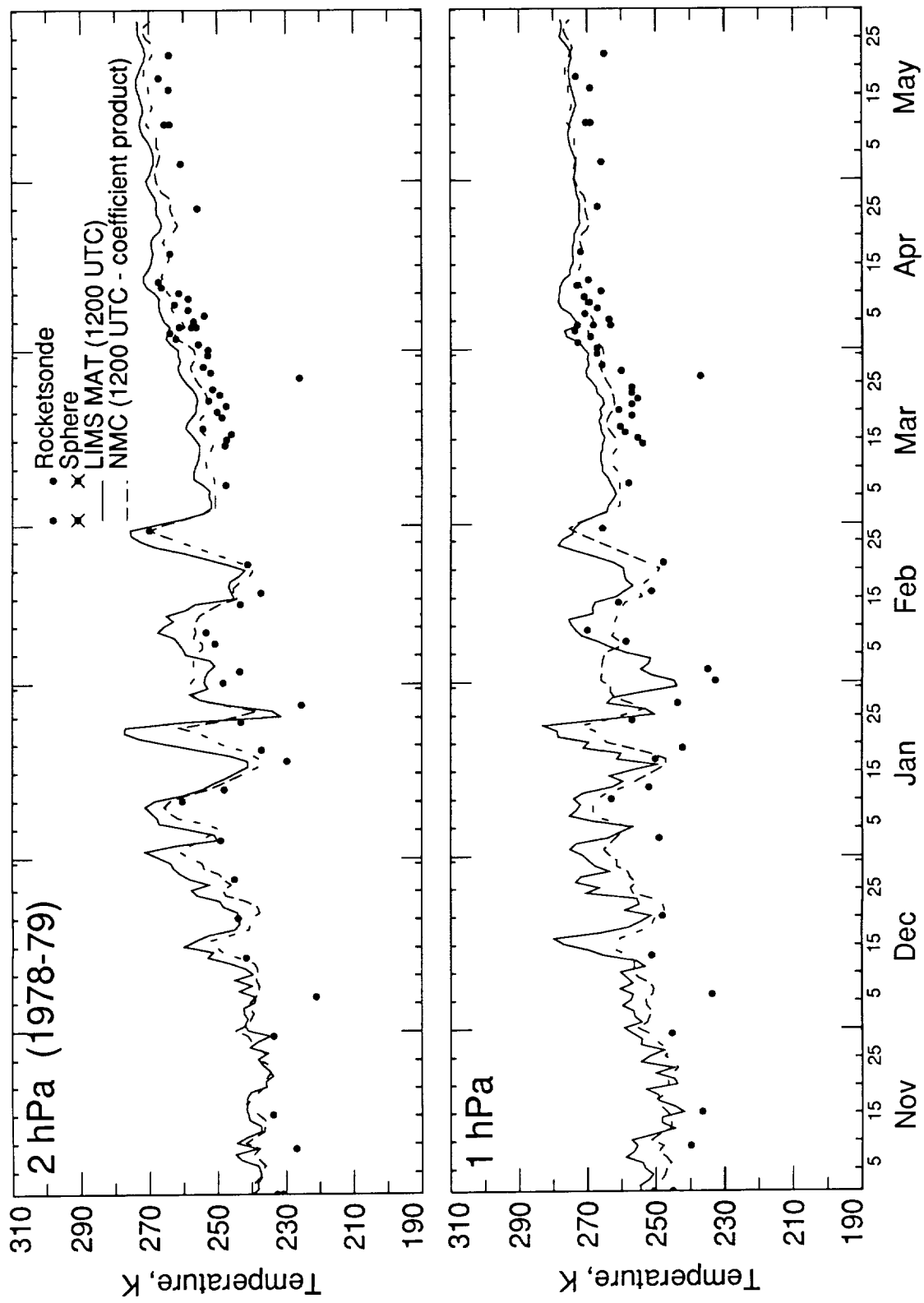
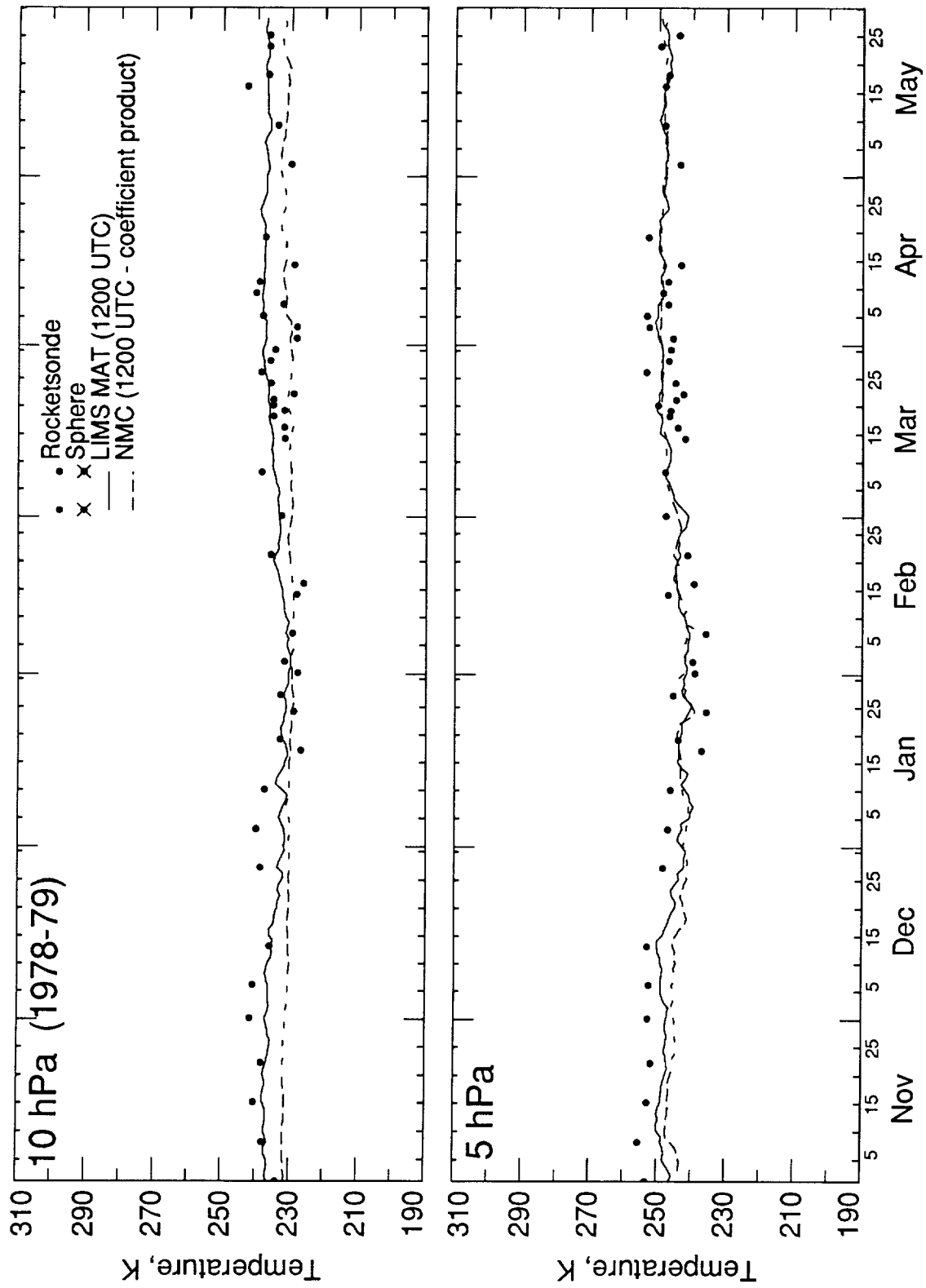Figure A12. Continued.
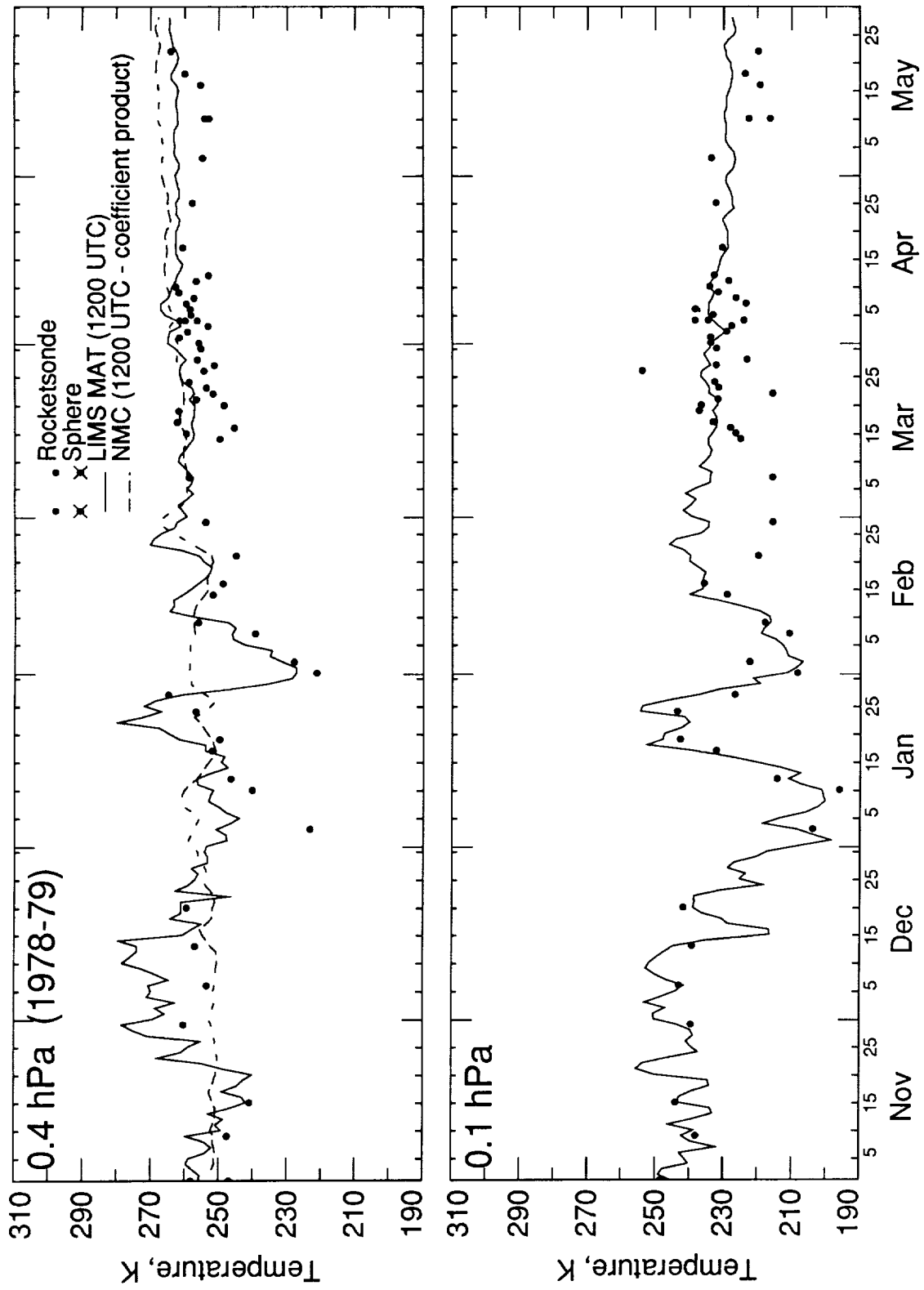
Figure A12. Continued.
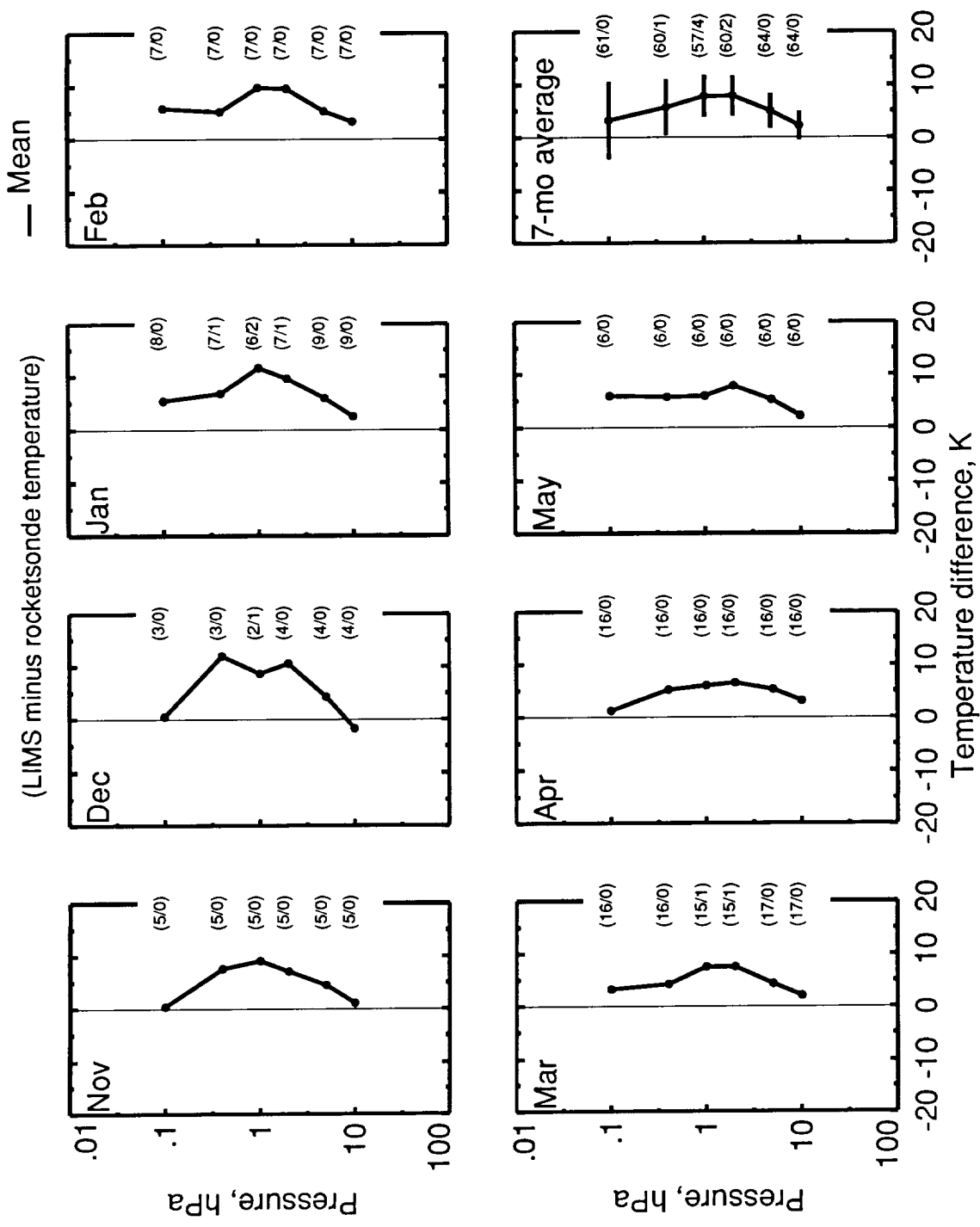
Figure A12. Concluded.

103
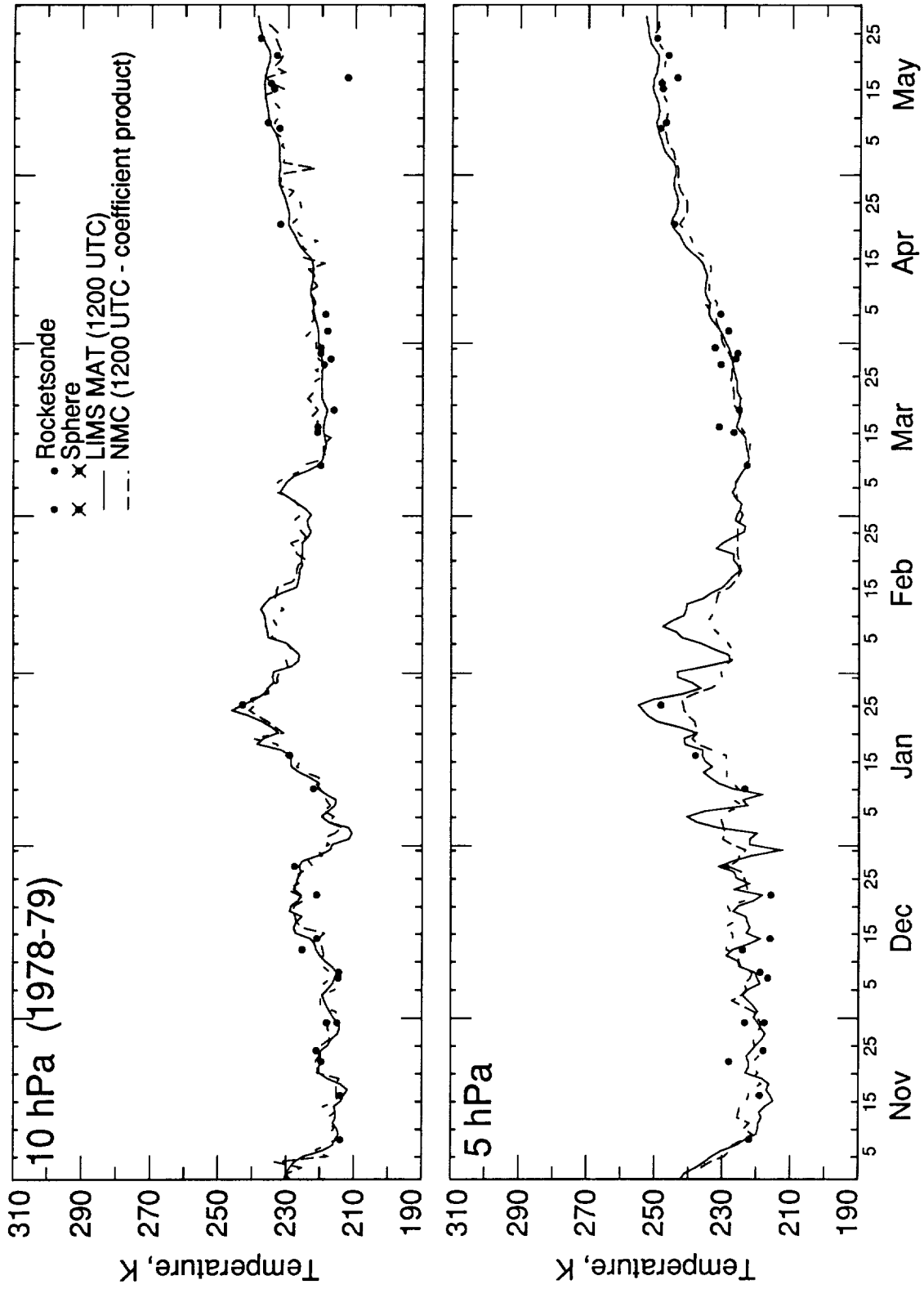
Figure A13. Shemya (53° N, 174° E).
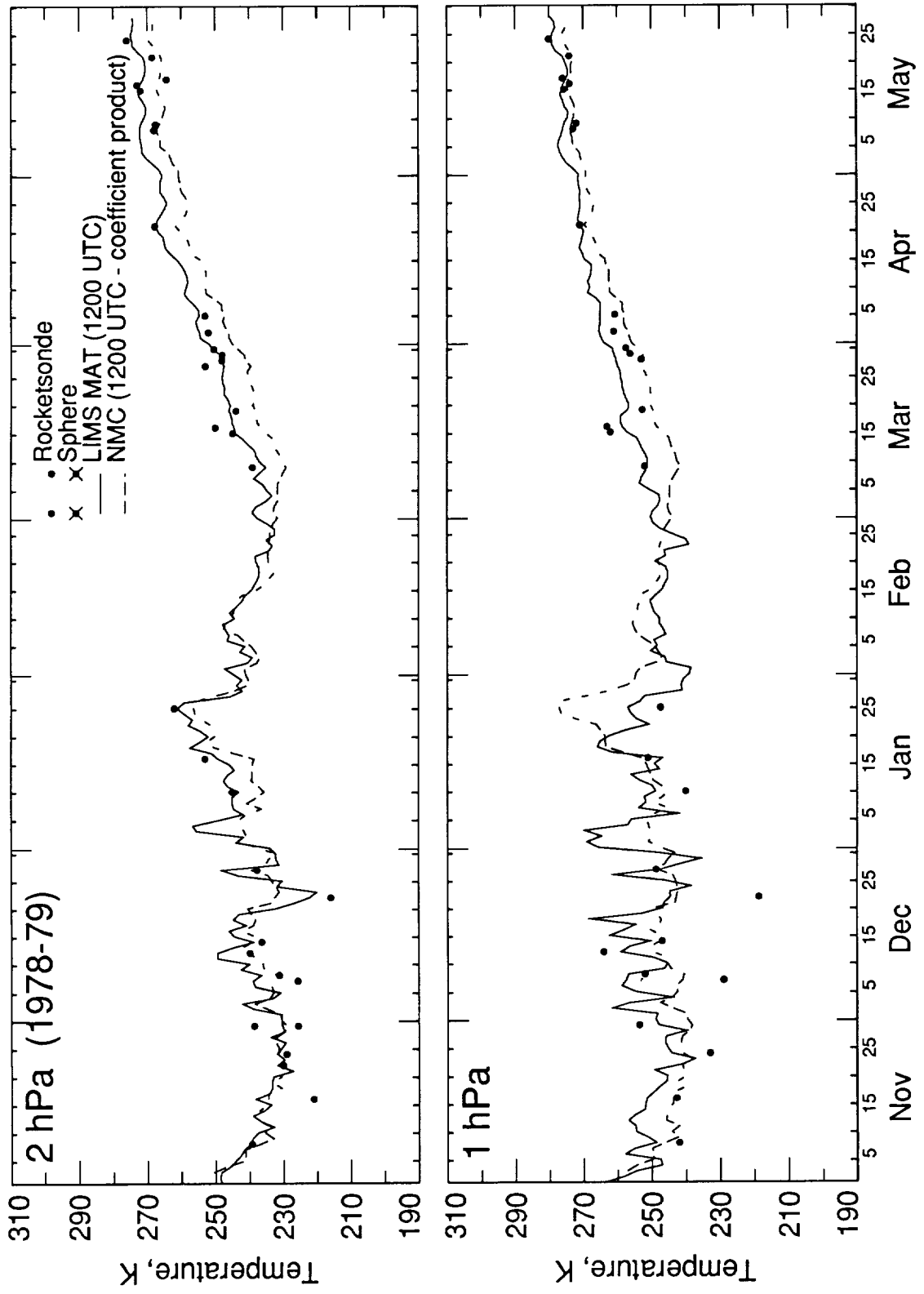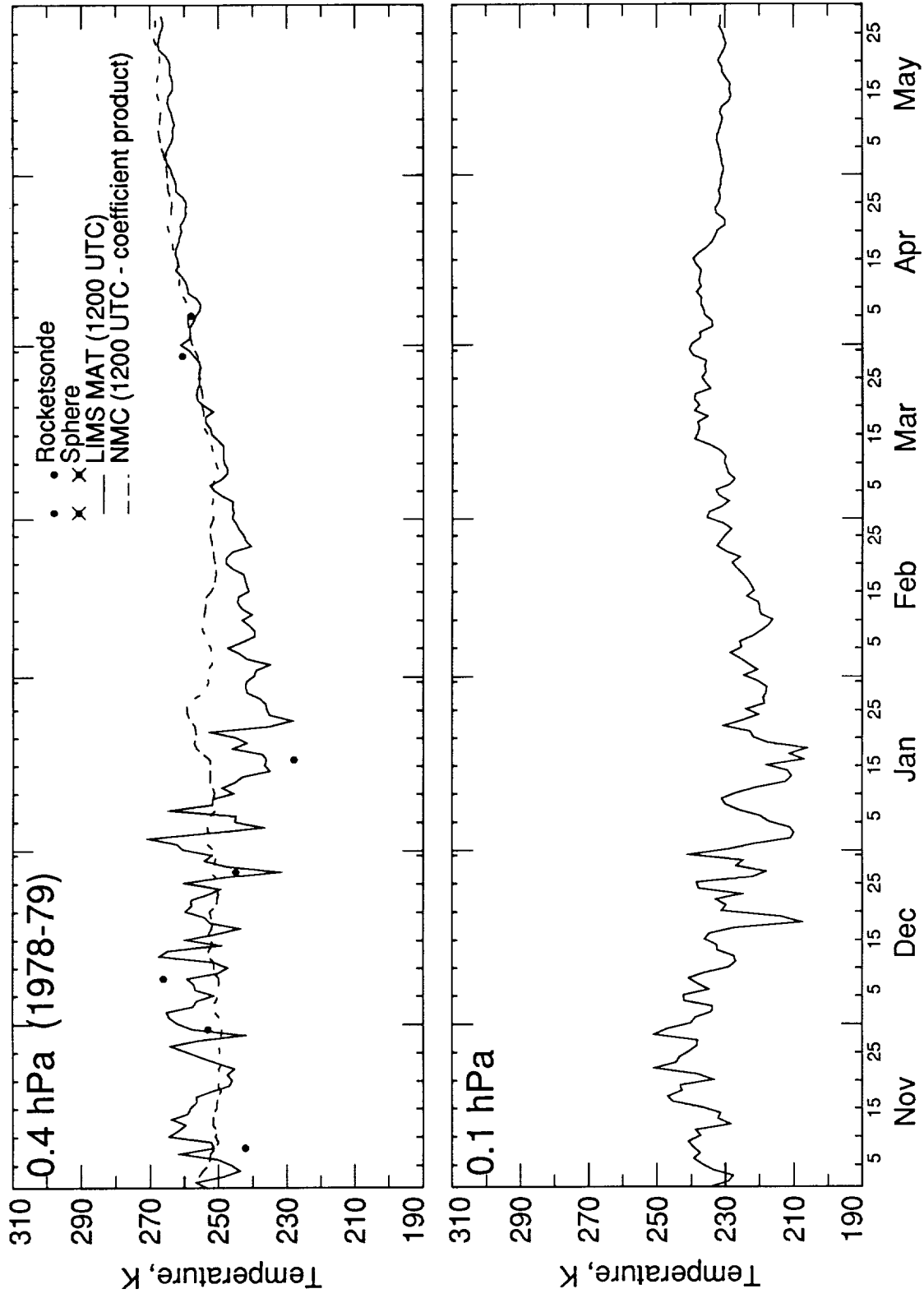
Figure A13. Continued.

Figure A13. Continued.

106
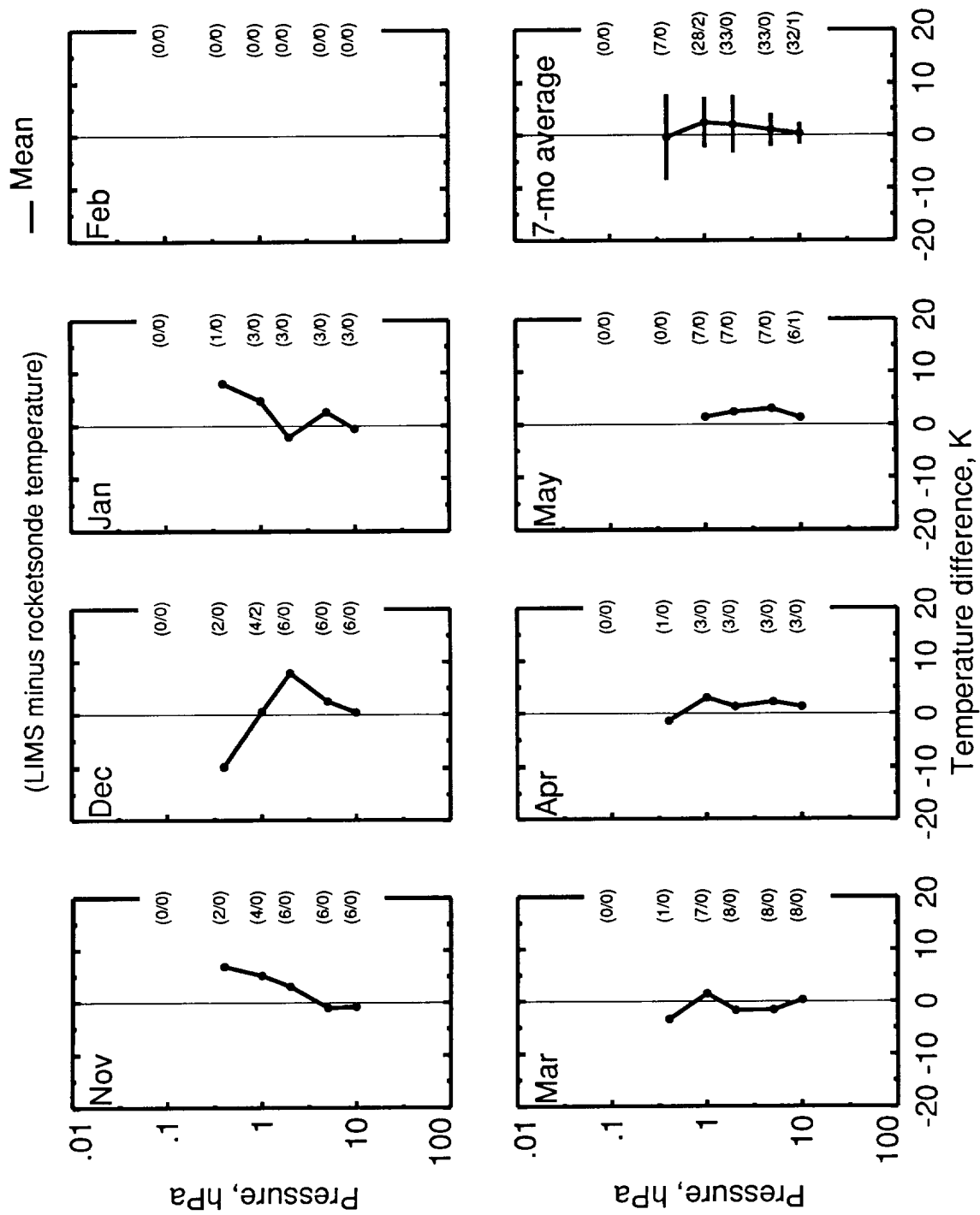
Figure A13. Concluded.

107
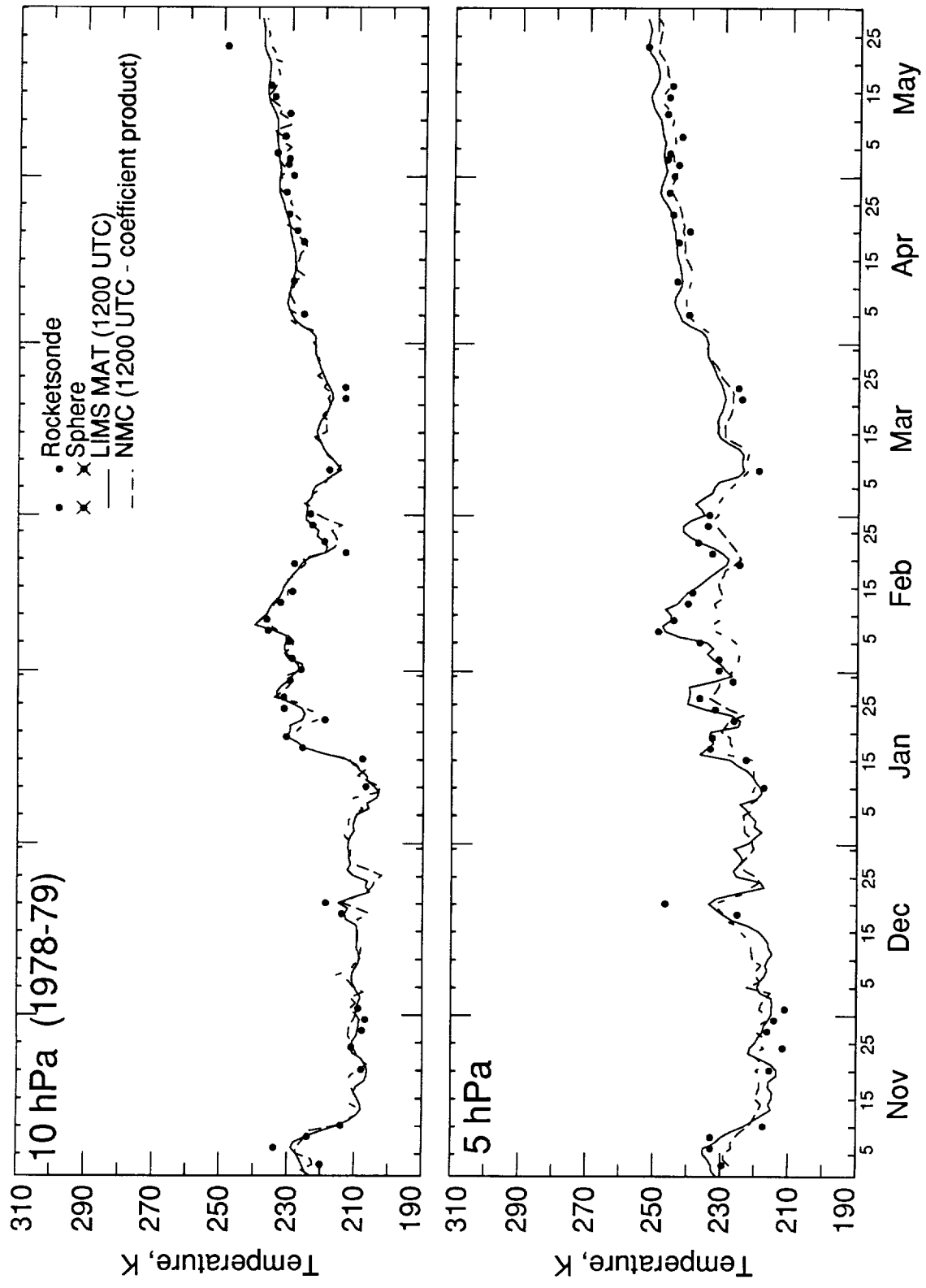
Figure A14. Primrose Lake (55° N, 250° E).

10 hPa (1978-79)

5 hPa

Temperature, K

Temperature, K

• Rocketsonde
× Sphere
—— LIMS MAT (1200 UTC)
—·— NMC (1200 UTC - coefficient product)
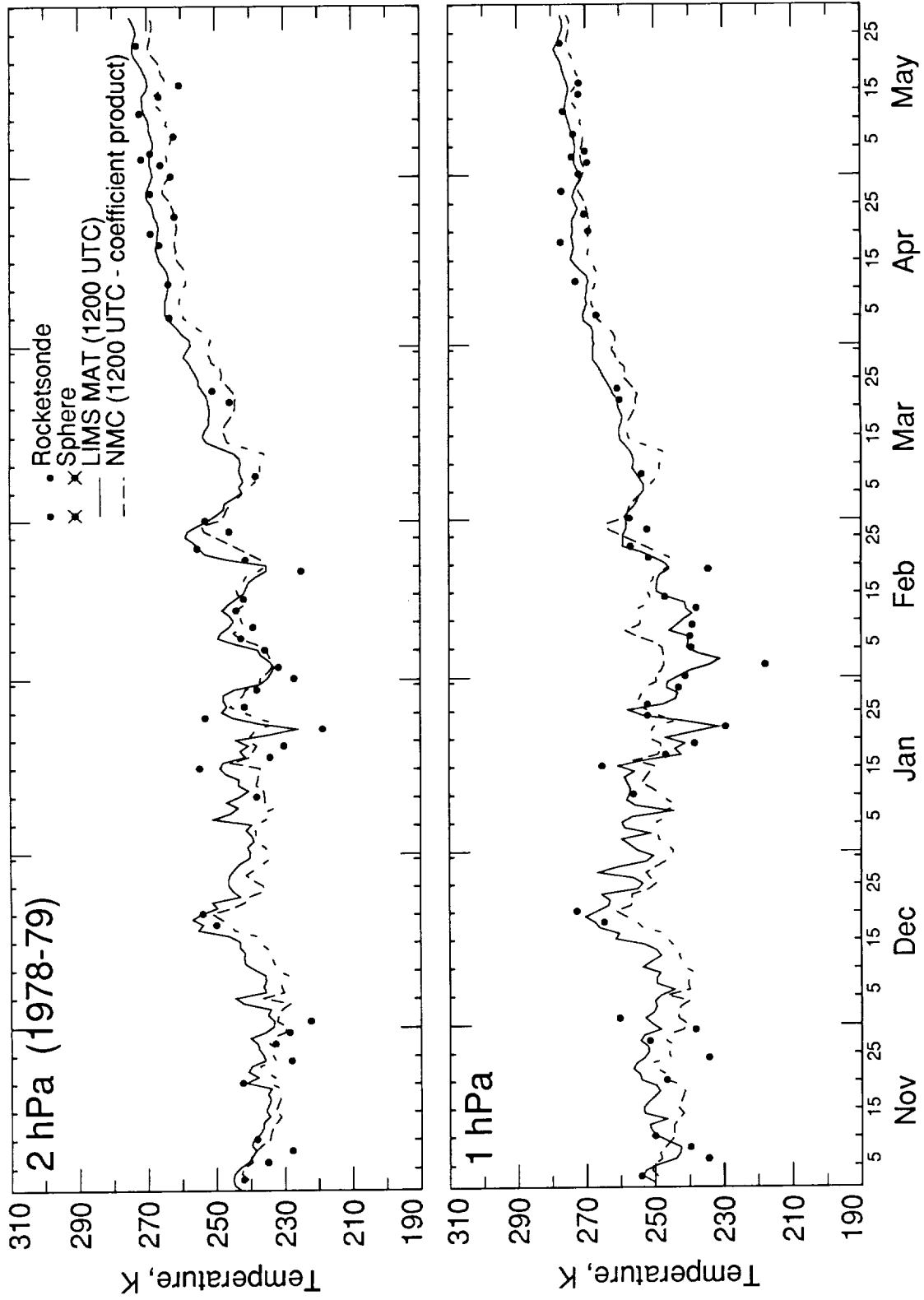
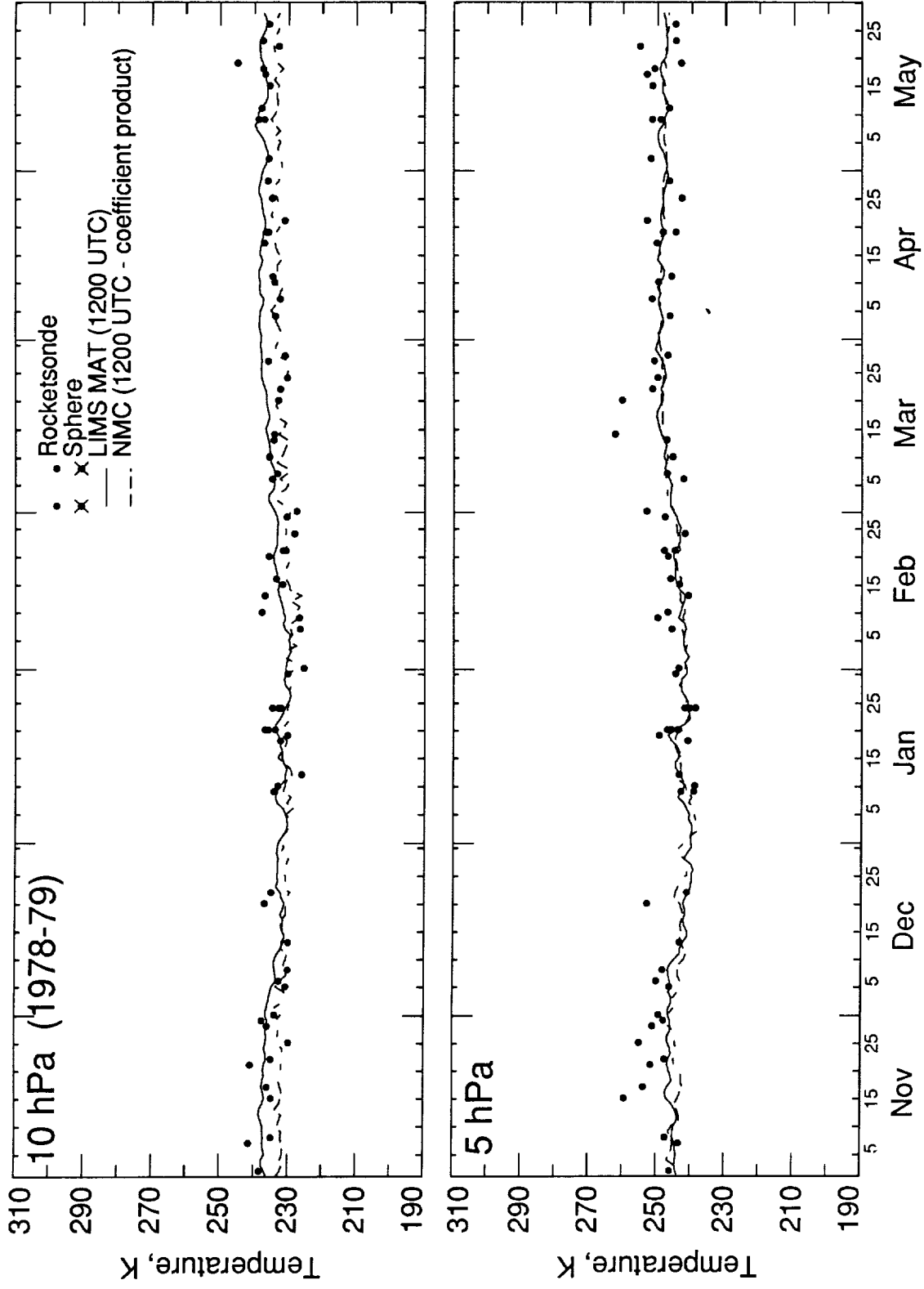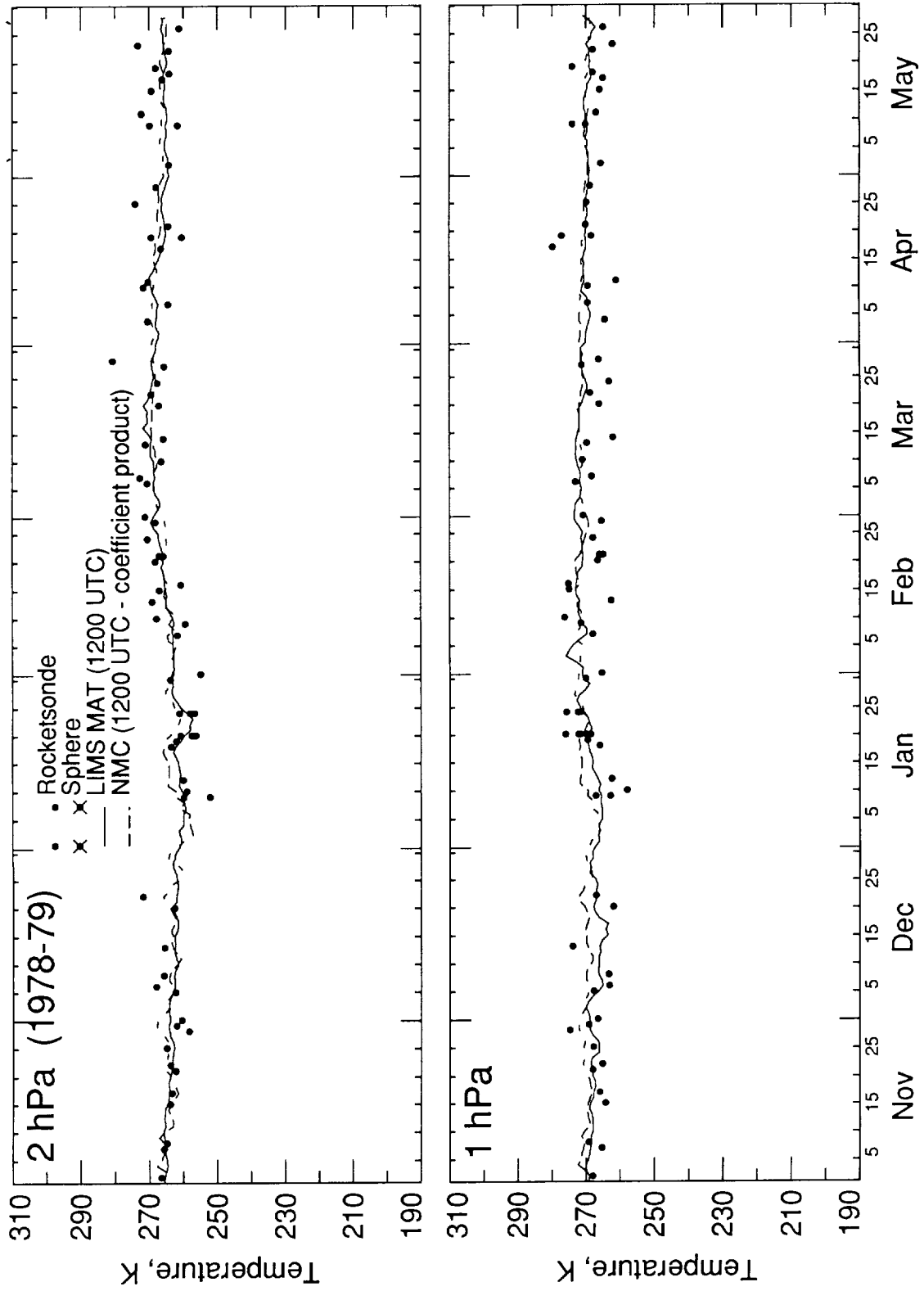Figure A14. Continued.
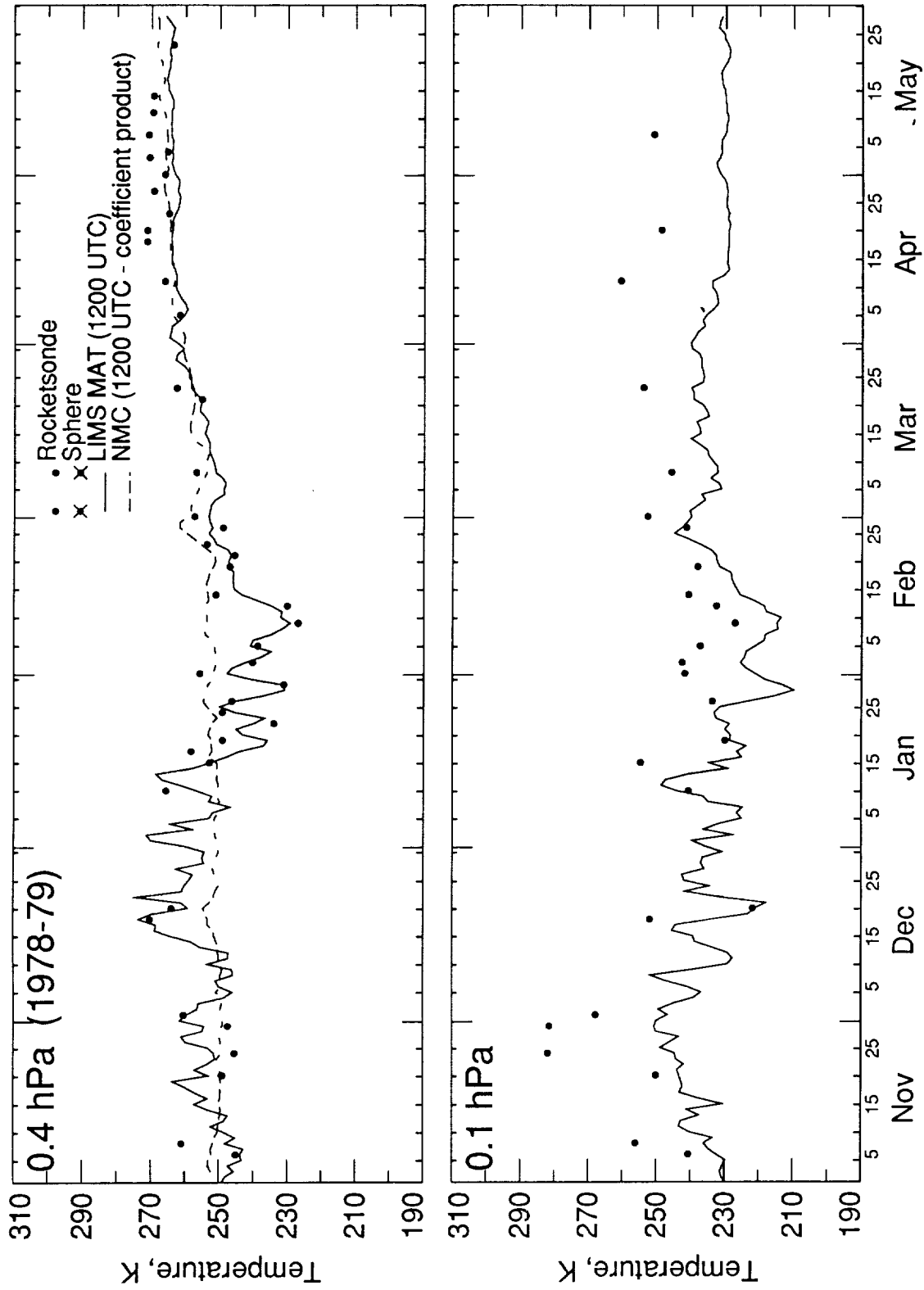
Figure A14. Continued.
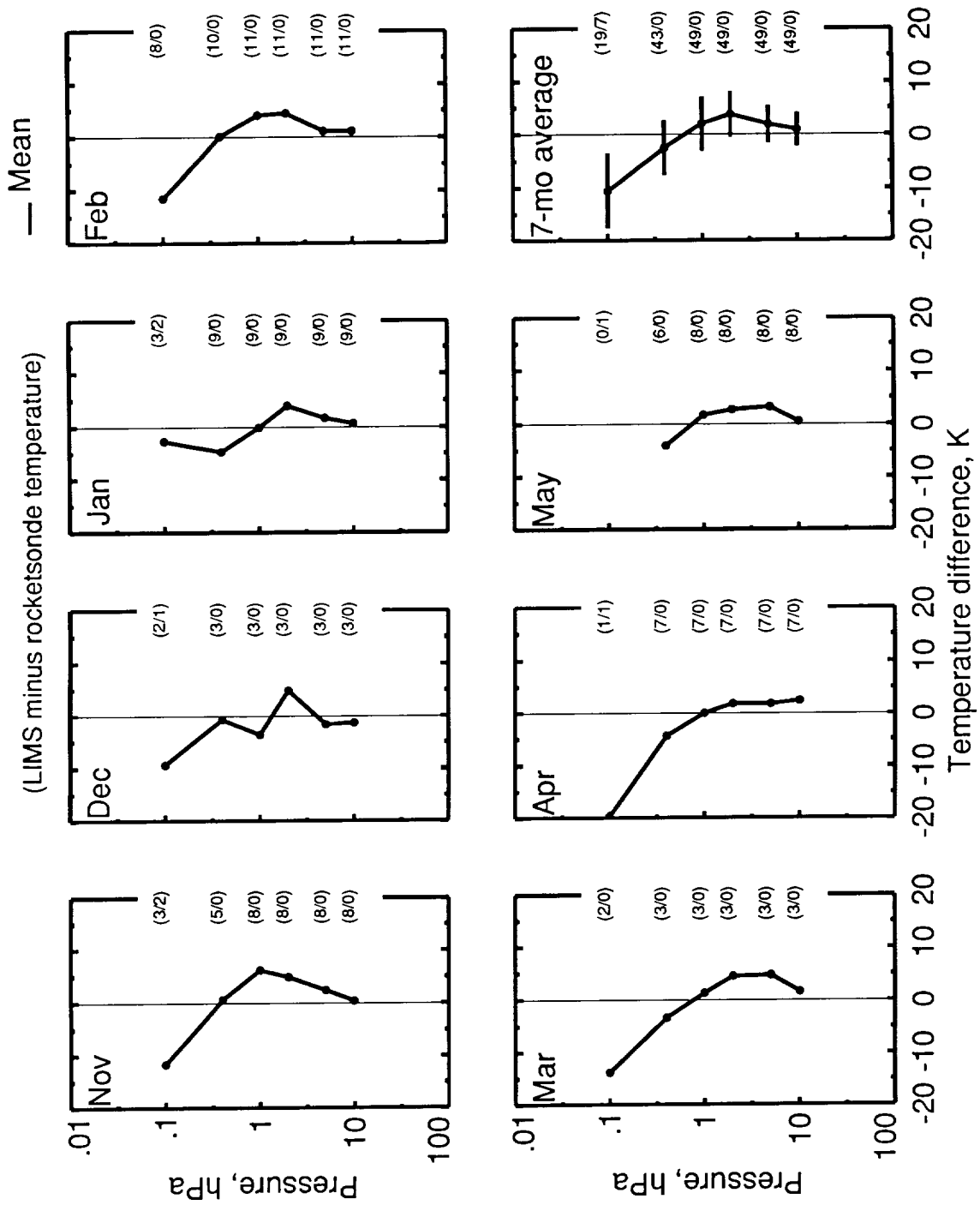
Figure A14. Concluded.

111
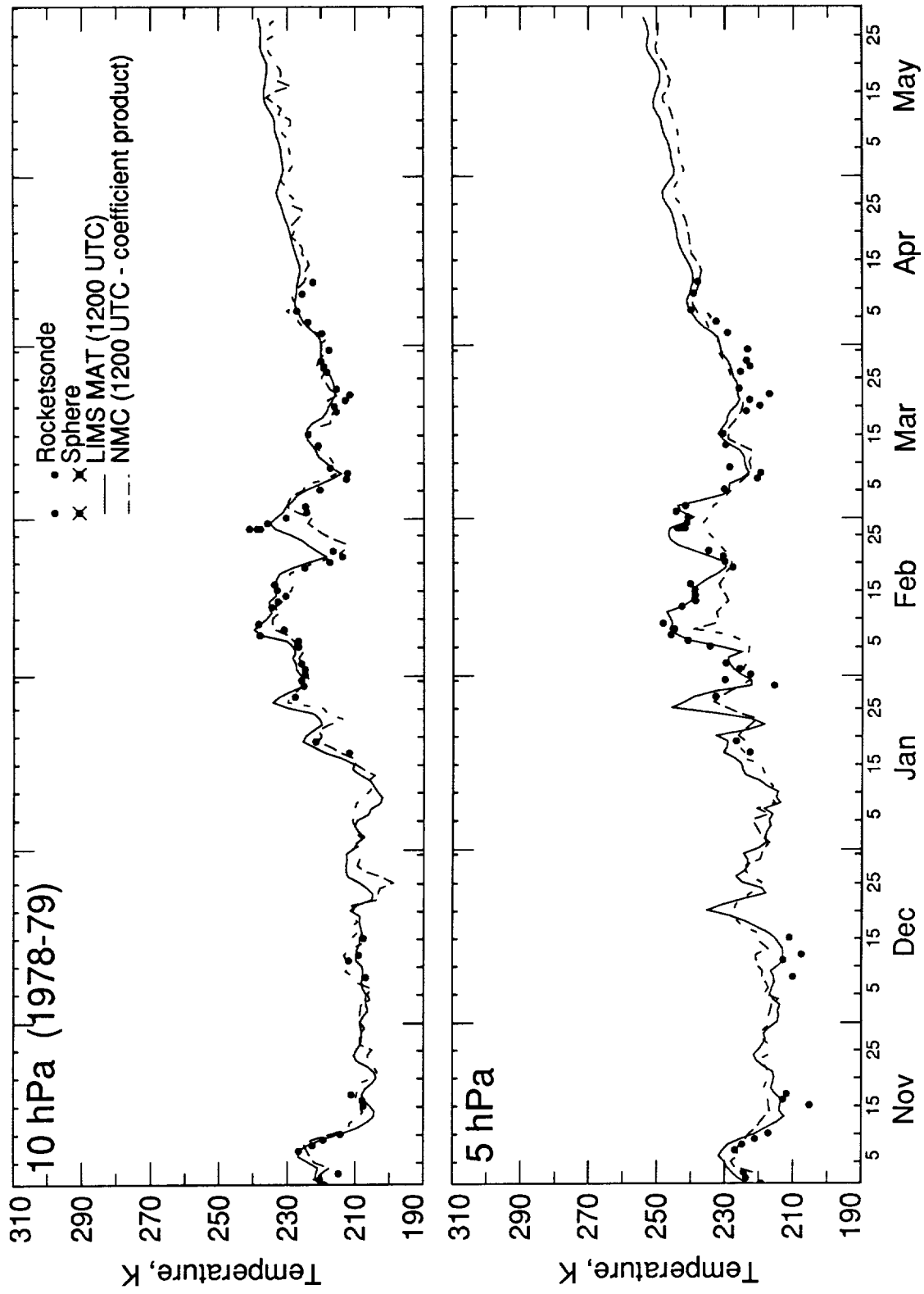
Figure A15. Fort Churchill (59° N, 266° E).
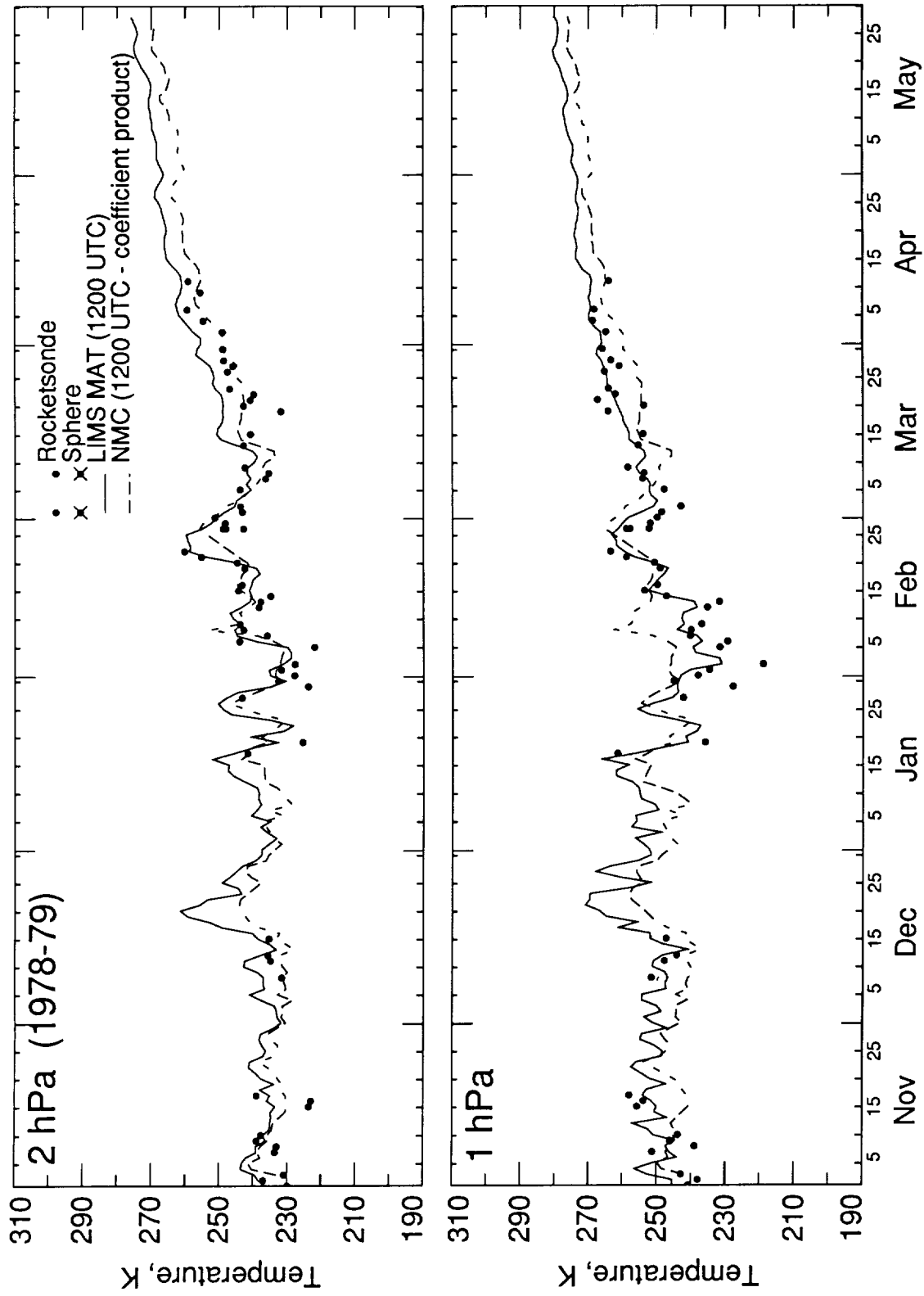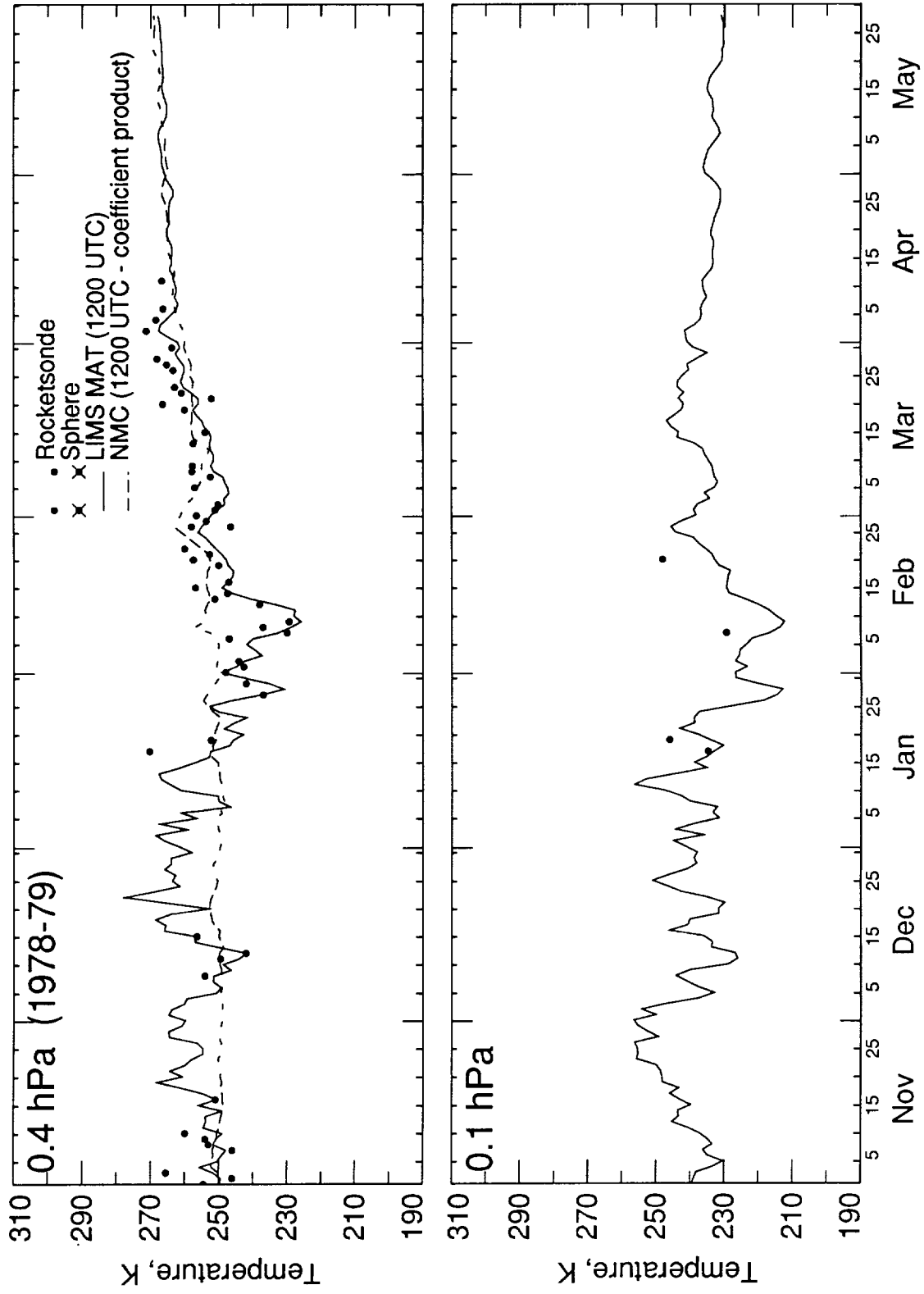
Figure A15. Continued.

Figure A15. Continued.

114
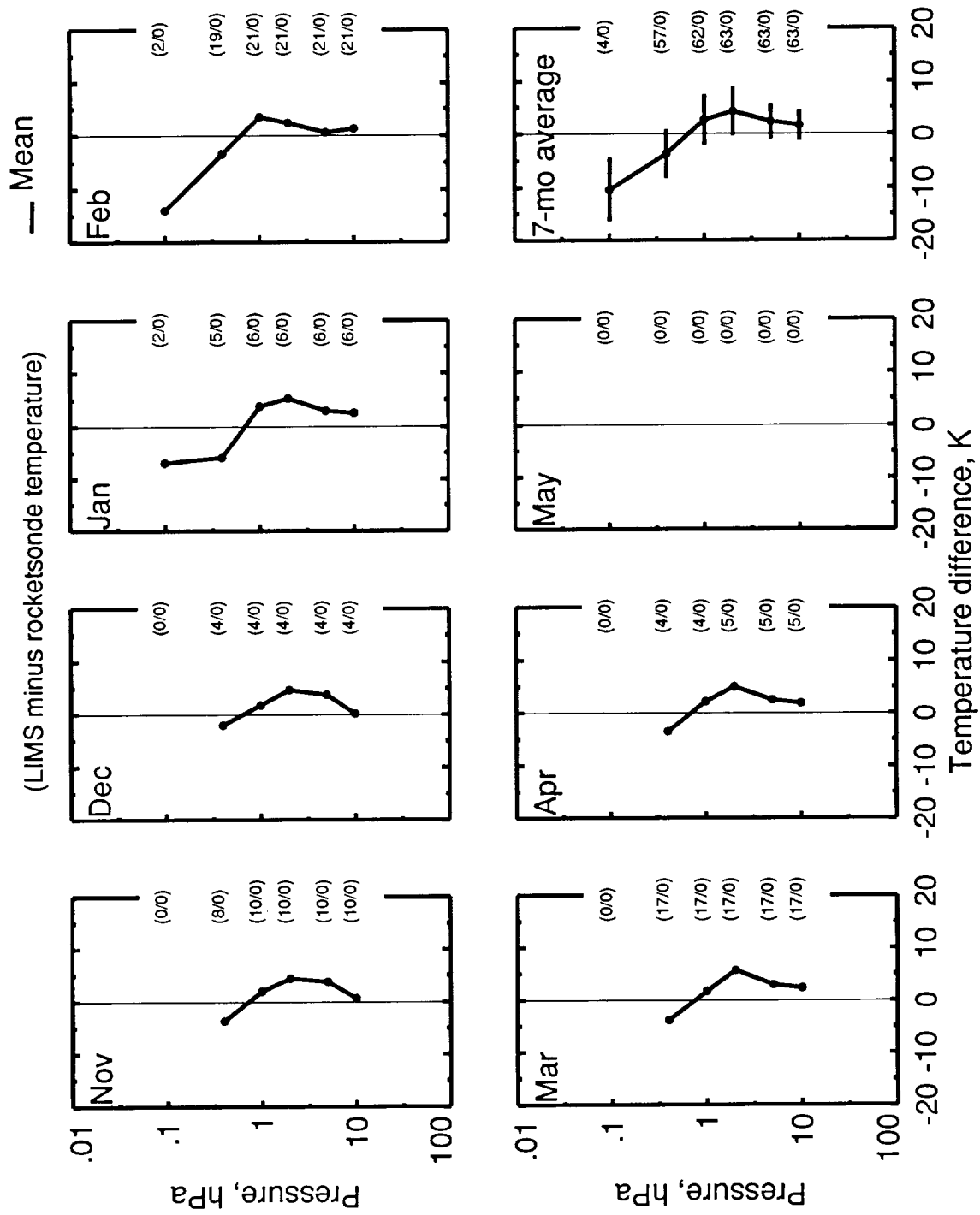
Figure A15. Concluded.

115
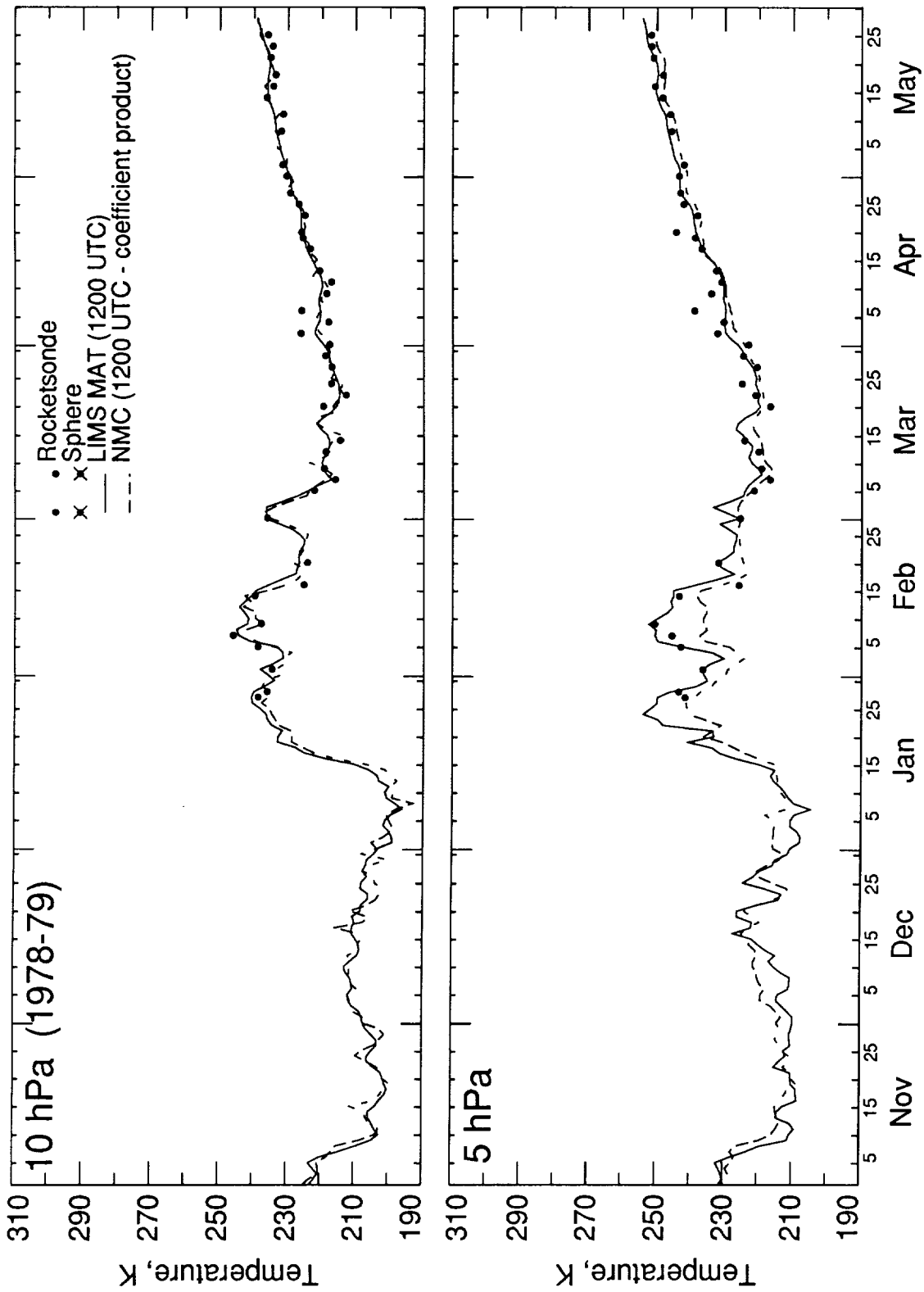
Figure A16. Poker Flat (65° N, 213° E).

Figure A16. Continued.

117
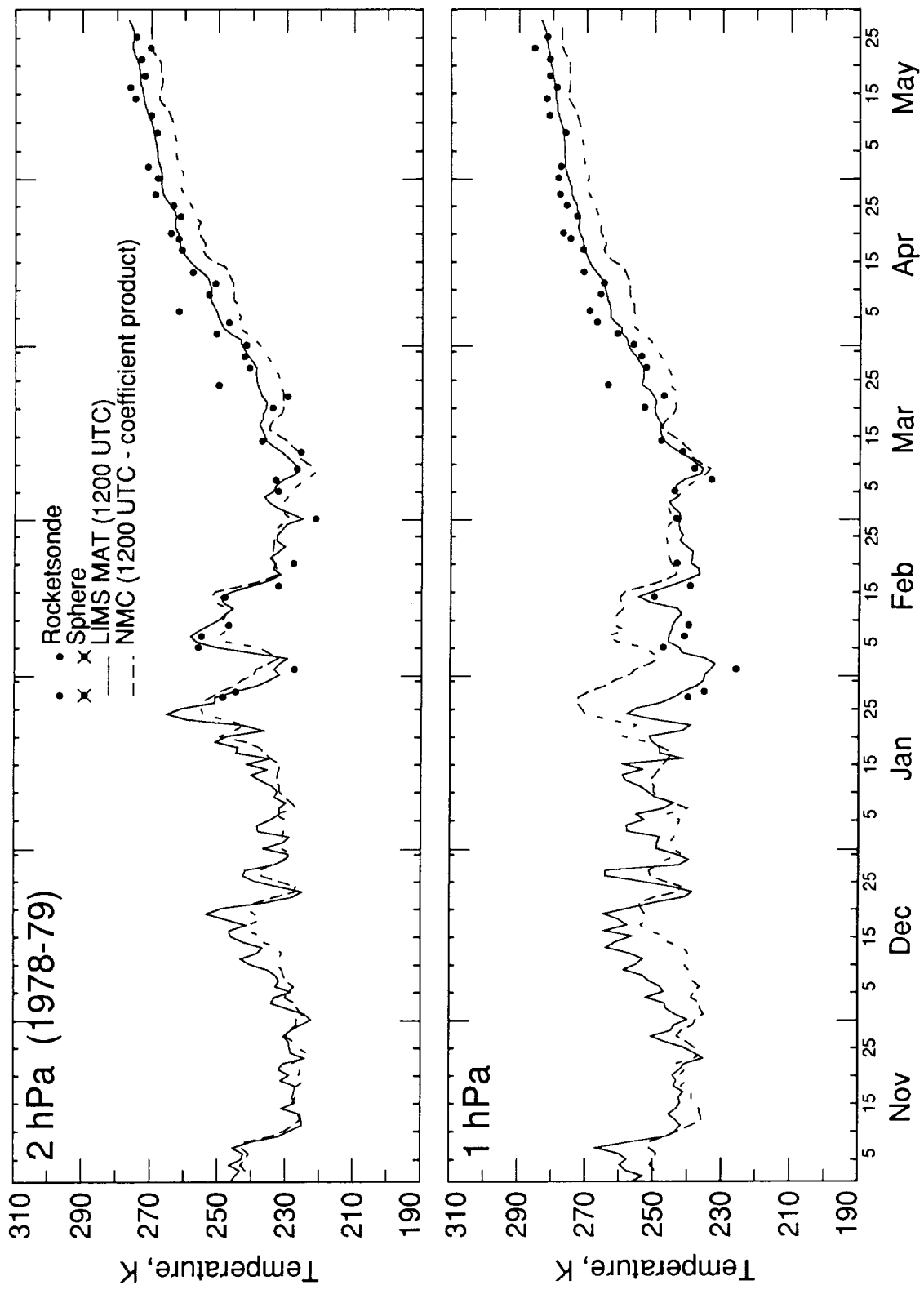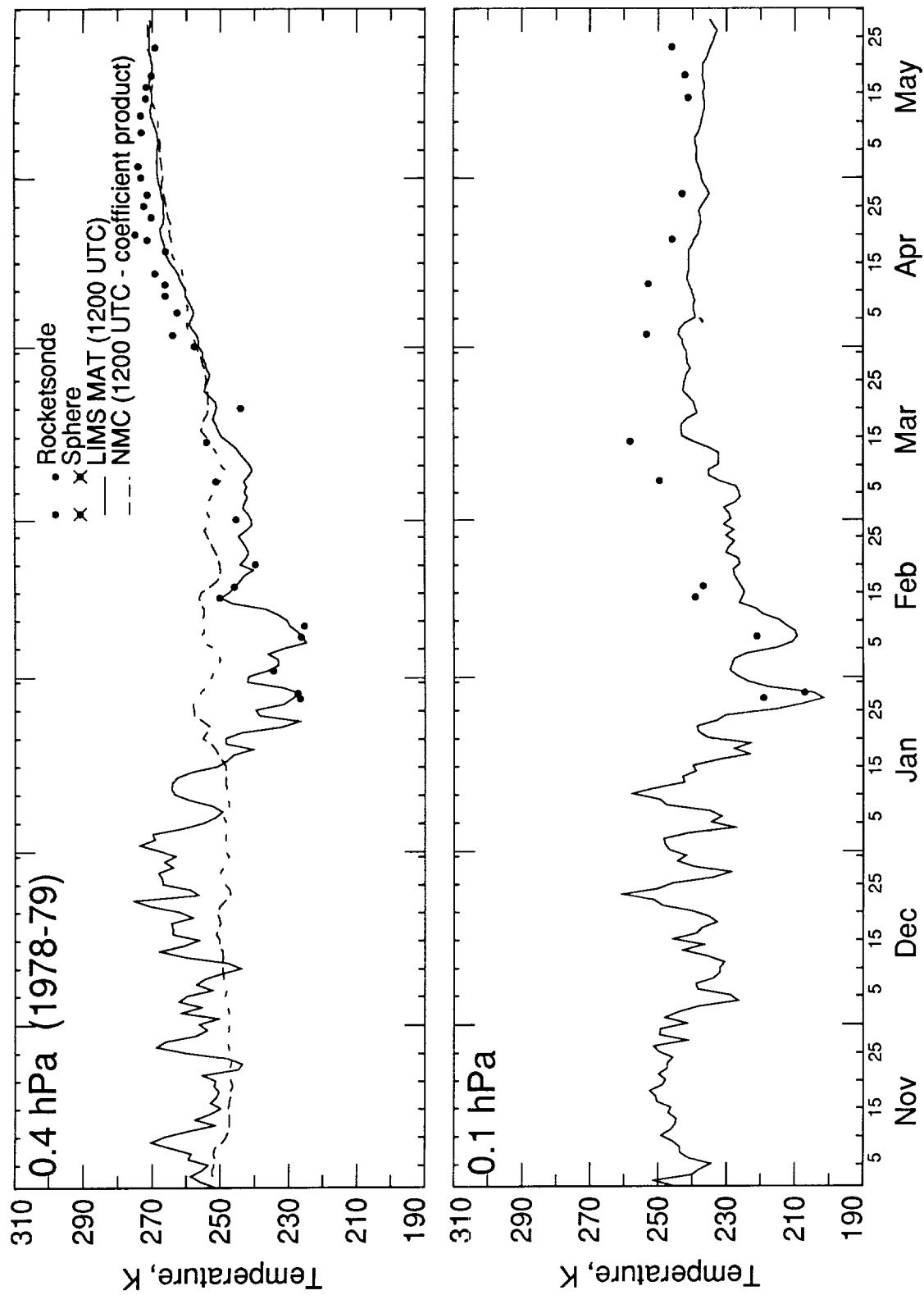
Figure A16. Continued.
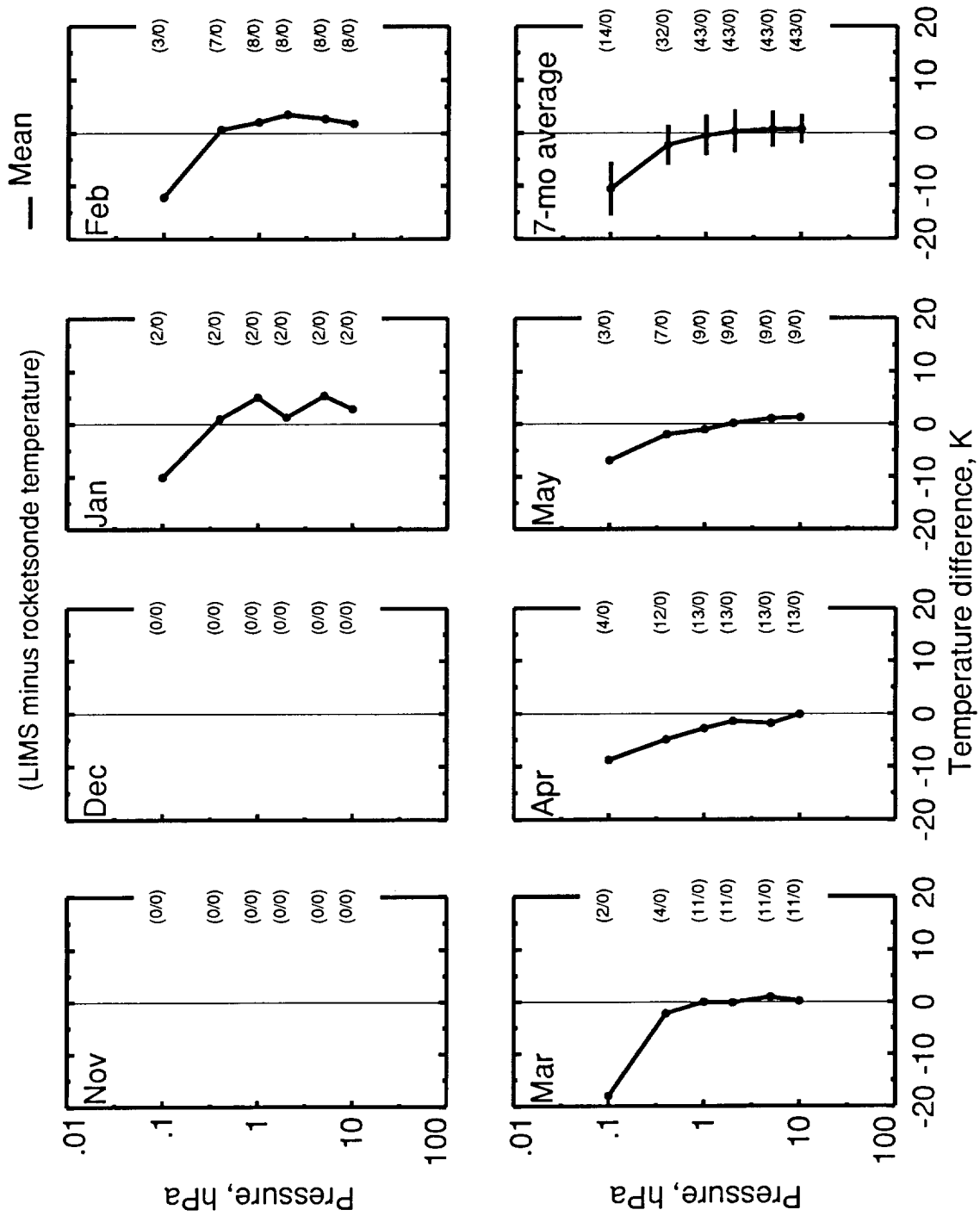
Figure A16. Concluded.

119
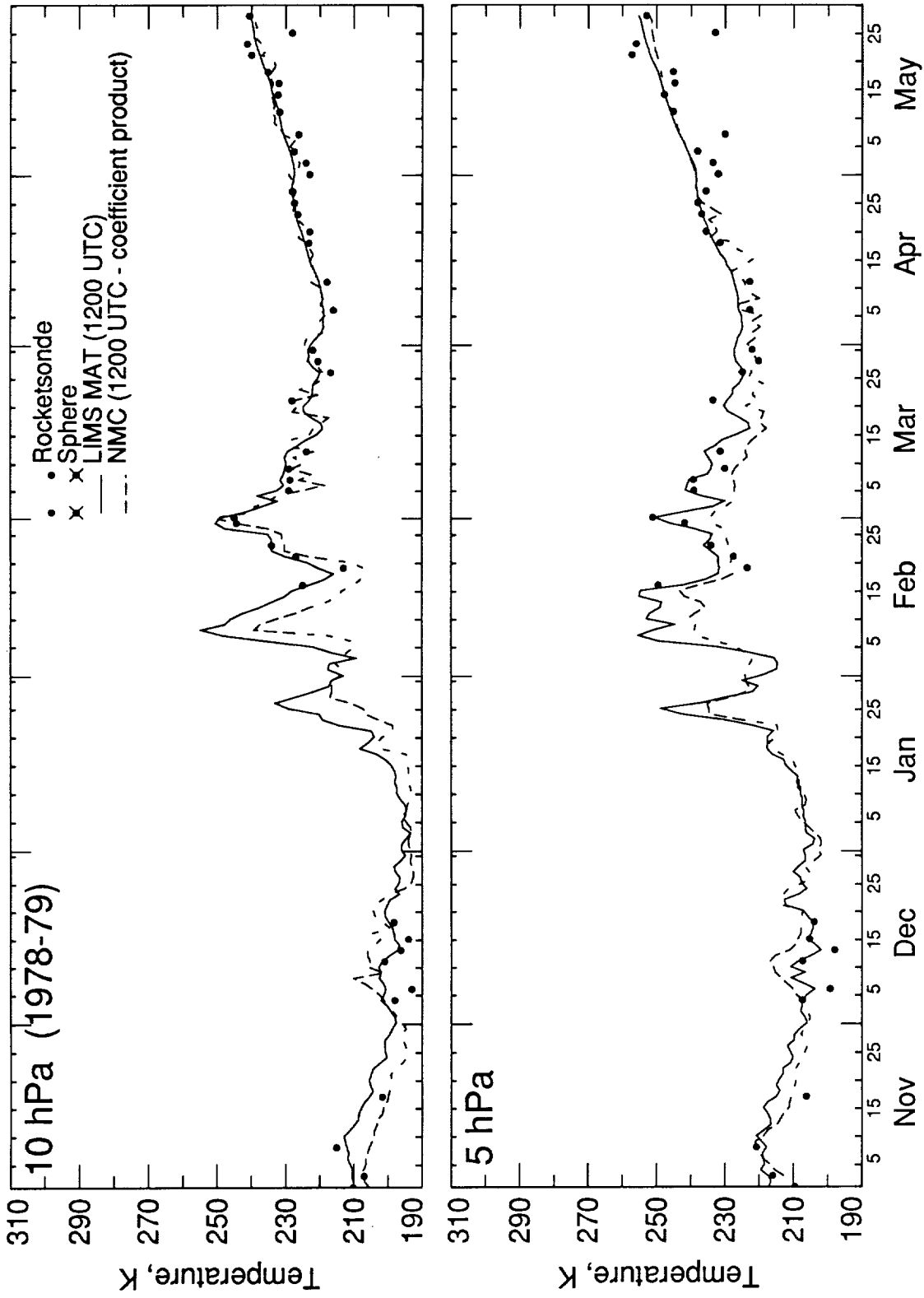
Figure A17. Thule (77° N, 291° E).
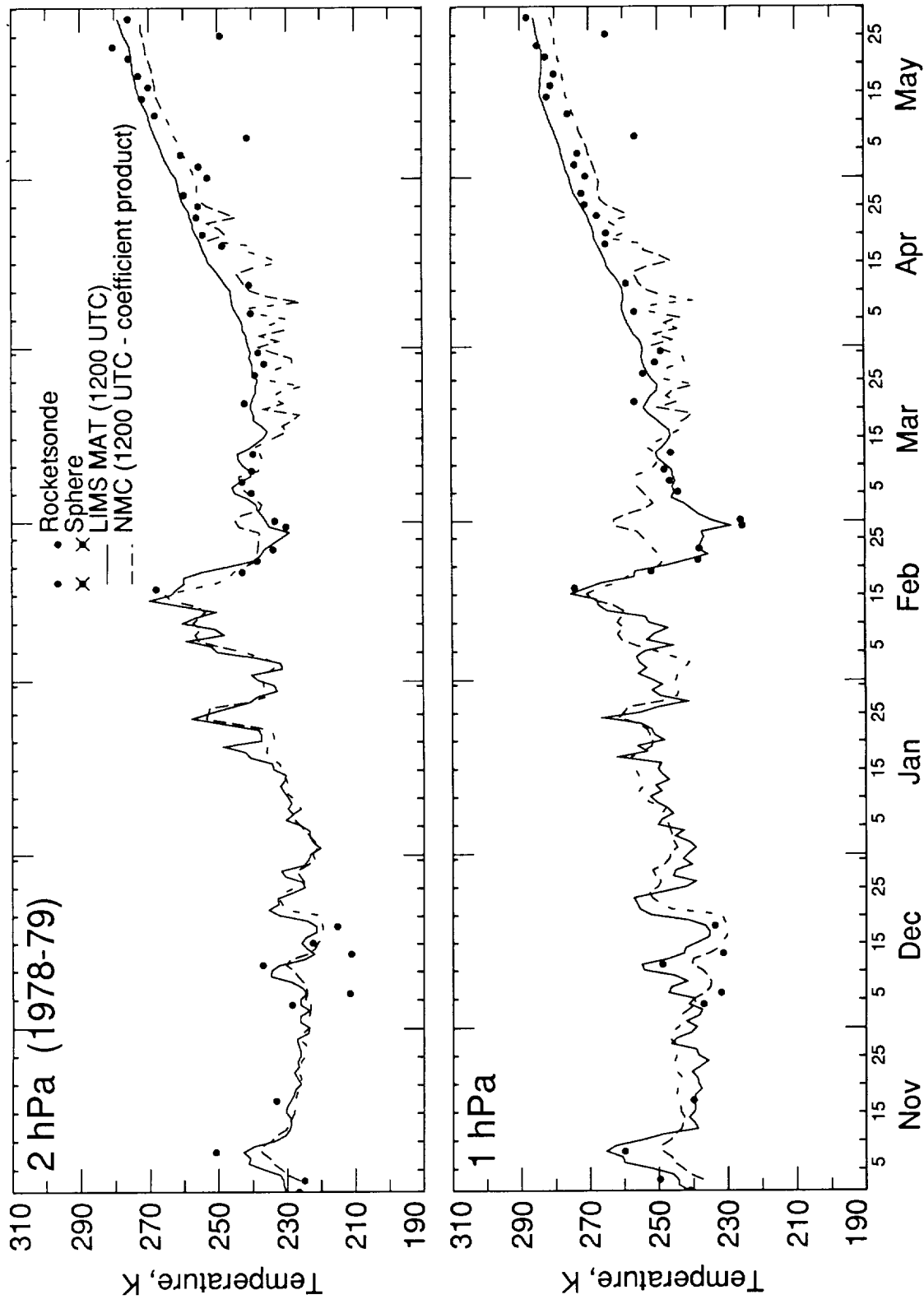
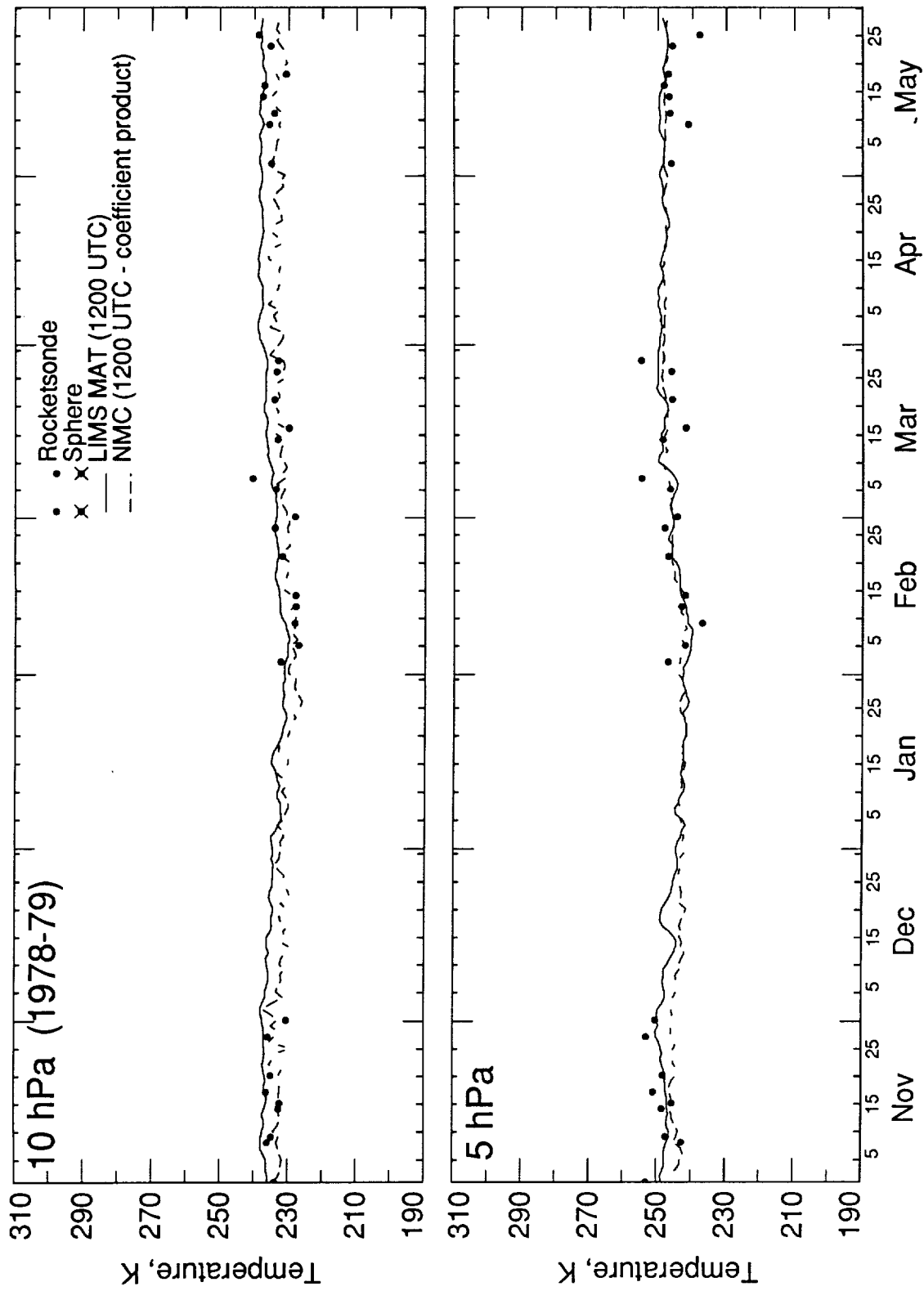Figure A17. Continued.
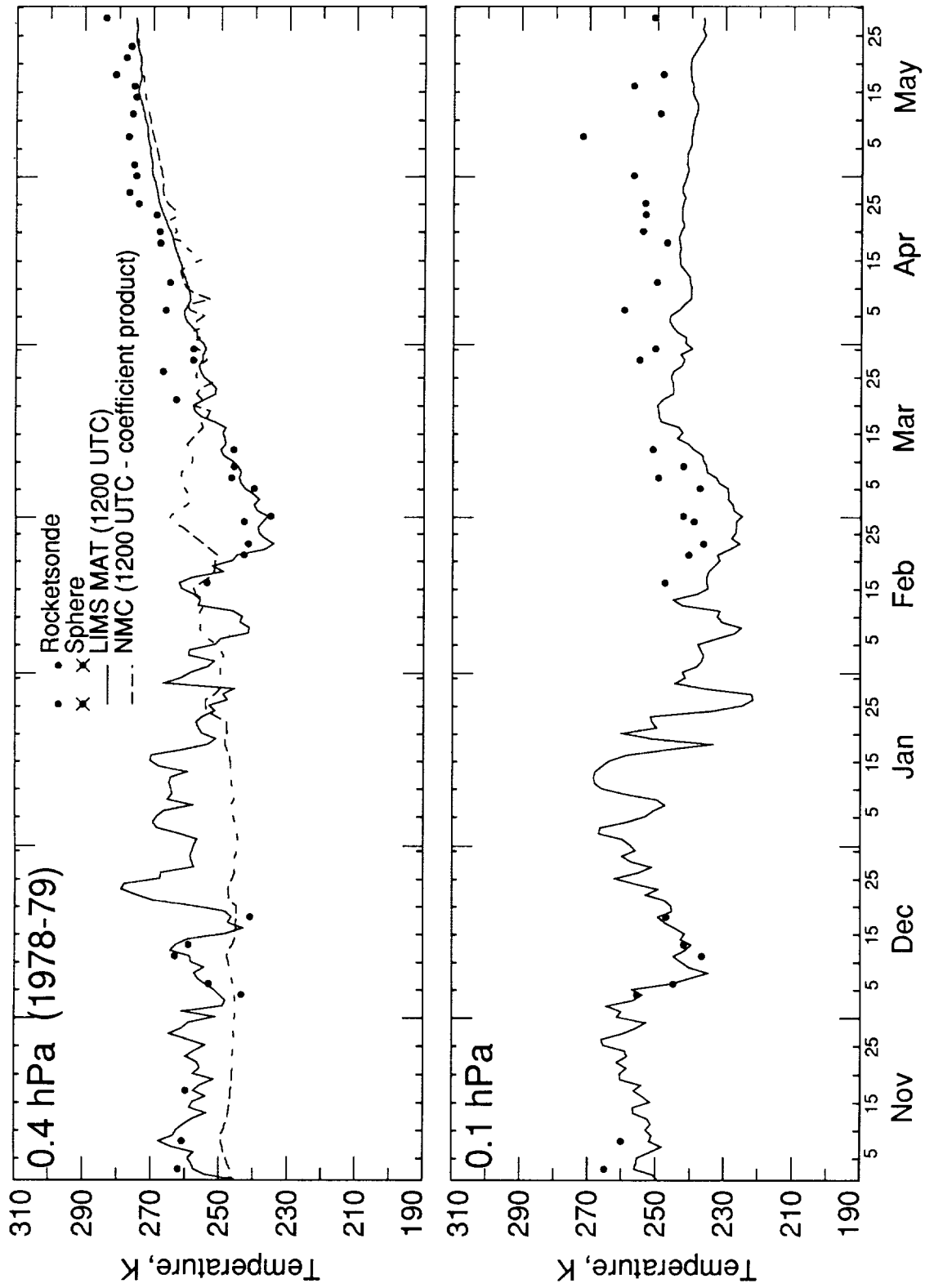
Figure A17. Continued.
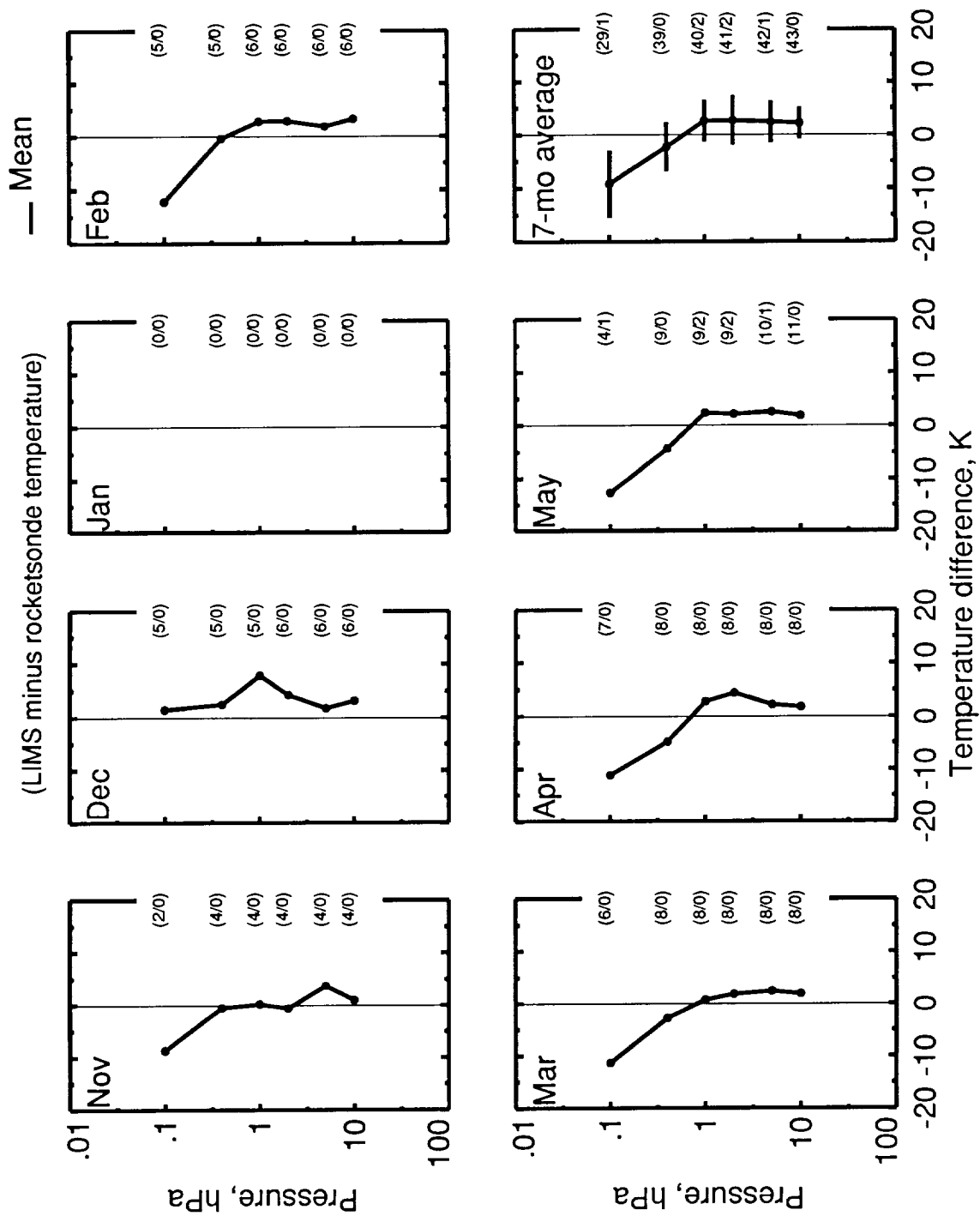
Figure A17. Concluded.

123
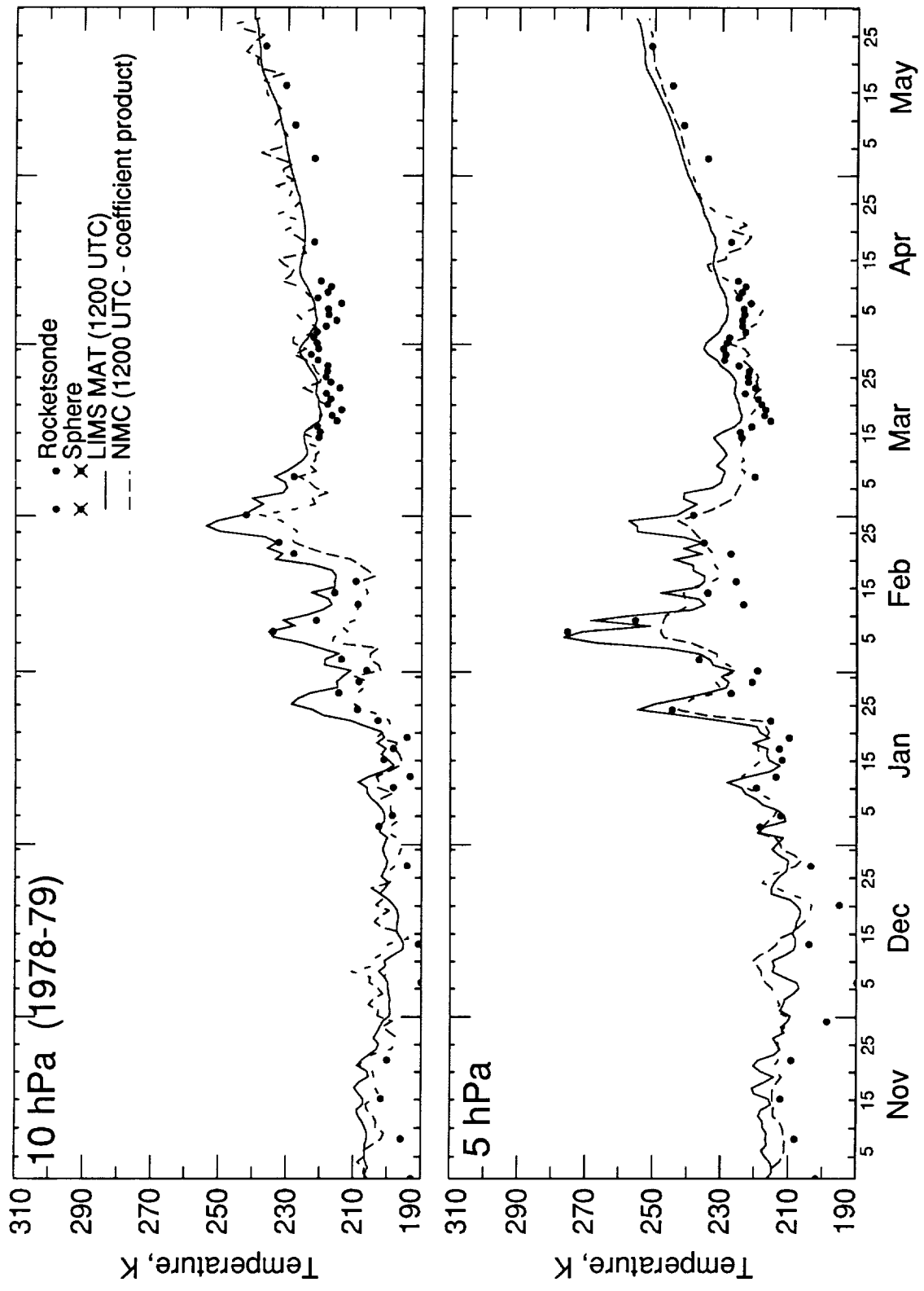
Figure A18. Heiss Island, USSR (81° N, 58° E).

124

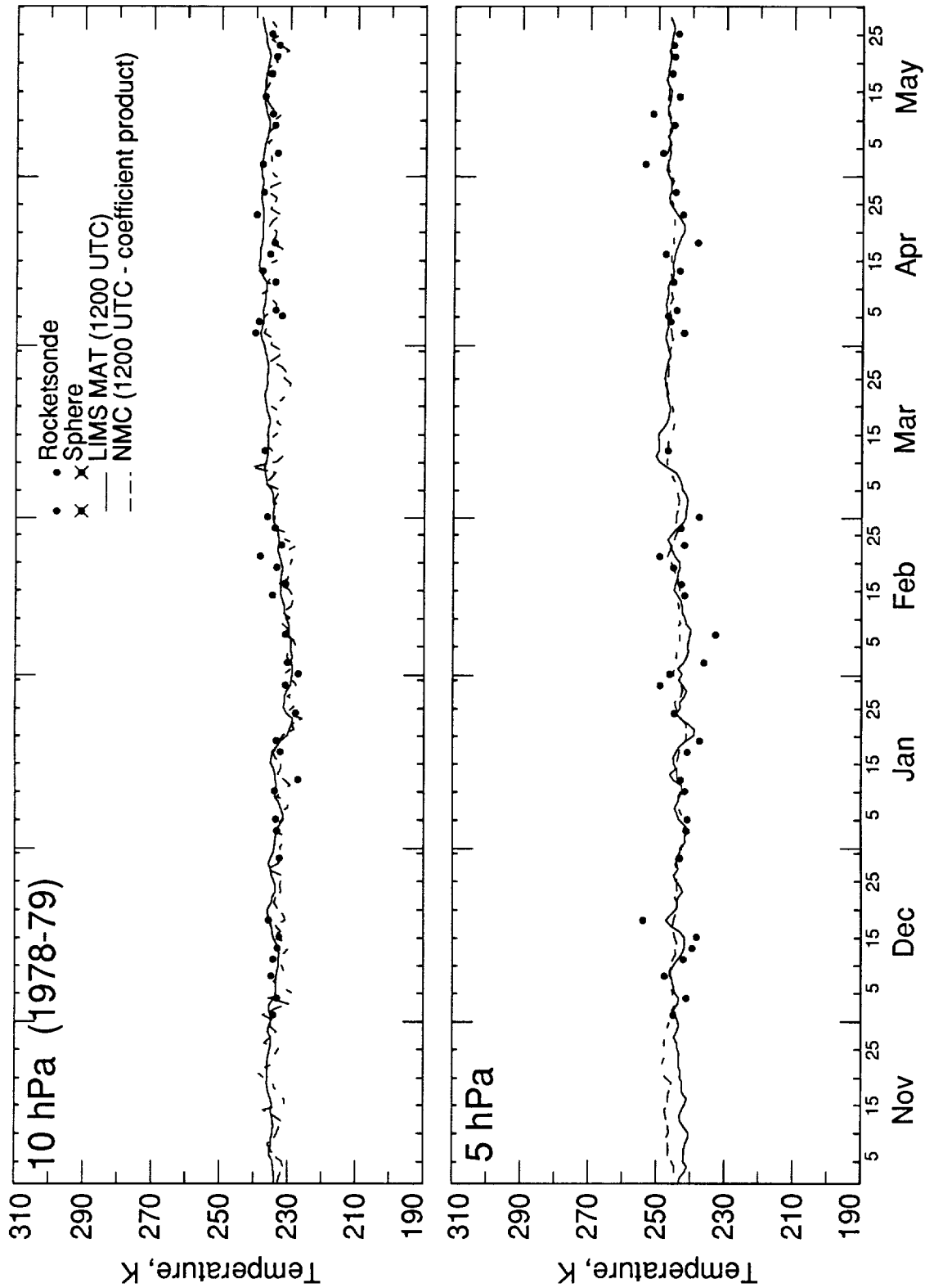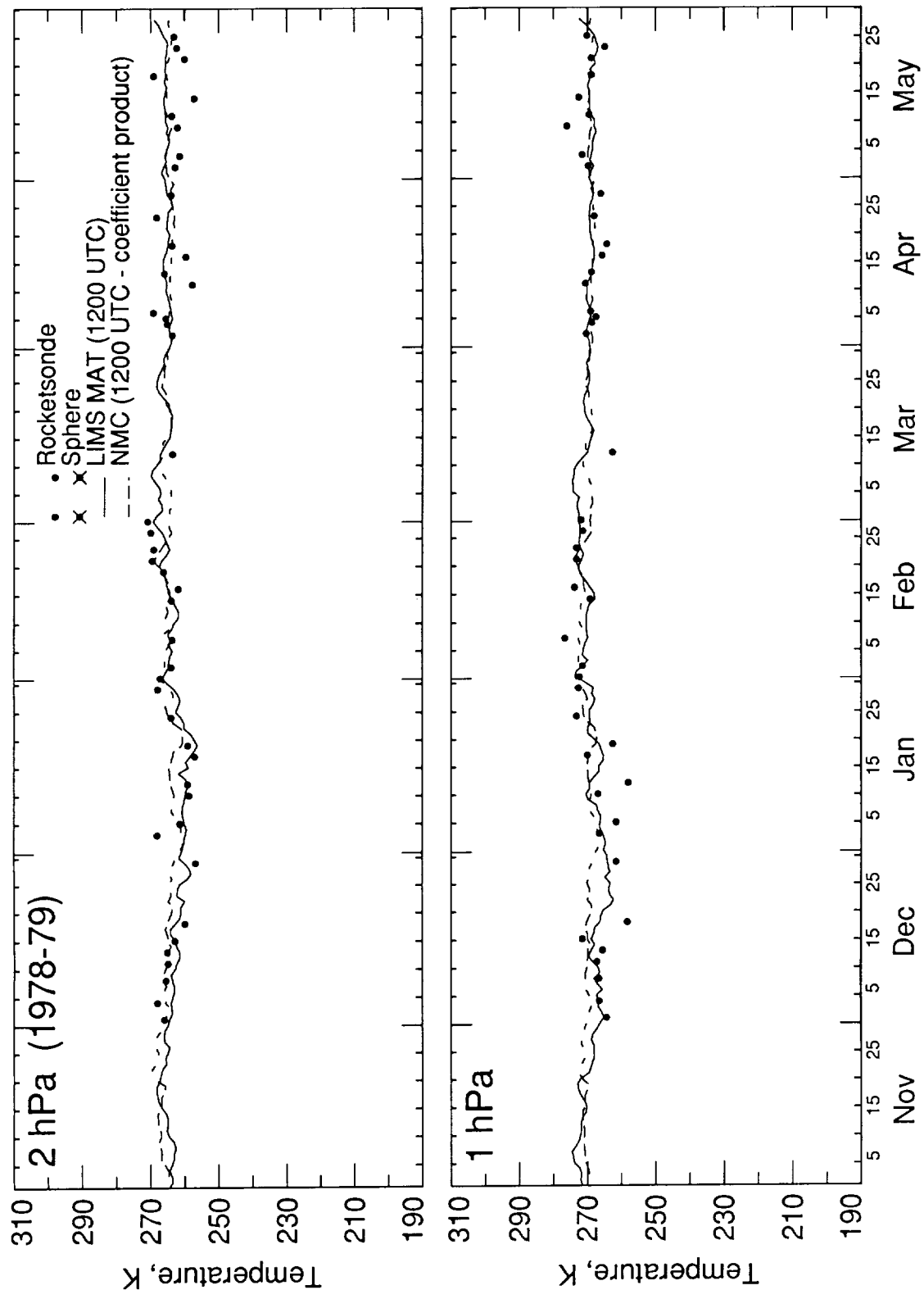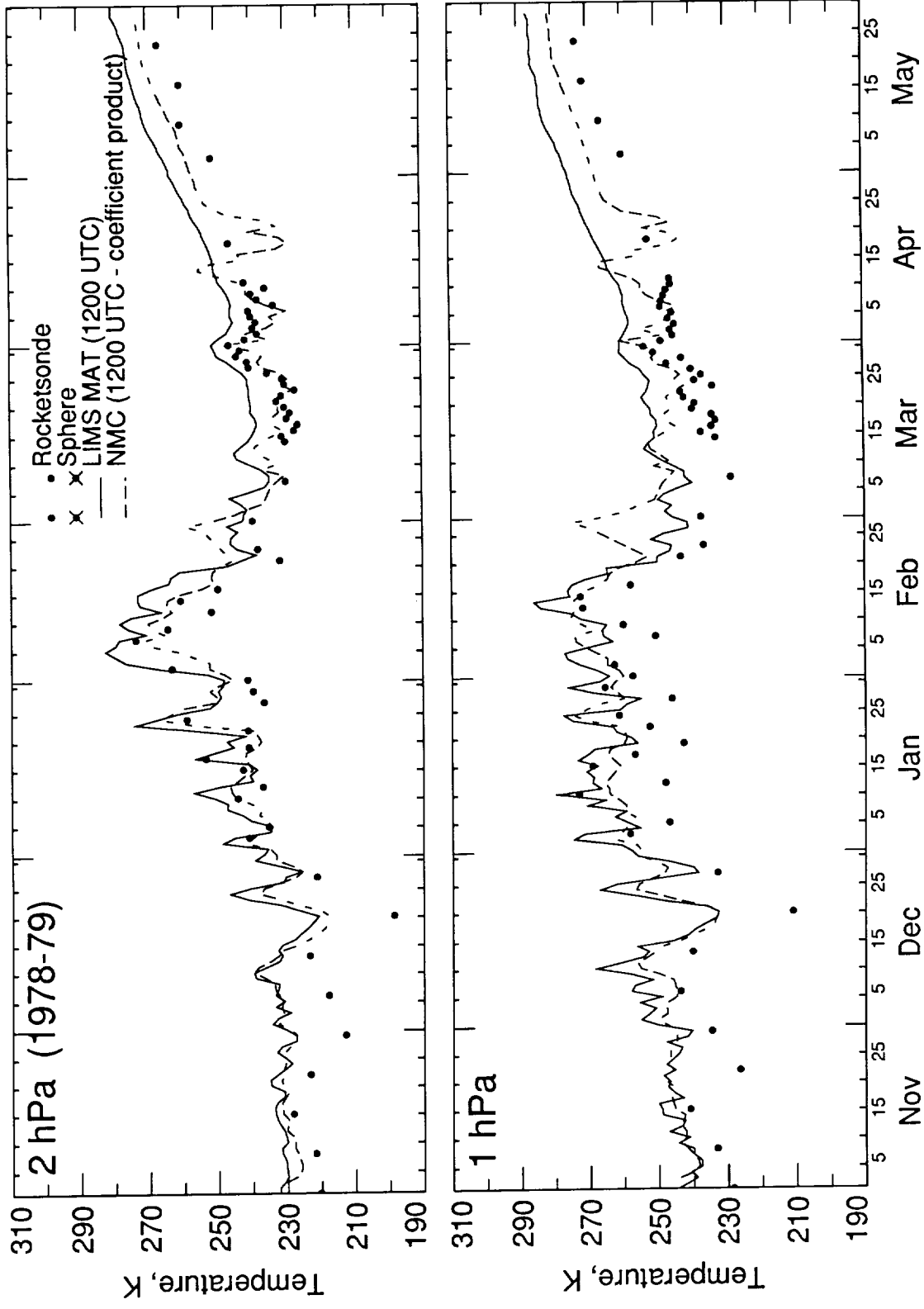Figure A18. Continued.
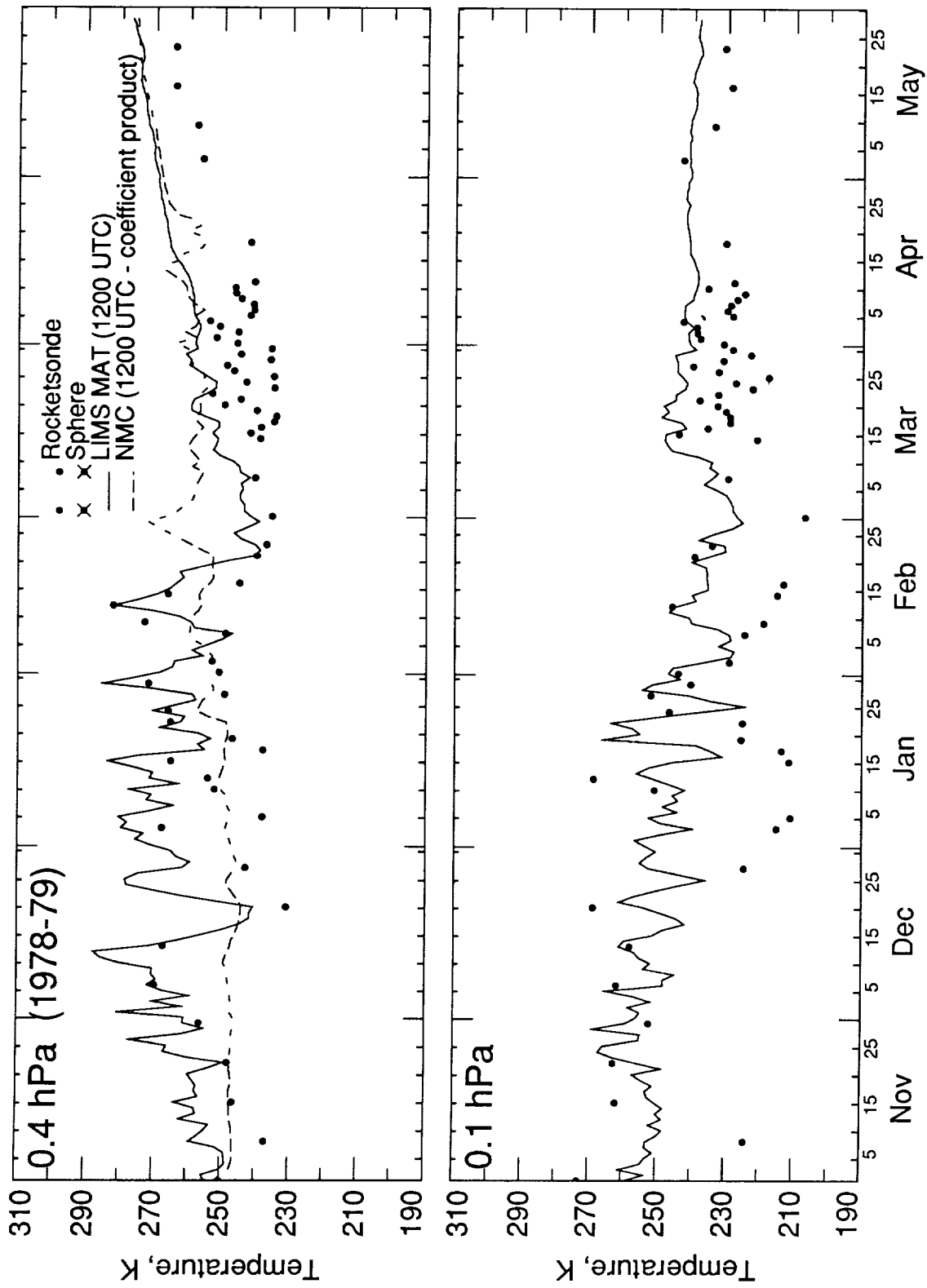
Figure A18. Continued.

Figure A18. Concluded.

(LIMS minus rocketsonde temperature)

Temperature difference, K

Pressure, hPa
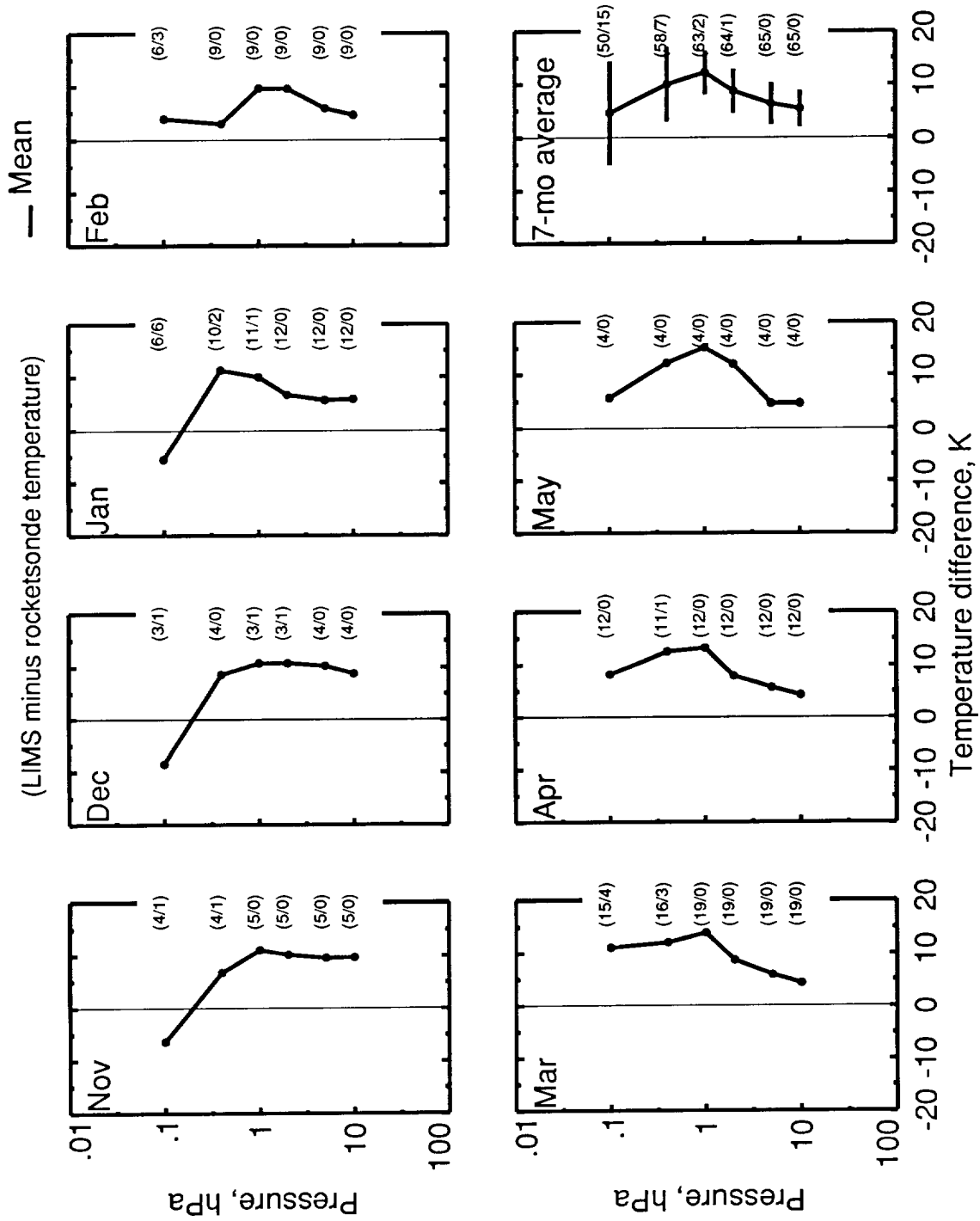
Appendix B

Tables of Temperature Statistics for Each Station

This appendix contains tables of temperature statistics (mean and standard deviation of temperature differences in K) at each of the 18 rocketsonde stations listed in table 1. Each table contains statistical comparisons between (a) LIMS minus rocketsonde, (b) LIMS minus NMC, and (c) NMC minus rocketsonde temperatures. The NMC data used here are from a Fourier coefficient product derived from the archived NMC gridded analyses.

The "Total of samples" is the number of samples used in computing the statistics. Along with the "Number rejected," the two values constitute the total number of observations at a given level for the corresponding period.

The row labeled "7 month" represents statistics for November 1, 1978, to May 28, 1979. The row "Nov.–Feb." represents the VTPR period (Nov. 1, 1978, to Feb. 22, 1979) for NMC data. The row "Feb.–May" represents the SSU period (Feb. 25, 1979, to May 28, 1979) for NMC data in this study. During the transition from VTPR to SSU (Feb. 22–25, 1979) for NMC, no data exists above 10 hPa for the days of February 22, 23, 24, and 25, 1979, even though the time series plots are continuous.

In table B1 for Molodezhnaya, the LIMS data are at 64° S and NMC is at station coordinates. The 7-month average LIMS minus rocketsonde results are plotted in appendix A.

Table B1. Statistics for Molodezhnaya (68° S, 46° E)

	Mean difference, K, at—						Total of samples/Number rejected at—						Standard deviation, K, at—					
	10 hPa	5 hPa	2 hPa	1 hPa	0.4 hPa	0.1 hPa	10 hPa	5 hPa	2 hPa	1 hPa	0.4 hPa	0.1 hPa	10 hPa	5 hPa	2 hPa	1 hPa	0.4 hPa	0.1 hPa
LIMS MAT minus rocketsonde																		
7 month	4.2	4.8	8.6	6.8	5.8	3.1	30/0	30/0	30/0	28/1	27/2	27/0	5.1	4.1	5.6	6.1	5.4	9.3
Nov.–Feb.	0.8	2.1	5.1	2.9	7.6	5.7	17/0	17/0	17/0	16/0	16/0	16/0	2.0	2.6	2.9	3.0	3.3	9.0
Feb. May	8.6	8.3	13.1	12.1	3.1	−0.7	13/0	13/0	13/0	12/1	11/2	11/0	4.4	3.0	5.0	5.3	6.8	8.6
LIMS MAT minus NMC (coefficient product)																		
7 month	1.0	0.7	0.2	−0.9	−0.3	0.0	193/0	186/0	186/0	186/0	186/0	0/0	2.7	3.1	3.6	3.6	4.4	0.0
Nov.–Feb.	0.7	−1.7	−2.2	−3.5	2.0	0.0	106/0	103/0	103/0	103/0	103/0	0/0	3.0	1.1	2.2	2.0	1.1	0.0
Feb.–May	1.3	3.8	3.1	2.3	−3.2	0.0	87/0	83/0	83/0	83/0	83/0	0/0	2.4	1.7	2.6	2.3	5.1	
NMC (coefficient product) minus rocketsonde																		
7 month	4.4	4.5	8.3	8.0	5.5	0.0	28/2	27/3	27/2	25/4	25/4	0/0	6.1	2.8	3.4	4.3	5.8	0.0
Nov.–Feb.	1.9	3.9	6.6	6.7	5.2	0.0	16/1	15/2	15/2	14/2	14/2	0/0	6.3	2.6	1.9	2.1	2.3	0.0
Feb.–May	7.8	5.3	10.5	9.7	5.9	0.0	12/1	12/1	12/1	11/2	11/2	0/0	4.1	3.0	3.7	5.7	8.6	0.0

Table B2. Statistics for Ascension (8° S, 346° E)

	Mean difference, K, at						Total of samples/Number rejected at—						Standard deviation, K, at—					
	10 hPa	5 hPa	2 hPa	1 hPa	0.4 hPa	0.1 hPa	10 hPa	5 hPa	2 hPa	1 hPa	0.4 hPa	0.1 hPa	10 hPa	5 hPa	2 hPa	1 hPa	0.4 hPa	0.1 hPa
LIMS MAT minus rocketsonde																		
7 month	0.7	−1.0	−1.9	−0.6	0.1	−8.0	34/0	34/0	34/0	34/0	34/0	3/0	2.7	4.0	4.2	3.1	3.4	6.4
Nov. Feb.	0.6	−0.8	−1.6	−0.8	0.1	−5.4	20/0	20/0	20/0	20/0	20/0	2/0	2.7	3.5	4.7	3.4	3.9	6.2
Feb. May	0.8	−1.2	−2.3	−0.3	0.2	−13.3	14/0	14/0	14/0	14/0	14/0	1/0	3.0	4.9	3.3	2.8	2.8	0.0
LIMS MAT minus NMC (coefficient product)																		
7 month	2.8	1.1	−1.2	−2.6	−2.2	0.0	193/0	186/0	186/0	186/0	186/0	0/0	1.6	1.8	2.1	2.5	3.7	0.0
Nov.–Feb.	3.2	1.6	−0.5	−4.0	−3.4	0.0	106/0	103/0	103/0	103/0	103/0	0/0	1.7	2.2	1.9	2.4	4.4	0.0
Feb.–May	2.3	0.5	−2.1	−0.8	−0.7	0.0	87/0	83/0	83/0	83/0	83/0	0/0	1.1	1.0	1.8	1.3	1.9	0.0
NMC (coefficient product) minus rocketsonde																		
7 month	−1.5	−1.0	−1.7	1.6	0.0	0.0	33/1	32/2	32/2	32/2	32/2	0/0	2.9	4.1	4.6	3.2	3.3	0.0
Nov. Feb.	−1.4	−0.2	−2.4	1.8	−0.5	0.0	20/0	19/1	19/1	19/1	19/1	0/0	2.7	3.4	4.3	3.6	3.5	0.0
Feb.–May	−1.5	−2.1	−0.5	1.2	0.7	0.0	13/1	13/1	13/1	13/1	13/1	0/0	3.3	4.8	4.8	2.5	3.0	0.0

Table B3. Statistics for Thumba (9° N, 77° E)

	Mean difference, K, at—						Total of samples/Number rejected at—						Standard deviation, K, at—					
	10 hPa	5 hPa	2 hPa	1 hPa	0.4 hPa	0.1 hPa	10 hPa	5 hPa	2 hPa	1 hPa	0.4 hPa	0.1 hPa	10 hPa	5 hPa	2 hPa	1 hPa	0.4 hPa	0.1 hPa
LIMS MAT minus rocketsonde																		
7 month	1.0	0.3	3.7	4.4	3.7	2.9	47/0	47/0	48/0	48/0	48/0	43/1	4.0	4.0	3.9	3.9	5.7	8.1
Nov.–Feb.	-0.6	-1.3	4.1	4.8	2.5	5.3	20/0	20/0	21/0	22/0	22/0	20/0	3.8	4.4	4.2	4.7	5.7	7.4
Feb.–May	2.2	1.4	3.4	4.0	4.8	0.8	27/0	27/0	27/0	26/0	26/0	23/0	3.8	3.4	3.8	3.0	5.7	8.2
LIMS MAT minus NMC (coefficient product)																		
7 month	4.5	0.8	-0.4	-2.0	-3.1	0.0	203/0	184/0	184/0	184/0	184/0	184/0	1.9	1.7	1.5	2.2	3.1	0.0
Nov.–Feb.	3.5	1.5	-0.5	-3.2	-4.3	0.0	111/0	101/0	101/0	101/0	101/0	101/0	1.8	1.9	1.7	2.1	3.6	0.0
Feb.–May	5.6	-0.1	-0.4	-0.4	-1.6	0.0	92/0	83/0	83/0	83/0	83/0	83/0	1.3	0.9	1.2	1.3	1.3	0.0
NMC (coefficient product) minus rocketsonde																		
7 month	-3.9	0.1	4.5	5.6	6.4	0.0	46/1	45/2	46/2	46/2	46/2	0/0	4.2	4.4	3.7	4.2	6.0	0.0
Nov.–Feb.	-4.0	-1.7	5.2	7.6	6.2	0.0	20/0	18/2	19/2	20/2	20/2	0/0	4.5	5.5	3.8	4.8	6.6	0.0
Feb.–May	-3.8	1.3	4.1	4.1	6.5	0.0	26/1	27/0	27/0	26/0	26/0	0/0	4.0	3.2	3.6	3.0	5.6	0.0

Table B4. Statistics for Kwajalein (9° N, 168° E)

	Mean difference, K, at—						Total of samples/Number rejected at—						Standard deviation, K, at—					
	10 hPa	5 hPa	2 hPa	1 hPa	0.4 hPa	0.1 hPa	10 hPa	5 hPa	2 hPa	1 hPa	0.4 hPa	0.1 hPa	10 hPa	5 hPa	2 hPa	1 hPa	0.4 hPa	0.1 hPa
LIMS MAT minus rocketsonde																		
7 month	1.1	-1.6	-0.3	1.3	-2.7	-9.0	76/0	76/0	76/0	76/0	74/0	38/4	3.2	3.9	3.7	4.0	3.5	4.2
Nov.–Feb.	0.2	-1.9	0.3	0.8	-3.3	-9.3	42/0	42/0	42/0	42/0	41/0	18/3	3.1	3.5	3.3	3.8	3.4	4.3
Feb.–May	2.3	-1.2	-1.0	-2.0	-1.9	-8.7	34/0	34/0	34/0	34/0	33/0	20/1	2.9	4.4	4.0	4.2	3.6	4.1
LIMS MAT minus NMC (coefficient product)																		
7 month	3.3	0.3	-0.6	-1.2	-3.2	0.0	203/0	184/0	184/0	184/0	184/0	184/0	1.9	1.4	1.6	1.9	3.5	0.0
Nov.–Feb.	2.5	0.3	-0.9	-2.0	-4.3	0.0	111/0	101/0	101/0	101/0	101/0	101/0	1.9	1.7	1.7	1.9	4.3	0.0
Feb.–May	4.3	0.2	-0.2	-0.2	-1.8	0.0	92/0	83/0	83/0	83/0	83/0	83/0	1.4	0.7	1.4	1.3	1.2	0.0
NMC (coefficient product) minus rocketsonde																		
7 month	-2.1	-2.2	0.9	2.4	-0.1	0.0	73/3	72/4	72/4	72/4	70/4	0/0	3.2	4.4	4.1	4.3	4.2	0.0
Nov.–Feb.	-2.3	-2.8	2.0	2.8	0.2	0.0	40/2	41/1	41/1	41/1	40/1	0/0	3.4	4.1	4.0	4.3	4.8	0.0
Feb.–May	-1.9	-1.5	-0.6	2.0	-0.4	0.0	33/1	31/3	31/3	31/3	30/3	0/0	2.9	4.7	3.9	4.3	3.3	0.0

Table B5. Statistics for Fort Sherman (9° N, 280° E)

Mean difference, K, at—

	10 hPa	5 hPa	2 hPa	1 hPa	0.4 hPa	0.1 hPa
LIMS MAT minus rocketsonde						
7 month	2.4	0.3	1.1	−1.1	−2.4	0.0
Nov.–Feb.	2.7	−0.9	2.8	−1.4	−2.6	0.0
Feb.–May	2.2	1.4	−0.4	−0.8	−2.3	0.0
LIMS MAT minus NMC (coefficient product)						
7 month	3.7	1.1	−0.7	−1.1	−2.2	0.0
Nov.–Feb.	3.2	1.4	−1.0	−2.5	−3.0	0.0
Feb.–May	4.3	0.6	−0.3	0.7	−1.1	0.0
NMC (coefficient product) minus rocketsonde						
7 month	−1.2	0.1	1.6	−1.1	−0.7	0.0
Nov.–Feb.	−0.2	−1.7	3.2	−0.5	−0.4	0.0
Feb.–May	−2.1	1.7	0.1	−1.8	−1.0	0.0

Total of samples/Number rejected at—

	10 hPa	5 hPa	2 hPa	1 hPa	0.4 hPa	0.1 hPa
LIMS MAT minus rocketsonde						
7 month	32/0	32/0	32/0	32/0	25/0	0/0
Nov.–Feb.	15/0	15/0	15/0	15/0	11/0	0/0
Feb.–May	17/0	17/0	17/0	17/0	14/0	0/0
LIMS MAT minus NMC (coefficient product)						
7 month	203/0	184/0	184/0	184/0	184/0	0/0
Nov.–Feb.	111/0	101/0	101/0	101/0	101/0	0/0
Feb.–May	92/0	83/0	83/0	83/0	83/0	0/0
NMC (coefficient product) minus rocketsonde						
7 month	29/3	28/4	28/4	28/4	22/3	0/0
Nov.–Feb.	13/2	14/1	14/1	14/1	10/1	0/0
Feb.–May	16/1	14/3	14/3	14/3	12/2	0/0

Standard deviation, K, at—

	10 hPa	5 hPa	2 hPa	1 hPa	0.4 hPa	0.1 hPa
LIMS MAT minus rocketsonde						
7 month	2.5	4.0	4.3	3.0	3.6	0.0
Nov.–Feb.	2.1	2.8	4.7	3.1	4.3	0.0
Feb.–May	2.9	4.7	3.3	2.9	3.2	0.0
LIMS MAT minus NMC (coefficient product)						
7 month	1.5	1.8	1.7	2.8	2.8	0.0
Nov.–Feb.	1.5	2.3	2.0	2.8	3.4	0.0
Feb.–May	1.4	0.9	1.1	1.7	1.2	0.0
NMC (coefficient product) minus rocketsonde						
7 month	2.7	3.9	4.1	4.1	4.4	0.0
Nov.–Feb.	1.8	3.3	4.8	4.7	5.6	0.0
Feb.–May	3.1	3.8	2.7	3.4	3.3	0.0

Table B6. Statistics for Antigua (17° N, 298° E)

Mean difference, K, at—

	10 hPa	5 hPa	2 hPa	1 hPa	0.4 hPa	0.1 hPa
LIMS MAT minus rocketsonde						
7 month	0.7	0.8	0.1	0.3	−2.6	−6.4
Nov.–Feb.	0.0	0.6	−1.1	0.5	−3.0	−7.5
Feb.–May	1.3	1.1	1.2	0.1	−2.3	−5.8
LIMS MAT minus NMC (coefficient product)						
7 month	1.8	−0.8	−0.7	−0.8	−3.3	0.0
Nov.–Feb.	1.3	−1.6	−2.2	−1.8	−4.0	0.0
Feb.–May	2.4	0.1	1.1	0.5	−2.4	0.0
NMC (coefficient product) minus rocketsonde						
7 month	−0.8	1.3	1.0	1.4	0.5	0.0
Nov.–Feb.	−0.9	1.4	1.6	2.7	0.5	0.0
Feb.–May	−0.8	1.2	0.3	0.1	0.5	0.0

Total of samples/Number rejected at—

	10 hPa	5 hPa	2 hPa	1 hPa	0.4 hPa	0.1 hPa
LIMS MAT minus rocketsonde						
7 month	46/0	46/0	46/0	45/0	43/0	32/2
Nov.–Feb.	23/0	23/0	23/0	22/0	20/0	12/2
Feb.–May	23/0	23/0	23/0	23/0	23/0	20/0
LIMS MAT minus NMC (coefficient product)						
7 month	203/0	184/0	184/0	184/0	184/0	0/0
Nov.–Feb.	111/0	101/0	101/0	101/0	101/0	0/0
Feb.–May	92/0	83/0	83/0	83/0	83/0	0/0
NMC (coefficient product) minus rocketsonde						
7 month	45/1	43/3	43/3	42/3	40/3	0/0
Nov.–Feb.	23/0	22/1	22/1	21/1	19/1	0/0
Feb.–May	22/1	21/2	21/2	21/2	21/2	0/0

Standard deviation, K, at—

	10 hPa	5 hPa	2 hPa	1 hPa	0.4 hPa	0.1 hPa
LIMS MAT minus rocketsonde						
7 month	2.3	3.2	3.5	3.6	3.5	4.9
Nov.–Feb.	2.5	3.6	2.7	4.3	3.9	4.7
Feb.–May	2.1	2.8	3.9	2.9	3.2	5.0
LIMS MAT minus NMC (coefficient product)						
7 month	1.9	1.9	2.2	2.3	2.4	0.0
Nov.–Feb.	1.7	2.0	1.7	2.3	2.8	0.0
Feb.–May	2.0	1.4	1.2	1.6	1.2	0.0
NMC (coefficient product) minus rocketsonde						
7 month	3.1	3.6	3.4	3.9	4.1	0.0
Nov.–Feb.	3.5	4.3	2.6	4.2	5.1	0.0
Feb.–May	2.7	2.9	4.0	3.1	3.2	0.0

Table B7. Statistics for Barking Sands (22° N, 200° E)

	Mean difference, K, at—						Total of samples/Number rejected at—						Standard deviation, K, at—					
	10 hPa	5 hPa	2 hPa	1 hPa	0.4 hPa	0.1 hPa	10 hPa	5 hPa	2 hPa	1 hPa	0.4 hPa	0.1 hPa	10 hPa	5 hPa	2 hPa	1 hPa	0.4 hPa	0.1 hPa
LIMS MAT minus rocketsonde																		
7 month	1.7	2.7	2.6	0.0	−3.5	−8.0	29/0	29/0	28/0	27/0	20/0	5/0	2.1	2.6	2.7	3.9	3.0	5.0
Nov.–Feb.	1.6	3.3	1.8	0.0	−3.6	−10.5	10/0	10/0	9/0	9/0	6/0	2/0	2.4	2.8	2.5	5.2	3.4	6.9
Feb.–May	1.7	2.5	2.9	0.0	−3.4	−6.4	19/0	19/0	19/0	18/0	14/0	3/0	2.0	2.5	2.8	3.2	2.9	4.1
LIMS MAT minus NMC (coefficient product)																		
7 month	0.3	−1.3	1.4	0.6	−3.4	0.0	203/0	184/0	184/0	184/0	184/0	0/0	2.1	3.6	2.1	2.5	2.0	0.0
Nov.–Feb.	−0.4	−2.8	1.7	0.6	−3.5	0.0	111/0	101/0	101/0	101/0	101/0	0/0	2.0	4.2	2.7	3.1	2.6	0.0
Feb.–May	1.1	0.6	1.1	0.6	−3.2	0.0	92/0	83/0	83/0	83/0	83/0	0/0	1.9	1.2	0.9	1.4	0.9	0.0
NMC (coefficient product) minus rocketsonde																		
7 month	0.9	3.3	1.3	−0.2	0.5	0.0	27/2	27/2	26/2	25/2	18/2	0/0	2.6	4.2	2.5	4.1	4.0	0.0
Nov.–Feb.	1.0	5.5	1.0	0.4	0.8	0.0	9/1	10/0	9/0	9/0	6/0	0/0	3.1	5.1	2.6	4.9	5.5	0.0
Feb.–May	0.8	2.0	1.5	−0.6	0.4	0.0	18/1	17/2	17/2	16/2	12/2	0/0	2.4	3.0	2.5	3.7	3.3	0.0

Table B8. Statistics for Cape Canaveral (29° N, 279° E)

	Mean difference, K, at—						Total of samples/Number rejected at—						Standard deviation, K, at—					
	10 hPa	5 hPa	2 hPa	1 hPa	0.4 hPa	0.1 hPa	10 hPa	5 hPa	2 hPa	1 hPa	0.4 hPa	0.1 hPa	10 hPa	5 hPa	2 hPa	1 hPa	0.4 hPa	0.1 hPa
LIMS MAT minus rocketsonde																		
7 month	0.1	0.5	0.0	−0.5	−4.5	−10.5	40/0	40/0	38/0	38/0	34/1	5/1	2.6	3.4	4.8	4.4	4.4	4.1
Nov.–Feb.	−0.5	−0.2	−1.9	−1.8	−6.5	−12.9	23/0	23/0	22/0	22/0	20/1	3/1	2.9	3.4	4.3	4.5	3.0	3.2
Feb.–May	1.0	1.3	2.6	1.4	−1.8	−6.9	17/0	17/0	16/0	16/0	14/0	2/0	1.8	3.2	4.3	3.8	4.6	1.9
LIMS MAT minus NMC (coefficient product)																		
7 month	0.3	−0.3	2.3	1.4	−4.4	0.0	203/0	184/0	184/0	184/0	184/0	0/0	1.5	5.0	3.0	3.7	3.6	0.0
Nov.–Feb.	−0.1	−2.2	2.6	2.9	−4.3	0.0	111/0	101/0	101/0	101/0	101/0	0/0	1.6	5.9	3.9	4.1	4.5	0.0
Feb.–May	0.7	2.1	2.1	−0.4	−4.6	0.0	92/0	83/0	83/0	83/0	83/0	0/0	1.3	2.0	1.4	2.0	1.9	0.0
NMC (coefficient product) minus rocketsonde																		
7 month	−0.4	0.1	−3.3	−2.1	0.2	0.0	39/1	37/3	35/3	35/3	31/4	0/0	2.7	6.0	5.9	6.6	6.1	0.0
Nov.–Feb.	−0.8	0.9	−5.8	−5.0	−1.6	0.0	23/0	22/1	21/1	21/1	19/2	0/0	2.9	7.0	5.4	6.3	6.2	0.0
Feb.–May	0.0	−1.1	0.5	2.2	3.0	0.0	16/1	15/2	14/2	14/2	12/2	0/0	2.4	4.3	4.5	4.3	5.1	0.0

Table B9. Statistics for White Sands (32° N, 254° E)

	Mean difference, K, at—						Total of samples/Number rejected at—						Standard deviation, K, at					
	10 hPa	5 hPa	2 hPa	1 hPa	0.4 hPa	0.1 hPa	10 hPa	5 hPa	2 hPa	1 hPa	0.4 hPa	0.1 hPa	10 hPa	5 hPa	2 hPa	1 hPa	0.4 hPa	0.1 hPa
LIMS MAT minus rocketsonde																		
7 month	0.3	0.6	0.3	−1.4	−4.6	−7.7	81/0	81/0	79/0	79/0	75/0	19/1	3.2	3.7	3.6	3.7	4.6	5.2
Nov. Feb.	0.0	0.1	−0.6	−2.3	−5.4	−8.7	52/0	52/0	50/0	50/0	47/0	13/1	3.4	3.4	3.7	4.0	3.9	5.2
Feb. May	0.7	1.3	1.8	0.1	−3.2	−5.4	29/0	29/0	29/0	29/0	28/0	6/0	2.8	4.2	2.9	2.6	5.3	5.0
LIMS MAT minus NMC (coefficient product)																		
7 month	0.7	2.1	2.9	3.2	−3.6	0.0	203/0	184/0	184/0	184/0	184/0	0/0	1.7	5.0	3.0	5.4	4.3	0.0
Nov.–Feb.	0.5	0.7	3.5	6.2	−2.6	0.0	111/0	101/0	101/0	101/0	101/0	0/0	1.7	6.0	3.5	5.4	5.3	0.0
Feb.–May	1.1	3.8	2.2	−0.3	−4.7	0.0	92/0	83/0	83/0	83/0	83/0	0/0	1.6	2.6	2.1	2.2	2.1	0.0
NMC (coefficient product) minus rocketsonde																		
7 month	−0.6	−1.2	−2.1	−4.5	−1.0	0.0	80/1	70/11	68/11	65/14	64/11	0/0	3.3	6.3	5.0	7.1	6.8	0.0
Nov.–Feb.	−0.6	−0.2	−3.3	−7.8	−2.6	0.0	51/1	46/6	44/6	41/9	41/6	0/0	3.4	6.5	5.4	6.7	6.8	0.0
Feb.–May	−0.4	−3.2	0.2	1.0	1.9	0.0	29/0	24/5	24/5	24/5	23/5	0/0	3.1	5.4	3.2	3.8	5.8	0.0

Table B10. Statistics for Point Mugu (34° N, 241° E)

	Mean difference, K, at—						Total of samples/Number rejected at—						Standard deviation, K, at					
	10 hPa	5 hPa	2 hPa	1 hPa	0.4 hPa	0.1 hPa	10 hPa	5 hPa	2 hPa	1 hPa	0.4 hPa	0.1 hPa	10 hPa	5 hPa	2 hPa	1 hPa	0.4 hPa	0.1 hPa
LIMS MAT minus rocketsonde																		
7 month	0.3	1.1	1.6	0.3	−3.0	−9.5	63/0	62/0	62/0	62/0	59/0	14/3	2.8	3.8	3.9	3.7	3.7	5.3
Nov. Feb.	−0.2	0.1	2.1	0.3	−4.2	−12.0	36/0	35/0	35/0	35/0	35/1	4/3	3.0	4.1	4.5	4.2	3.5	3.5
Feb.–May	0.9	2.5	1.0	0.3	−1.3	−8.5	27/0	27/0	27/0	27/0	24/0	10/0	2.4	2.9	2.8	2.9	3.3	5.8
LIMS MAT minus NMC (coefficient product)																		
7 month	0.7	1.4	2.3	2.8	−3.4	0.0	203/0	184/0	184/0	184/0	184/0	0/0	1.9	5.3	2.4	5.3	4.0	0.0
Nov.–Feb.	0.0	−0.5	2.3	5.2	−2.6	0.0	111/0	101/0	101/0	101/0	101/0	0/0	1.7	6.2	2.9	5.9	5.1	0.0
Feb.–May	1.6	3.8	2.3	−0.1	−4.4	0.0	92/0	83/0	83/0	83/0	83/0	0/0	1.8	2.6	1.6	2.0	1.6	0.0
NMC (coefficient product) minus rocketsonde																		
7 month	−0.7	0.3	−0.5	−2.2	0.8	0.0	60/3	53/9	53/9	53/9	50/9	0/0	3.4	5.6	4.3	6.1	5.5	0.0
Nov. Feb.	−0.3	1.4	0.1	−3.9	−0.9	0.0	34/2	30/5	30/5	30/5	30/5	0/0	3.7	6.4	4.9	7.3	6.0	0.0
Feb.–May	−1.2	−1.2	−1.3	0.1	3.3	0.0	26/1	23/4	23/4	23/4	20/4	0/0	3.1	4.1	3.2	3.0	3.4	0.0

Table B11. Statistics for Wallops Island (38° N, 285° E)

	Mean difference, K, at—						Total of samples/Number rejected at—						Standard deviation, K, at—					
	10 hPa	5 hPa	2 hPa	1 hPa	0.4 hPa	0.1 hPa	10 hPa	5 hPa	2 hPa	1 hPa	0.4 hPa	0.1 hPa	10 hPa	5 hPa	2 hPa	1 hPa	0.4 hPa	0.1 hPa
LIMS MAT minus rocketsonde																		
7 month	−2.2	−1.7	−1.0	−1.9	−3.6	−11.0	35/0	35/0	36/0	35/0	25/0	15/2	3.6	3.9	5.0	3.8	5.0	4.5
Nov.–Feb.	−4.2	−4.4	−3.9	−3.9	−5.2	−11.8	13/0	13/0	13/0	13/0	13/0	7/1	3.1	2.9	5.2	4.3	3.8	5.3
Feb.–May	−1.0	−0.1	0.6	−0.8	−1.9	−10.4	22/0	22/0	23/0	22/0	12/0	8/1	3.3	3.6	4.1	3.0	5.7	4.0
LIMS MAT minus NMC (coefficient product)																		
7 month	0.7	0.8	2.8	2.7	−3.7	0.0	203/0	184/0	184/0	184/0	184/0	0/0	1.7	4.0	3.4	5.5	4.5	0.0
Nov.–Feb.	0.5	−0.6	2.4	4.6	−3.2	0.0	111/0	101/0	101/0	101/0	101/0	0/0	1.9	4.6	4.4	6.5	5.5	0.0
Feb. May	0.8	2.5	3.3	0.4	−4.3	0.0	92/0	83/0	83/0	83/0	83/0	0/0	1.4	2.3	1.6	2.3	2.7	0.0
NMC (coefficient product) minus rocketsonde																		
7 month	−2.9	−3.0	−3.4	−2.5	1.3	0.0	33/2	30/5	31/5	29/6	21/4	0/0	4.5	5.5	5.0	5.4	7.0	0.0
Nov.–Feb.	−5.3	−4.0	−5.8	−7.4	−0.3	0.0	13/0	11/2	11/2	10/3	11/2	0/0	3.5	6.1	6.2	6.1	8.1	0.0
Feb.–May	−1.4	−2.5	−2.1	0.0	3.1	0.0	20/2	19/3	20/3	19/3	10/2	0/0	4.4	5.3	3.8	2.6	5.4	0.0

Table B12. Statistics for Volgograd (49° N. 44° E)

	Mean difference, K, at						Total of samples/Number rejected at—						Standard deviation, K, at—					
	10 hPa	5 hPa	2 hPa	1 hPa	0.4 hPa	0.1 hPa	10 hPa	5 hPa	2 hPa	1 hPa	0.4 hPa	0.1 hPa	10 hPa	5 hPa	2 hPa	1 hPa	0.4 hPa	0.1 hPa
LIMS MAT minus rocketsonde																		
7 month	2.2	5.0	7.9	7.8	5.7	3.2	64/0	64/0	60/2	57/4	60/1	61/0	2.7	3.3	3.8	4.0	5.3	7.3
Nov.–Feb.	1.8	5.3	9.4	10.2	7.1	3.1	24/0	24/0	22/1	19/3	21/1	22/0	3.5	4.3	5.1	4.5	7.0	7.2
Feb.–May	2.5	4.8	7.1	6.6	4.9	3.2	40/0	40/0	38/1	38/1	39/0	39/0	2.0	2.7	2.5	3.3	4.1	7.5
LIMS MAT minus NMC (coefficient product)																		
7 month	2.2	0.7	3.7	3.7	0.3	0.0	203/0	184/0	184/0	184/0	184/0	0/0	3.0	3.7	3.8	5.5	10.1	0.0
Nov.–Feb.	2.2	0.7	4.0	4.8	2.6	0.0	111/0	101/0	101/0	101/0	101/0	0/0	3.4	4.8	4.9	6.9	13.0	0.0
Feb.–May	2.1	0.8	3.3	2.4	−2.6	0.0	92/0	83/0	83/0	83/0	83/0	0/0	2.5	1.5	1.4	2.4	2.3	0.0
NMC (coefficient product) minus rocketsonde																		
7 month	0.5	4.9	4.4	3.8	5.4	0.0	63/1	57/7	53/9	51/10	52/9	0/0	3.4	5.0	3.8	5.2	6.3	0.0
Nov.–Feb.	−0.4	5.2	6.1	5.6	2.5	0.0	24/0	21/3	19/4	17/5	17/5	0/0	4.2	7.3	4.8	6.6	8.6	0.0
Feb.–May	1.1	4.8	3.4	2.8	6.9	0.0	39/1	36/4	34/5	34/5	35/4	0/0	2.8	3.0	2.7	4.0	4.3	0.0

Table B13. Statistics for Shemya (53° N, 174° E)

	Mean difference, K, at –						Total of samples/Number rejected at						Standard deviation, K, at					
	10 hPa	5 hPa	2 hPa	1 hPa	0.4 hPa	0.1 hPa	10 hPa	5 hPa	2 hPa	1 hPa	0.4 hPa	0.1 hPa	10 hPa	5 hPa	2 hPa	1 hPa	0.4 hPa	0.1 hPa
LIMS MAT minus rocketsonde																		
7 month	0.3	1.0	2.0	2.4	-0.4	0.0	32/1	33/0	33/0	28/2	7/0	0/0	2.0	3.1	5.4	4.7	8.1	0.0
Nov.–Feb.	-0.2	1.1	3.9	3.1	0.5	0.0	15/0	15/0	15/0	11/2	5/0	0/0	2.1	3.3	6.7	6.3	9.8	0.0
Feb.–May	0.8	0.8	0.4	1.7	-2.4	0.0	17/1	18/0	18/0	17/0	2/0	0/0	1.8	3.0	3.3	3.3	1.4	0.0
LIMS MAT minus NMC (coefficient product)																		
7 month	0.2	1.1	3.9	3.1	-2.4	0.0	203/0	184/0	184/0	181/0	184/0	0/0	2.7	4.2	3.9	7.3	7.8	0.0
Nov.–Feb.	0.1	1.1	2.0	1.4	-2.7	0.0	111/0	101/0	101/0	101/0	101/0	0/0	2.7	5.5	4.2	9.2	10.3	0.0
Feb.–May	0.3	1.1	6.3	5.2	-2.1	0.0	92/0	83/0	83/0	83/0	83/0	0/0	2.7	1.5	1.5	2.7	2.2	0.0
NMC (coefficient product) minus rocketsonde																		
7 month	0.3	0.5	-3.3	-2.2	-1.3	0.0	32/1	30/3	30/3	26/4	6/1	0/0	3.0	4.1	6.6	6.7	9.2	0.0
Nov.–Feb.	-0.1	1.3	0.0	-0.9	-1.0	0.0	15/0	13/2	13/2	10/3	4/1	0/0	3.1	5.6	7.8	9.6	11.7	0.0
Feb.–May	0.7	0.0	-5.9	-3.0	-1.8	0.0	17/1	17/1	17/1	16/1	2/0	0/0	3.0	2.5	4.0	4.2	3.8	0.0

Table B14. Statistics for Primrose Lake (55° N, 250° E)

	Mean difference, K, at –						Total of samples/Number rejected at						Standard deviation, K, at					
	10 hPa	5 hPa	2 hPa	1 hPa	0.4 hPa	0.1 hPa	10 hPa	5 hPa	2 hPa	1 hPa	0.4 hPa	0.1 hPa	10 hPa	5 hPa	2 hPa	1 hPa	0.4 hPa	0.1 hPa
LIMS MAT minus rocketsonde																		
7 month	0.9	1.9	3.8	2.0	-2.5	-10.6	49/0	49/0	49/0	49/0	43/0	19/7	3.1	3.5	4.3	5.0	5.1	7.1
Nov.–Feb.	0.6	1.2	4.6	2.6	-1.5	-10.2	28/0	28/0	28/0	28/0	24/0	14/5	3.0	4.1	4.6	6.2	6.2	7.1
Feb.–May	1.3	2.9	2.8	1.3	-3.6	-11.8	21/0	21/0	21/0	21/0	19/0	5/2	3.3	2.3	3.9	2.7	3.0	7.8
LIMS MAT minus NMC (coefficient product)																		
7 month	0.7	2.5	4.8	2.8	-1.5	0.0	203/0	184/0	184/0	184/0	184/0	0/0	2.2	4.0	3.1	6.4	8.2	0.0
Nov.–Feb.	0.3	2.2	4.2	2.3	-1.0	0.0	111/0	101/0	101/0	101/0	101/0	0/0	2.3	5.2	3.9	8.3	10.8	0.0
Feb.–May	1.2	2.9	5.4	3.5	-2.1	0.0	92/0	83/0	83/0	83/0	83/0	0/0	1.9	1.4	1.5	2.7	2.5	0.0
NMC (coefficient product) minus rocketsonde																		
7 month	-0.1	-2.0	0.2	0.9	0.2	0.0	46/3	45/4	45/4	43/6	36/7	0/0	3.5	5.5	6.7	8.4	7.6	0.0
Nov.–Feb.	-0.4	-3.1	1.5	2.2	0.5	0.0	27/1	28/0	28/0	26/2	21/3	0/0	3.5	6.5	7.8	10.0	9.2	0.0
Feb.–May	0.3	-0.2	-2.1	-1.1	-0.3	0.0	19/2	17/4	17/4	17/4	15/4	0/0	3.5	2.3	3.8	4.5	4.9	0.0

Table B15. Statistics for Fort Churchill (59° N, 266° E)

	Mean difference, K, at—						Total of samples/Number rejected at—						Standard deviation, K, at—					
	10 hPa	5 hPa	2 hPa	1 hPa	0.4 hPa	0.1 hPa	10 hPa	5 hPa	2 hPa	1 hPa	0.4 hPa	0.1 hPa	10 hPa	5 hPa	2 hPa	1 hPa	0.4 hPa	0.1 hPa
LIMS MAT minus rocketsonde																		
7 month	1.6	2.3	4.2	2.6	−3.7	−10.4	63/0	63/0	63/0	62/0	57/0	4/0	2.9	3.3	4.6	4.7	4.5	5.9
Nov.–Feb.	1.8	2.1	3.2	2.5	−4.1	−10.4	36/0	36/0	36/0	36/0	32/0	4/0	2.7	3.3	4.7	5.3	5.1	5.9
Feb.–May	1.2	2.6	5.5	2.6	−3.1	0.0	27/0	27/0	27/0	26/0	25/0	0/0	3.2	3.2	4.2	3.8	3.7	0.0
LIMS MAT minus NMC (coefficient product)																		
7 month	1.5	2.1	4.5	3.6	0.4	0.0	203/0	184/0	184/0	184/0	184/0	0/0	3.3	4.0	3.6	6.3	8.9	0.0
Nov.–Feb.	1.0	1.7	3.8	2.9	1.6	0.0	111/0	101/0	101/0	101/0	101/0	0/0	3.4	5.1	4.3	7.9	11.5	0.0
Feb.–May	2.1	2.6	5.4	4.5	−1.0	0.0	92/0	83/0	83/0	83/0	83/0	0/0	3.2	2.0	2.3	3.4	3.3	0.0
NMC (coefficient product) minus rocketsonde																		
7 month	−0.1	−1.2	1.3	0.6	0.1	0.0	61/2	56/7	56/7	51/11	47/10	0/0	5.2	7.2	5.2	9.3	7.8	0.0
Nov.–Feb.	0.5	−1.8	1.1	1.9	0.9	0.0	34/2	32/4	32/4	28/8	25/7	0/0	2.9	8.3	5.4	9.6	8.3	0.0
Feb.–May	−0.8	−0.5	1.5	−0.8	−0.8	0.0	27/0	24/3	24/3	23/3	22/3	0/0	7.1	5.6	5.1	8.9	7.2	0.0

Table B16. Statistics for Poker Flat (65° N, 213° E)

	Mean difference, K, at—						Total of samples/Number rejected at—						Standard deviation, K, at—					
	10 hPa	5 hPa	2 hPa	1 hPa	0.4 hPa	0.1 hPa	10 hPa	5 hPa	2 hPa	1 hPa	0.4 hPa	0.1 hPa	10 hPa	5 hPa	2 hPa	1 hPa	0.4 hPa	0.1 hPa
LIMS MAT minus rocketsonde																		
7 month	0.7	0.7	0.3	−0.5	−2.3	−10.6	43/0	43/0	43/0	43/0	32/0	14/0	2.7	3.4	4.1	3.8	3.8	5.0
Nov.–Feb.	2.2	3.6	3.0	3.2	1.4	−11.3	9/0	9/0	9/0	9/0	8/0	5/0	4.3	4.4	4.0	4.4	2.1	5.5
Feb.–May	0.4	−0.1	−0.4	−1.4	−3.6	−10.2	34/0	34/0	34/0	34/0	24/0	9/0	2.0	2.6	3.8	3.1	3.4	5.1
LIMS MAT minus NMC (coefficient product)																		
7 month	0.7	1.9	3.5	2.1	0.0	0.0	203/0	184/0	184/0	184/0	184/0	0/0	2.1	4.9	4.0	9.1	11.2	0.0
Nov.–Feb.	1.0	1.6	2.0	−0.3	1.2	0.0	111/0	101/0	101/0	101/0	101/0	0/0	2.7	6.6	4.5	11.6	14.6	0.0
Feb.–May	0.4	2.1	5.3	5.0	−1.5	0.0	92/0	83/0	83/0	83/0	83/0	0/0	1.2	1.3	2.1	2.6	3.9	0.0
NMC (coefficient product) minus rocketsonde																		
7 month	0.0	−3.2	−4.2	−5.6	−1.0	0.0	42/1	40/3	40/3	35/8	26/6	0/0	2.5	4.0	6.7	6.0	6.8	0.0
Nov.–Feb.	−0.2	−6.7	2.1	7.6	10.3	0.0	9/0	9/0	9/0	4/5	4/4	0/0	3.6	5.9	8.9	4.9	5.2	0.0
Feb.–May	0.0	−2.2	−6.0	−7.3	−3.1	0.0	33/1	31/3	31/3	31/3	22/2	0/0	2.1	2.5	4.7	3.5	4.8	0.0

Table B17. Statistics for Thule (77° N, 291° E)

	Mean difference, K, at—						Total of samples/Number rejected at—						Standard deviation, K, at—					
	10 hPa	5 hPa	2 hPa	1 hPa	0.4 hPa	0.1 hPa	10 hPa	5 hPa	2 hPa	1 hPa	0.4 hPa	0.1 hPa	10 hPa	5 hPa	2 hPa	1 hPa	0.4 hPa	0.1 hPa
LIMS MAT minus rocketsonde																		
7 month	2.2	2.4	2.7	2.6	−2.3	−9.2	43/0	42/1	41/2	40/2	39/0	29/1	3.0	3.9	4.6	3.9	4.6	6.2
Nov.–Feb.	2.4	2.4	2.3	3.7	1.9	−3.3	13/0	13/0	13/0	12/0	11/0	9/0	3.2	4.5	7.1	5.7	4.6	6.6
Feb.–May	2.0	2.3	2.8	2.2	−4.0	−11.9	30/0	29/1	28/2	28/2	28/0	20/1	3.0	3.7	3.1	2.8	3.4	3.7
LIMS MAT minus NMC (coefficient product)																		
7 month	3.1	2.7	3.9	2.5	4.0	0.0	203/0	184/0	184/0	184/0	184/0	0/0	5.8	4.9	4.8	8.4	10.2	0.0
Nov.–Feb.	4.8	1.7	2.1	0.8	9.1	0.0	111/0	101/0	101/0	101/0	101/0	0/0	6.9	5.4	3.6	7.4	9.2	0.0
Feb.–May	0.9	4.0	6.1	4.7	−2.2	0.0	92/0	83/0	83/0	83/0	83/0	0/0	3.0	3.8	5.2	9.1	7.7	0.0
NMC (coefficient product) minus rocketsonde																		
7 month	0.9	0.1	−2.0	−3.1	−4.8	0.0	41/2	37/6	36/7	34/8	31/8	0/0	5.1	7.1	6.8	6.4	7.1	0.0
Nov.–Feb.	0.1	2.9	−0.7	−1.2	−6.0	0.0	12/1	12/1	12/1	11/1	10/1	0/0	8.0	6.7	8.1	7.6	9.0	0.0
Feb.–May	1.2	−1.2	−2.6	−3.9	−4.3	0.0	29/1	25/5	24/6	23/7	21/7	0/0	3.3	7.0	6.1	5.7	6.2	0.0

Table B18. Statistics for Heiss Island (81° N, 58° E)

	Mean difference, K, at—						Total of samples/Number rejected at—						Standard deviation, K, at—					
	10 hPa	5 hPa	2 hPa	1 hPa	0.4 hPa	0.1 hPa	10 hPa	5 hPa	2 hPa	1 hPa	0.4 hPa	0.1 hPa	10 hPa	5 hPa	2 hPa	1 hPa	0.4 hPa	0.1 hPa
LIMS MAT minus rocketsonde																		
7 month	5.4	6.3	8.7	12.2	10.0	4.6	65/0	65/0	64/1	63/2	58/7	50/15	3.4	3.9	4.1	4.1	7.0	9.7
Nov.–Feb.	7.0	7.4	8.9	10.3	7.7	−4.5	28/0	28/0	27/1	26/2	25/3	17/11	4.2	5.5	5.3	4.8	8.4	9.1
Feb.–May	4.1	5.5	8.6	13.5	11.8	9.2	37/0	37/0	37/0	37/0	33/4	33/4	1.9	1.9	2.8	2.8	5.1	6.1
LIMS MAT minus NMC (coefficient product)																		
7 month	2.9	3.5	5.5	4.0	6.7	0.0	203/0	184/0	184/0	184/0	184/0	0/0	6.7	5.6	5.9	7.4	12.2	0.0
Nov.–Feb.	4.4	2.2	4.2	2.5	13.8	0.0	111/0	101/0	101/0	101/0	101/0	0/0	7.0	6.4	5.4	5.4	10.7	0.0
Feb.–May	1.0	5.0	7.1	5.8	−2.0	0.0	92/0	83/0	83/0	83/0	83/0	0/0	6.0	3.7	6.1	9.1	7.4	0.0
NMC (coefficient product) minus rocketsonde																		
7 month	2.7	1.6	2.3	6.4	6.0	0.0	61/4	57/8	59/6	56/9	50/15	0/0	5.8	5.2	7.1	6.4	10.7	0.0
Nov.–Feb.	0.8	5.0	5.1	7.4	−1.4	0.0	26/2	24/4	26/2	24/4	24/4	0/0	7.4	5.2	7.7	7.5	10.5	0.0
Feb.–May	4.2	−1.0	0.0	5.7	12.8	0.0	35/2	33/4	33/4	32/5	26/11	0/0	3.8	3.4	5.8	5.4	4.7	0.0

REPORT DOCUMENTATION PAGE		Form Approved OMB No. 0704-0188

1. AGENCY USE ONLY *(Leave blank)*	2. REPORT DATE April 1994	3. REPORT TYPE AND DATES COVERED Technical Paper

4. TITLE AND SUBTITLE	5. FUNDING NUMBERS
Time Series Comparisons of Satellite and Rocketsonde Temperatures in 1978-79	WU 579-21-44-70

6. AUTHOR(S)

Ellis E. Remsberg, Praful P. Bhatt, and Francis J. Schmidlin

7. PERFORMING ORGANIZATION NAME(S) AND ADDRESS(ES)	8. PERFORMING ORGANIZATION REPORT NUMBER
NASA Langley Research Center Hampton, VA 23681-0001	L-17250

9. SPONSORING/MONITORING AGENCY NAME(S) AND ADDRESS(ES)	10. SPONSORING/MONITORING AGENCY REPORT NUMBER
National Aeronautics and Space Administration Washington, DC 20546-0001	NASA TP-3409

11. SUPPLEMENTARY NOTES

Remsberg: Langley Research Center, Hampton, VA; Bhatt: SAIC, Hampton, VA; Schmidlin: Wallops Flight Facility, Wallops Island, VA.

12a. DISTRIBUTION/AVAILABILITY STATEMENT	12b. DISTRIBUTION CODE
Unclassified-Unlimited Subject Category 47	

13. ABSTRACT *(Maximum 200 words)*

The Limb Infrared Monitor of the Stratosphere (LIMS) experiment on Nimbus 7 yielded temperature-versus-pressure $(T(p))$ profiles for each radiance scan. The present report describes time series comparisons between LIMS and rocketsonde $T(p)$ values at rocketsonde station locations. Sample size has increased up to 665 by this new approach, leading to better statistics for a $T(p)$ validation. The results indicate no clearly significant bias for LIMS versus Datasonde from 10 hPa at low and mid latitudes. There is a positive LIMS bias of 2 to 3 K in the upper stratosphere at high latitudes for the Northern Hemisphere in both winter and spring. LIMS is progressively colder than Datasonde from 0.4 hPa (about −3 K) to 0.1 hPa (about −9 K) at all latitudes. A similar comparison between LIMS and the more accurate falling sphere measurements reveals an equivalent mid-latitude LIMS bias at 0.4 hPa but a much smaller bias at 0.1 hPa (−4.6 K). Because the biases do not vary noticeably with season, it is concluded that they are not a function of atmospheric state. This result confirms the robustness of the LIMS temperature retrieval technique.

14. SUBJECT TERMS	15. NUMBER OF PAGES 140
LIMS (Limb Infrared Monitor of the Stratosphere); Nimbus 7; Satellite temperature; Rocketsonde; Middle atmosphere	16. PRICE CODE A07

17. SECURITY CLASSIFICATION OF REPORT Unclassified	18. SECURITY CLASSIFICATION OF THIS PAGE Unclassified	19. SECURITY CLASSIFICATION OF ABSTRACT	20. LIMITATION OF ABSTRACT

National Aeronautics and
Space Administration
Langley Research Center
Mail Code 180
Hampton, VA 23681-00001